FCT Fundação para a Ciência e a Tecnologia
MINISTÉRIO DA CIÊNCIA, TECNOLOGIA E ENSINO SUPERIOR Portugal

POPH PROGRAMA OPERACIONAL POTENCIAL HUMANO

QREN QUADRO DE REFERÊNCIA ESTRATÉGICO NACIONAL PORTUGAL 2007.2013

UNIÃO EUROPEIA
Fundo Social Europeu

LISTA DE PUBLICAÇÕES

Esta investigação foi realizada no Centro de Investigação em Química (CIQ), no Departamento de Química e Bioquímica da Faculdade de Ciências da Universidade do Porto, com o apoio financeiro de uma bolsa de Doutoramento (SFRH/BD/65350/2009) atribuída pela Fundação para a Ciência e Tecnologia.

Esta dissertação integra resultados que foram publicados em congressos científicos internacionais através de comunicações em painel e comunicações orais e em revistas de circulação internacional com arbitragem científica:

Artigos em revistas de circulação internacional com arbitragem científica:

Fernandes, A., Brás, N., Mateus, N., de Freitas, V. Study of Anthocyanins Self-Association by NMR spectroscopy*, New Journal of Chemistry*, **submitted.**

Fernandes, A., Brás, N., Mateus, N., de Freitas, V. Understanding the molecular mechanism of anthocyanins binding to pectin*, Langmuir*, **2014**, *30* (28), 8516-8527;
doi: *10.1021/la501879w.*

Fernandes, A., Ivanova, G., Brás, N., Mateus, N., Ramos. M.J., de Freitas, V. Structural characterization of inclusion complexes between cyanidin-3-*O*-glucoside and β-cyclodextrin, *Carbohydrate Polymers*, **2014**, *102*, 269-277;
doi: *10.1016/j.carbpol.2013.11.037.*

Fernandes, A., Sousa, A., Azevedo, J., Mateus, N., de Freitas, V. Effect of Cyclodextrins on the Thermodynamic and Kinetic Properties of Cyanidin-3-*O*-glucoside*, Food Research International*, **2013**, *51*, 748-755;
doi: *10.1016/j.foodres.2013.01.037.*

Gago, S., Basílio, N., Fernandes, A., de Freitas, V., Quintas, A., Pina, F. Photochromism of the complex between 4'-(2-hydroxyethoxy)-7-hydroxyflavylium and β-cyclodextrin, studied by ^{1}H NMR, UV-Vis, continuous irradiation and circular dichroism, *Dyes and Pigments*, **2014,** *110*, 106-112;
doi: *10.1016/j.dyepig.2014.04.038.*

Basílio, N., Fernandes, A., de Freitas, V., Gago, S., Pina, F. Effect of β-cyclodextrin on the chemistry of 3',4',7-trihydroxyflavylium, *New Journal of Chemistry*, **2013**, *37*, 3166-3177;
doi: *10.1039/C3NJ00588G.*

Petrov, V., Stanislav, S., Petrov, I., Fernandes, A., de Freitas, V., Pina, F. Emptying the β-Cyclodextrin Cavity by Light. Photochemical Removal of the Trans-Chalcone of 4',7-Dihydroxyflavylium, *Journal of Physical Chemistry A, **2013**, 117 (41),* 10692–10701;
doi: *10.1021/jp4060582.*

Comunicações orais:

Fernandes, A., Mateus, N., de Freitas, V. Chemical structure and stability of microencapsulated anthocyanins. 10º Encontro Nacional de Química Orgânica – 1º Simpósio Luso-Brasileiro de Química Orgânica, Lisboa, Portugal, 4-6 September, 2013.

Comunicações em painel:

Fernandes, A., Ivanova, G., Brás, N., Mateus, N., Ramos. M.J, de Freitas, V. Structural characterization of inclusion complexes between cyanidin-3-*O*-glucoside and β-cyclodextrin. 7th International Workshop on Anthocyanins, Porto, Portugal, 9-11 September, 2013.

Fernandes, A., Mateus, N., de Freitas, V. Physical-chemical properties of microencapsulated anthocyanins. 26th International Conference on Polyphenols, Florence, Italy, 22-26 July 2012.

AGRADECIMENTOS

A realização deste trabalho não teria sido possível sem a colaboração e o apoio de várias pessoas e instituições. Desta forma gostaria de expressar o meu sincero agradecimento:

Ao Professor Doutor Victor de Freitas, orientador deste trabalho, agradeço a sua orientação e conhecimentos científicos que me transmitiu ao longo destes últimos anos, as suas críticas e sugestões, o apoio incondicional e principalmente por toda a confiança que depositou em mim.

Ao Professor Doutor Nuno Mateus, agradeço todos os conselhos e disponibilidade que sempre demonstrou. Agradeço a sua boa disposição e sentido de humor.

Ao grupo de investigação em Química Física de Centro de Investigação em Química, em particular ao Professor Doutor Luís Belchior agradeço pela realização dos ensaios de DSC.

À Mariana Andrade, agradeço a incansável ajuda e motivação nas longas experiências de RMN. Agradeço por todo o apoio técnico e pela sua total disponibilidade e interesse.

À Doutora Galya Ivanova, agradeço a ajuda na realização de algumas experiências de RMN e todos os ensinamentos que me transmitiu.

Ao Professor Doutor Eurico Cabrita, agradeço pelas sugestões na realização das experiências de STD.

Ao Professor Doutor Fernando Pina, agradeço pelo apoio e ensinamentos na realização das experiências de *pH jump*.

À Natércia Brás, agradeço por toda a colaboração nos estudos computacionais e por todos os conhecimentos que me transmitiu na área da Química Teórica. Mas especialmente agradeço o seu apoio, a sua amizade, companheirismo e disposição contagiante

A todos os meus amigos e colegas de laboratório agradeço por terem tornado este percurso muito mais fácil e possível. Agradeço-lhes a ajuda, o apoio e especialmente a motivação nestes últimos tempos de escrita. Agradeço-lhes também por todos momentos de que temos partilhado, quer profissionalmente quer pessoalmente.

Por último, mas não menos importante, agradeço à minha família, em particular aos meus pais, ao meu irmão, à Marta e ao Mário por todo o apoio, incentivo e

principalmente pelo entusiasmo ao longo deste projeto. Agradeço os empurrões que me foram dando ao longo deste percurso. Agradeço especialmente ao Rui, por inúmeras razões, entre as quais toda a ajuda na escrita desta tese, todo o apoio e incentivo incansável, pela sua compreensão, paciência e claro, pelo amor que partilhamos. À Leonor, um agradecimento muito especial. És a minha fonte de inspiração, a minha vontade de ser melhor a cada dia que passa.

De entre as várias entidades que contribuíram para a realização deste trabalho destaco as seguintes:

A Fundação para a Ciência e Tecnologia (FCT), pelo apoio financeiro concedido através de uma bolsa de Doutoramento (SFRH/BD/65350/2009).

A Faculdade de Ciências da Universidade do Porto (FCUP) e em particular o Departamento de Química e Bioquímica, por me ter aceite no Programa Doutoral em Química.

A Linha 2 do Centro de Investigação em Química (CIQ), pelos apoios logísticos e financeiros concedidos para a realização deste trabalho.

RESUMO

Os compostos polifenólicos são metabolitos secundários ubíquos na Natureza. Estes compostos estão presentes em alimentos e bebidas de origem vegetal tendo uma contribuição importante em algumas propriedades organoléticas tais como a cor e o sabor. Por outro lado, o consumo dos polifenóis está associado a efeitos benéficos para a saúde humana, o que tem fomentado a aplicação tecnológica destes compostos. As antocianinas constituem um grupo relevante de polifenóis sendo responsáveis pela grande diversidade de cores que se podem observar nas plantas e em produtos alimentares delas resultantes. Apesar do enorme potencial de aplicação das antocianinas na indústria alimentar, a sua utilização como corantes alimentares apresenta ainda algumas limitações, principalmente devido à sua instabilidade.

Nos últimos anos a interação entre antocianinas e carboidratos tem despertado a atenção por parte da comunidade científica uma vez que estes compostos são frequentemente encontrados juntos nas plantas e nos alimentos. Diversos estudos demonstraram que a interação entre estes compostos poderá influenciar a estabilidade e a extração destes pigmentos. Deste modo, com este projeto pretendeu-se estudar a interação entre antocianinas e carboidratos habitualmente usados na indústria alimentar. Por outro lado, vários estudos evidenciaram que a acilação das antocianinas aumenta a sua estabilidade, tendo esta estabilização sido atribuída a mecanismos de copigmentação intra- e inter-molecular (auto-associação). Assim, neste projeto pretendeu-se estudar igualmente a ocorrência de mecanismos de auto-associação em antocianinas mono-aciladas e não aciladas.

Os resultados obtidos neste trabalho foram divididos em três partes: o estudo da interação entre flavílios e ciclodextrinas (Capítulo III), antocianinas e pectina (Capítulo IV) e o estudo da ocorrência de mecanismos de auto-associação entre antocianinas (Capítulo V).

A associação entre uma antocianina (cianidina-3-*O*-glucósido) e três tipos de ciclodextrinas (α, β e γ) e a avaliação do impacto desta associação nos equilíbrios termodinâmicos e cinéticos das suas reações ácido-base foi estudada por espectrofotometria de ultravioleta-visível. A adição de β-ciclodextrina resultou numa diminuição da cor da solução antociânica, sendo este efeito mais evidente a pH mais

elevado e a concentrações superiores de β-ciclodextrina. Este efeito de anti-copigmentação indicou claramente que os equilíbrios ácido-base foram afetados pela presença da ciclodextrina. A inclusão molecular das formas incolores da antocianina na cavidade da β-ciclodextrina resultou num aumento da velocidade observada de isomerização (k_{obs}) a pH 5.3 e no aumento da constante de equilíbrio de hidratação (K_h), com o aumento da concentração da espécie hemiacetal e diminuição do catião flavílio de cor vermelha. Pelo contrário, para as outras duas ciclodextrinas testadas, α- e γ-ciclodextrina, não foram observadas alterações significativas nas constantes de equilíbrio termodinâmico e nas velocidades de reação, o que sugere que a inclusão de cianidina-3-*O*-glucósido nestas ciclodextrinas não foi efetiva.

Foi igualmente possível observar que a inclusão molecular de cianidina-3-*O*-glucósido na cavidade da β-ciclodextrina originou uma estabilização desta antocianina, traduzindo-se num aumento do seu tempo de semi-vida.

Posteriormente, a estrutura molecular dos complexos de inclusão cianidina-3-*O*-glucósido-β-ciclodextrina foi caracterizada por ressonância magnética nuclear e por estudos computacionais. A existência de interações inter-moleculares foi evidenciada através de experiências de DOSY (*Difusion Ordered spectroscopy*) e de NOE (*Nuclear Overhauser Effect*). A alteração dos desvios químicos dos protões da cavidade da β-ciclodextrina e dos protões pertencentes à forma hemiacetal da cianidina-3-*O*-glucósida, em conjunto com os valores de coeficientes de difusão (*D*) e das correlações de NOE, evidenciou a formação de um complexo de inclusão entre esta forma de equilíbrio e a β-ciclodextrina. Esta antocianina formou um complexo de inclusão de 1:1 com a β-ciclodextrina em que o anel pirânico C da antocianina se encontra incluído no interior da cavidade da ciclodextrina, enquanto o anel B se encontra no plano da extremidade mais larga da ciclodextrina. Por outro lado, a análise dos dados obtidos nas experiências de ressonância magnética nuclear não evidenciou a existência de uma interação entre o catião flavílio ou a *trans*-chalcona da cianidina-3-*O*-glucósido e a β-ciclodextrina.

A interação entre as diferentes formas de equilíbrio de três flavílios sintéticos (4',7-dihidroxiflavílio, 4'-(2-hidroxietoxi)-7-hidroxiflavílio e 3',4',7-trihidroxiflavílio) e a β-ciclodextrina e a formação dos respetivos complexos de inclusão foi igualmente estudada por ressonância magnética nuclear (ROESY – *Rotational Overhauser Effect spectroscopy*). Para estes três flavílios sintéticos, as respetivas espécies *trans*-chalcona interagiram preferencialmente com a ciclodextrina. Pelo contrário, as

restantes espécies em equilíbrio não evidenciaram qualquer interação com a β-ciclodextrina. Os dados obtidos através das experiências de ROESY sugerem uma estrutura em que a *trans*-chalcona dos flavílios sintéticos é incluída na cavidade da β-ciclodextrina através do anel A, sendo evidente a interação entre os hidrogénios H8, H6, H5, H4 e H3 e os protões da superfície interna da β-ciclodextrina. A menor polaridade do composto 4'-(2-hidroxietoxi)-7-hidroxiflavílio pareceu resultar numa penetração mais profunda deste flavílio sintético na cavidade β-ciclodextrina.

Numa segunda parte deste trabalho, foi estudada interação entre duas antocianinas naturais (cianidina-3-*O*-glucósido e delfinidina-3-*O*-glucósido) e a pectina, que é um polissacarídeo presente nas paredes celulares vegetais. Esta interação foi caracterizada por ressonância magnética nuclear de diferença de transferência de saturação (STD) o que permitiu determinar a respetiva constante de dissociação (K_d). Esta interação foi igualmente estudada por espectrofotometria de ultravioleta-visível e por estudos de modelação molecular. A pH 4.0, em que as antocianinas se encontram sobretudo na sua forma hemiacetal, foi possível verificar a existência de uma interação fraca entre as duas antocianinas e a pectina. Uma variação na extensão dessa ligação foi também verificada para a delfinidina-3-*O*-glucósida (com três grupos hidroxilo) que revelou uma afinidade superior para a pectina comparativamente à cianidina-3-*O*-glucósido (K_d ≈ 180 μM para delfinidina e K_d ≈ 250 μM para cianidina-3-*O*-glucósido). Experiências realizadas a pH 1.5 (antocianina na forma de catião flavílio) revelaram uma interação superior (K_d ≈ 2 μM) entre as antocianinas e a pectina comparativamente ao pH 4.0. Estes resultados foram complementados por estudos computacionais teóricos, que confirmaram uma interação mais forte da forma do catião flavílio da antocianina com a pectina e especialmente para a dp3glc (AH^+_{dp3glc}>B_{dp3glc}> B_{cy3glc}).

A possibilidade de ocorrência de reações de associação em antocianinas aciladas com ácido cumárico (malvidina-3-*O*-(6-cumaroíl)glucósido) e antocianinas não-aciladas (malvidina-3-*O*-glucósido) foi estudada por espectroscopia de ressonância magnética nuclear e dinâmica molecular. Experiências de NOESY (*Nuclear Overhauser Effects spectoscopy*) e DOSY a pH ácido (1.0) evidenciaram a ocorrência de dois mecanismos de associação das formas flavílio das antocianinas aciladas, nomeadamente copigmentação intra-molecular e associação inter-molecular. As variações espectrais observadas (deslocamentos químicos, δ e coeficientes de difusão, *D*) resultantes das concentrações crescentes das antocianinas foram

analisadas recorrendo a um modelo isodésmico. Nas condições experimentais testadas, a malvidina-3-*O*-(6-cumaroíl)glucósido evidenciou uma constante de associação superior (1402 M^{-1} (δ) e 2203 M^{-1} (*D*)) em comparação com a malvidina-3-*O*-glucósido (819 M^{-1} (δ) e 1002 M^{-1} (*D*)), indiciando que as antocianinas aciladas apresentam uma maior afinidade para a auto-associação. Em D_2O/DMSO o valor de concentração de agregação crítica (cac) determinado foi muito semelhante para as duas antocianinas.

De um modo geral, este projeto contribuiu para a elucidação da interação entre carboidratos e antocianinas, principalmente do ponto de vista estrutural, permitindo a obtenção de informações determinantes sobre o impacto de ciclodextrinas nos equilíbrios termodinâmicos e cinéticos das antocianinas. Os resultados alcançados neste projeto contribuíram igualmente para a elucidação da interação entre antocianinas e pectinas, importante não só para a estabilização destes pigmentos, mas também um aspeto fundamental na extração e biodisponibilidade das antocianinas. Este estudo permitiu também obter informações sobre os mecanismos de estabilização de antocianinas.

PALAVRAS-CHAVE: Antocianinas; auto-associação; carboidratos; ciclodextrinas; complexos de inclusão molecular; copigmentação intra-molecular; Dinâmica Molecular; DOSY; flavílios; NOESY; pectina; RMN; ROESY; STD; UV-Vis

ABSTRACT

Polyphenolic compounds are secondary metabolites widespread in the Nature. These compounds are also present in food and beverages derived from plants in which they are responsible for major organoleptic properties. The consumption of these compounds has been associated with health benefits which have stimulated their technological application in diverse industries. Among polyphenols, anthocyanins are a relevant group of compounds which play a detrimental role in the color of plants. Although the great potential of application that anthocyanins represents for food-industry, their use as food colorants is seriously limited due to their instability problems, which has prompted the search for new methods to enhance anthocyanin's stability.

Association between anthocyanins and carbohydrates has drawn attention over the past few years and this interaction is of particularly importance in food chemistry since these compounds are often found together in plants and foodstuffs. Several studies have revealed that this interaction may affect not only color but also the stability and the extraction of anthocyanins. Moreover, research involving the development of anthocyanin-containing food colorants has led to the discovery that acylated anthocyanins exhibit remarkable stability, with this improved stabilization being attributed to intra and inter-molecular copigmentation.

This project intended to bring insights regarding the structural interaction between anthocyanins and carbohydrates (β-cyclodextrin and pectin) and the occurrence of intra and inter-molecular association in anthocyanins. This project also intended to study the formation and the structure of inclusion complexes between synthetic flavylium compounds and β-cyclodextrin.

The results obtained in this work was divided into three main chapters focusing the binding between flavyliums (anthocyanins and synthetic flavylium salts) and several cyclodextrins (α, β and γ) (Chapter III), anthocyanins and pectin from *citrus* fruit (Chapter IV) and anthocyanins association reactions (Chapter IV).

The interaction between α, β and γ-cyclodextrin and cyanidin-3-*O*-glucoside and the impact of this binding on anthocyanin's network of chemical reactions was investigated through ultraviolet-visible absorption techniques. It was shown that the addition of β-cyclodextrin resulted in the fading of anthocyanin solution and this fading effect was

greater at higher pH. This anti-copigmentation effect clearly indicated that the equilibrium and kinetic constants of the network of chemical reactions taking place in cyanidin-3-*O*-glucoside was affected by the presence of β-cyclodextrin. Molecular inclusion in the cyclodextrin cavity resulted in the increase of the isomerization observed rate constant (k_{obs}) at pH 5.3 and in the increase of the hydration equilibrium constant (K_h) which is in agreement with the fading of anthocyanin solution. Oppositely, for the other two macrocycles α- and γ-cyclodextrin, no significant changes were observed on the equilibrium and kinetic constants, which suggests that the inclusion of cyanidin-3-*O*-glucoside in these cyclodextrins was not favored.

Molecular inclusion of this anthocyanin into β-cyclodextrin cavity induced a thermal stabilization of the pigment with an increase of the half-time values in the presence of this cyclodextrin.

The formation and the structure of cyanidin-3-*O*-glucoside-β-cyclodextrin inclusion complexes were investigated using a combined approach of nuclear magnetic resonance spectroscopy and Molecular Dynamics simulation. Diffusion ordered spectroscopy (DOSY) and study of nuclear Overhauser effects (NOE) were used to determine the selective intermolecular interactions and structure of these complexes in aqueous solution. The observed chemical shift displacements of resonance signals of protons from the interior of β-cyclodextrin cavity and protons belonging to the hemiketal, together with the diffusion coeficients measurements and the NOE studies have anticipated the formation of an inclusion complex between this equilibrium form and β-cyclodextrin. The analysis of the spectral data have shown no evidence of internal interaction between this cyclodextrin and the flavylium cation or *trans*-chalcone forms of cyanidin-3-*O*-glucoside. The hemiketal formed a 1:1 inclusion complex with β-cyclodextrin in which the pyranic C ring is deeply included inside the cyclodextrin cavity while B ring lies on the plan of the wider rim. The structure of the complexes was also clarified through a theoretical approach by Molecular Dynamics simulation.

The interaction between the network of chemical reactions of three synthetic flavyliums (4',7-dihydroxyflavylium; 4'-(2-hydroxyethoxy)-7-hydroxyflavylium and 3',4',7-trihydroxyflavylium) and β-cyclodextrin and the structure of the molecular inclusion complexes was also studied by nuclear magnetic resonance spectroscopy (ROESY experiments). The *trans*-chalcone was the network specie exhibiting stronger interaction with the host. In contrast, the flavylium cation does not interact with β-cyclodextrin. ROESY experiments suggests a structure where the synthetic flavylium

salts are deeply included on β-cyclodextrin cavity with the hydrogens in positions H8, H6, H5 (ring A), H4 and H3 interacting with the internal surface of the cyclodextrin. The decrease polarity of 4'-(2-hydroxyethoxy)-7-hydroxyflavylium resulted on a deeper penetration of this synthetic flavylium into β-cyclodextrin cavity.

The binding between natural anthocyanins (delphinidin- and cyanidin-3-*O*-glucoside) and cell wall carbohydrates was characterized by saturation transfer difference (STD) nuclear magnetic resonance spectroscopy and the respective dissociation constant (K_d) was obtained. This interaction was also studied through computational calculations and ultraviolet-visible spectrophotometry. A pH 4.0, in the presence of the anthocyanin hemiketal form a weak interaction between anthocyanins and pectin seems to occur. A variation in the extent of this interaction was also noticed for the two anthocyanins with delphinidin-3-*O*-glucoside bearing three hydroxyl groups, revealing to be a stronger binder to pectin (K_d ≈ 180 μM for delphinidin-3-*O*-glucoside and K_d ≈ 250 μM for cyanidin-3-*O*-glucoside). Experiments performed at acidic pH (flavylium cation) revealed a stronger interaction (K_d ≈ 2 μM). These experimental results were also supported by theoretical studies which also revealed a stronger interaction in the presence of the anthocyanin flavylium cation and also a stronger interaction between pectin and delphinidin-3-*O*-glucoside than with cyanidin-3-*O*-glucoside (AH^+_{dp3glc}>B_{dp3glc}>B_{cy3glc}).

The association reactions (intra- and inter-molecular association) occurring in a mono-acylated (malvidin-3-*O*-(6-coumaroyl)glucoside) and non-acylated anthocyanin (malvidin-3-*O*-glucoside) in the flavylium form (pH 1.0) was studied using a synergistic combination of nuclear magnetic resonance spectroscopy and Molecular Dynamics simulation. NOESY experiments have showed the occurrence of two association mechanisms on the acylated anthocyanin namely intra-molecular and self-association. The spectral variations (chemical shifts, δ, and diffusion coefficients, *D*) resulting from the increasing of the anthocyanins concentration were analyzed using an isodesmic model. In the concentration range tested in this work malvidin-3-*O*-(6-coumaroyl)glucoside was found to self-associate with a higher affinity constant (1402 M^{-1} (δ) and 2203 M^{-1} (*D*)) compared to the malvidin-3-*O*-glucoside (819 M^{-1} (δ) and 1002 M^{-1}(*D*)) revealing that in acylated anthocyanins the combined aggregation phenomenon could be responsible for this higher affinity towards self-association. In this study the critical aggregation concentration (cac) value determined for both anthocyanins were very similar.

Overall, this work brings more insights on the carbohydrate-anthocyanin interaction, particularly from a structural point of view and represents valuable insights regarding the impact of cyclodextrins on the pH dependent equilibrium network of anthocyanins. The results achieved also offer a contribution to the elucidation of the binding between anthocyanins and carbohydrates from plants cell wall, important not only for the color and stabilization of these pigments but also a possible fundamental aspect in the extraction and bioavailability of anthocyanins. This study also provides information regarding anthocyanins stabilization mechanism, particularly intra and inter-molecular association.

From a technological perspective, the results presented on this thesis contribute to the increasing knowledge regarding the phenomena that drive the stabilization of flavylium compounds, a major issue for the putative application of these compounds in several industries.

KEYWORDS: Anthocyanins; carbohydrates; cyclodextrins; DOSY; flavyliums; intra-molecular copigmentation; Molecular Dynamics; molecular inclusion complexes; NMR; NOESY; pectin; ROESY; self-association; STD; UV-Vis.

TABLE OF CONTENTS

LIST OF FIGURES

LIST OF TABLES

ABBREVIATIONS / ACRONYMS

Abs	Absorbance
A	Anthocyanin quinoidal base
AH^+	Anthocyanin flavylium cation
B	Anthocyanin hemiketal
C	Anthocyanin content after a predetermined time
C_0	Initial anthocyanin content
cac	Critical aggregation concentration
CB	Conjugated base
C*c*	Anthocyanin *cis*-chalcone
C*t*	Anthocyanin *trans*-chalcone
CD	Cyclodextrins
COSY	Correlation Spectroscopy
Cy3glc	Cyanidin-3-*O*-glucoside
d	Duplet
D	Diffusion coeficient
D_2O	Deuterium oxide
DAD	Diode Array Detector
DCl	Deuterium chloride
dd	Doublet of duplet
DMSO-d_6	Dimethyl sulfoxide hexadeuterated
DOSY	Difusion Ordered spectroscopy
Dp3glc	Delphinidin-3-*O*-glucoside
DSC	Differencial scanning calorimetry
EU	European Union
FAO/WHO	Food and Agriculture Organization/ World Health Organization

Gal*p*A	Galacturonic Acid
Gal*p*	Galactose
Glc	Glucose
HMBC	Heteronuclear Multiple Bond Connectivity
HGs	Homogalacturonans
HPLC-DAD	High Performance Liquid Chromatography with Diode Array Detector
HSQC	Heteronuclear Singlet Quantum Connectivity
i.d.	Internal Diameter
J	Coupling constant
k	Degradation rate constant
k_{ass}	Association constant
K_a'	Apparent acidity equilibrium constant
K_a	Acidity equilibrium constant
$K^{\wedge}_a$	Acidity pseudo-equilibrium constant
K_d	Dissociation constant
K_h	Hydration equilibrium constant
k_{obs}	First observed rate constant
k_h	Rate constant of hydration reaction
k_{-h}	Rate constant of dehydration reaction
K_i	Isomerization equilibrium constant
K_t	Tautomerization equilibrium constant
m	Multiplet
MD	Molecular Dynamics
Mv3cumglc	Malvidin-3-(6-coumaroyl)-glucoside
Mv3glc	Malvidin-3-*O*-glucoside
n.a.	Non assigned
NaOD	Sodium deuteroxide
NMR	Nuclear Magnetic Resonance
NOE	Nuclear Overhauser Effect

NOESY	Nuclear Overhauser Effects spectroscopy
R^2	Correlation factor
RGs I or II	Rhamnogalacturonans type I or II
Rha*p*	Rhamnose
RMSD	Root-mean square deviation
RMSF	Root-mean square fluctuation
ROESY	Rotational Overhauser Effects spectroscopy
s	Singlet
SASA	Solvent accessible surface area
STD	Saturation Transfer Difference
t	Triplet
t	Time
$t_{1/2}$	Half-life value
UV	Ultraviolet
UV-Vis	Ultraviolet-Visible
α-CD	α-cyclodextrin
β-CD	β-cyclodextrin
γ-CD	γ-cyclodextrin
δ	Chemical shift
λ_{max}	Maximum wavelength
4',7-DHF	4',7-dihydroxyflavylium
4'-(2-hydroxyethoxy)-7-HF	4'-(2-hydroxyethoxy)-7-hydroxyflavylium
3',4',7-THF	3',4',7-trihydroxyflavylium

OUTLINE OF THIS THESIS

This thesis is organized in six chapters. This is a formal organization and does not necessarily reflect the order of the experimental work. This is an author´s option in order to present the results in a concise and clear way.

A general approach regarding the scope and the aims defined for this thesis are presented on Chapter **I**. Following this chapter:

Chapter **II** consists on a bibliographic review of the most relevant literature, which includes a general description of polyphenols, particularly some flavonoids and the main nutritional and health properties attributed to these compounds. A more detailed explanation regarding anthocyanins chemistry, occurrence in the human diet, toxicity, reactivity and technological application is also presented. Information regarding anthocyanin's stabilization mechanisms and anthocyanin-carbohydrate interaction is also described in this bibliographic review.

Chapters **III, IV** and **V** concerns the results obtained during the PhD work. Chapter **III** reports the interaction and the formation of inclusion complexes between flavylium derivatives (anthocyanins and synthetic flavyliums) and cyclodextrins (α, β and γ). This chapter is divided in three parts (**A**, **B** and **C**). In part **A** the impact of α, β and γ-cyclodextrins on the thermodynamic and kinetic constants occurring in cy3glc is presented. The assessment of these parameters was made through an UV-Vis approach. The evaluation of the thermal stability of cy3glc in the presence of β-CD was also evaluated.

In part **B** the formation of molecular inclusion complexes between cy3glc different equilibrium forms and β-CD was studied. This molecular inclusion was evaluated through several NMR experiments, including DOSY and ROESY and through Molecular Dynamics simulation.

The content of part **A** and **B** was adapted from two papers published in peer-reviewed journals.

Part **C** of this chapter reports the inclusion complex formation between three synthetic flavyliums (4',7-DHF, 4'-(2-hydroxyethoxy)-7-HF and 3',4',7-THF) and β-

cyclodextrin. This interaction was studied by NMR spectroscopy (ROESY experiments). The content of this part results from the adaptation of some data presented on three papers published in peer-reviewed journals.

Chapter **IV** reports the study of the interaction between anthocyanins and carbohydrates present in plant cell walls. More specifically, in this chapter the binding between cy3glc and dp3glc and low methoxylated pectin from *citrus* fruit is described. This binding was assessed using several experimental techniques including UV-Vis spectroscopy and NMR (STD experiments) and also through a theoretical approach (Molecular Dynamics simulation). The content of this chapter was adapted from a paper published in a peer-reviewed journal.

Chapter **V** describes the occurrence of copigmentation mechanisms (intra-copigmentation and auto-association) in mono-acylated and non-acylated anthocyanins. These anthocyanin's stabilization mechanisms were studied by the variation of several NMR parameters (δ and *D*) with anthocyanin concentration and by Molecular Dynamics simulation. The content of this chapter was adapted from a submitted manuscript in a peer-reviewed journal.

Chapter **VI** presents a general conclusion of the main results obtained, representing not only a summary of the main results obtained as also a global comparative analysis of different results. Final remarks and recommendations for future research activities are also presented in this chapter.

The adaptation of these chapters from published and submitted papers involved the standardization of the formatting and nomenclature. Some sentences and images were added, in order to clarify some aspects. Also, in **Part A** from chapter **III**, some unpublished results related to the impact of γ-CD on cy3glc's thermodynamic and kinetic constants and results related to cy3glc's thermal stability in the presence of β-CD (studied by DSC and thermal degradation) were added.

I. SCOPES AND AIMS

I.1. Scopes

Nowadays plant polyphenols enjoy an ever-increasing recognition not only by the scientific community but also, and most remarkably, by the general public because of their presence in fruits, seeds, vegetables and derived foodstuffs or beverages. The economic implications of polyphenolic compounds are thus substantial. They are used in numerous sectors of the food-industry as natural additives (natural coloring agents, conservative agents, natural antioxidants, nutritional additives, functional foods). However, it is probably in the field of human health that the economic implication of polyphenols is the most important. Actually, many plant extracts rich in phenolic molecules of interest are used as food complements or can be integrated into cosmetic or pharmaceutical formulations *(1)* (Figure I.1).

Figure I.1. Representation of some industrial and technological applications of polyphenols (pharmaceutical, cosmetic and food-industry).

In addition to aroma, taste and texture, color is the most important quality parameter of foods because it is one of the first characteristics perceived by the senses and is used by consumers for the rapid identification and ultimate acceptance of foods *(2)*. Consumers judge the quality of a food product principally by its color and for this reason the food-industry has commonly used synthetic colorants to enhance or to restore original appearance of foods due to processing and storage, to ensure

uniformity and raw material heterogeneity and as an indicator of food quality. Synthetic dyes have also been used because of their outstanding stability against light, oxygen and heat. However, the safety of these colorants commonly used in the food industry has been questioned in the past years and consumers had become increasingly concerned about the adverse health effect. For instance, azo dyes used in drinks, are associated with detrimental effects on children's health, particularly with attention deficit hyperactivity disorder (ADHD) *(3)*. As a consequence, besides the requirement for the labelling of food containing synthetic colorants, there is a worldwide trend in the search of nutritious, safe and environmentally friendly food colorants from natural sources *(4, 5)*.

Replacing artificial pigments by their natural counterparts is therefore a major challenge for the food-industry. In this context, anthocyanins are particularly promising candidates and in the last two decades an intense research activity on anthocyanins has been promoted *(6)* mainly related to their possible use as natural colorants and their potential health-promoting properties, which could allow their application in functional foods, in nutraceutical and in the pharmaceutical industries. These phenolic compounds are ubiquitous colorants of most flowers and fruits and are considered as suitable candidates for food pigments as they can contribute for the most spectacular red, blue and purple color. Anthocyanins provide high colorant power, they are hydrophilic colorants which facilitates their incorporation into many food systems *(7)* and they are specifically compatible with a water-based gel formulation. Furthermore they have been consumed for centuries without adverse effects and studies indicates that anthocyanins are non-toxic and non-mutagenic *(8)*. On the opposite, several positive therapeutic properties have been attributed to anthocyanins, like for instance antioxidant, anti-carcinogenic, anti-inflammatory, and anti-angiogenic properties *(9, 10)*. Anthocyanins can also improve the nutritional value of processed foods by preventing oxidation of lipids and proteins in the food products *(11)*.

In response to consumer demand for "greener" additives, combinations of various extracts of anthocyanins and also winery by-products, which are particularly rich in anthocyanins due to their poor extraction in the course of vinification, have been used. For instance, application of anthocyanins based colorants in pastry, fruit yogurt and many types of fruit-flavored dry mixes is becoming more popular. Indeed, synthetic dyes are not allowed in the rapidly growing natural food market, where anthocyanins are becoming increasingly important *(12)*.

Although the great potential of application that anthocyanins represents for food-industry, their applications as food colorants are seriously limited due to their stability problems. Their stability is affected by many factors and the limitation to the application of anthocyanins as pigments in food systems is related to the process conditions, formulation and storage. Anthocyanin's stability is affected by pH, storage temperature, presence of enzymes, light, oxygen, structure, concentration of the anthocyanins, and the presence of other compounds such as other flavonoids, proteins, and minerals *(13)*. Besides this they present low extraction percentages.

These drawbacks have stimulated a search for new methods to enhance the anthocyanin's stability and to increase the possibilities for the use of these compounds *(5)*. Scientific research on the chemistry of colors, in theoretical and applied level, is essential to the technology of foods, cosmetics and drugs, since with alternative anthocyanins stabilization mechanisms and with better understanding of their influence in the anthocyanins degradation may improve the application of natural compounds *(13)*. The need to avoid the use of synthetic colorants and move towards the use of natural food colors has also increased the research in this field during the past decades.

I.2. Aims

The detailed knowledge of the factors that governs anthocyanins color is a key step towards the implementation of strategies for the stabilization of these pigments which would allow a putative application in food matrices as natural colorants. On the other hand, the impact of polymeric compounds (*e.g.* pectins) on anthocyanins extractability from plant materials is also an important issue regarding several industries. Despite some information have already been reported, it has not been carried out a systematic and fundamental study concerning the mechanisms of anthocyanins color stabilization, particularly the interaction between these pigments and some carbohydrates.

Bearing this, the overall objective of this thesis was to gain knowledge of anthocyanins physical-chemical behavior in the presence of some carbohydrates and particularly to better understand the impact of these carbohydrates (cyclodextrins and pectin) on anthocyanin's color and on the physic-chemical equilibria of these pigments. The occurrence of self-association and intra-molecular co-pigmentation mechanisms on mono-acylated and non-acylated anthocyanins was also of interest for this thesis.

In this context several objectives were defined for this work:

- Understand the impact of cyclodextrins (α, β, and γ) on the color of an anthocyanin bearing a catechol moiety (cy3glc). Study the effect of these carbohydrates on the thermodynamic and kinetic constants of cy3glc's network of chemical reaction by UV-Vis spectroscopy. Evaluate β-cyclodextrin impact on cy3glc's thermal stability (**III**– Part A);

- Study the formation of molecular inclusion complexes between β-cyclodextrin and cy3glc equilibrium forms and structure establishment of the inclusion complex cy3glc-β-CD using NMR spectroscopy and a theoretical approach (**III** – Part B);

- Study the formation of molecular inclusion complexes between synthetic flavyliums (as anthocyanins model compounds) and β-cyclodextrin by NMR spectroscopy. Evaluate the affinity of different equilibrium forms towards molecular inclusion and the structure of these complexes (**III** – Part C);

- Study the mechanism governing the binding between anthocyanins bearing a catechol and a pyrogallol moiety (cy3glc and dp3glc, respectively) and polymeric carbohydrate (pectin from *citrus* fruit). Evaluate the extent of the binding between anthocyanins flavylium cation or hemiketal equilibrium form and pectin. To perform this study a combined approach of UV-Vis, NMR and MD simulation was used (**IV**);

- Understand the self-association and intra-molecular copigmentation mechanisms occurring in mono-acylated and non-acylated anthocyanins. This stabilization mechanisms were assessed by different NMR parameters and by a theoretical approach (**V**);

II. General Introduction

II.1. Polyphenols

Polyphenols are secondary metabolites widely distributed in the plant kingdom. These phytochemicals are distinguished for their roles in many biotic and abiotic interactions, including plant resistance against fungal or bacterial infections and also in the defense against insects and mammalian herbivorous. Polyphenols also play an important role in plant's color and maturation and in pollinator's attraction *(14)* and are also known for their general protective roles (*e.g.*, as antioxidant, free radical-scavenging, UV light-absorbing) *(15, 16)*. These compounds are commonly found in both higher and edible plants and consequently they are abundant in our diet particularly in plant-derived foods and beverages (*e.g.* wine, coffee, tea, fruit juices).

Dietary polyphenols are important for food nutritional properties *(17)* and also for major organoleptic characteristics, particularly color and flavor properties (astringency and bitterness) *(18)*. These compounds have also received attention after recognition of their potential health benefits. High intake of fruits, vegetables and whole grains, which are rich in polyphenols, has been linked to lowered risks of many chronic diseases, particularly cancer, cardiovascular diseases, chronic inflammation and many degenerative diseases *(19)*. For instance, drinking red wine has been correlated with the relatively low incidence of coronary heart disease in French population despite a high fat diet, well known as the French Paradox *(20)* (Table II.1). Polyphenols are also strong antioxidants, defending against oxidative stress caused by excess reactive oxygen species (ROS), chelating transition metal ions and inhibiting enzymes involved in oxidative stress *(19, 21-23)*.

Table II.1. The French Paradox *(20)*.

Region	Plasma cholesterol (mg/dl)	Mortality from coronary heart disease (per 10^4)
France	216	102
Toulouse	224	78
USA (Stanford)	209	182
UK	240	380

Plant polyphenols comprise a large diversity of structures and their composition is highly variable both qualitatively and quantitatively; some of the compounds are

ubiquitous whereas others are restricted to specific families or species *(24)*. For instance, quercetin can be found in all plant products (fruits, vegetables, cereals, leguminous plants, fruit juices, tea, wine, etc) while isoflavones can be found specially in soya *(16, 17)*.

Although the term polyphenol is often used as a synonym of phenolic compound, it should be restricted in a strict chemical sense to molecules bearing at least two phenolic rings regardless of the number of hydroxyl groups they each bear *(25)*. These compounds may be classified into different groups as a function of the number of phenol rings that they contain and the structural elements that bind these rings to one another *(16)*. Classes of non-flavonoids and flavonoids are usually distinguished with this latter group of polyphenols being the most abundant *(14)*. In fact, in the last years more than 8000 flavonoids have been reported in plants and the list is constantly growing *(26)*. In addition to this diversity, polyphenols may be associated with various carbohydrates and organic acids and with one another, occurring as oligomers and polymers (*i.e.* condensed and hydrolysable tannins) *(16)*.

II.2. Non-Flavonoids

The non-flavonoids are mostly rather simple molecules, such as phenolic acids (benzoic and hydroxycinamic acids, based on C_1-C_6 and C_3-C_6 skeletons, respectively) and stilbenes (C_6-C_2-C_6), although also include complex molecules derived from them (*eg*, stilbene oligomers, gallotannins, ellagitannins and lignins) *(16)* (Figure II.1).

Hydroxybenzoic acids	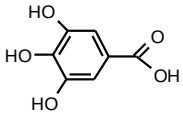 *Gallic acid*	
Hydroxycinnamic acids	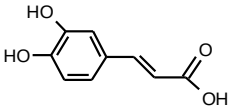 *Cafeic acid*	
Stilbenes	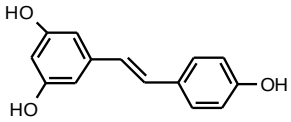 *Resveratrol*	
Ellagitannins	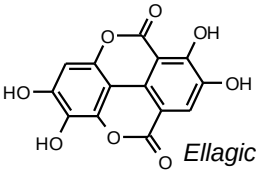 *Ellagic acid*	

Figure II.1. Chemical structures of some representative classes of non-flavonoids with some examples of plants where they can be found.

II.3. Flavonoids

The flavonoids are the most abundant polyphenols in our diet and they share a common nucleus containing a three-ring core, consisting on two phenolic rings (A and B) that are bound together by three carbon atoms that form an oxygenated heterocycle (C ring) (C_6-C_3-C_6 skeleton) *(16)* (Figure II.2).

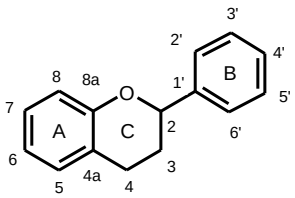

Figure II.2. Basic structure of flavonoids with rings denomination and numeration.

The flavonoids composition in plants is highly variable both qualitatively and quantitatively and they are present predominantly as glycosides *(27)*. This group of polyphenols can themselves be divided into several groups differing in the oxidation state (degree of unsaturation) of the heterocyclic pyran ring (flavanols, anthocyanidins, flavonols, flavones, isoflavones, flavanones). The shift of B-ring substitution from C_2 to C_3 position allows the separation of the isoflavones from others subclasses *(12)* (Figure II.3).

The structural diversity of dietary polyphenols is not limited to differences in the structure of the carbon skeleton and in the oxidation state of the heterocycle of flavonoids. It is further complicated by varying patterns of hydroxylation or methoxylation of the phenolic rings, by glycosylation of most flavonoids, by acylation with phenolic acids and by the existence of stereoisomers, among others *(28)*.

Among flavonoids, the flavanols and the anthocyanidins are abundant flavonoids in our diet. These two classes also play a detrimental role in the quality and in the sensorial properties of plant-derived foods and beverages, particularly in the taste properties (flavanols) and in the color definition (anthocyanindins). Due to these characteristics a brief description of the flavanols will be presented. A more detailed description of the anthocyanindins chemistry will be presented as the work present in this thesis is essentially focused in this sub-class.

Flavonols	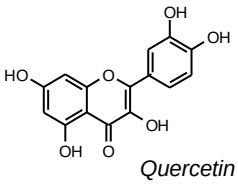 *Quercetin*	
Flavones	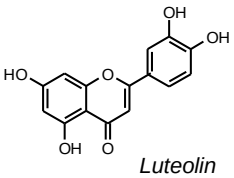 *Luteolin*	
Flavanols	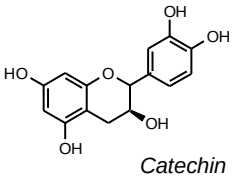 *Catechin*	
Flavanones	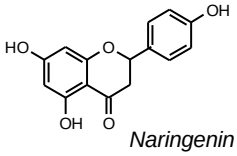 *Naringenin*	
Anthocyanidins	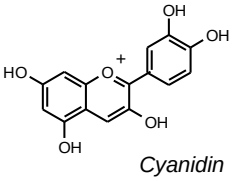 *Cyanidin*	
Isoflavones	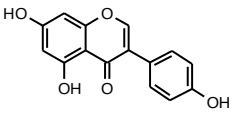 *Genestain*	

Figure II.3. Chemical structures of some representative classes of flavonoids with some examples of plants or plant derived beverages where they can be found.

II.3.1. Flavanols

The sub-class of flavanols exists in both form of monomers (flavanol), oligomers and polymers (proanthocyanins or condensed tannins) and in contrast to other class of flavonoids, in the flavanols there is no double bond between C_2 and C_3 and no C_4 carbonyl in the C-ring. This and the hydroxylation at C_3 allows flavan-3-ols to have two chiral centers on the molecule (on C_2 and C_3), thus four possible diastereoisomers *(22)*. In the plant kingdom flavan-3-ols are usually hydroxylated in positions C_5 and C_7 (ring A) and depending on the variation in the stereochemistry of the two asymmetric centers and on the differences in the pattern of hydroxylation of B ring, flavan-3-ols can be classified as afzlechin (or epiafzlechin), catechin (or epicatechin) and gallocatechin (or epigallocatechin) (Figure II.4). Moreover, the flavanols can be esterified in position C_3 with gallic acid *(29)*. Catechin and epicatechin are the main flavan-3-ols in fruits while gallocatechin, epigallocatechin and epigallocatechin gallate are found in certain seeds of leguminous plants and in tea *(30, 31)*.

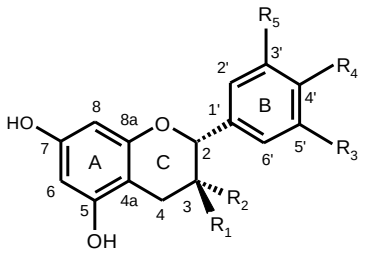

Flavan-3-ol	R_1	R_2	R_3	R_4	R_5
(+)-afzelechin	OH	H	H	OH	H
(-)-epiafzelechin	H	OH	H	OH	H
(+)-catechin	OH	H	H	OH	OH
(-)-epicatechin	H	OH	H	OH	OH
(+)-gallocatechin	OH	H	OH	OH	OH
(-)-epigallocatechin	H	OH	OH	OH	OH

Figure II.4. Chemical structure of the flavan-3-ols units in proanthocyanidins with characteristic numeration and rings denomination.

Condensed tannins are derived from the oligomerization of flavan-3-ol units that are bound together by interflavanic bonds (Figure II.5). The condensed tannins can also be referred to proanthocyanidins as an acid-catalyzed cleavage of the polymeric chains produces anthocyanidins *(22)*. Their structure is dependent on the kind of monomer, the nature of the interflavanic linkage between monomers, by their chain length and by

the degree of esterification with gallic acid *(29)*. Depending on the interflavanic linkages, oligomeric proanthocyanidins can be A-type structure in which the monomers are linked through C_2-*O*-C_7 or C_2-*O*-C_5 bonding or B-type in which C_4-C_8 or C_4-C_6 are common.

The reactivity of condensed tannins with molecules of biological significance has important nutritional and physiological consequences *(32)*. Their multiple phenolic hydroxyl groups lead to the formation of complexes with proteins *(33, 34)* with metal ions *(35)* and with other macromolecules like polysaccharides *(36)*.

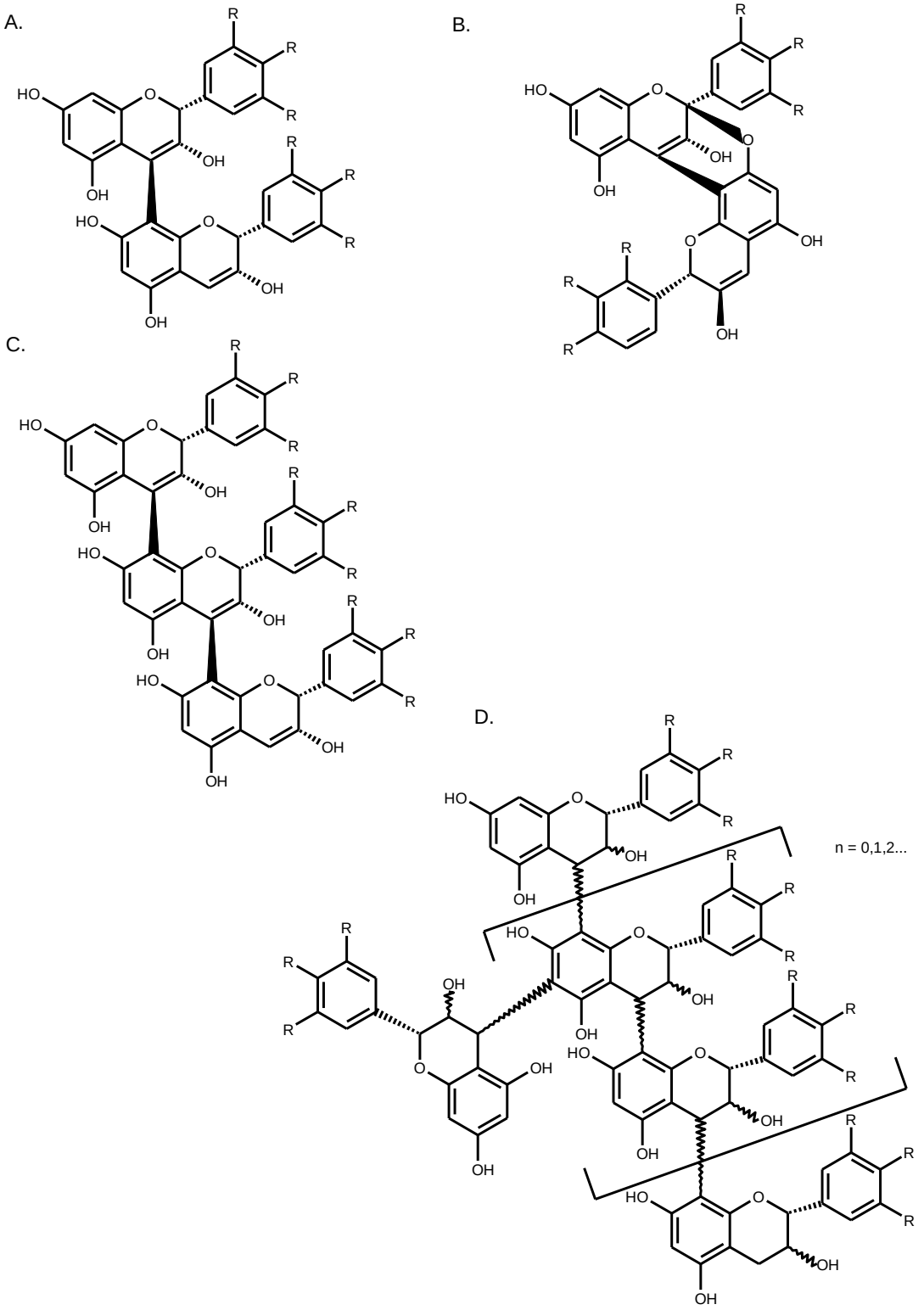

Figure II.5. Chemical structure of some condensed tannins: type B dimeric procyanidin (**A**); type A dimeric procyanidin (**B**); trimeric procyanidin (**C**); polymerized procyanidins (**D**). R is aH or OH.

II.3.2. Anthocyanins

Anthocyanins (in Greek *anthos* means flower and *kyanos* means blue) constitute the largest and the most important group of water soluble and vacuolar pigments with appealing colors ranging from pink through scarlet, magenta and violet to purple and blue *(37-39)*. The total number of anthocyanins structures identified after isolation from plant extracts is about 700. However, nearly 200 different anthocyanins have also been presented with tentative structures *(40)*.

Anthocyanins occur in all tissues of higher plants, including flowers and fruits where they play a definite role in the attraction processes involved in pollination and in seed dispersal. For this reason, anthocyanins are of considerable value in the co-evolution of these plant-animal interactions *(10)*. These flavonoids are also quite common in young leaves and together with other flavonoids they might exert a deterring effect against herbivores *(41)*. Anthocyanins can act as antioxidants, phytoalexins or as antibacterial agents *(42)* and owing to strong absorption of light they may also be important in protecting plants from UV-induced damage, thereby protecting the tissues from photoinhibition or high-light stress *(14, 43)*.

In addition to the physiological functions in plants and the color attributes particularly relevant for the food industry, interest in anthocyanins has increased due to their possible health benefits *(5)*. An important function of anthocyanins extracts is their antioxidant activity *(44-49)*, although health benefits also include enhancement of sight acuteness *(50)*, treatment of various blood circulation disorders resulting from capillary fragility , inhibition of platelet aggregation, maintenance of normal vascular permeability *(44)*, vaso-protective and anti-inflammatory properties *(51, 52)*, controlling diabetes, anti-neoplastic and chemoprotective agents *(53, 54)*, radiation-protective agents *(55)* and possibly others due to their diverse action on various enzymes and metabolic processes *(56)*.

II.3.2.1. Anthocyanins chemistry

Anthocyanins belong to a large group of flavonoids. Chemically, they are glycosides of polyhydroxy and polymethoxy derivatives of 2-phenyl-benzopyrylium salts. Anthocyanidins share a C_6-C_3-C_6 carbon skeleton *(41)* and are usually penta- (C_3, C_5, C_7, $C_{3'}$, $C_{4'}$) or hexa-substituted (C_3, C_5, C_7, $C_{3'}$, $C_{4'}$, $C_{5'}$) (Figure II.6). Owing to the long chromophore with eight conjugated double bonds carrying a positive charge,

anthocyanins are intensely colored under acidic conditions and the maximum absorption in the visible range is usually between 465 and 550 nm while the other maximum absorption band falls in the UV range between 270 and 280 nm *(57)*.

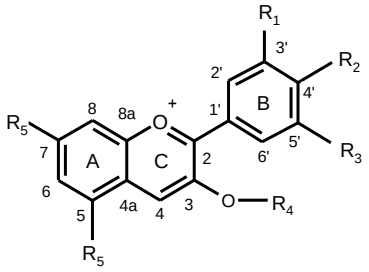

Figure II.6. General structure of anthocyanins. R_1 and R_3 are H, OH or OCH_3; R_2 is OH; R_4 is a glycosyl or H; R_5 is a OH or a *O*-glycosyl.

Depending on the pattern of hydroxylation and methylation on A and B rings, there are close to 31 different anthocyanidins (aglicone) that have been properly identified in nature *(13)* of which only six are the most common in vascular plants. In fact, approximately 90% of all anthocyanins isolated in the plant kingdom are derived from these six anthocyanidins: pelargonidin (Pg), cyanidin (Cy), peonidin (Pn), delphinidin (Dp), petunidin (Pt) and malvidin (Mv) *(9, 10)*. The distribution of the six most common anthocyanidins in the edible parts of plants is cyanidin (50%), pelargonidin (12%), peonidin (12%), delphinidin (12%), petunidin (7%) and malvidin (7%) *(10)*.

Under acidic conditions, the color of anthocyanidins is determined largely by the pattern of hydroxylation and methoxylation of the ring B. In general, B ring possessing more hydroxyl groups falls on the blue end of the spectrum (bathochromic shift) while those possessing more methoxyl groups fall on the red end of the spectrum *(39, 58)*. Other factors such as glycosylation pattern, *i.e.*, sugar *vs.* acylated sugar can also affect the color of anthocyanin compounds (Table II.2).

Table II.2. Differences on chemical structure, color and λ_{max} of anthocyanidins most commonly found in nature *(12)*. *In HCl acidified MeOH

	R_1	**R_3**	**R_4**	**R_5**	**Color**	**λ_{max} (nm)**
Cianidin (**Cy**)	OH	H	H	OH	Magenta	535
Peonidin (**Pn**)	OCH_3	H	H	OH	Magenta	532
Pelargonidin (**Pg**)	H	H	H	OH	Red	520
Malvidin (**Mv**)	OCH_3	OCH_3	H	OH	Purple	542
Delphinidin (**Dp**)	OH	OH	H	OH	Purple	546
Petunidin (**Pt**)	OCH_3	OH	H	OH	Purple	543

Additionally, the sugar moieties of anthocyanins (Figure II.6) may in turn be further linked to other sugars through glycosidic bonds (at C_1) or acylated with organic aromatic or aliphatic acids through ester bonds (at C_6). The nature, the number and the position of the sugar moiety attached to the aglycone as well as the nature and number of organic acids attached to the sugars result on a wide variety of anthocyanins *(43)*. Anthocyanins most frequently occur as 3-monosides, 3-biosides and 3-triosides as well as 3,5-diglycosides and more rarely 3,7- diglycosides *(10)*.

Glucose (glu) is the most common monosaccharide attached to the aglycone, but rhamnose (rha), galactose (gal), arabinose (ara) and xylose (xyl) are also commonly attached to the aglycone. The di- and trisaccharides most often found in anthocyanins are rutinose (rut), sophorose (sop) and sambubiose (sam) *(9, 24, 37)* (Figure II.7).

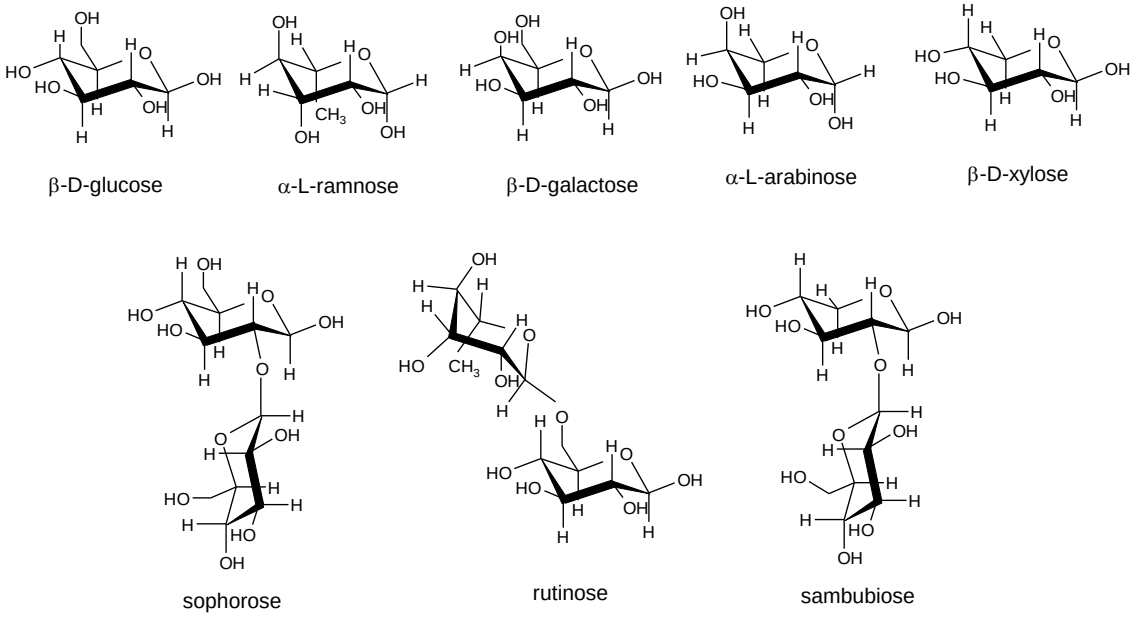

Figure II.7. Chemical structure of the most common saccharides present in anthocyanins.

The sugar residues may occur acylated with aromatic acids including cinnamic (*e.g. p*-coumaric, caffeic, ferulic, or sinapic acid) as well as aliphatic acids (*e.g.* malonic, acetic, malic, succinic or oxalic acid) *(5)* (Figure II.8) and more than 69% of the reported anthocyanins contain one or more acyl group *(40)*. Cinnamic acids may themselves bear glycosidic sugar and aromatic and aliphatic acylation may occur in the same molecule, forming the polyacylated structure. These acyl substituents are commonly bound to the C_3 sugar, esterified to the OH groups of the sugars at position 6 or less frequently at position 4 *(59, 60)*. Nevertheless, anthocyanins containing rather

complicated acylation patterns attached on different sugar moieties have also been reported *(61, 62)*.

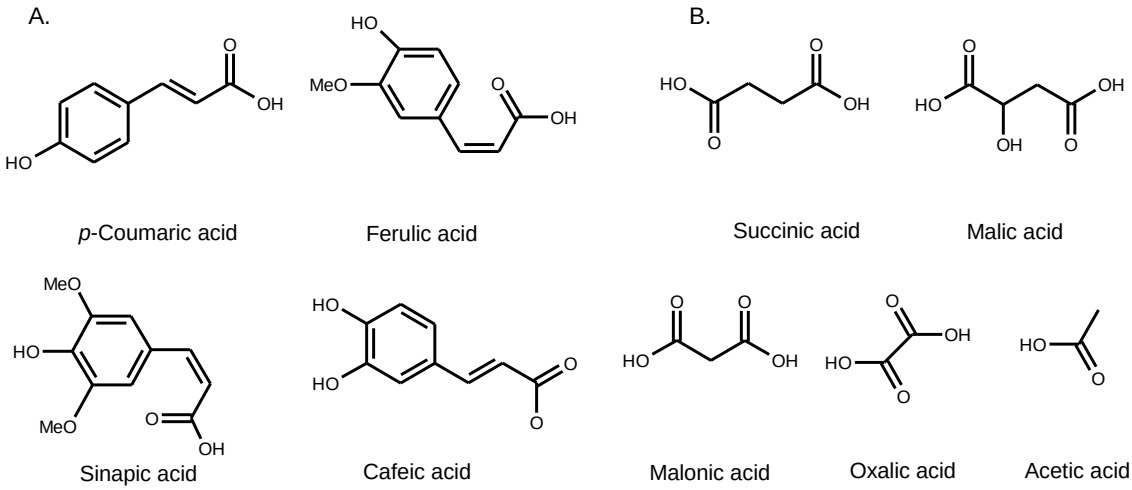

Figure II.8. Chemical structure of common cinnamic acids (**A**) and aliphatic acids (**B**) acylated with sugar moieties of anthocyanins.

Both glycosylation and acylation affect the physical and chemical properties of anthocyanins in that they modify the molecular size and polarity of the molecule, affecting also the stability and reactivity of the anthocyanin molecule.

In general, acylation of the sugar moieties of the anthocyanins involves a loss of polarity causing a decrease in water solubility whereas glycosylation increases water solubility. On the opposite, the aglycone form of anthocyanins is rarely found in nature due to the poor solubility. Besides this, anthocyanin molecules with complex patterns of glycosylation and acylation exhibit remarkable stability to pH changes, heat treatment and light exposure, which could be explained through the formation of intramolecular H-bonding network within the anthocyanin molecule *(63-65)*. Hydroxylation degree has also an important effect on the anthocyanins stability. Increasing the number of hydroxyl groups in the structure of anthocyanins cause a decrease in their stability. Further, high methoxylation increases the stability of anthocyanins *(66)*.

The various types of glycosidic and acyl substituents that can be found attached to the anthocyanidins molecule, as well as the different numbers of substitutions that can be attached to the molecule, are responsible for the wide variability of anthocyanin chemical structures reported in plant kingdom *(12)*.

II.3.2.2. Anthocyanins in the human diet

In the human diet anthocyanins can be found in many sources including certain varieties of cereals, colored fruits such as berries, cherries, peaches, grapes, pomegranates and plums as well as many dark-colored vegetables (*e.g.* red cabbage, beans, onions, red raddish) *(57, 67)*. Dietary anthocyanins sources also include fruit-based processed foods and beverages such as juices and red wine (

Table II.3). Abundance of the more common anthocyanins in the edible parts of plants varies substantially across plant species and even cultivars with environmental factors such as light, temperature and altitude affecting anthocyanins concentration *(67, 68)*. Food contents are generally proportional to color intensity and reach values up to 1000-4000 mg/kg in blackcurrants or blackberries and 200-350 mg/kg in red wine *(16)*. With regard to mass consumed, anthocyanins constitute the most important subclass of flavonoids with an estimated consumption of anthocyanin of 10,000 tons annually *(9)* with cyanidin being the most common anthocyanidin in foods. The daily intake of anthocyanins had been estimated in a wide range (3–215 mg *per* day) *(69)*, but the more recent estimates indicates that the average adult intake of anthocyanins in Europe and the United States is in the scale of 10 mg per day *(40)*. However the dietary habits and choices have also a large influence on anthocyanin consumption. For example, regular red wine or fruit juices drinkers can also benefit higher anthocyanins intake *(9)*.

Animals and humans have consumed anthocyanins since ancient times and no adverse impact on health has been reported with oral consumption of anthocyanins in foods *(70)*. Based on toxicological studies including mutagenicity, reproductive toxicity, teratogenicity as well as acute and short-term toxicity evolutions, the Joint FAO/WHO Expert Committee on Food Additives (JECFA) concluded that anthocyanin-containing extracts are harmless compounds with a very low order toxicity *(71)*. Bearing this, the use of anthocyanins from natural sources is widely permitted as food colorants in many countries. In the United States anthocyanins are approved as food colorants under the category of fruit (21CFR73.250) or vegetable (21CFR73.260) juice color. Under these categories only the edible portion of plants are to be used. Extracts from dried materials are permitted under this classification but the extracting solvent is restricted to water *(5)*. The EU classifies anthocyanins (as grape color extract, grape skin extract, concentrated juice of black currant, cherry, red cabbage, etc) as food additives under classification number E163 *(57, 72)*.

Table II.3. Selected data for the content of anthocyanins in foods and beverages *(9)*.

Commodity	Content ($mg.L^{-1}$ or $mg.kg^{-1}$)
Blackberry	1150
Blueberry	825 – 4200
Boysenberry	1609
Cherry	20 – 4500
Chokeberry	5060 – 10000
Cranberry	600 – 2000
Cowberry	1000
Currant (black)	1300 – 4000
Elderberry	2000 – 10000
Grape (red)	300 – 7500
Loganberry	774
Blood orange (juice)	2000
Plum	20 – 250
Raspberry (black)	1700 – 4277
Raspberry (red)	100 – 600
Raspberry (red - juice)	4 – 1101
Sloe	1600
Strawberry	150 – 350
Red cabbage	250
Eggplant	7500
Onion	up to 250
Rhubard	up to 2000
Red Wine	240-350
Port Wine	140-1100

II.3.2.3. Anthocyanins reactivity

As already described, the flavonoids are built on a three-ring core consisting of two aromatic systems and a pyran ring. Except for flavanols that have a fully saturated central ring, all major flavonoids molecules are pigments absorbing in higher wavelengths as the unsaturation increases (resulting in an extent of electron delocalization): from yellow for flavones and flavonols to red and blue for anthocyanins. A specific type of reactivity can characterize each ring (Figure II.9) *(73)*.

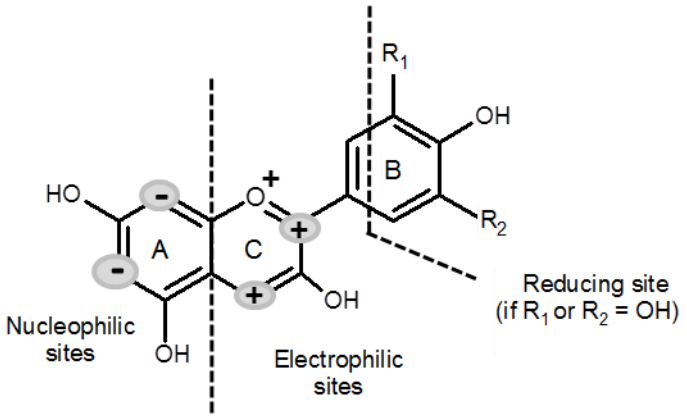

Figure II.9. Flavonoids general reactivity.

For anthocyanins, the central pyranic C-ring tends to have a positive charge delocalized especially on positions C_2 and C_4. Therefore, the reactions of this ring are dominated by nucleophilic attack on the electrophilic carbons C_2 and C_4. In fact, the most important reaction of the anthocyanins is the water attack on C_2 of the flavylium cation forming the hemiketal *(40)*. The electrophilic character of C_4 is mostly reported in connection with the use of SO_2 as preservative in the food industry. SO_2 will attack C_4 and form colorless adducts in a reversible reaction *(74)* (Figure II.10).

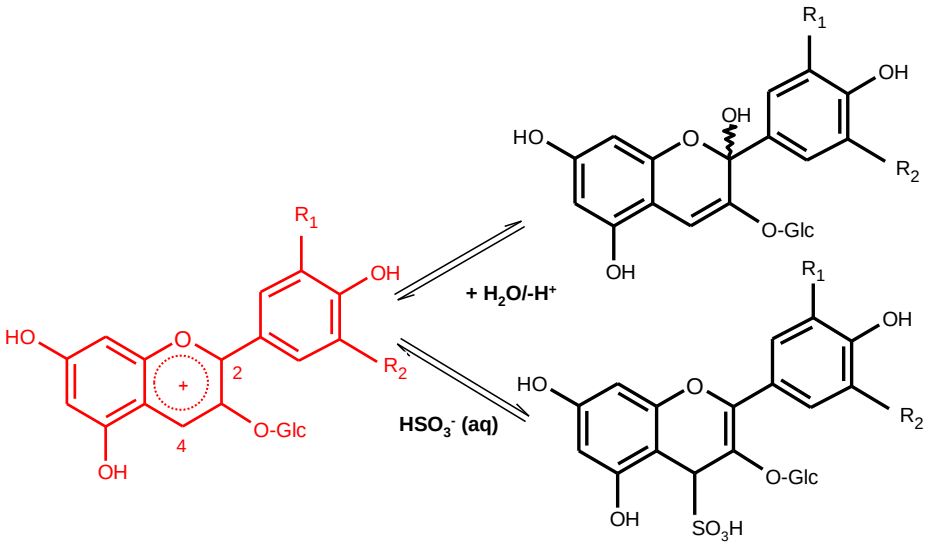

Figure II.10. Anthocyanins C-ring reactivity exemplified by the nucleophilic attack of water and bisulfite.

On the other hand, and although its positive charge, anthocyanins can react with electrophilic compounds through hydroxyl groups and positions C_6 and C_8. The A-ring is a phloroglucinol type structure possessing two nucleophilic sites activated by three hydroxyl groups, two located on *ortho* position and one in *para* position and the chemistry of this ring is dominated by the nucleophilic nature of the carbon atoms in position C_6 and C_8 *(73)*. This ring facilitates electrophilic aromatic substitution in these

positions. As a consequence, the hydrogens at the C_6 and C_8 positions are relatively acidic and involved, for instance, in exchange with deuterium in deuterated solvents in contrast to the hydrogens of the B- and C-rings, which are directly linked to the carbon skeleton *(75)*.

The increased nucleophilic reactivity of these positions can be detected in aqueous media (juices, wines, etc.), where anthocyanins readily react with other phenolic compounds such as flavanols, giving rise to flavanol (4→8) anthocyanins *(76)* (Figure II.11). For anthocyanins, the nucleophilic character of A-ring is provided by their hydrated forms.

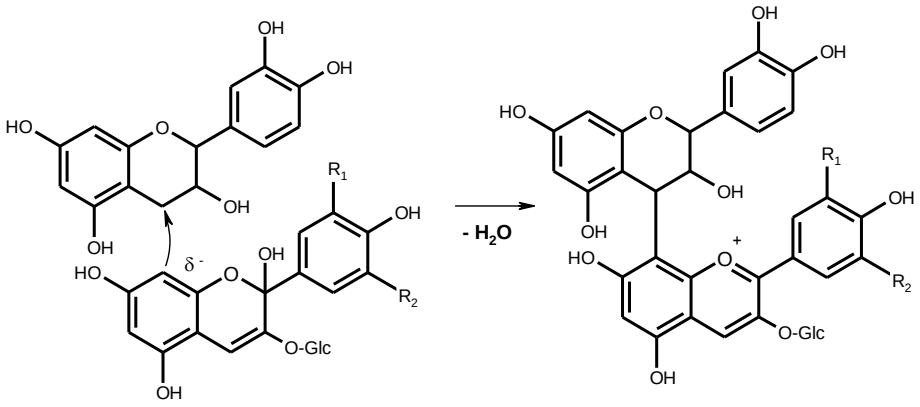

Figure II.11. Flavanol–anthocyanin type pigments.

The presence of at least two adjacent hydroxyl groups on the B-ring (like in Cy, Dp, or Pt) allows the occurrence of metal chelation (Figure II.12). A more discussed function of the *ortho*-positioned hydroxyl groups found in the B-ring of delphinidin (pyrogallol) and in cyanidin and petunidin (catechol) is their ability to act as antioxidants *(77)*.

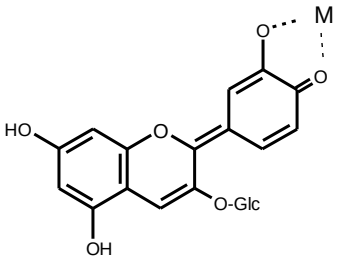

Figure II.12. Anthocyanins B-ring metallic complexation.

Another kind of reaction has been demonstrated for anthocyanin's cationic form, and results in the formation of a second pyran ring. This happens in cycloaddition reactions in the presence of pyruvic acid to form pyranoanthocyanins and the mechanism involves both the electron deficient C_4 and the 5-hydroxyl group on the A-ring of the anthocyanin *(78)* (Figure II.13).

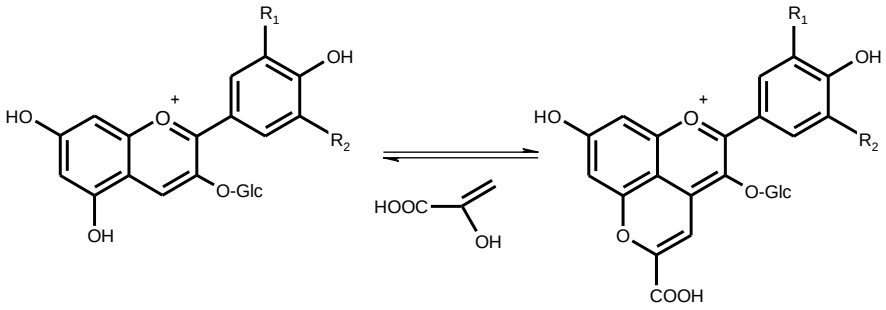

Figure II.13. Pigment issued from cycloadditions.

II.3.2.4. Anthocyanins stability

Anthocyanins are highly reactive species and they are structurally depending on the conditions and composition of the media where they are dissolved and suffer interactions among them and with other compounds that influence their structural equilibria and modify their color *(79)*. These changes are well known to food chemistry and technology specialist and have large effects on food quality, affecting the performance and biological activity of anthocyanin-containing food.

The common simple anthocyanins show instability toward a variety of chemical and physical parameters, including structure and concentration, oxygen, high temperatures, light intensity and specially the pH value *(70, 80)*. In fact, the stability of the anthocyanin molecules is mostly linked to the distribution of the anthocyanins on their various equilibrium forms, with the formation of hemiketal forms being the most critical component for anthocyanin instability *(81-83)*. The opening of the C-ring of the flavylium cation by hydration and subsequent formation of the chalcones is postulated as the first degradation step of anthocyanins *(40)*.

Anthocyanins also react with sulfur dioxide, with some cations, ascorbid acid, proteins and other phenolic compounds and will undergo transformations under storage. These pigments are also highly influenced by enzymatic activity of glycosidases and polyphenoloxidases which break the covalent bond between the glycosyl residue and the aglycone of an anthocyanin pigment, resulting in the degradation of the highly unstable anthocyanidin *(40)*.

Finally, anthocyanin color properties can be strongly modified by interaction mechanisms, including metal complexation, copigmentation and self-association

processes. For this reason anthocyanins chemical stabilization is a subject of major interest and many studies have been conducted with the aim to increase the stability of these substances *(13)*.

II.3.2.4.1. Structure

With respect to molecular structure, some anthocyanidins are more stable than others and the stability of these compounds is influenced by the B-ring substituents. Generally, increased hydroxylation decreases stability, whereas increased methylation increases it *(70)*. In contrast with aglycons, monoglycosides and mostly diglycosides derivatives are most stable in neutral pH conditions. This behavior can be explained because the sugar molecules avoid the degradation of instable intermediaries into phenolic acid and aldehyde compounds *(84)*. Moreover, anthocyanins containing galactose are more stable than those containing arabinose *(85)*.

Recent researches have also shown that anthocyanins with aromatic acyl substituents (especially polyacylated anthocyanins) are more resistant to color fading with increased pH than their unacylated analogs. These anthocyanins are also more stable during processing and storage. The improved stabilization has been attributed to the stacking of the acyl groups with the pyrylium ring of the flavylium cation, thereby reducing the susceptibility of nucleophilic attack of water and subsequent formation of colorless equilibrium forms (intra-molecular copigmentation) *(5)*.

Anthocyanin derivatives with substituents connected to the C-ring, for instance pyranoanthocyanins, have different reactivity than the original anthocyanins and are more stable in a wider pH range, exhibit higher resistance to bleaching by sulfur dioxide and higher color intensities as compared to analogous anthocyanidin 3-glucosides *(86, 87)*. This is because the substitution at C_4 of the flavylium cation affects the distribution of the charge throughout the C-ring. As a result, the C_2 and C_4 positions at the flavylium cation become less reactive toward nucleophilic attack (hydration).

II.3.2.4.2. Concentration effects

Increased anthocyanin concentration promotes higher color stability *(5)* and higher color intensity. Change of cyanin concentrations from 10^{-4} to 10^{-2} (100 fold increase) produced a 300-fold increment of the color intensity *(88)*. Increasing the content of anthocyanins improves their stability through self-association processes between anthocyanins which protects against water attack and consequently the formation of hemiketal forms *(70)*.

II.3.2.4.3. Temperature, oxygen and light

The stability of anthocyanins was found to decrease during processing and storage as temperature rises. The increase on anthocyanins degradation occurs since the equilibriums are displaced toward the *trans*-chalcone form *(89)*. This effect is observed as paler anthocyanin solution after heating. At pH 2–4, higher temperatures will also imply higher hydrolysis rates of the *O*-glycosyl moieties forming unstable anthocyanidins which leads to further loss of anthocyanins color. Thermal degradation of anthocyanins follows first order kinetics *(90)*.

Oxygen amplifies the impact of other anthocyanin degradation processes and the presence of oxygen, together with elevated temperature was the most detrimental combinations of many factors tested against color deterioration of isolated anthocyanins *(7)*. The combined degradation action between oxygen and ascorbic acid, pH or light caused an growth on anthocyanins degradation *(91)*. The deleterious effect of oxygen on anthocyanins can take place through direct oxidative mechanism and/or through indirect oxidation, where the oxidized components of the media further react with anthocyanins giving rise to colorless or brown products *(92)*.

Light also accelerates anthocyanin degradation *(7)*. It has been shown that anthocyanins photochemical degradation products are the same as the ones obtained in thermal reaction, although a different kinetic pathway involving the excitation of the flavylium cation *(93)*.

II.3.2.4.4. pH

Evaluation of the factors that affect the stability of anthocyanins indicates pH as a marked effect on anthocyanins stability, being the most important extrinsic factor of anthocyanins degradation. Anthocyanins are unique among flavonoids as their aglycone part undergoes pH-dependent transformation in aqueous solutions. These dynamic equilibriums have a profound impact on anthocyanins color and stability and even on their nutraceutical properties.

The structures and interconversions between the different molecular structures of anthocyanins are well established and are summarized in Figure II.14 *(89, 94-100)*. The red flavylium cation (**AH^+**) is the predominant species in the equilibrium under sufficiently acidic conditions (pH<2). When the pH is raised up to pH values of 3-4 the flavylium cation is involved in two parallel reactions: (i) deprotonation to form the quinoidal base (**A**); (ii) hydration in position C_2 or C_4 followed by proton loss to give the non-colored hemiketal (**B**). The hemiketal form has lost its conjugated double bond between the A- and B-ring and therefore does not absorb visible light. The *cis*-chalcone (**C*c***) is formed from **B** by a tautomeric process and the *trans*-chalcone (**C*t***) by the isomerization of the former. These two equilibrium forms present a yellowish color. The proton transfer is much faster than the hydration but in the case of the anthocyanins the other forms (**B**, **C*c***, **C*t***) at the equilibrium are more stable than **A**. This means that **A** can be formed as a kinetic product and later totally or partially disappears to yield the thermodynamic equilibrium. As pH increases above 8, the quinoidal base can be ionized to carry one or two negative charges *(100)*. The tautomeric reaction is favoured by increased temperature. However, at any pH condition, the chalcone form exists in a much smaller proportion as compared with the hemiketal form. The colored species are the flavylium cation (**AH^+**) and the quinoidal base (**A**) that may appear as red and purple/blue in common anthocyanins, respectively *(97)*. The relative composition of the different molecular structures of anthocyanins coexisting in aqueous solution at any given time will be dependent on pH, structure of a certain anthocyanin, temperature, time and even concentration (Figure II.15).

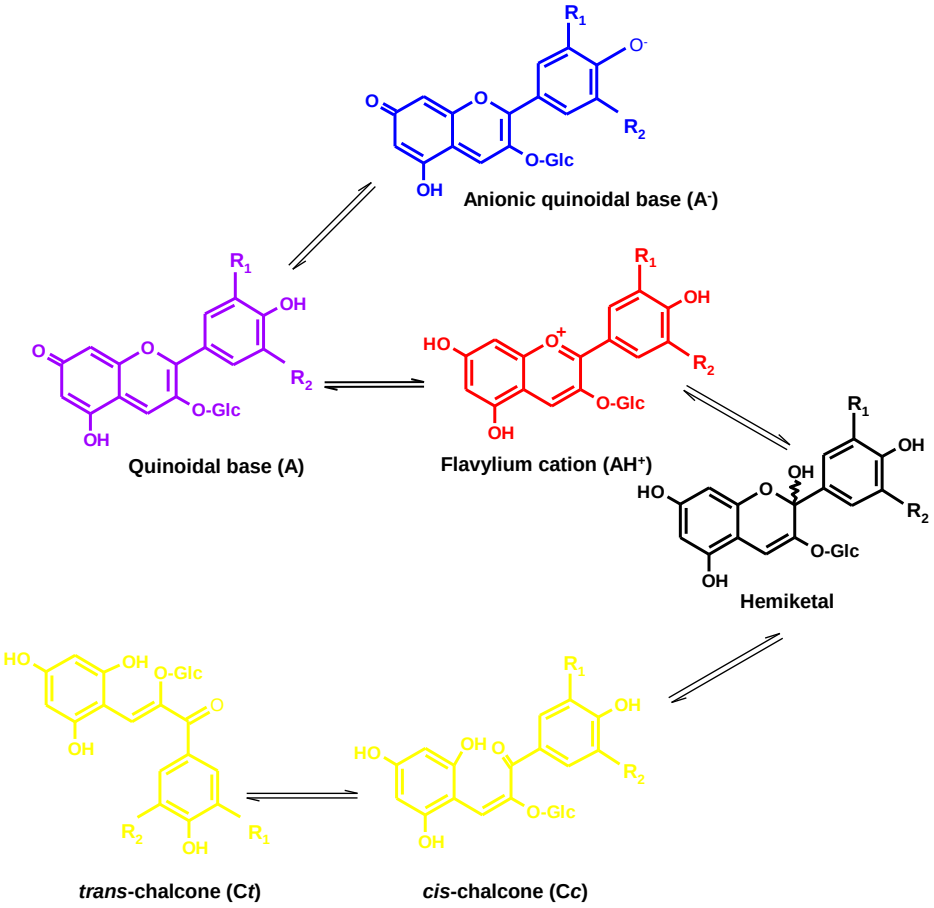

Figure II.14. General scheme for anthocyanins equilibrium forms. R_1 and R_2 can be OH and/or OCH_3 groups depending on the type of aglycone.

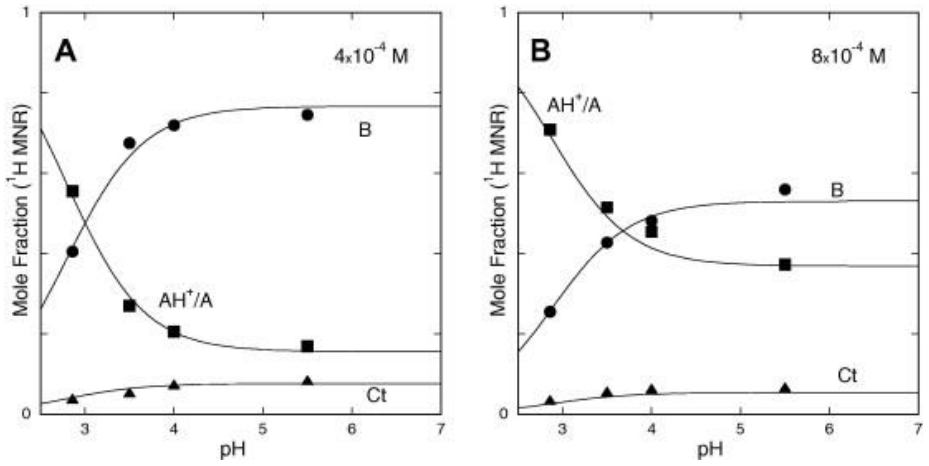

Figure II.15. Mole fraction distribution of **AH**$^+$(■), **B** (●) and **Ct** (▲) as a function of pH for delphinidin-3-*O*-glucoside at 0.4 mM (**A**) and 0.8 mM (**B**) *(6)*.

II.3.2.4.5. Anthocyanins thermal degradation affected by pH

Among the already reported factors that affect anthocyanins stability, the effects of pH and temperature have been studied thoroughly. According to various proposals for the thermal degradation pathways, it was clear that pH has a strong influence in the conditions for shaping the different pathways of anthocyanins degradation. At pH 3.5, the first step in anthocyanins thermal degradation was the hydrolytic opening of the pyrylium ring giving the chalcone-glycosides (Figure II.16). The chalcone-glycosides would then be cleaved to yield the corresponding chalcones, which degraded to the hydroxybenzaldehyde derivatives originated from A-ring and the 4-hydroxybenzoic acid derivatives originated from B-ring (*e.g.*, 3,4-dihydroxybenzoic acid for Cy and 4-hydroxy-3,5-dimethoxybenzoic acid for Mv) *(101)*. At pH 1, the degradation pathway seemed to be slightly different (Figure II.16). When acylated and non-acylated anthocyanins were heated at 95ºC they were cleaved by successive loss of the sugar moieties. The anthocyanidins were further degraded by scission into the same final products as observed in the experiments performed at pH 3.5. It was also reported the existence of intermediate degradation products such as chalcones *(102)*.

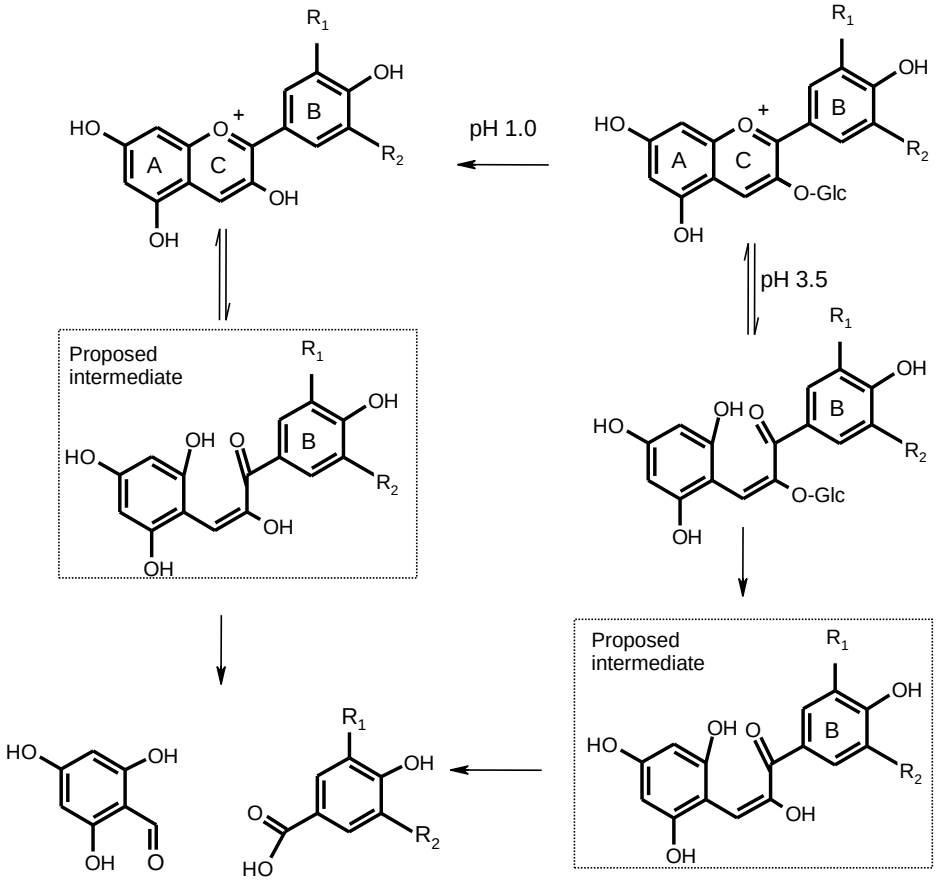

Figure II.16. Thermal degradation pathways of anthocyanins influenced by pH. Adapted from Andersen & Jordhein, 2013 *(40)*.

II.3.2.5. Anthocyanins stabilization mechanisms

Although the already mentioned instability of anthocyanins, nature has found many mechanisms to stabilize the colored forms of these pigments. Several factors that enhance the stability of anthocyanins have been reported including: acylation *(103-105)*, glucuronidation with enzymes and several types of association like auto-association (self-assembling), intra and inter-molecular copigmentation, metal complexation *(8, 80, 88, 106, 107)* and reaction with other molecules leading to the formation of more stable anthocyanin-derived compounds *(108, 109)*. The association of anthocyanins with other compounds affects not only its color but also its stability and in general, independently of the type of association of anthocyanins involved, an increase in their stability is observed. Factors such as solvent, light, pH, temperature, structure and concentration of copigments and anthocyanins, among others, significantly influence the association reactions *(13, 110)*.

II.3.2.5.1. Metallic ions interaction

One of the main characteristics of anthocyanins and anthocyanidins with vicinal hydroxyl groups in the B-ring (cyanidin, delphinidin and petunidin), is their ability to form metal-anthocyanin complexes (supermolecules) *(111)* and this reaction influences anthocyanins color. Some studies regarding the color variety and stability in flowers, suggest that the variety of blue and purple colors can be due to the formation of chelates between some bi- and trivalent metals ions (Al, Fe, Cu, Sn, Mg, Mo) and anthocyanins *(9)*. The metal selectively links with anthocyanin quinoidal forms, modifying anthocyanin equilibria towards these structures and provoking a change of the color to more violet hues *(112)*. In the metal-anthocyanin interaction, the complexation was found to stabilize the blue ionised quinoidal base by avoiding its degradation by oxidation *(113)*. More recent studies have shown that the complexation between *o*-di-hydroxyl anthocyanins and Fe (III) or Mg (II) ions at pH 5 are essential for the formation of blue color in plants *(114)*. Anthocyanins – metal complexation have also been shown to stabilize the color of different berry products *(13)*. Schreiber *et al*., 2010 analysed the chemical mechanism for Al^{3+} complexing with delphinidin and divided it in two steps: first, production of the blue quinoidal base anion of delphinidin that complexes with the Al^{3+}, second, this complex is stabilized by the π-π stacking of a second delphinidin as a flavylium cation on the top of the blue complex, creating a

bathochromic shift of the cation spectral signature and accentuating the blue color *(115)*.

Despite the low interest in the food industry about the anthocyanin-metal complexation, this interaction constitutes a viable alternative for color stabilization, particularly if the metals involved do not imply a risk for health or even they are part of the essential minerals diet *(116)*.

II.3.2.5.2. Copigmentation

The color of anthocyanins can be stabilized and enhanced by copigmentation mechanisms which consist of hydrogen-bind interaction and hydrophobic interactions (π-π stacking) between the planar polarizable nuclei of the colored forms of the anthocyanins (*i.e.*, flavylium cation ion and quinoidal forms) with other colorless organic molecules (*i.e.*, copigments) or other anthocyanins. Copigmentation complexes adopt a sandwich configuration (vertically stacked) that protects the flavylium chromophore from the nucleophilic attack of water, thus preventing at least in part the formation of colorless hemiketal and chalcone forms *(79)*. The final result is that the anthocyanin solutions show a more intense color (hiperchromism) due to the formation of the π-π complexes *(111)*. Occasionally a bathochromic effect (the shift of the maximum absorption wavelength towards higher wavelength), which is also called the bluing effect, can also be produced due to the proton transfer equilibrium between quinoidal forms and/or preferent association quinoidal forms and copigments *(117)*.

Copigmentation will induce a stabilization of the flavylium form by the π complex displacement of the anthocyanin hydration equilibrium toward the pigmented forms and color enhancement (Figure II.17).

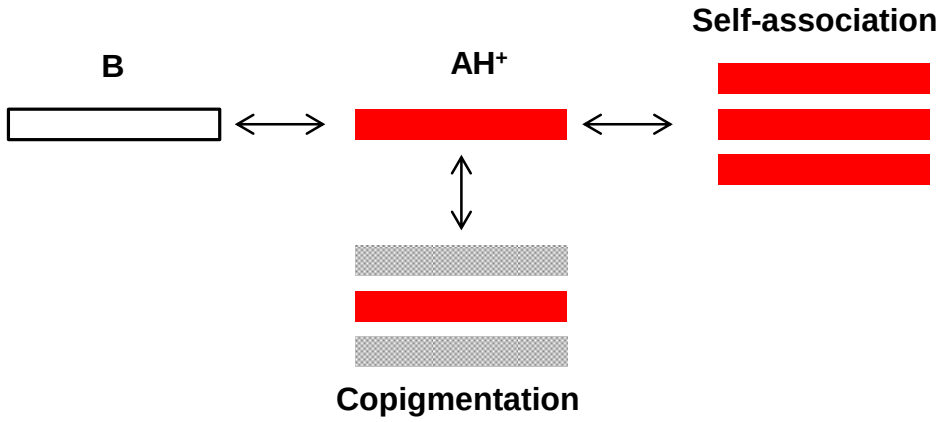

Figure II.17. Copigmentation mechanism. Adapted from Fulcrand et al., 2004 *(73)*.

Copigmentation reactions are strongly affected by pH *(118)*, temperature *(107)*, concentrations *(119)*, solvents *(120, 121)* and molecule structures. For instance, the magnitude of the copigmentation is higher at pH 2-5, since at this pH values the anthocyanin is in its hemiketal colorless form and also the quinoidal equilibrium form is present *(116, 118)*. The solvent system also affects the copigmentation phenomenon. The structure of water, in liquid state, governs the molecular association between an anthocyanin and its copigment. The stronger the network of hydrogen bonded tetrahedral water molecules is the stronger copigmentation phenomenon can be achieved. Therefore, the addition of organic solvents or salts to the solvent reduces the copigmentation effect.

In food science, this physico-chemical phenomenon is considered a very important interaction because color is one of the main quality factors crucial in a product acceptance. Copigmentation can take place through several interaction: i) inter-molecular copigmentation when anthocyanins associate with other molecules (*e.g.* flavonols, flavanols, phenolic acids); ii) self-association, which is a particular case of inter-molecular copigmentation, when it involves anthocyanins themselves; and iii) intra-molecular copigmentation when the anthocyanin chromophore interacts with other residues of its own molecule (*e.g.* aromatic groups of hydroxycinnamic acids). This latter is restricted to anthocyanins which are acylated and occurs predominantly in flower vacuoles while inter-molecular copigmentation occurs mostly in fruits and berries *(122)* (Figure II.18).

A wide range of different molecules has been found to act as copigments. The most common copigment compounds are flavonoids (flavones, flavonols, flavanones, and flavanols), alkaloids, amino acids, and organic acids. Phenolic acids, *i.e.* hydroxycinnamic acids and hydroxybenzoic acids, have also been of interest for co-pigmentation researchers, and have shown a prominent effect on the enhancement and stabilization of anthocyanin *(123)*.

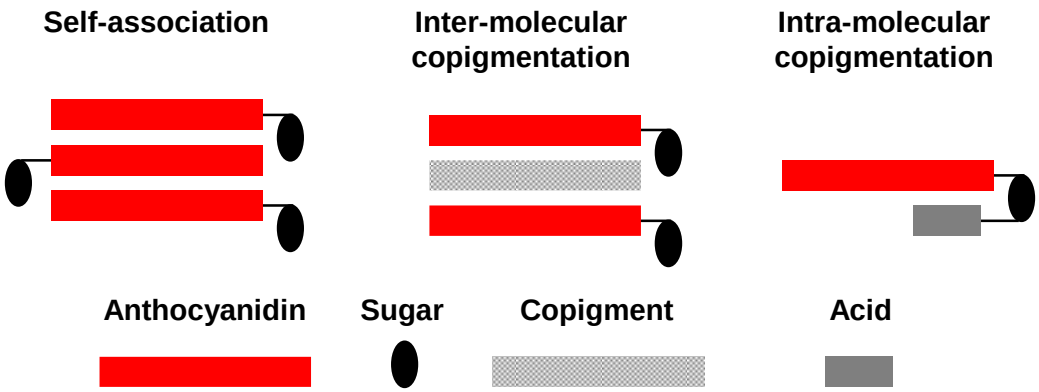

Figure II.18. Self-association, inter-molecular and intra-molecular copigmentation mechanisms occurring on anthocyanins. Adapted from Rein, 2005 *(124)*

II.3.2.5.2.1. Inter-molecular copigmentation

Inter-molecular copigmentation can be defined as a physico-chemical interaction between a colored anthocyanin and a colorless copigment, which is not bound covalently to the anthocyanin molecule *(125)*. Hydrophobic interactions and hydrogen bonding have been suggested as the main mechanistic driving forces for inter-molecular copigmentation *(64, 88)*. These interactions can occur with both the flavylium cation (**AH^+**) and the neutral quinoidal base (**A**) forms of the anthocyanin once both forms are almost planar with efficiently delocalized π-electrons. This inter-molecular association results in an overlapping arrangement of the molecule, which prevented the nucleophilic attack of water on the anthocyanin molecule. Several studies have evaluated the color enhancement and stability of anthocyanins present in wines, juices and fruit products due to the interaction of these pigments with phenolic cofactors. These results indicate that the presence and amount of hydroxyl, methyl and/or glycosylated groups on the copigment structure has great influence on the copigmentation as well on the color enhancement and anthocyanins stabilization *(13)*.

Copigmentation is thermodynamically rather than kinetically controlled, which allows the use of UV-Vis spectroscopy to determine stability and thermodynamic parameters associated with copigmentation *(126)*.

II.3.2.5.2.2. Self-association

Anthocyanins stability can be achieved by self-association, in which two or more anthocyanin molecules are associated *(127)*. The self-association of the anthocyanins was first suggested by Asen *et al*., (1972) and is demonstrated as a positive deviation from Beer´s law, which occurs on increasing the concentration of anthocyanins in the medium *(88)*. Unlike inter-molecular copigmentation, self-association is characterized by a hypsochromic shift in the wavelength of the absorbance maximum *(128)*. Gonzalez-Manzano et al., (2008) demonstrated the existence of this association in wine-like solutions and its positive influence on the color and stabilization of anthocyanins *(129)*. The mechanism of self-association has been claimed to be analogous to the stacking-like interactions, in which vertical stacking of the molecules of anthocyanins are formed and stabilized mainly through the hydrophobic interactions that take place between their aromatic nuclei *(130-132)*. Like for the other two copigmentation mechanisms, this interaction protects anthocyanins from water attack and thereby limits the formation of the hemiketal forms *(133)*.

Self-association takes place with the colored flavylium cation as well as with the quinoidal bases. At acidic pH, cross aggregation involving the colored species (flavylium cation) with the colorless *trans*-chalcone were also described for malvidin-3-*O*-glucoside *(134)*. The possibility for the cross aggregation is probably due to the *trans*-chalcone planar structure, favoring closer packing with the flavylium cation.

II.3.2.5.2.3. Intra-molecular copigmentation

Intra-molecular copigmentation is a type of association restricted to acylated anthocyanins in which the chromophore of the anthocyanin (aglycone) and the co-pigment (phenolic acids) are covalently linked to the same sugar residue *(125)*. This association, through hydrophobic interaction, is thought to be stronger and more effective in stabilizing the anthocyanin color than inter-molecular copigmentation probably due to strengths of the bonds *(70)*.

The intra-molecular copigmentation occurs through the alignment of aromatic acyl residues with the flavylium cation difficulty the hydration process at the position C_2 and C_4 in the pyrilium ring *(81)*. When acylation occurs through position 6 of the sugar, it allows the free rotation of the acyl group, allowing the folding of the molecule and intra-molecular stacking. The flexible saccharide chains are considered spacers, allowing

the folding of the acyl aromatic rings over the planar pyrylium ring *(5)* and protecting it from hydration *(135)*, contributing to the color stabilization of the system.

The number of acyl groups, their structure and the position of attachment to glycosyl residues, as well as the structure and number as saccharides affect the intra-molecular copigmentation *(125, 135)*. Polyacylated anthocyanins can be stabilized by a sandwich type stacking caused by hydrophobic interactions between the planar aromatic residues of the acyl groups and the positively charged pyrilium nucleus, and thus diminishing the formation of the hemiketal *(130)*. In the case of mono-acylated anthocyanins, only on side of the pyrilium ring can be protected against the nucleophilic attack of water and therefore only a weak intermolecular affect and a partial stabilization might occur.

II.3.2.6. Anthocyanins – carbohydrate interaction

Anthocyanins – carbohydrates interaction has been examined primarily focusing on the effect on color. For instance, several works have reported anthocyanin's color stability with pectins *(136-138)*. Other carbohydrates like fructose and glucose have been found to produce no change or slightly increase the absorbance of anthocyanin solution. This was probably due to a decrease in water activity which is known to cause anthocyanins color increase. This color enhancement occurs by the displacement of the hydration/dehydration equilibrium towards the colored species upon the removal of water *(139, 140)*. Similar observations were made for polysaccharides like mannoproteins. On the other hand, amylopectin, amylose and cyclodextrins (α and β) have been shown to produce a decrease in anthocyanin color *(140, 141)*. In the particular case of β-cyclodextrin, interaction with anthocyanins has been shown to improve the pigments thermal stability *(142)* but also to affect the equilibrium and rate constants of the flavylium network *(143, 144)*. Sucrose has also been shown to protect anthocyanins from degrading during frozen storage, prevented browning and the formation of polymeric pigments, which is probably due to the inhibition of enzymatic reactions or the hindering of different condensation reactions by sucrose *(145)*.

In anthocyanins-carbohydrate interaction the degree of color change appeared to be related primarily to the identity of the anthocyanin aglycone and only secondarily to its sugar substitution and/or acylation pattern *(140)*. Beside this, the size and conformation of both the anthocyanin and the polysaccharide are important. The effect of added sugar on anthocyanin stability depends also seems to be influenced by the concentration and sugar type *(146)*.

For food industry and nutrition perspective, the interaction between anthocyanins and carbohydrates is a very important issue to be considered on anthocyanin's stabilization as these pigments are bio-synthetized in a polysaccharide rich environment where intensive contact between these compounds may occur *(147, 148)*. In fact, anthocyanins along with other polyphenols are located uniformly within the vacuole of plant cells, enclosed by the tonoplast and cytoplasmic lipid membranes which are in turn encapsulated by the plant cell wall *(149)*. Cellulose and pectin are the key constituents of the plant cell wall of fruits and vegetables with these polysaccharides providing structural support, strength and flexibility *(150)*. They also regulate the inflow and outflow of nutrients and waste material from the cell whilst also affecting the textural properties of fruits and vegetables *(151)*. With the disruption of plant tissues during the food processing or oral mastication and digestion, lipid membranes and the plant cell walls are fractured allowing the contents within the cell, including anthocyanins to be released. During exit form the cell, anthocyanins and plant cell walls become into contact for the first time with the potential for binding interaction to take place *(149)* (Figure II.19). The association between macromolecules resulting from disrupted cell walls (*e.g.* pectins) and anthocyanins may affect pigments extractability, chemical stability and color properties thus playing an important role in the final color of food products *(152)*.

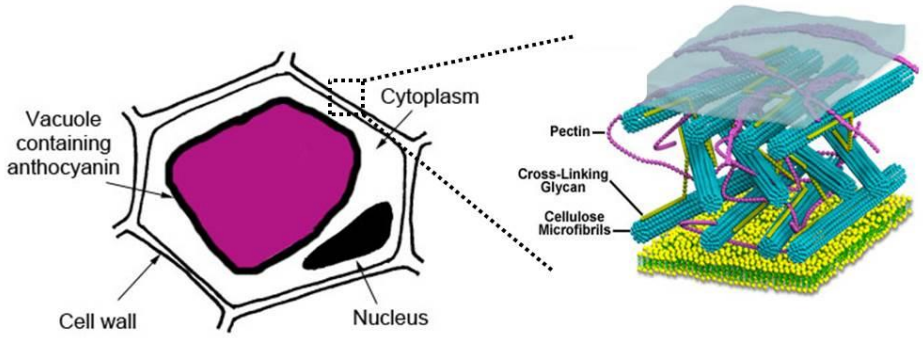

Figure II.19. Schematic representation of the grape cell structure evidencing the presence of the vacuoles where anthocyanins are located[1] and schematic representation of the primary cell wall evidencing the most important carbohydrates[2].

On the other hand, natural cyclodextrins macrocyles have been widely employed as additives in food, cosmetics and pharmaceutical industries and are thus promising matrices for several applications *(153)*. This has prompted the research concerning the use of these oligosaccharides in the stabilization of natural pigments, particularly regarding the impact of host-guest formation on anthocyanins stability and also the

[1] http://hschools.haifanet.org.il/ironi_a/hisc/subjects/biotech/DocLib7/sugars.aspx
[2] http://micro.magnet.fsu.edu/cells/plants/cellwall.html

nature of the anthocyanin equilibrium species preferentially interacting with cyclodextrins.

Different mechanisms of association between anthocyanins and carbohydrates have been suggested. Anthocyanin retention could be primarily a surface phenomenon due to adsorption *(154)*. On the other hand, the formation of these complexes could also be attributed to hydrophobic interactions and hydrogen bonding. Some polysaccharides have the ability to form gel-like structures or to develop secondary structure in solution forming hydrophobic pockets able to encapsulate and complex polyphenols. In the case of cyclodextrins, the presence of hydrophobic cavities favors the interaction with anthocyanins of appropriate shape or mobility *(155)*. However, independently of the mechanism of association, polysaccharides must have a suitable structure, composition, as well as a sufficient size and conformational flexibility to be able to complex polyphenols *(156)*.

As already reported, anthocyanin – carbohydrate interaction has been primarily studied focusing anthocyanin´s color stability. On the other hand anthocyanins extractability is also an important parameter to evaluate theirs prospective use as natural colorants has anthocyanin's extractability could be largely influenced by their association with carbohydrates *(157)*. Since the knowledge regarding the aspects driving the structural interaction between anthocyanins and carbohydrates is scarce, the main purpose of this project was to perform a fundamental and systematic study on the interaction between flavylium compounds (anthocyanins pigments and synthetic flavyliums) and some carbohydrates usually used in the food industry.

Relevant properties of selected carbohydrates studied in this project are summarized below.

II.3.2.6.1. Structure of pectin and cyclodextrin

Pectins are a high value functional food ingredient widely used as gelling agent and stabilizer for instance in jams, jellies and spreads *(138)*. These carbohydrates are a complex family of polysaccharides, mostly present in the middle lamella and primary cell wall. They comprise smooth and hairy regions *(158)*. The "smooth regions", also known as homogalacturonans (HGs), consist of a long chain of (1→4) linked α-D-galacturonic acid (Gal*p*A) *(159)* (Figure II.20). Some of the carboxyl groups can be partially methyl-esterified at C-6 and acetyl-esterified at positions *O*-2 and/or *O*-3,

depending on plant species. The linear units of HGs in which more than 50% of the Gal*p*A are esterified with methyl (or methoxy) groups are conventionally called high methyl-esterified HGs; otherwise they are referred as to low methyl-esterified HGs *(160)*. The level of methylation also influences strongly the physicochemical properties of pectins. As it affects the hydrophobicity of the polymer, the degree of methylation of pectins can modulate their interaction with other biomolecules *(161)*.

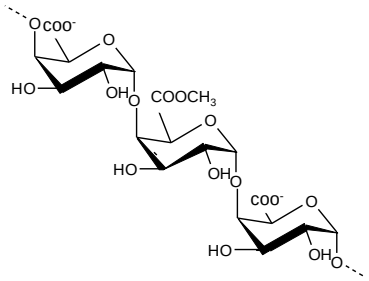

Figure II.20. Representation of a homogalacturonan structure.

The hairy regions, named rhamnogalacturonans (RGs) are of two types (I and II). Rhamnogalacturonans I are formed by the repeating unit of disaccharides →4)-α-D-Gal*p*A-(1→2)-α-L-Rha*p*-(1→), with the rhamnose residues of the RG fractions being partially esterified by chains composed mainly of arabinose and galactose *(162, 163)*. RG II, is a minor pectic component and as homogalacturonans possesses a backbone of (1→4) linked α-D-Gal*p* with side chains containing rhamnose and a variety of rare monosaccharides *(164)*.

Cyclodextrins are oligosaccharides that contain six, seven or eight glucose monomers (α, β and γ-cyclodextrins, respectively) that are joined together to form circular entities with α-(1→4) linkages *(165)*. This gives to cyclodextrins a molecular structure that is relatively rigid and has a hollow cavity of specific diameter and volume. β-cyclodextrin is the most accessible, the lowest-priced and generally the most useful compared to its homologues especially because of its wide use in the food industry *(166)* (Figure II.21).

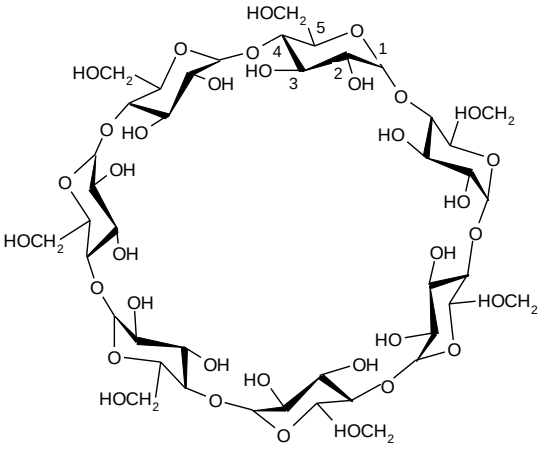

Figure II.21. Chemical structure of β-cyclodextrin.

The possibility of these molecules to form inclusion complexes, which can change the physical and chemical properties of guest molecules, offers a variety of potential uses. Molecular inclusion may lead to dissolution rate enhancement, increased membrane permeability and bioavailability of low-solubility nutraceuticals. Cyclodextrins may also provide protection against oxidation, light-induced decomposition and heat-induced changes *(167)*. For these reasons, cyclodextrins are widely used in food, pharmaceuticals, cosmetics, environment protection, bioconversion, packing and in the textile industry *(166)*. The polar hydroxyl groups of the glucose monomers are located on the rim of the molecule and are directed away from the cavity. These groups interact with water giving cyclodextrins their aqueous solubility properties and will interact with polar groups of some molecules to form hydrogen bonds. While the outer surfaces (top and bottom) are hydrophilic, the internal cavity has a relatively high electron density and is hydrophobic in nature due to the hydrogen and glycosidic oxygen atoms being oriented to the interior of the cavity. Organic molecules of suitable size, shape and hydrophobicity are able to interact non-covalently with cyclodextrins to form stable complexes. Several forces, such as van der Waals forces, hydrophobic interaction and dipole-dipole interaction are involved in the binding of guest molecules to the cyclodextrins cavity *(168)*. The main driving force of complex formation is the release of enthalpy-rich water molecules from the cavity. Water molecules are displaced by more hydrophobic guest molecules present in the solution to attain an apolar-apolar association and decrease of cyclodextrins ring strain resulting in a more stable lower energy state *(169)*. While the initial equilibrium to form the complex is very rapid (often within minutes), the final equilibrium can take much longer to reach. Once inside the cyclodextrin cavity, the guest molecule makes conformational adjustments to take maximum advantage of the weak van der Waals forces that exist. The binding of guest molecules within the host cyclodextrins is not

fixed or permanent but rather is a dynamic equilibrium and the binding strength depends on how well the host-guest complex fits together. In fact, the dimensions of the cyclodextrins cavity allow some selectivity for the complexation of guest molecules. Strong binding results if more interaction occurs between the walls of the cyclodextrins and the guest molecule. If the molecule to be encapsulated is small compared to the cavity, then only a part of its surface will be in contact with the walls and the full potential of the guest molecule to interact with the cyclodextrins is not realized. On the opposite, for larger molecules, the guest molecule might be totally excluded from the cavity or only a portion of it would fit. As more of the molecule can fit into the cavity, a stronger binding results *(168)*.

III. MOLECULAR INCLUSION FORMATION BETWEEN FLAVYLIUM COMPOUNDS AND CYCLODEXTRIN

SYNOPSE:

- **PART A: Effect of cyclodextrins (α, β and γ) on the thermodynamic and kinetic properties of cyanidin-3-*O*-glucoside. Thermal stability in the presence of β-cyclodextrin.**
- **PART B: Structural characterization of inclusion complexes between cyanidin-3-*O*-glucoside and β-cyclodextrin.**
- **PART C: Molecular inclusion of synthetic flavylium compounds in β-cyclodextrin.**

A - Effect of Cyclodextrins (α, β and γ) on the Thermodynamic and Kinetic Properties of Cyanidin-3-*O*-glucoside. Thermal stability in the presence of β-cyclodextrin.

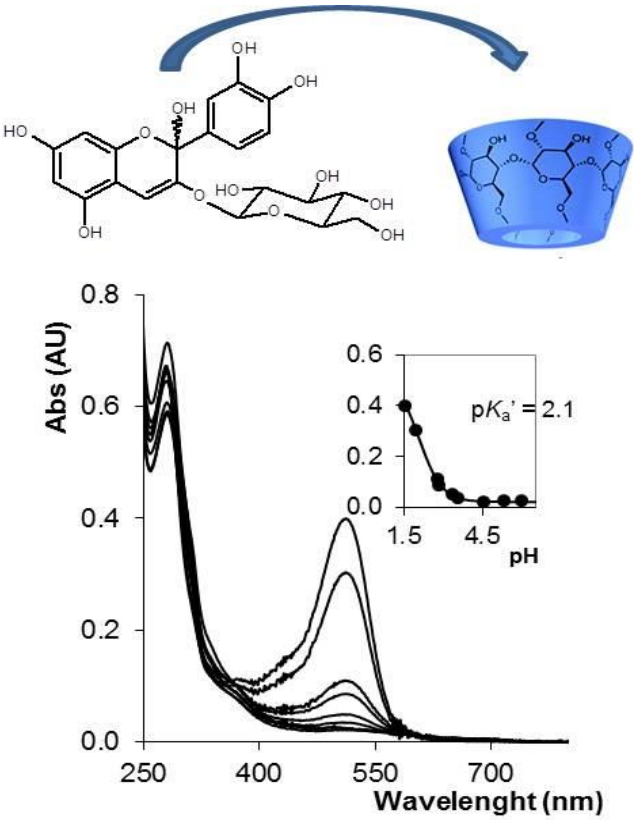

Adapted from:

Fernandes, A., Sousa, A., Azevedo, J., Mateus, N., de Freitas, V.
Effect of Cyclodextrins on the Thermodynamic and Kinetic Properties of Cyanidin-3-*O*-glucoside*, Food Research International*, **2013**, *51*, 748-755. doi: 10.1016/j.foodres.2013.01.037

With the exception of the DSC experiments, the experimental design and work described in this part was carried out by the author.

III.1. Introduction

Color is one of the most important attributes in food products, as it affects the acceptability of products by consumers *(170)*. Nowadays, as a consequence of perceived consumer preferences as well as legislative action, there is a worldwide trend towards the development of food colorants from natural sources, and the replacement of synthetic dyes by these natural colorants has been increasing *(171)*. In this context, anthocyanins are attractive as food colorants since these natural pigments are responsible for the colors of flowers, fruits and vegetables, provide high colorant power and present a low toxicity and water solubility, which permit their incorporation in many food systems *(172, 173)*. Moreover, several studies have suggested that these compounds are beneficial to human health, being responsible for several positive therapeutic effects *(8, 9)*. However, the use of these colorants in food products may face some problems due to their instability *(66)*. The color and stability of anthocyanins is highly dependent on pH, due to changes in the concentration of the four species present in acidic and neutral aqueous solutions: flavylium cation (**AH^+**), quinoidal base (**A),** hemiketal (**B)** and chalcone (**C**) (Figure II.14) *(94, 97, 174)*. Conversion of one species to another is typically accompanied by dramatic changes in color and stability *(170, 175)*.

To increase the stability of anthocyanins, molecular inclusion and encapsulation with several carbohydrates has been used *(170, 171, 173, 176, 177)* and in particular with cyclodextrins (CDs) *(140, 142, 178)*. These compounds are cyclic oligosaccharides composed of β-D-glucopyranosyl units linked by α-(1,4) bonds. The most common are α-, β- and γ-cyclodextrin which have six, seven and eight glucose units, respectively (Figure II.21). The glucose monomers are orientated in a cyclic manner, forming a typical conical or truncated cone structure with a hydrophobic hollow cavity of specific diameter and volume and a relatively hydrophilic outer surface *(168)*. The hollow molecular shape gives cyclodextrins their unique ability to form reversible inclusion complexes with a wide variety of organic compounds (often phenolic substances) yielding supramolecules *(179)*. Formation of the host-guest complex can be easily monitored using techniques such as nuclear magnetic resonance *(180-182)*, UV-visible spectroscopy (UV-vis) *(183)*, fluorescence spectroscopy *(184)*, infrared spectroscopy, electrochemical approaches and solubility measurements *(179)*. Concerning anthocyanins, they include in their structure hydrophobic aromatic moieties and hydrophilic polar groups like hydroxyl groups. This amphiphilic character makes anthocyanins very good candidates for molecular complexation with cyclodextrins

(143). Several studies have reported the formation of inclusion complexes of anthocyanins with cyclodextrin macrocycles *(140-144, 185-187)*. However, interaction between cyclodextrins and some anthocyanins was found to promote the anthocyanins discoloration and lead to an anti-copigmentation effect *(140, 141, 143, 187)*.

The main goal of this study was to verify the effect of cyclodextrins (α, β and γ) on the color of cy3glc. The effect of these three cyclodextrins on the equilibrium and kinetic constants of the network of chemical reactions taking place in cyanidin-3-*O*-glucoside was evaluated by UV-visible absorption techniques. The assessment of cy3glc thermal stability was also studied in the presence of β-CD.

III.2. Materials and Methods

III.2.1. Materials

α-CD, β-CD and γ-CD were purchased from Sigma-Aldrich® (Madrid, Spain). Cy3glc was extracted and purified from blackberries (*Rubus fruticosus*) by semipreparative HPLC with C_{18} reversed phase column (250 mm x 4.6 mm i.d., Merck, Lichrospher®), as described elsewhere *(188)*.

An universal buffer of Theorell Stenhagen was prepared in distilled water (1L) by dissolving 2.25 mL of phosphoric acid (85% w/w), 7.00 g of monohydrated citric acid, 3.54 g of boric acid and 343 mL of 1 M NaOH solution in water (until 1 L completion) *(189)*. The concentration of the buffer (Theorell Stenhagen universal buffer) was maintained low in order to avoid the buffer effects. Different buffers solutions (pH 1–7) were prepared by the addition of small amounts of HCl (37% v/v) to the universal buffer.

III.2.2. pH measurements

All pH measurements were made in a pH meter WTW pH 320 fitted with a Crison® 52 09 electrode. The calibration was made with standard buffers pH 7.0, pH 4.0 and pH 1.0 purchased from Crison®.

III.2.3. Effect of cyclodextrins on the color of cyanidin-3-*O*-glucoside

A stock solution of cy3glc (1.50 x 10^{-4}M) was prepared in HCl 0.1 M. The low pH value of the stock solution ensured that most of the cy3glc was in the flavylium form and thus prevented pigment degradation. Solution composed of 1.0 mL of cy3glc stock solution, 1.0 mL of solution of NaOH (0.1 M) and 0.5 mL of universal buffer solution at pH 1.0 and 2.0 was allowed to equilibrate for 2 hours. To these anthocyanin solutions α, β and γ-CD were added at various concentrations (6.00x10^{-4}; 1.80x10^{-3} and 7.50x10^{-3} M) and the solutions were left to equilibrate for 2 hours. The absorbance (260-700 nm) was measured in an UV-Vis spectrophotometer (Thermo Scientific Evolution Array®) fitted with a thermostatized 1.0 cm path length quartz cuvette device at 25º C.

III.2.4. pH jump

All thermodynamic and kinetic constants of cy3glc solution and of the inclusion complexes cy3glc-α-CD, cy3glc-β-CD and cy3glc-γ-CD were determined by spectrophotometric method, as described elsewhere *(96, 190)*. A stock solution of cy3glc (1.50 x 10^{-4}M) was prepared as described above (control). For the molecular inclusion complex, α-CD, β-CD and γ-CD solution (7.50 x 10^{-3}M) were prepared in HCl 0.1 M. Cy3glc was dissolved in this solution at an approximate molar ratio of 1:50 (cy3glc-α, β, or γ-CD, molar ratio which induced the largest flavylium cation absorbance decrease) and left to equilibrate. pH jumps were carried out by adding the necessary amount of NaOH (0.1 M) to neutralize the stock solution of flavylium cation (cy3glc) and the necessary amount of an universal buffer solution (at different pH values). The ionic strength was maintained at 0.1 M so that the effect of ion-pair formation could be minimized. Throughout the whole experiment the temperature was kept at 25º C.

III.2.5. Thermal degradation studies

The thermal degradation of cy3glc was studied in aqueous solution, at pH 4.0 (which is typical to products that contain anthocyanins) at temperatures of 60 and 90º C. Aliquots of 10 mL of cy3glc aqueous solution (0.01% w/v) were placed into hydrolysis tubes already equilibrated in a thermostatic oil bath. At predetermined intervals, aliquots were removed from the water bath and rapidly cooled at -20º C. Before

analysis, each sample was allowed to come to room temperature. The anthocyanin content of the samples was determined by HPLC-DAD as described elsewhere *(188)*. The thermal degradation of anthocyanins in the presence of β-CD was studied by dissolving β-CD at a w/w ratio of anthocyanin-β-CD 1:10, in the initial aqueous solution, followed by the same thermal treatment and analysis as previously described. This study was performed in triplicate and the results presented are an average of the obtained values. Data analysis was carried out using ANOVA.

III.2.6. Study of the decomposition of cyanidin-3-*O*-glucoside and its β-CD complex by DSC

The thermal analysis of the β-CD, cy3glc, and it's β-CD complex were performed by differential scanning calorimetry. DSC studies were performed using a power compensation differential scanning calorimeter, model SETARAM DSC 141, using a heating rate of 1.67×10^{-1} $K\cdot s^{-1}$ and hermetically sealed aluminum crucibles. The experiments were done under constant flow of nitrogen, 1.683×10^{-6} $m^3\cdot s^{-1}$. The temperature and heat flux scales were calibrated by measuring the temperature and the enthalpy of fusion of some reference materials *(191)*: *o*-terphenyl, benzoic acid, indium, triphenylene, tin, perylene and zinc.

Cy3glc was dissolved in water and left under stirring for 24 hours at room temperature. The complex was prepared by dissolving cy3glc in a β-CD solution (ratio w/w 1:10, anthocyanin-β-CD) and was also left under stirring for 24 hours. Subsequently, the control (cy3glc and β-CD) and the mixture (cy3glc-β-CD) were frozen and lyophilized in a freeze dryer. Approximately 2 mg of cy3glc, β-CD or a quantity of the complex cy3glc-β-CD containing the same amount of anthocyanin were placed in aluminum crucibles and were heated from room temperature to 298.15 K in nitrogen atmosphere at a heating rate of 1.67×10^{-1} $K\cdot s^{-1}$. The samples remained at 298.15 K for 600 s to ensure a homogeneous temperature distribution within the sample and then were heated up to 673.15 K at the same heating rate.

III.3. Results and Discussion

The ability of cyclodextrins to form an inclusion complex with a guest molecule is a function of two key factors. The first concerns the steric requirements and depends on

the relative size of the cyclodextrin to the size and to the physical-chemical properties of the molecule to include. The second critical requirement corresponds to the thermodynamic interactions between the different components of the system (cyclodextrin, molecule to include and solvent) *(166)*. For a complex to be formed there must be a favorable net energetic driving force that pulls the guest into the cyclodextrins and a variety of non-covalent forces such as van der Waals forces, hydrogen bonds and other forces are responsible for the formation of a stable complex *(148)*.

Among different naturally occurring anthocyanins, cyanidin-3-*O*-glucoside (Figure III.1) was selected for this study because of its structural simplicity and reduced steric hindrance, a property needed for a good interaction with cyclodextrin *(144)*. Indeed for sterically hindered pigments such as anthocyanidin diglycosides and anthocyanidin monoglycosides heavily substituted on their aromatic rings, the inclusion on the β-CD cavity is not favored *(143)*.

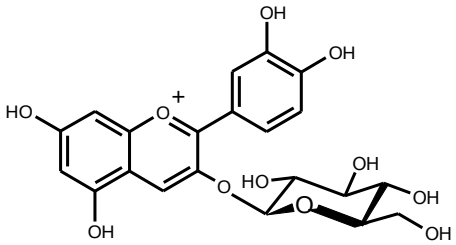

Figure III.1. Structure of cyanidin-3-*O*-glucoside extracted from blackberries (*Rubus fruticosus*).

III.3.1. Effect of cyclodextrins on the color of cyanidin-3-*O*-glucoside

Addition of β-CD to an acidic solution of cy3glc induces a strong decrease in the anthocyanin visible absorption band (hypochromism) (Figure III.2) and this decrease was greater with higher concentrations of β-CD added. This effect was lower at pH 1.0, in which cy3glc is practically 100% in its flavylium equilibrium form (8% absorbance decrease at pH 1.0 instead of 38% absorbance decrease at pH 2.0, at molar ratio 1:50). This fading effect, also known as anti-copigmentation phenomenon has previously been reported in several works *(140, 141, 143, 144)*. Since no change in the shape of the absorption band corresponding to the flavylium form was observed, it can be assumed that the flavylium cation is not the species interacting with β-CD *(144)*. Indeed, anthocyanin flavylium cation maximum absorption is very sensitive to solvent effects and the formation of inclusion complex of the flavylium cation with cyclodextrin would induce a large modification in its solvation shell, shifting the visible maximum of

absorption of flavylium *(144)*. The large loss of color following the addition of β-CD to the cy3glc solution points to the preferential inclusion of the colorless forms (**B**, **Cc** or **Ct**) into the β-CD cavity, a phenomenon leading to the shifting of the pigment hydration equilibrium towards the formation of more colorless forms through the flavylium cation which result in the loss of color *(141, 172)*. A small increase of absorbance at λ_{max} in the ultraviolet region (≈280 nm) was observed with the addition of β-CD, which agrees with the formation of the anthocyanin colorless forms. These forms are more abundant at pH 2.0 comparing to pH 1.0 which could explain the higher anti-copigmentation effect at the prior pH.

On the other hand, addition of α-CD or γ-CD (at the same molar ratio) to a cy3glc solution at pH 2.0 caused only a small increase at λ_{max} in the UV-Visible spectrum (≈280 and 360 nm) and no change could be observed in the band corresponding to the flavylium cation (≈516 nm). These results appear to indicate that the inclusion of cy3glc on the α or γ-CD's cavity is not favored (Figure III.2). As already described, the dimensions of the cyclodextrin cavity allow some selectivity for the complexation of guest molecules. In fact the three cyclodextrins tested in this study differs only in the number of glucose units, having six, seven or eight glucose units, which corresponded to an internal diameter of 5.7 Å, 7.8 Å and 9.5 Å (α, β, and γ-cyclodextrin, respectively) *(168)*. Probably the dimensions of α and γ-CD cavity could not allow so many interactions between the colorless forms of cy3glc and the cavity walls, thus resulting in weaker binding *(192)*.

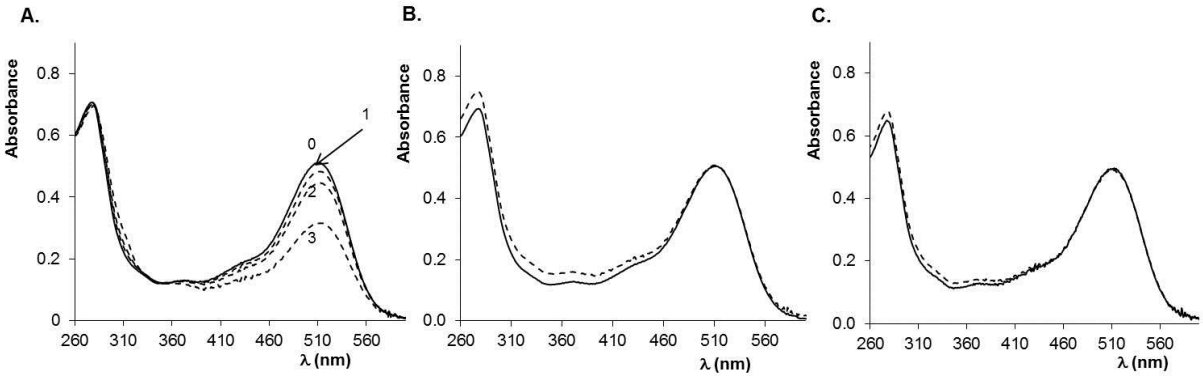

Figure III.2. UV-Vis spectra of cy3glc (full line) and UV-Vis spectra of molecular complex cy3glc-β–CD (dotted line) at pH 2.0; Cy3glc: $1.50x10^{-4}$ M (0); β-CD: $6.00x10^{-4}$ M (1); $1.80x10^{-3}$ M (2); $7.50x10^{-3}$ M (3) (**A**); UV-Vis spectra of cy3glc (full line) and UV-Vis spectra of molecular complexes cy3glc-α-CD (dotted line) (**B**) and cy3glc-γ-CD (**C**) at pH 2.0; Cy3glc: $1.50x10^{-4}$ M; α or γ-CD: $7.50x10^{-3}$ M.

III.3.2. pH jumps

One useful way to follow the kinetic process occurring in the network of flavylium compounds is the use of relaxation techniques, in which the equilibrium of the system is shifted by means of an external influence, applied very rapidly, forcing the metastable system thus formed to shift to the new state of equilibrium. The evolution to a new state of equilibrium can be followed by the monitorization of some parameters (*e.g.* UV-Vis and ^{1}H NMR spectrum) which allow the establishment of both kinetic *(193)* and thermodynamic equilibrium *(194)*. The most common perturbations used are instantaneous variations of temperature, pressure, concentration or pH, the latter being more advantageous since it does not produce secondary physical effects *(195)*. For anthocyanins the flavylium cation (**AH$^+$**) is the predominant species in the equilibrium under sufficiently acidic conditions. When the pH is raised the flavylium cation is involved in parallel reactions that occur in distinct scales of time. The proton transfer is quite instantaneous occurring in the nano- to micro-second range *(194, 196-198)* while the hydration reaction is a relatively slow processes occurring in seconds to a few minutes, depending on the pH of the system *(96)*. The hemiketal is involved in a tautomeric process that leads to the ring opening (and closure) with formation of *cis*-chalcone. This reaction is also pH dependent and usually occurs in the sub-second scale of time. By contrast, the *cis-trans* chalcone isomerization is much slower and pH independent and its equilibrium state are fully established in a time of scale of seconds to weeks, depending on the *cis-trans* isomerization barrier *(199)*.

The impact of cyclodextrins (α, β and γ) in the network of chemical reactions taking place in cyanidin-3-*O*-glucoside was studied using a standard UV-visible spectrophotometer, by performing direct pH jumps from acidic to basic, in thermally equilibrated solutions. In acidic media the following equations account for the thermodynamic and kinetic processes occurring in anthocyanins (Figure II.14) *(94, 96, 97)*:

$AH^+ + H_2O \overset{K_a}{\Longleftrightarrow} A + H_3O^+$	K_a proton transfer	*(III.1)*
$AH^+ + H_2O \overset{K_h}{\Longleftrightarrow} B + H_3O^+$	K_h hydration	*(III.2)*
$B \overset{K_t}{\Longleftrightarrow} Cc$	K_t tautomerization	*(III.3)*
$Cc \overset{K_i}{\Longleftrightarrow} Ct$	K_i isomerization	*(III.4)*

These can be simplified in one single acid-base equilibrium with constant K'_a, equations *(III.5 to III.8)*, if the **A**, **B**, **Cc** and **Ct** species are represented together as one generic conjugate base **CB** (given by the sum of the species **A**, **B**, **Cc** and **Ct**), which is in equilibrium with the acidic flavylium cation $\mathbf{AH^+}$:

$$\mathrm{AH^+ + H_2O \overset{K'_a}{\Longleftrightarrow} CB + H_3O^+} \qquad (III.5)$$

$$K'_a = K_a + K_h + K_h K_t + K_h K_t K_i \qquad (III.6)$$

$$K'_a = \frac{[CB][H_3O^+]}{AH^+} \qquad (III.7)$$

$$[CB] = [A] + [B] + [Cc] + [Ct] \qquad (III.8)$$

III.3.2.1. Thermal equilibrium

Determination of the cy3glc and the cy3glc-β-CD K'_a value was carried out by spectrophotometric measurement *(96, 200)* from the pH dependence of the absorption spectra of equilibrated solutions. Several pH jumps were performed from thermally equilibrated solutions at pH 1.0 to higher pH values (between 1.5 and 6.2 approximately). The decreasing of the absorbance of the flavylium cation was fitted for a single acid-base equilibrium according to equation *(III.6)*. The cy3glc:β-CD molar ratio tested was 1:50 since at this ratio the anti-copigmentation effect was superior.

The pH dependence of the absorption spectra of thermal equilibrated solutions of cy3glc (**A**) and of inclusion complex cy3glc-β-CD (**B**) together with the representation of the fitting of the experimental data to equation *(III.6)* was displayed in Figure III.3. The main feature that emerges from these spectra was the progressive decrease, with increasing pH, of the absorption band centered at ≈511 nm, which can be attributed to the flavylium cation, accompanied by a bathochromic shift to higher λ_{max}. At lower pH values these spectra suggested the predominance of the hemiketal form (lack of absorbance in the visible region) a more evident effect in the presence of β-CD. It was also possible to notice the presence of small amounts of *cis*-chalcone in equilibrium with the hemiketal form through the existence of a band at ≈330 nm *(89)*.

From the data represented in this figure and the fitting of the equation *(III.6)* allowing the calculation of pK'_a = 2.8 for cy3glc and pK'_a = 2.1 for inclusion complex cy3glc-β-CD. The difference observed on the pK'_a calculated for cy3glc and for cy3glc-β-CD probably indicates that in the presence of β-CD the colorless forms are more favorable.

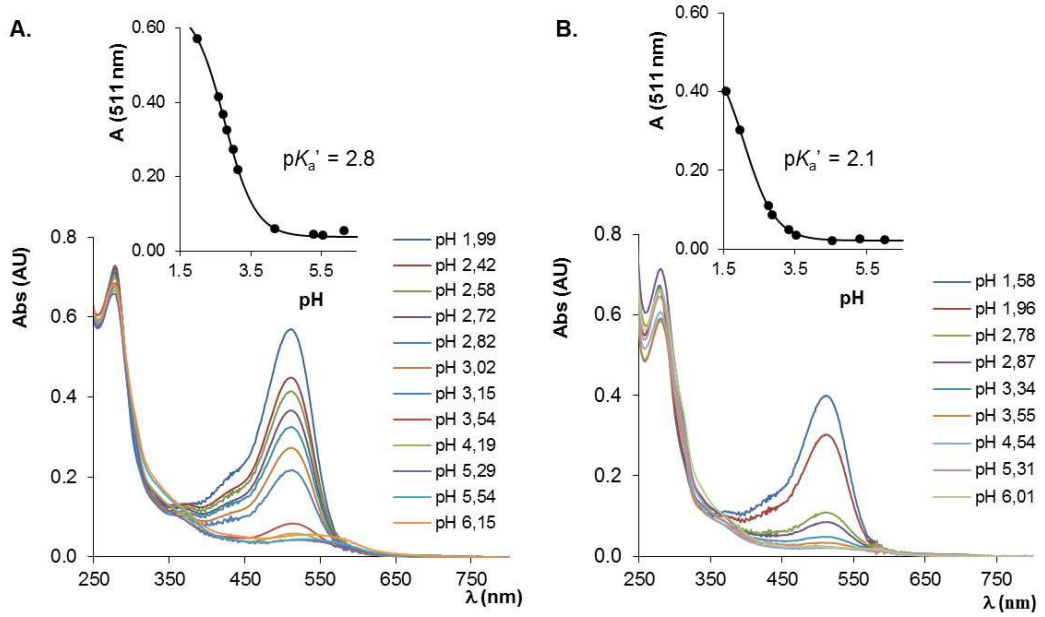

Figure III.3. UV-Vis spectra of equilibrated solutions of cy3glc ($6.0x10^{-5}$M) (**A**) and of molecular complex cy3glc-β-CD ($6.0x10^{-5}$M-$3.0x10^{-3}$M) (**B**) as a function of pH; Inset: Determination of pK_a' through the fitting of the absorption data taken at 511 nm for each pH values.

III.3.2.2. Equilibrium constants

As already reported three main processes with very different timescales can generally be observed for anthocyanins: (i) proton transfer is the fastest and occurs in the micro-second timescale; (ii) hydration (including tautomerization) takes place on a timescale from seconds to several minutes (if pH is not much higher than pK_a); (iii) isomerization occurs on a timescale of seconds or days, depending on the *cis-trans* isomerization barrier.

III.3.2.2.1. Proton transfer

The first process that occurs upon a pH jump from pH < 1 to higher values is the transfer of a proton. This reaction is very fast and for this reason, conventional spectrophotometry including stopped-flow analysis is useless *(96, 201)*. The acidity constant K_a, can be calculated through an alternative method as follows: pH jump from pH<1 to a value where pH >> pK_a+2. At this pH the flavylium cation is totally converted into quinoidal base and hydration process is generally slow enough to be followed by a conventional spectrophotometer. Under these conditions, the absorbance taken immediately after the pH jump, A_0, corresponds to the maximum of concentration of this

species. At the end of the kinetic process (final equilibrium) the absorbance of the quinoidal base indicates its final concentration A_1. The ratio A_1/A_0 is equal to the molar fraction distribution of the quinoidal base at the equilibrium (when β' = 1, there is practically no flavilyum cation) (equation *(III.9)*). For cy3glc, K_a/K'_a = 0.12, giving pK_a = 3.7. For the molecular complex cy3glc-β-CD, K_a/K'_a = 0.07, giving pK_a = 3.1 (Figure III.4). Once again, in the presence of the cyclodextrin a decrease in the K_a value was noticed suggesting a higher stability of the colorless forms.

$$\frac{[A]}{C_0} = \frac{K_a}{K'_a}\,\beta' \;;\quad \beta' = \frac{[A]+[B]+[Cc]+[Ct]}{C_0} \qquad (III.9)$$

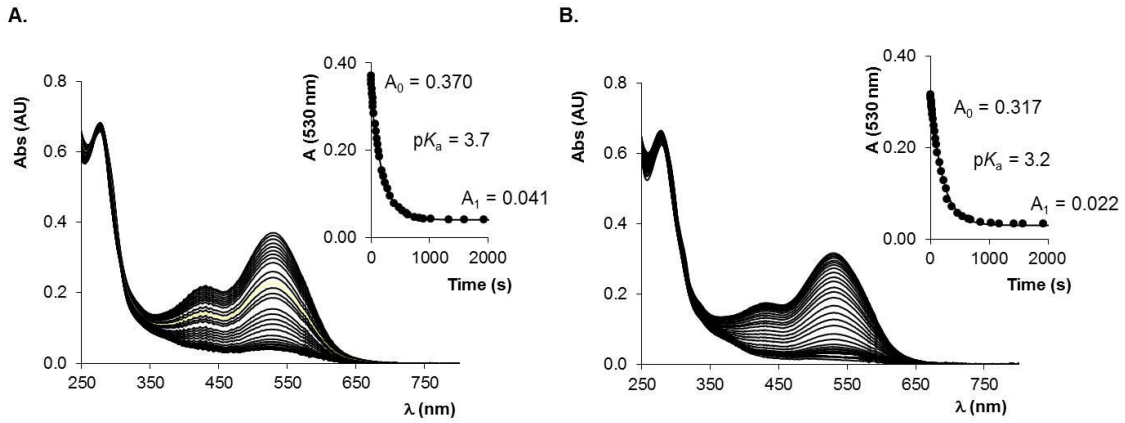

Figure III.4. Spectral variations *versus* time of cy3glc (**A**) (6.0x10^{-5}M) and spectral variations *versus* time of molecular complex cy3glc-β-CD (6.0x10^{-5}M-3.0x10^{-3}M) upon a direct pH jump from pH1.0 to pH 5.3; Inset: Variation of the absorbance at 530 nm *versus* time, giving pK_a = 3.7 (cy3glc) and pK_a = 3.2 (cy3glc-β-CD) through equation *(III.9)*.

III.3.2.2.2. Hydration reaction

For anthocyanins the different reaction rate of proton transfer, hydration, tautomerization and isomerization reactions allowed the separation of these processes. Also the cases where the *cis-trans* isomerization barrier is very high, as in the case anthocyanins, the system can be separated into the sequence of reactions $A \rightleftharpoons AH^+ \rightleftharpoons B \rightleftharpoons Cc$ on one hand and $Cc \rightleftharpoons Ct$ on the other. Besides these, according to previous works *(134, 190)* for anthocyanins the value of K_t is very small. Considering only the fastest process (hydration reaction) and neglecting the tautomerization (K_t = 0) and the isomerization equilibria (K_i = 0) in the acid-base equilibrium, it was possible to determine the pseudo equilibrium constant ($K^\wedge_a$). Bearing this in mind, equation *(III.6)* could be simplified to give equation *(III.10),* which allows the calculation of K_h.

$$K\hat{}_a = K_a + K_h \qquad (III.10)$$

At the end of the hydration reaction it can be assumed that the system is in pseudo equilibrium, from which the respective constants could be obtained. Nevertheless, this only constitutes an approximation in the measurement of K_h. The pseudo equilibrium ($K\hat{}_a$) was obtained considering the absorption spectra of solution in pseudo equilibrium (end of hydration reaction) which was obtained in different time ranges considering the pH of the system. Values of p$K\hat{}_a$ =2.69 (2.0x10^{-3} M^{-1}, $K\hat{}_a$) and 2.48 (3.3x 10^{-3} M^{-1}, $K\hat{}_a$) were determined for cy3glc and for the molecular complex cy3glc-β-CD, respectively.

Taking the absorbance values of the consecutive spectra at λ_{max} and plotting them against time, one can obtain the graph depicted on Figure III.5. The experimental data were fitted to mono $k_{\mathrm{obs}} = \mathrm{A}_0 + \left(\mathrm{A}_1 \times \mathrm{e}^{(-\mathrm{k}_1 \mathrm{t})}\right)$ or biexponential curves $k_{\mathrm{obs}} = \mathrm{A}_0 + \left(\mathrm{A}_1 \times \mathrm{e}^{(-\mathrm{k}_1 \mathrm{t})}\right) + \left(\mathrm{A}_2 \times \mathrm{e}^{(-\mathrm{k}_2 \mathrm{t})}\right)$ which allowed the determination of the observed rate constants (k_{obs}) of the hydration process (fastest reaction) and for the isomerization process (slowest reaction) *(196)*.

The graphical representation of the first observed rate constants (k_{obs}) for cy3glc and for the molecular complex cy3glc-β-CD against pH of the system allowed the determination of its variation (Figure III.5). Hydration reaction revealed to be pH dependent: at higher pH values the observed rate constants was smaller. On the other hand, the hydration reaction becomes faster in acidic solutions. However, direct pH jumps from pH 1.0 to very acidic pH values are useless for observing the variation of the rate constants of hydration since at very acidic pH, AH^+ is the most stable specie and no spectral modifications can take place *(190)*. For these reasons for the determination of the hydration constant (K_h) several pH jumps from pH 1.0 to higher pH values were performed (between 2.5 and 6.2, approximately). The fitting of the experimental data by equation *(III.11)* allowed k_h and k_{-h} determination together with K_h calculation for cy3glc (K_h = 1.8x10^{-3} M^{-1}) and for the inclusion complex cy3glc-β-CD (K_h= 2.7x10^{-3} M^{-1}) (through equation *(III.12)*).

$$k_{obs} = \frac{[\mathrm{H}^+]}{[\mathrm{H}^+] + K_a} k_h + k_{-h}[\mathrm{H}^+] \qquad (III.11)$$

$$K_h = \frac{K_h}{K_{-h}} \qquad (III.12)$$

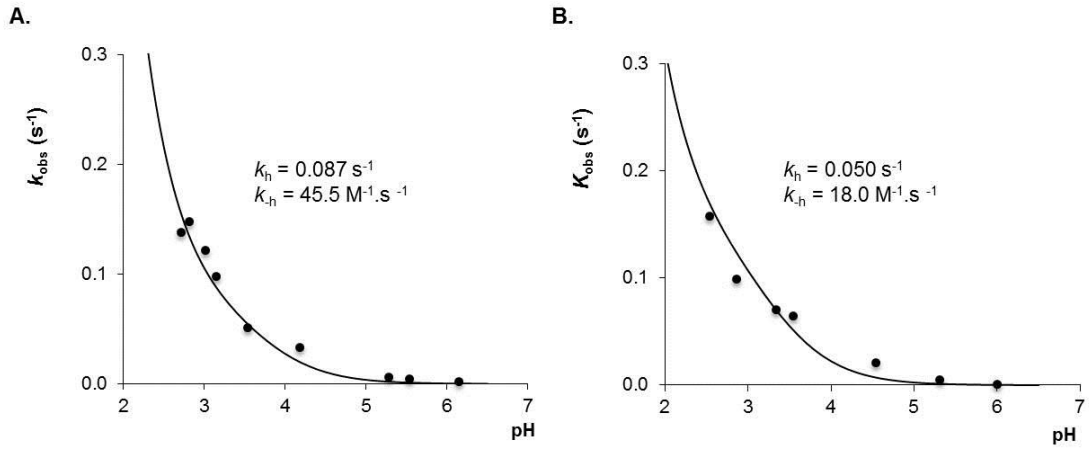

Figure III.5. Fitting of the first observed rate constant as a function of pH for cy3glc solution ($6.0x10^{-5}$M), pK_h = 2.9 (**A**) and for cy3glc-β-CD solution ($6.0x10^{-5}$M-$3.0x10^{-3}$M), pK_h = 2.5 (**B**), determined through equations *(III.11)* and *(III.12)*.

Hydration of cy3glc was speeded up by the presence of β-CD and this reaction appears to be about 1.5 times faster inside the β-CD cavity which could explain the anti-copigmentation effect observed in the presence of this macrocyclic. Simultaneously K_h was higher than K_a reflecting the well-known stability of the anthocyanin hemiketal form (compared to the quinoidal forms) in aqueous solution.

III.3.2.2.3. Isomerization reaction

Direct pH jumps followed in a longer scale of time put in evidence the existence of a much slower process that was assigned to the **C*c*-C*t*** isomerization. Three pH jumps to pH 4.5, 5.3 and 6.1 were performed and followed during several hours to study the isomerization process. An example of one of those experiments is displayed in Figure III.6 at pH 5.3, in which the decrease of absorbance at 530 nm together with the increase of absorbance at 340 nm could be an indication of the isomerization process, which led to the formation of the *trans*-chalcone (**C*t***).

Taking the absorbance values of the consecutive spectra at λ_{max} = 530 nm and 340 nm and plotting them against time, one can obtain two distinct graphs. The fitting of the biexponential curve at 340 nm allowed the determination of the observed rate constants (k_{obs}) of the hydration (fastest process – absorbance decrease) and the isomerization process (slowest process – absorbance increase) *(96)*. It was possible to observe that at pH 5.3, the isomerization occurs with a mean lifetime of 0.96 h for cy3glc and of 0.55 h for inclusion complex cy3glc-β-CD ($1/k_{obs}$). Inclusion of this

anthocyanin on the β-CD cavity clearly induced acceleration on the isomerization observed rate constant (approximately 1.7 times faster).

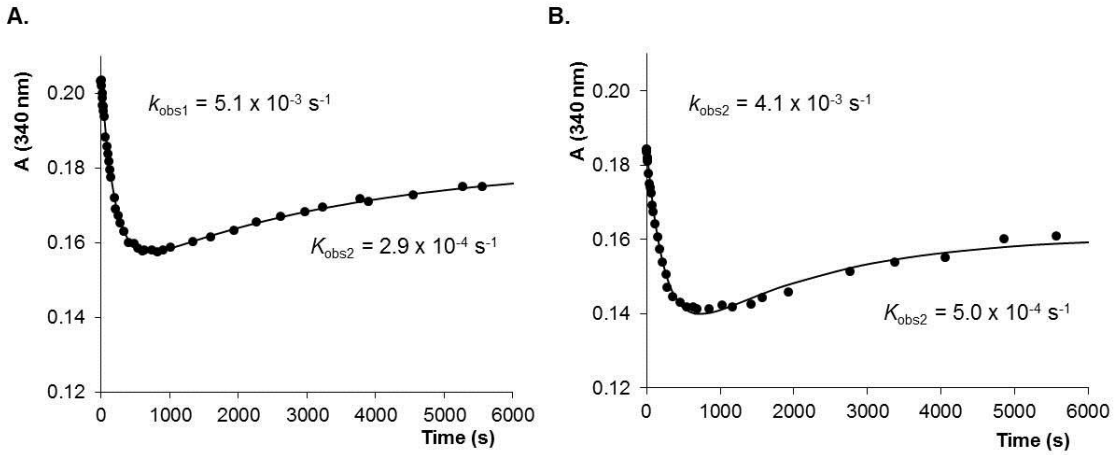

Figure III.6. Variation of the absorbance at 340 nm *versus* time of cy3glc solution (6.0x10^{-5}M) (**A**) and cy3glc-β-CD solution (6.0x10^{-5}M-3.0x10^{-3}M) (**B**) upon a direct pH jump from pH 1.0 to pH 5.3, showing two kinetic processes (k_{obs1} e k_{obs2}).

The observed rate constant (isomerization, k_{obs2}) and hydration constant (K_h) obtained for the molecular inclusion complex cy3glc-β-CD are in agreement to previous works. Dangles *et al*., (1992) reported the inclusion-induced acceleration for the hydration and isomerization reaction of a synthetic, non-natural anthocyanin, the 3,4'-dimethoxy-7-hydroxyflavylium. In this work, the evaluation of hydration reaction was made through one pH jump to pH 3.5 and observed rate constant was about twice as fast inside de β-CD cavity. Similarly, this macrocycle catalyzed the chalcone *cis-trans* isomerization, and the isomerization observed rate constant has been estimated to be about ten times faster inside the β-CD cavity *(143)*.

Similar studies were performed with β-CD's homologues, α- and γ-CD. As previously reported the cyclodextrins tested in this study differs only in the number of glucose units. The interaction of these two macrocycles with cy3glc did not alter significantly the equilibrium and kinetic rate constants of this anthocyanin which clearly suggests that the inclusion of cy3glc on the α- and γ-CD's cavity was not favored. These weak interactions resulted only on a reduced impact on cy3glc's color and on the equilibrium and kinetic constants (Table III.1).

Table III.1. Thermodynamic and kinetic constants determined by UV-Vis absorption for the transformations of cy3glc ($6.0x10^{-5}$M) and of inclusion complexes cy3glc-β-CD, cy3glc-α-CD and cy3glc-γ-CD ($6.0x10^{-5}$M-$3.0x10^{-3}$M). Thermodynamic and kinetic constants described for malvidin-3-*O*-glucoside in the literature (Mv3glc) *(190)*.

	Determined values				**Described values**
	Cy3glc	Cy3glc-α-CD	Cy3glc-β-CD	Cy3glc-γ-CD	Mv3glc
K'_a (M^{-1})	$1.8x10^{-3}$	$2.3x10^{-3}$	$8.4x10^{-3}$	$1.5x10^{-3}$	$5.35x10^{-3}$
pK'_a	2.8 ± 0.1	2.6 ± 0.1	2.1 ± 0.1	2.8 ± 0.1	2.3 ± 0.1
K_a(M^{-1})	$2.1x10^{-4}$	$2.9x10^{-4}$	$5.9x10^{-4}$	$2.4x10^{-4}$	$1.6x10^{-4}$
pK_a	3.7 ± 0.1	3.5 ± 0.1	3.2 ± 0.1	3.6 ± 0.1	3.8 ± 0.1
K_h (M^{-1})	$1.5x10^{-3}$	$2.0x10^{-3}$	$2.7x10^{-3}$	$1.7x10^{-3}$	$4.3x10^{-3}$
pK_h	2.8	2.7	2.5	2.8	2.4
k_h (s^{-1})	0.08 ± 0.01	0.08 ± 0.01	0.05 ± 0.01	0.14	0.08 ± 0.01
k_{-h} ($M^{-1}s^{-1}$)	48 ± 1	40 ± 1	18 ± 1	81. ± 1	19 ± 1

III.3.3. Thermal degradation studies

The data obtained by HPLC-DAD analysis (anthocyanin content) was fitted by a first-order kinetics models (equation (*III. 13*)), where C_0 is the initial anthocyanin content and C is the anthocyanin content after predetermined time (t). Degradation rate constants, *k*, were obtained from the slope of a plot of the natural logarithmic of anthocyanin retention (ln(C/C_0) *versus* time (t). For a first order reaction, half-life values ($t_{1/2,}$ the time needed for 50% degradation of anthocyanins) were determined by equation (*III. 14*) *(202)*.

$$ln(C/C_0) = -k\mathrm{t} \qquad \textit{(III.13)}$$

$$\mathrm{t}_{1/2} = ln0.5/k \qquad \textit{(III.14)}$$

The kinetic plots from the HPLC-DAD data at 60 and 90º C are illustrated in Figure III.7. In general, linear relationships were observed between ln(C/C_0) and time for both control (cy3glc) and complex sample (cy3glc-β-CD) (R^2 between 0.9552 and 0.9926), apparently indicating a first order reaction kinetics for pigment degradation. Similar kinetic responses for anthocyanins have been reported by other authors *(142, 171, 173, 203)*. Table III.2 shows the first order degradation rate constant (*k*) obtained from the slope of logarithmic plots of anthocyanins retention *versus* time. Half-life value ($t_{1/2}$) was calculated from the degradation rates. As expected, the degradation rate constant

(*k*) of anthocyanins increased with increasing heat temperature and time. The results show that the effect of temperature on degradation kinetic rates for anthocyanins in control and complexed with β-CD were significantly different (p<0.05) for both temperatures tested with the rate of degradation being lower in the presence of β-CD. Comparison of $t_{1/2}$ values revealed that anthocyanins were more resistant in the presence of β-CD, as the presence of this macrocycle increased the half-time value. This possible anthocyanin stabilization could be due to anthocyanin complexation with β-CD.

The equilibrium forms of anthocyanins present at the pH 4.0 (pH tested in the thermal degradation studies) are the flavylium cation, the hydrated hemiketal (major specie), the chalcone forms and the quinoidal base form. As pointed out by the UV-vis data obtained, a preferential inclusion of the neutral and more flexible colorless forms is expected, while the flavylium cation appears to be a poor candidate for inclusion in the cyclodextrin cavity due to its polarity and planar structure. As described on section II.3.2.4.5, at pH 3.5 anthocyanin degradation is generally accepted to be initiated by hydration at position C_2 and subsequent cleavage of the flavonoid skeleton to form the chalcone form. The significant protection towards thermal degradation observed in the presence of β-CD could be due to the preferential inclusion of the hydrated forms that could prevent extended tautomerization reaction leading to the formation of the chalcone form and subsequent formation of hydroxybenzaldehyde and 4-hydroxybenzoic acid anthocyanin derivatives. However further studies needed to be performed in order to clarify the equilibrium form interacting with β-CD cavity.

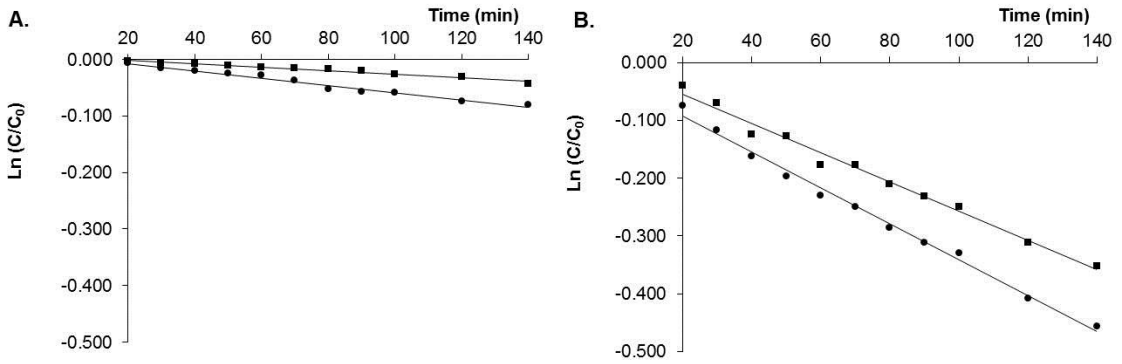

Figure III.7. Degradation of cy3glc (•) and cy3glc-β-CD complex (▪) in aqueous solutions (pH 4.0) at 60º C (**A**) and 90º C (**B**).

Table III.2. Degradation kinetics parameters of cy3glc and cy3glc-β-CD complex. Columns with the same symbol (*) indicate that there is significance difference (p<0.05).

Temperature	K (min $^{-1}$)		$t_{1/2}$ (h)		R^2	
	Cy3glc*	Cy3glc-β-CD*	Cy3glc	Cy3glc-β-CD	Cy3glc	Cy3glc-β-CD
60º C	-0.0008 ± 0.0002	-0.00029 ± 0.00003	14.4	39.8	0.9809	0.9552
90º C	-0.0032 ± 0.0001	-0.0026 ± 0.0001	3.6	4.4	0.9926	0.9899

III.3.4. Study of the decomposition of cyanidin-3-*O*-glucoside and its β-CD complex by DSC

DSC is widely used to confirm the formation of a complex in the solid state. For instance, the disappearance of thermal events of guest molecules, such as endothermic peak assigned to melting, when examined as CD complexes is generally considered as a proof of inclusion *(204)*. Moreover, DSC can be used to study the thermal degradation of a compound. Figure III.8 shows the combined DSC thermograms of cy3glc (blue line), β-CD (green line) and of the inclusion complex of cy3glc-β-CD (red line) as a function of temperature.

Through the thermogram analysis there is a clear indication of complex formation, between cy3glc and β-CD, based on the shape of the dehydration process in the complex. In the complex form, cy3gc dehydration process was shifted to higher temperatures. It was also noticed a decrease on the thermal stability of the dehydration process in the β-CD in the complex form (a shift of 20 ºC) (**A**).

The DSC thermogram of cy3glc (blue line) demonstrated the occurrence of a decomposition / polymerization process at 170º C (**B**). However, after complexation with β-CD this decomposition process is not present in the thermogram of the complex (red line) which is a good indication of anthocyanin-β-CD interaction. The absence of this peak in the thermogram of the complex could also be an indication of the anthocyanin thermal protection due to inclusion formation.

In the complex form, the pre-melting peak were shifted to higher temperature (a shift of 30 ºC) than the previous observed temperature of melting for cy3glc and pre-melting for β-CD (**C**). This indicates a significant interaction between cy3glc and β-CD, that is maintained until the pre-melting temperature of the β-CD. The shifted to higher temperature is followed and supported by an increase of the process enthalpy.

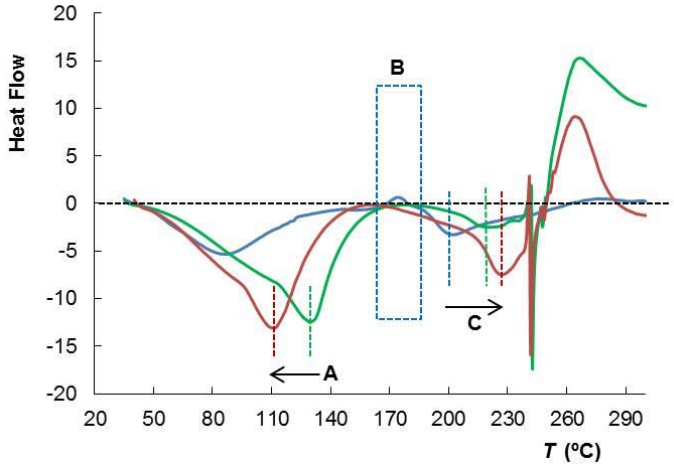

Figure III.8. DSC thermograms of cy3glc (blue line), β-CD (green line) and inclusion complex (cy3glc-β-CD) (red line) under nitrogen atmosphere.

III.4. Conclusion

The need for safe natural food colors has prompted researchers all over the world to look for new sources of food colors. In order to increase the knowledge about the impact of cyclodextrins on the equilibrium and kinetic constants of the network of chemical reactions taking place in cyanidin-3-*O*-glucoside a spectroscopic study was performed. The spectral properties of cy3glc were changed by the molecular inclusion with β-CD. The anti-copigmentation phenomenon observed shows dependence on the pH and on the β-CD concentration. The comparison of the values of the equilibrium and kinetic equilibrium constants between cy3glc and inclusion complex cy3glc-β-CD showed that the inclusion causes significant modifications in the kinetic and thermodynamic properties. Inclusion of cy3glc in the β-CD cavity induced acceleration on hydration constant (K_h) and on the isomerization observed rate constant (k_{obs}), which is in agreement with the anti-copigmentation phenomenon observed. β-CD's homologues (α and γ-CD) didn't cause significant changes on the network of chemical reactions taking place in cy3glc probably indicating that this interaction is not favorable.

Moreover, molecular inclusion of cy3glc into β-CD cavity was shown to enhance the thermal stability of this anthocyanin, which could be an advantage for efficient utilization in food systems.

B - Structural characterization of inclusion complexes between cyanidin-3-*O*-glucoside and β-cyclodextrin

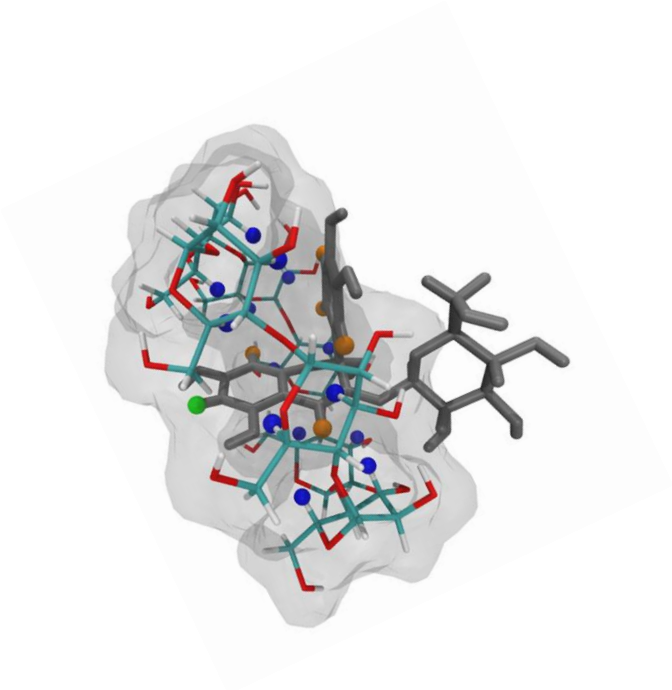

Adapted from:

Fernandes, A., Ivanova, G., Brás, N., Mateus, N., Ramos. M.J, de Freitas, V.
Structural characterization of inclusion complexes between cyanidin-3-*O*-glucoside and β-cyclodextrin, *Carbohydrate Polymers*, **2014**, *102*, 269-277. doi: 10.1016/j.carbpol.2013.11.037

With the exception of the computational calculations, the experimental design and work described in this part was carried out by the author.

III.1. Introduction

Cyclodextrins (CD) are cyclic oligosaccharides consisting of six or more (1→4)-α-D-glucopyranose units, possessing the remarkable ability of forming inclusion complexes with a variety of organic molecules *(205, 206)*. Due to their unique structural features, these molecules are invaluable in a variety of industrial applications namely in the food industry, where they have been used for controlling flavor release, masking odors and tastes, stabilizing emulsions, controlling or masking color, and protecting ingredients from oxidation and from thermal decomposition *(165, 166)*.

In recent years, replacing synthetic dyes by natural colorants has become a major issue for the food industry since the use of synthetic additives is becoming less popular among the consumers as they easily associate these colorants to toxic issues.
Anthocyanins are potentially very interesting as natural food colorants due to their ability to impart vibrant colors. These polyphenolic compounds provide colors ranging from salmon-pink to red and violet, they are water-soluble pigments which simplifies their incorporation in aqueous food systems and do not pose any particular problems in terms of food safety *(83)*. On the contrary, these compounds are antioxidant and were described to have some putative beneficial health effects *(9, 12)*.

However, the application of anthocyanins as food colorants requires improvement of their chemical stability since they are very unstable and susceptible to be transformed in food matrices during storage *(173)*. The fact that anthocyanins co-exist in aqueous solution in a complex network of equilibrium species depending on pH is an important factor related to the color displayed by these compounds. In very acidic aqueous solutions, the red flavylium cation (**AH^+**) is predominant. As pH increases, water addition on flavylium cation gives rise to the colorless hemiketal (**B**). This specie is in fast equilibrium with some yellow *cis*-chalcone (**C*c***). Finally, the slowest process is the *cis-trans* isomerization to lead to a small mole fraction of yellow *trans*-chalcone at equilibrium (**C*t***). Concurrently, deprotonation of the flavylium cation also occurs, leading to blue-purple quinoidal bases (**A**) *(89, 94, 95)*. For anthocyanins, the quinoidal bases are not the most stable specie at the equilibrium and they tend to disappear to form the most stable hemiketal (**B**) form *(97)*.

The formation of inclusion complexes between cyclodextrins and anthocyanins was found to improve the anthocyanin stability and prevent losses during storage *(140, 142, 178, 207, 208)*. However, in several studies an anti-copigmentation effect was

described, resulting from the better inclusion of the colorless forms into the cyclodextrin cavity *(140, 141, 144)*. Some preliminary kinetic results have also demonstrated the preferable inclusion of these forms, established on the increase of the hydration constant (K_h) and on the isomerization observed rate constant (k_{obs}) *(143, 144)*.

Therefore, a correct knowledge of the factors that govern anthocyanin's color stability seems to be decisive in terms of a putative application in food matrices. The aim of the present work was to distinguish the different anthocyanin (Figure II.14) colorless forms by their tendency for associating with β-cyclodextrin in aqueous solution. For this purpose, a combination of NMR experiments (ROESY and DOSY) and a theoretical approach has been undertaken.

III.2. Materials and Methods

III.2.1. Materials

β-CD, deuterium oxide (99.9%) was purchased from Sigma-Aldrich® (Madrid, Spain). NaOD (99.5%) was purchased from Euriso-top® Cy3glc was extracted and purified in the laboratory from blackberries (*Rubus fruticosus*) by semipreparative HPLC with C_{18} reversed phase column (250 mm x 4.6 mm i.d., Merck, Lichrospher®), as described elsewhere *(188)*.

III.2.2. NMR samples preparation

Solutions of cy3glc at different concentrations (8.6 mM, 5.2 mM, 2.7 mM, 2.1 mM and 1.4 mM) and β-CD (8.6 mM) were prepared in 99.9% D_2O at room temperature and pH was adjusted to 3.5 by the addition of NaOD *(209)*. For the study of the inclusion complexes formation 1.4 mM of cy3glc was dissolved in 99.9% D_2O and appropriate amounts of β–cyclodextrin were added (1.2 mM; 1.4 mM; 2.2 mM; 3.4 mM and 4.5 mM). pH was also adjusted to 3.5. Samples were allowed to equilibrate for at least 8 hours before the NMR study.

III.2.3. UV-Vis absorption spectra

Absorption spectra of cy3glc solution (1.4 mM) and absorption spectra of samples of cy3glc and β-CD at different concentrations were obtained in an UV-Vis spectrophotometer (Thermo Scientific Evolution Array®) fitted with a thermostatized 1.0 cm path length quartz cuvette device at 25º C.

III.2.4. NMR spectroscopy

All NMR experiments were recorded on a Bruker Avance III 600 HD spectrometer, operating at 600.13 MHz for protons and 150.92 MHz for carbon, equipped with 5 mm CryoProbe Prodigy and pulse gradient units, capable of producing magnetic field pulsed gradients in the z-direction of 50 G/cm. The NMR measurements have been done with standard BRUKER pulse sequences, in D_2O, at 300K and at pH 3.5. ^{1}H NMR experiments were performed with water suppression using excitation sculpting with gradients *(210)*, acquisition time 1.36 s, relaxation delay 2 s, 128 or 256 transients of a spectral width of 10000 Hz were collected into 32 K time domain points. Typical measuring conditions for the ^{1}H/^{1}H and 2D spectra (COSY, TOCSY, ROESY, NOESY) recorded in phase sensitive mode and with water suppression were: relaxation delay 2 s, 64-128 scans, a total 2K data points in *F*2 and 256 data points in *F*1 over a spectral width of 10000 Hz. TOCSY spectra were recorded MLEV-17 sequence with a mixing time of 80 ms. ROESY experiments were carried out using a mixing time of 100, 200, 400, 500, 700 and 800 ms in the phase-sensitive mode. 2D 1H/13C HSQC and HMBC experiments were carried out with a spectral width of *ca* 10000 Hz for 1H and 32000 Hz for 13C, relaxation delay 1.5 s, Fourier transform (FT) size 2 K × 1K.

Proton registered diffusion-ordered NMR (^{1}H DOSY) experiments were acquired using the bipolar longitudinal eddy current delay (BPPLED–Bipolar Pulsed Field Gradient Longitudinal Eddy Delay) pulse sequence *(211)*. The experimental conditions (5mm NMR tubes, amount of the solute and solvent, a temperature of 300 K, no sample rotation and high air flow of 535 L/h to avoid convections in the samples) for all DOSY experiments were kept constant. Before the NMR experiments, the temperature was equilibrated and maintained at 300 K, as measured using the spectrometer thermocouple system. Typically, in each experiment a number of 16 spectra of 32K data points and 128 or 256 scans were collected, with values for the duration of the magnetic field pulse gradients (δ) of 2.4 ms, diffusion times (Δ) of 120 ms and an eddy

current delay set to 5 ms. The pulse gradient (g) was incremented from 2 to 98% of the maximum gradient strength in a linear ramp. The spectra were processed with the Bruker Topspin software package (version 3.2). The diffusion coefficients (*D*) were obtained by measuring the signal intensity of characteristic resonances of the species presented in the samples studied and were all scaled to the absolute *D* value obtained for acetone (0.001 M; 1.69×10^{-9} m^2 s^{-1}, calculated standard deviation of 1.15×10^{-3}) used as an internal reference.

III.2.5. Molecular Dynamics simulation

The initial structure of β-cyclodextrin was obtained from its complex with cyclo/maltodextrin-binding protein (pdb id: 2ZYN at 1.7 Å resolution) *(212)* retrieved from the protein databank. Given the absence of cy3glc structure in this database, the initial geometry of this compound was built with the GaussView software *(213)*. To calculate the optimized geometries and electronic properties for the subsequent parameterization of this compound, the Gaussian 09 suite of programs *(214)* was used to perform restricted Hartree-Fock calculations (RHF), with the 6-31G(d) basis set. Atomic charges were further recalculated using RESP algorithm *(215)*. This methodology was chosen for its consistency with that adopted for the parameterization process in AMBER 10.0 simulation package *(216)*. The geometry optimizations and a Molecular Dynamics (MD) simulation on cy3glc-β-CD complex were performed with the parameterization adopted in AMBER 10.0, using the GAFF force field, the general Amber force field for small organic molecules, and the Glycam2004 force field (Glycam-04 parameters) for carbohydrates *(217-219)*. In this simulation, an explicit solvation model with pre-equilibrated TIP3P water molecules was used, filling a truncated octahedral box with a minimum distance of 12 Å between the box faces and any atom of the cy3glc-β-CD complex. The size of this system was 6,004 atoms. The complex geometry was minimized in two stages: first both compounds were kept fixed and only the position of the water molecules was minimized. Afterwards the full system was minimized. Subsequently, an MD simulation of 100 ps at constant volume and temperature, and considering periodic boundaries conditions was run, followed by 30 ns of MD simulation with NPT ensemble, in which Langevin dynamics was used (collision frequency of 1.0 ps^{-1}) to control the temperature at 303.15 K *(220)*. These simulations were carried out using the Sander module, the bond lengths involving hydrogen atoms were constrained using the SHAKE algorithm, and the equations of motion were integrated with a 2 fs time step using the Verlet leapfrog algorithm *(221)*.

The Particle-Mesh Ewald (PME) method *(222)* was used to include the long-range interactions, and the nonbonded interactions were truncated with a 10 Å cutoff. The MD trajectory was saved every 2 ps and the MD results were analyzed with the PTRAJ module of AMBER 10.0 *(216)*.

III.3. Results and Discussion

In the present work, the ability for inclusion complex formation between the different equilibrium forms of cy3glc and β-CD in aqueous solution and the structure of these inclusion complexes were studied by NMR spectroscopy and theoretical calculations. pH 3.5 was selected to perform this study since at this pH value approximately 75% of the anthocyanin corresponds to the hemiketal form with the remaining 25% corresponding to the flavylium cation, to the *cis* and *trans*-chalcone and to the quinoidal base form *(97)*.

III.3.1. NMR spectral characterization of cy3glc

The detailed knowledge of the structural and spectral characteristics of anthocyanins is of primary significance prior to the investigation of the molecular structure of inclusion complexes with β-cyclodextrin. It is well known that anthocyanins can co-exist in aqueous solution in equilibrium between five species depending on pH (Figure II.14). Additionally, the relative species population is affected by the possible self-association of anthocyanins as a result of the vertical stacking caused by hydrophobic interaction between aromatic rings (self-association) *(134)* .

Therefore, a preliminary NMR spectral characterization of cy3glc in aqueous solution, at pH 3.5 and different concentrations was performed. The assignment of the resonance signals in ^{1}H NMR spectra of anthocyanin was based on the analysis of one and two dimensional (COSY, TOCSY, HSQC, HMBC) NMR spectra. The NMR data are consistent with the data already published *(99, 134, 223)* and the assignments of the chemical shifts and coupling constants of protons H2', H6', H5' and H4 in the different equilibrium forms are presented in Table III.3 The resonance signals of protons H6 and H8 in the A ring disappeared from the spectrum a few hours after sample preparation due to protons exchange with deuterium *(134, 224)*. The hemiketal can be easily identified not only because it is the major specie at this pH value but also because of the existence of twin peaks related to the presence of the two epimers

(*R*/*S*) on carbon 2 (C2). The *cis*- and *trans*-chalcones usually appear at low concentrations *(6)*.

Table III.3. ^{1}H (600.13 MHz) NMR data (proton chemical shift (ppm), multiplicity and spin-spin coupling constant (Hz)) and diffusion coefficient (*D*) for the flavylium cation, hemiketal, *cis*-chalcone and *trans*-chalcone equilibrium forms of 8.6 mM and 1.4 mM cyanidin-3-*O*-glucoside solutions in D_2O at pH 3.5 (*s*, singlet; *d*, doublet; *dd*, double doublet).

	Cyanidin-3-*O*-glucoside							
	Flavylium (AH^+)		**Hemiketal (B)**		***Cis*-chalcone (Cc)**		***Trans*-chalcone (Ct)**	
	8.6 mM	*1.4 mM*	*8.6 mM*	*1.4 mM*	*8.6 mM*	*1.4 mM*	*8.6 mM*	*1.4 mM*
Aglicone								
H2'	7.23 *s*	7.67 *s*	7.08 *d*/7.04 *d (2.2)*	7.09 *d*/7.06 *d (2.2)*	-	7.23 *d (2.0)*	-	7.39 *d (2.2)*
H5'	6.50 *d (8.2)*	6.84	6.86 *d (8.6)*	6.88 *d (8.6)*	-	6.70 *d (8.6)*	-	6.95 *d (8.5)*
H6'	7.44 *d (8.2)*	7.79	6.99 *dd*/6.95 *dd (8.6; 2.2)*	7.02 *dd*/6.99 *dd (8.4; 2.2)*	-	7.21 *dd* (8.0; 2.0)	-	7.42 *dd* (8.6; 2.0)
H4	8.21 *s*	8.60 *s*	6.33 *s* / 6.32 *s*	6.41 *s* / 6.38 *s*	-	6.54 *s*	-	6.73 *s*
$Dx10^{-10}$ (m^2s^{-1})	3.24	4.20	5.34	5.55	-	5.50	-	5.59

From the analysis of the ^{1}H NMR spectra performed at decreasing concentrations (8.6 to 1.4 mM) a systematically downfield shift of the resonance signals of the flavilyum and a significant accumulation of hemiketal form and appearance the of weak signals form *cis*- and *trans*-chalcone were observed (Figure III.9). The self-association of anthocyanins is a well-known phenomenon taking place with the flavylium cation as well as with the quinoidal base. Cross aggregation involving flavylium cation and *trans*-chalcone was also described *(132, 134)* and in this work, the self-association of the flavylium cation was perceived through the downfield shift with the anthocyanin concentration decrease. Perceptibly, the disruption of the aggregation phenomenon affects the equilibrium between the four species in the aqueous solution resulting in a significant increase of the **B** form and appearance of **C*c*** and **C*t*** forms at solution concentration under 1.4 mM.

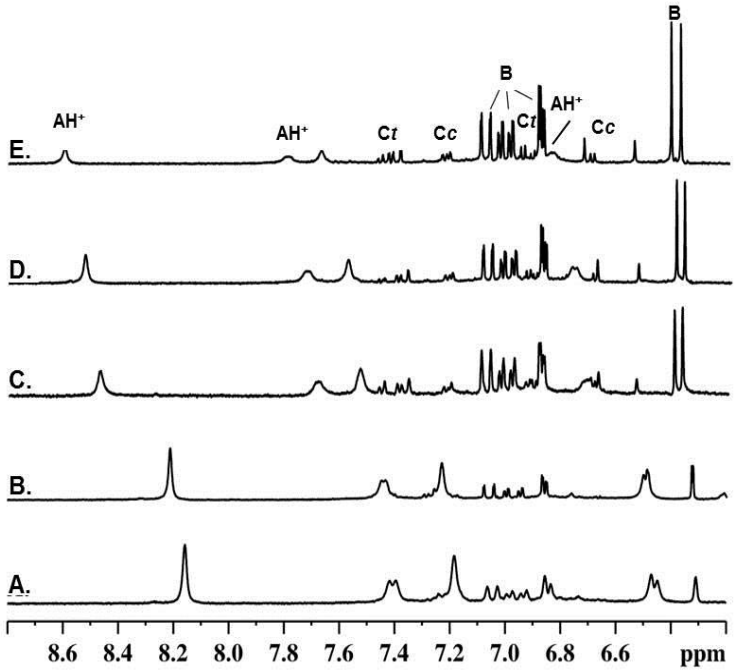

Figure III.9. ^{1}H NMR spectra of cyanidin-3-*O*-glucoside in D_2O at pH 3.5 as a function of concentration (8.6 mM-**A**; 5.2 mM-**B**; 2.7 mM-**C**; 2.1 mM-**D**, 1.4 mM-**E**).

The concentration dependence of self-association of cy3glc species was additionally estimated on the basis of the alteration of their self-diffusion coefficients as measured by DOSY experiments. The diffusion coefficients measured for the different species presented in the solution of cy3glc at 9 and 1.4 mM are presented in Table III.4. It is possible to observe that the *D* value for the flavylium cation form was significantly affected by the concentration as a result of its self-aggregation. Micellarization process is a well-known phenomenon taking place in procyanidins *(225, 226)* and similarly to these polyphenolic compounds, by plotting the flavylium cation *D* value against the

inverse anthocyanin concentration we could obtain an approximated cac, critical aggregation concentrations (~1g.L^{-1}) (Figure III.10). However to ensure that the flavylium cation behaves such as procyanidins undergoing a micellarization process, more anthocyanin concentration should be tested.

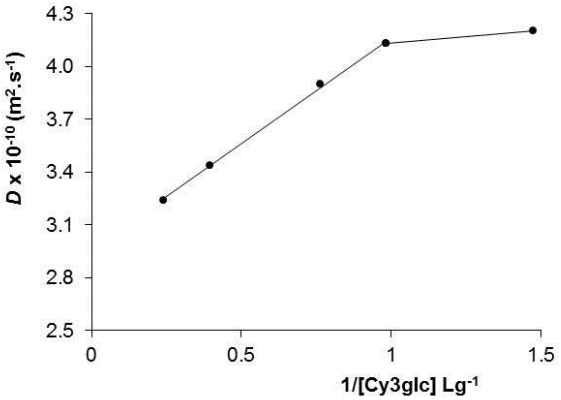

Figure III.10. Estimation of cac's value from the diffusion coefficients. The intercept of slopes obtained for concentrated and diluted regions of *D* versus inverse anthocyanin concentration gives the cac value.

III.3.2. NMR analysis and stoichiometry of the inclusion complex cy3glc-β-CD

Evaluation of the changes in chemical shifts of β-cyclodextrin upon complexation provided the first information about the host-guest interaction allowing the determination of the stoichiometry of the inclusion complexes. The reasoning is based on the expectation that if the guest molecule is imbedded in the CD cavity, the screening environment should be sensed by magnetic nuclei inside the β-CD cavity (H3 and H5) but not by outside protons (H1, H2 and H4) *(227)*.

In order to minimize the effect of the self-aggregation of the anthocyanin, the lowest solution concentration (1.4 mM) was selected to perform the subsequent NMR study of the interaction between cy3glc and β-CD and for structural characterization of cy3glc-β-CD complex (Figure III.11). ^{1}H NMR spectra with high resolution were recorded for cy3glc-β-CD in D_2O at pH 3.5. The spectra are dominated by the intense resonance signals of β-CD and upfield shifts of the resonance signals of H3 and H5 β-CD's protons was detected. This behavior may result mainly from the magnetic anisotropic shielding by the aromatic rings in cy3glc molecules, included within the cavity of β-CD *(224, 228)*. Only minor alterations in the chemical shift of protons H1, H2 and H4 which lie on the outer surface of the cavity was observed.

In the ^{1}H NMR spectra of cy3glc-β-CD, signals belonging to the protons of **AH**$^{+}$, **B**, **C*c*** and **C*t*** forms of cy3glc were clearly observed. Moreover, it was found that the addition of β-CD to the aqueous solution of cy3glc immediately induced the appearance of new set of resonance signals identified as $\mathbf{B_{CD}}$ (Figure III.11). The intensity of these signals increased while the intensity of the resonance signals of the **B** form decreased with time. On the basis of 1D and 2D (TOCSY, HMBC) NMR analysis, these new signals were attributed to the hemiketal anthocyanin form complexed with β-CD ($\mathbf{B}_{CD}$). Well defined long range correlations were observed in the ^{1}H/^{13}C HMBC spectra between characteristic signals of the $\mathbf{B_{CD}}$, such as between the protons at δ 7.16 ppm (H2'), δ 6.98 ppm (H6') and δ 6.76 ppm (H4) with carbon C2 at 102.3 ppm, characteristic of hemiketal form. The ^{1}H signals of $\mathbf{B_{CD}}$ were found to be downfield shifted with respect to the spectra of **B** before the addition of β-CD. The two epimeric forms could not be distinguishable after complexation, which could be a result of a preferable inclusion of one of the two epimers into β-CD's cavity. Indeed, the use of cyclodextrins for the separation of isomers was already been reported in the literature *(228, 229)*. Also, for the protons signals of **C*c*** a downfield shifted were observed. Interconversion between *cis*- and *trans*-chalcone is in slow exchange (in the NMR time scale) while the chemical exchange between the hemiketal and the *cis*-chalcone is much faster *(96, 97)*. Bearing this, the chemical shifts changes observed for the *cis*-chalcone could result from the faster chemical exchange. However based on the NOE interaction observed between this equilibrium form and β-CD and on the alteration of the *D* value, we assume that the chemical shift changes may be a result from the interaction with β-CD's internal protons, namely a steric compression effect *(230)* instead of chemical exchange. Only minor chemical shifts changes were detected in ^{1}H NMR spectra of cy3glc:β-CD for the protons and **C*t*** forms.

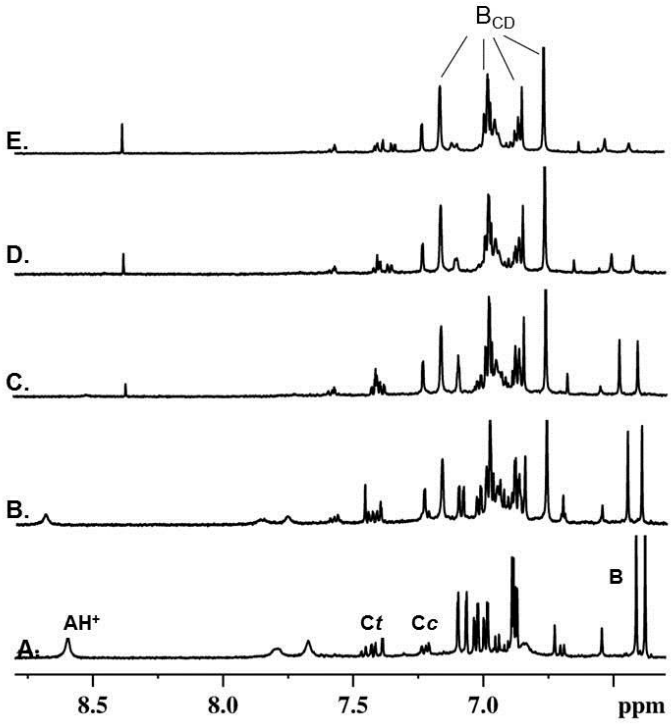

Figure III.11. ^{1}H NMR spectra of 1.4 mM cyanidin-3-*O*-glucoside solution in D_2O at pH 3.5 (**A**) and ^{1}H NMR spectra of cyanidin-3-*O*-glucoside with increasing ratios of β-CD after reaching equilibrium (1:0-**A**; 1:0.8-**B**; 1:1.6-**C**; 1:2.4-**D**; 1:3.2-**E**).

For the evaluation of the stoichiometry of the inclusion complexes cy3glc-β-CD, Job´s continuous variation technique was applied *(231)*. For this purpose, solutions with different cy3glc-β-CD molar ratios were prepared and the data were plotted in the form $X_H\Delta\delta$ versus X_H, where X_H is the mole fraction of β-CD. The Job's plot showed a maximum at r = 0.5 (where r = [β-CD]/([β-CD]+[Cy3glc])), indicating that the complexes possessed a 1:1 stoichiometry (Figure III.12).

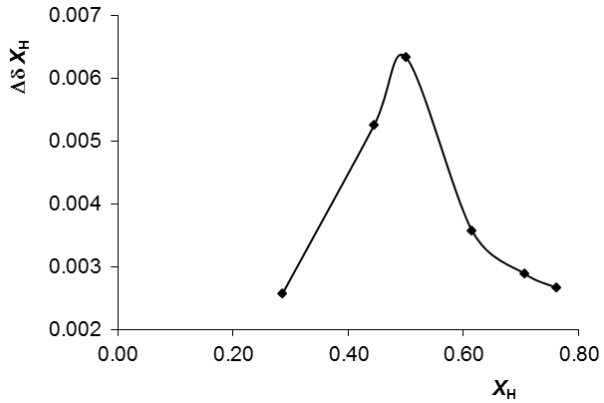

Figure III.12. Job's plot obtained to determine the stoichiometry of the complex (X_H is β-CD molar fraction).

Moreover, when performing the NMR titration it was noticed that the addition of β-CD affected principally the hydration reaction, mainly disturbing the normalized molar proportions between the flavylium cation and the hydrated hemiketal. The other equilibrium forms, *cis*- and *trans*-chalcones were almost unaffected with the increase of β-CD (Figure III.13). These preliminary results suggest the preference inclusion of the hemiketal into β-CD with this compound catalyzing the transformation of the flavylium cation into the hemiketal, a phenomenon leading to the shifting of the pigment hydration equilibrium towards the formation of more hemiketal with the addition of more β-CD. The normalized molar proportion of the various equilibrium forms were determined by integration of signals in the ^{1}H NMR spectra. Concurrently, during the same experiments with the addition of β-cyclodextrin a clear change in the color of the anthocyanin solution was observed. β-cyclodextrin induces a strong decrease in the anthocyanin visible absorption band and this decrease was greater with higher concentrations of β-CD added (Figure III.13). This behavior had already been described in the literature *(143, 144)* and once again suggests a preferential interaction between the anthocyanin hemiketal form and β-CD.

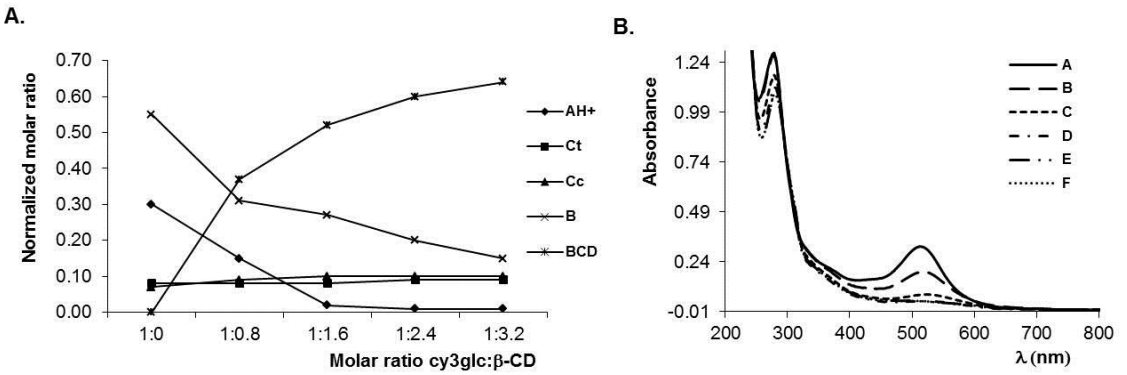

Figure III.13. Normalized molar proportion of the **AH^{+}**, **B**, **C*c***, **C*t*** and hemiketal complexed (**B_{CD}**) as a function of different β-CD ratios, determined by integration of signals in the ^{1}H NMR spectra (**A**). Uv-visible spectra of cyanidin-3-*O*-glucoside alone and in the presence of β-cyclodextrin at different concentrations (**B**).

III.3.3. Diffusion Ordered spectroscopy

Diffusion Ordered NMR (DOSY) is a well-established technique for characterizing the structure and dynamics of complex systems. The self-diffusion coefficients of these systems reveal structural characteristics such as molecular size, weight and shape *(232, 233)*. This methodology relies on the determination of the diffusion coefficients in the absence and presence of host molecules (β-cyclodextrin in this study), thus

providing information about the size and evidence on the magnitude of the binding constants *(234, 235)*.

Typically, cy3glc is approximately one half of the average size of β-CD. In these DOSY studies it was intended not only in confirming the interactions between cy3glc and β-CD but also distinguishing the affinity of the existing anthocyanin equilibrium species at pH 3.5 for inclusion complex formation with β-CD. Since a modification in a solution composition was expected to induce changes in the behavior of the anthocyanin equilibrium forms, cy3glc-β-CD samples containing cy3glc to β-CD ratio of 1:0.8, 1:1.6, 1:2.4 and 1:3.2 were studied. The diffusion coefficients of β-CD and the existing equilibrium forms of cy3glc in cy3glc-β-CD samples were determined and compared with the corresponding values of cy3glc and β-CD alone. The diffusion measurements using DOSY were performed under identical experimental conditions taking special attention on the concentration, pH and temperature of the samples. The diffusion coefficients (*D*) of cy3glc equilibrium forms were obtained by measuring the signal intensity at more than one place in the spectra and those for β-CD from the resonance signals of the anomeric protons. To account for changes in the samples solution viscosity or drift on the experimental conditions, the diffusion coefficient values were all scaled to the absolute *D* value obtained for acetone (0.001 M; 1.69×10^{-9} m^2 s^{-1}, calculated standard deviation of 1.15×10^{-3}) used as an internal reference.

In the absence of β-CD the *D* value of **B**, **C*c*** and **C*t*** was found to be very similar to 5.5×10^{-10} m^2s^{-1} (Table III.4). The significantly lower *D* value observed for $\mathbf{AH^+}$ was attributed to the tendency of this equilibrium form to self-aggregate resulting on a specie with higher hydrodynamic diameter. Concerning the results obtained for the inclusion complexes cy3glc-β-CD, diverse behaviour of the different anthocyanin equilibrium forms in the presence of β-CD was observed. The diffusion coefficients measured for the new set of signals detected in cy3glc-β-CD ($\mathbf{B_{CD}}$) form was found to be similar to the corresponding values of β-CD (4.0×10^{-10} m^2s^{-1}). This is an indication of intermolecular interactions and complexation between these two species was hence assumed. Likewise, the decrease of the diffusion coefficient of *cis*-chalcone in cy3glc-β-CD samples, to values close to that of β-CD reveal a possible interaction between these two species. However, only small changes in the self-diffusion of *trans*-chalcone was observed in the presence of β-CD. This fact and the registered absence of chemical shift displacements of **Ct** resonance signals in the ^{1}H NMR spectra of cy3glc-β-CD strongly suggest a lack of intermolecular interactions between and β-CD.

Table III.4. Diffusion coefficients (*D*) obtained for β-cyclodextrin and for **AH^+**, **B**, ***Cc*** and ***Ct*** equilibrium forms of 1.4 mM cyanidin-3-*O*-glucoside solutions with increasing amounts of β-CD in D_2O at pH 3.5; * undetected.

	***D* x 10^{-10} (m^2s^{-1})**				
Ratio cy3glc:β-CD	**AH^+**	**B**	**C*c***	**C*t***	**B_{CD}**
1:0.0	4.2	5.4	5.5	5.6	-
1:0.8	4.2	5.5	4.0	5.4	3.9
1:1.6	*	5.7	3.9	5.5	3.8
1:2.4	*	5.8	4.0	5.5	3.8
1:3.2	*	5.7	4.0	5.5	3.9

$D_{\beta\text{-CD}}$ x 10^{-10} (m^2s^{-1}) = 4.0;

The flavylium cation diffusion coefficient was almost unchanged and lower than β-CD's during the experiments until the third anthocyanin:β-CD ratio was achieved. At this ratio only traces of the AH^+ equilibrium form was detected, not allowing the correct *D* determination (Table III.4). The results from the analysis of DOSY spectra of the inclusion complex cy3glc:β-CD indicate that only two of the anthocyanin equilibrium forms, **B** and **C*c***, showed preference for association and affinity for intermolecular complex formation with β-CD. These results are in agreement with the observed chemical shifts alterations registered for protons of **B**, **C*c*** and β-CD in ^{1}H NMR spectra of cy3glc:β-CD. The observed changes in the chemical shifts and self-diffusion change for **B** and **C*c*** suggest an inclusion of these species into the cavity of β-CD.

III.3.4. Putative structure of the inclusion complex of cy3glc with β-CD

Beside the chemical shifts changes and changes of diffusion constants initiated by complexation with CD, changes of NOE for the species in the solution serve as a measure of intermolecular binding and inclusion complex formation. Further reliable information on the inclusion complex formation can be obtained by the evaluation of the intermolecular proximity of protons in the guest species to the H3 and H5 protons, located inside of the cyclodextrin cavity by measurements of NOE. Additionally, information can be extracted for the preferred structural arrangement of the guest molecules in the cyclodextrin cavity in the process of inclusion complexes formation.

Therefore, structural investigations based on NOE studies were performed to further determine the behavior and way of interaction of the different forms of anthocyanin co-existing in aqueous solution at pH 3.5 with β-CD and to define the structure of the

cy3glc-β-CD complex. The NOE relies on different correlation times (τ_c) of free and bound molecules and the observation of intermolecular NOE between molecules in solution is a strong indication for intermolecular association processes.

Rotating frame nuclear Overhauser spectroscopy (ROESY) was applied to study solutions containing equimolar amounts of β-CD and cy3glc in D_2O. A number of ROESY experiments using a mixing time in the range between 100 and 800 ms were recorded with the aim to discriminate the NOE originating from the bound state of cy3glc with β-CD (inter-molecular NOE) and NOE of the non-bounded species in the solution (intra-molecular NOE). In the ROESY spectrum, the cross-peak connecting two proton resonances indicates that those proton nuclei are in close proximity in the ground state of the molecule *(224)*. The intensity of the rotating frame nuclear Overhauser effect (ROE) was estimated from the integral volume of the cross-peak and was classified as strong, medium, weak or very weak *(228)*.

Concerning the NOE experiments, a prior ROESY spectrum of cyanidin-3-*O*-glucoside in the absence of β-cyclodextrin was performed (500 ms mixing time). A characteristic intramolecular correlation between the anthocyanin H4 and glucose H1'' was detected. Also very weak correlations could be observed between protons from anthocyanin B-ring and glucose protons revealing the proximity of these two rings (Figure III.14).

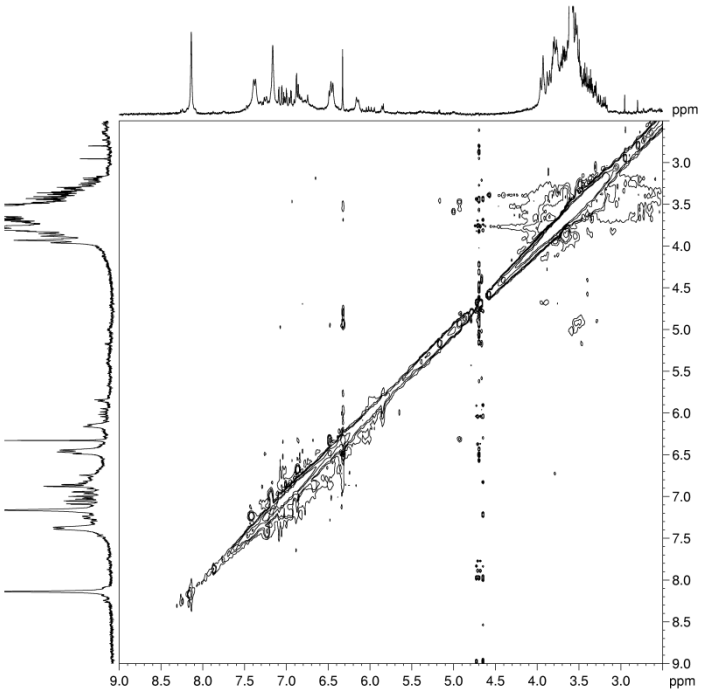

Figure III.14. 2D ROESY (600 MHz) spectra of cy3glc acquired in D_2O (pH 3.5) with a mixing time of 500 ms, showing characteristic intra-molecular NOE interactions.

In transient experiments such as ROESY, the NOE dynamically builds up and then decays due to relaxation during the mixing time. In general, large molecules build-up NOE quickly and the point of maximum NOE is shifted to shorter mixing time while small molecules build-up NOE more slowly. When the mixing time is increased, for larger molecules (such as the complex cy3glc-β-CD) the ROE signal becomes weaker. For this reason, in order to discriminate inter from intramolecular NOE, several ROESY experiments were performed with different mixing times. At lower mixing time (100-200 ms) only inter-molecular interactions could be detected. The analysis of 2D ROESY spectra of cy3glc-β-CD showed correlations between protons of cy3glc's hemiketal form complexed with β-CD and H3 and H5 protons lying on the inner surface of β-CD (Figure III.15). The H3 protons of β-CD shares strong inter-molecular ROE correlations with protons H4 from C-ring and H6' from ring B, medium inter-molecular correlations with proton H2' and weak inter-molecular correlations with proton H5' (also from B ring) of the hemiketal form $\mathbf{B_{CD}}$. H5 of β-CD shares strong ROE correlations with protons H4 (Figure III.15). These observations strongly suggest that the cy3glc's C-ring is deeply included in the β-CD cavity. No NOE interactions were detected between protons from the anthocyanin $\mathbf{B_{CD}}$ with the outer protons H2 and H4. All together, these data suggest that probably the A- and C-ring are included from the wide secondary hydroxyl group side of the β-CD cavity being closer to the narrow rim, whilst the B-ring lies on the plane of the wider rim of β-CD. This type of molecular inclusion had already been described for other polyphenols, namely for (-)-epicatechin gallate (also presenting a catechol B ring) and (-)-epigallocatechin gallate (presenting a pyrogallol B ring) *(224, 228)*.

In this spectrum no dipole-dipole interactions were registered between protons of the flavylium cation and *trans*-chalcone equilibrium forms and β-CD. However, small but detectible NOE was observed between characteristic protons of *cis*-chalcone and β-CD's H3. The structural similarity of the two equilibrium forms $\mathbf{B_{CD}}$ and **C*c*** was assumed to be a reason for their similar behavior in a presence of CD. The presence of a tetrahedral carbon atom in the neutral hemiketal makes it much less rigid then the almost planar flavylium cation and probably allows a closer fit to the macrocyclic cavity. Additionally, for the charged and highly polar flavylium cation the relative desolvation of the guest molecule when it enters the cyclodextrin cavity is probably more endothermic. In the *cis*-chalcone the presence of an open chain probably also allows a better molecular inclusion in the hydrophobic cyclodextrin cavity.

In the 2D ROESY spectra recorded at longer mixing time (500 and 800 ms) weak intramolecular interactions between the anthocyanin protons were observed in the aromatic spectral area besides weak intermolecular dipole interaction between **B_{CD}** and **C*c*** with the interior β-CD cavity protons.

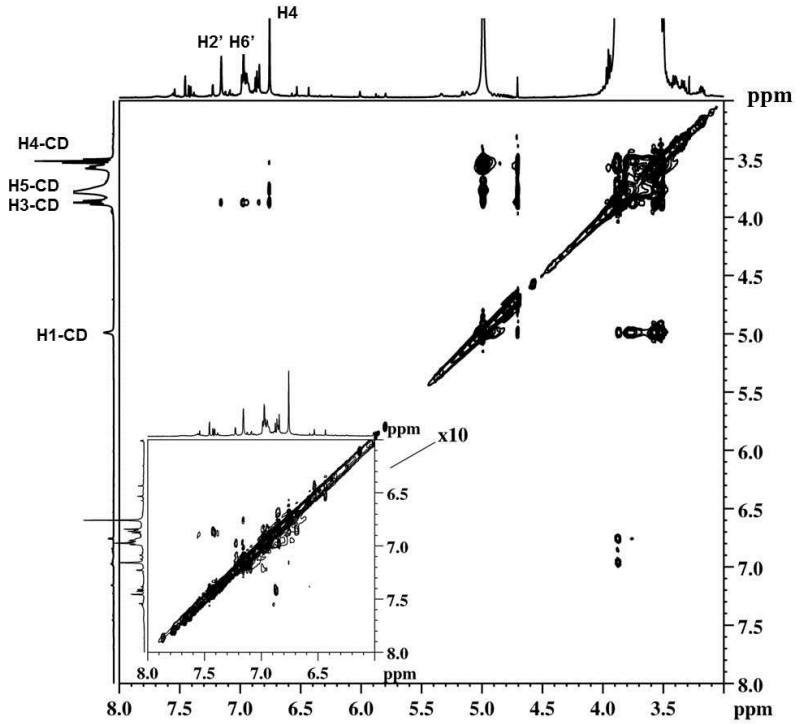

Figure III.15. 2D ROESY (600 MHz) spectra of cy3glc-β-CD (1:1) acquired in D_2O (pH 3.5) with a mixing time of 500 ms, showing characteristic inter- and intra- (expanded spectral area) molecular NOE interactions in the complex. The assignment of resonances of B_{CD} and β-CD is included.

III.3.5. Structure of the inclusion complex cy3glc-β-CD by Molecular Dynamics simulation studies

To better understand the inclusion of the hemiketal cy3glc form in the hydrophobic β-CD's internal cavity, computational studies were additionally carried out. An MD simulation of 30 ns was performed for this complex, which allowed the respective conformational space to be sampled. The last 20 ns of this MD simulation were used for the subsequent structural analysis. The root-mean-square deviation (RMSD) value obtained for this compound was 2.92 ± 0.62 Å. This small value reveals higher equilibration and stability of this complex during the MD simulation. Figure III.16 shows the closest structure to the average geometry of cy3glc-β-CD complex, which is in good agreement with the data obtained in the NMR studies.

In order to measure the movement of the cy3glc molecule relative to the average structure over the whole simulation, root-mean-square fluctuation values by atom were also calculated. Analyzing these values it was noticed higher RMSF values for the main hydroxyl groups of the glucose unit and the HO-C3' group of the B ring, as well as for the H5' and H6' atoms which reveal a higher degree of flexibility during the MD simulation. The dynamic behavior of these atoms agrees with their previously referred close contact with solvent molecules.

To clarify the binding and inclusion mode of cy3glc-β-CD complex, the distances between all H atoms of A-, B- and C- rings of the hemiketal and the H1, H2, H3, H4 and H5 atoms of each glucose unit from the β-CD were also calculated during the MD simulation. Table III.5 shows the average distances of the closest contacts between the hydrogen atoms of cy3glc and the β-CD molecules. As seen in the Molecular Dynamics simulation, the binding and inclusion of cy3glc in the cavity of β-CD are ensured by the establishment of hydrophobic interactions between the polyphenolic and glucose rings, as well as hydrogen bonds with the hydrophilic hydroxyl polar groups of both compounds. All these crucial interactions contribute to the formation and stabilization of this complex. As seen in Figure III.16, the A- and C- nucleus of cy3glc provide the major contribution to the binding driving force, followed by the B-ring, whilst its glucose residue seems to perturb the cy3glc's inclusion in the β-CD and is facing the solvent. Similarly to the present NMR studies, these results also reveal a higher proximity between the H4, H2', H5' and H6' atoms of cy3glc and the internal H3 and H5 atoms of several glucose units, in particular the Glc3, Glc5 and Glc7 units. It was also obtained large distances to the outer H1, H2 and H4 atoms of β-CD, and it is noteworthy that the H6 at the A-ring of cy3glc is very distant to the hydrogen atoms of β-CD and directed to the solvent molecules during the whole simulation (data not shown).

Table III.5. Distance values obtained for the closest contacts between the hydrogen atoms of cy3glc and β-CD compounds.

Atom of cy3glc	Atom of β-CD	Distance (Å)
H4	H3-Glc7 and H5-Glc7	3.29 ± 1.02 and 3.22 ± 0.82
H6	-	-
H8	H3-Glc3 and H5-Glc3	3.60 ± 1.24 and 2.93 ± 0.93
H2'	H3-Glc5	4.87 ± 1.47
H5'	H3-Glc5	4.66 ± 1.77
H6'	H3-Glc5	4.56 ± 1.65

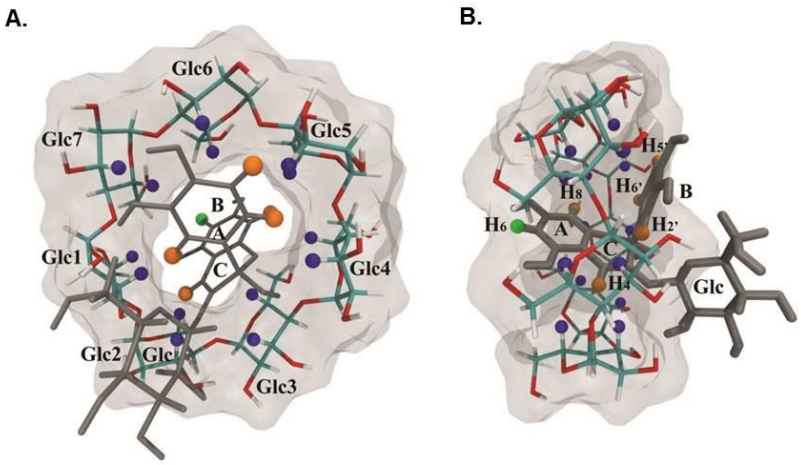

Figure III.16. Structure of cy3glc-β-CD complex in front-view (**A**) and side-view (**B**). The β-CD is represented with surface and colored by atom type, the cy3glc is represented with sticks and colored in gray. All H_3 and H_5 protons of each glucose unit from β-CD are colored in blue, while the nonpolar hydrogen atoms from the cy3glc are colored in orange (H4, H8, H2', H5' and H6') and green (H6).

To better characterize this cy3glc-β-CD inclusion mode, the solvent-accessible surface area (SASA) values for some nonpolar H atoms of both cy3glc (H4, H6, H8, H2', H5' and H6') and β-CD (H1, H2, H3, H4 and H5) molecules during the MD simulation were calculated. The SASA defines the surface area of a group/atom that is accessible to a solvent probe and indicates which atoms are most exposed to the solvent.

Table III.6 shows the obtained SASA values with standard deviations for each atom. As expected, the outer H1, H2 and H4 atoms of β-CD have shown higher values. On the other hand, the internal H3 and H5 atoms present smaller values of SASA, which agrees with the hydrophobic environment of β-CD's cavity. Relatively to the cy3glc molecule, the higher SASA value was obtained for the H6 atom (7.82 ± 2.83 $Å^2$), which indicates that this specific atom is highly exposed to the solvent. On the other hand, minimal SASA values were obtained for H4, H8, H2', H5' and H6'. According to the SASA values obtained, a higher protection of H4, H8, H2', H5' and H6' atoms was noticed due to the interaction with the β-CD molecule. Therefore, the hydrophilic environment around the H6 of cy3glc point out by this data demonstrates that this atom is proximal to solvent water molecules and is directed to the exterior of the β-CD cavity.

Table III.6. SASA values obtained for several hydrogen atoms of cy3glc and β-CD molecules.

Atom	SASA (Å^2)
H1-Glc of β-CD	74.55 ± 4.89
H2-Glc of β-CD	108.42 ± 3.85
H3-Glc of β-CD	2.03 ± 3.37
H4-Glc of β-CD	44.90 ± 3.98
H5-Glc of β-CD	0.20 ± 0.56
H4 of cy3glc	0.03 ± 0.32
H6 of cy3glc	7.82 ± 2.83
H8 of cy3glc	0.05 ± 0.28
H2' of cy3glc	2.26 ± 2.63
H5' of cy3glc	5.34 ± 3.43
H6' of cy3glc	2.61 ± 3.54

III.4. Conclusion

Nuclear Magnetic Resonance analysis and Molecular Dynamics simulation performed in this study have clearly proved the selective inclusion of the anthocyanin hemiketal form into the β-CD cavity. This assumption was based on the anthocyanin chemical shift alteration after complexation with β-CD, decrease on the diffusion coefficient of the hemiketal equilibrium form to values close to the corresponding values of β-CD and on the observed NOE effect between this equilibrium form with CD's interior protons. The computational data support and clarify the successful inclusion of the cy3glc molecule inside the hydrophobic cavity of β-CD proposed by the present experimental studies.

The results achieved offer a contribution to the elucidation of the formation and the structure of inclusion complexes between the equilibrium network of anthocyanins forms and cyclodextrins increasing the knowledge regarding the phenomena that drive the stabilization of these natural colorants.

C - Molecular inclusion of synthetic flavylium compounds in β-cyclodextrin

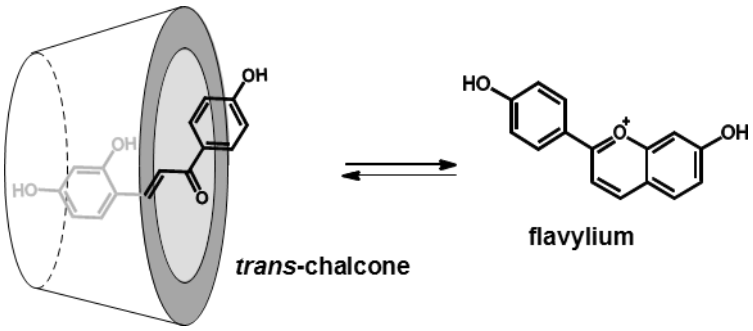

Adapted from:

Gago, S., Basílio, N., Fernandes, A., de Freitas, V., Quintas, A., Pina, F.
Photochromism of the complex between 4'-(2-hydroxyethoxy)-7-hydroxyflavylium and β-cyclodextrin, studied by ^{1}H NMR, UV-Vis, continuous irradiation and circular dichroism, *Dyes and Pigments*, **2014,** *110*, 106-112. doi: *10.1016/j.dyepig.2014.04.038.*

Basílio, N., Fernandes, A., de Freitas, V., Gago, S., Pina, F.
Effect of β-cyclodextrin on the chemistry of 3',4',7-trihydroxyflavylium, *New Journal of Chemistry*, **2013**, *37*, 3166-3177. doi: *10.1039/C3NJ00588G.*

Petrov, V., Stanislav, S., Petrov, I., Fernandes, A., de Freitas, V., Pina, F.
Emptying the β-Cyclodextrin Cavity by Light. Photochemical Removal of the Trans-Chalcone of 4',7-Dihydroxyflavylium, *Journal of Physical Chemistry A,* ***2013****, 117 (41),* 10692–10701. doi: *10.1021/jp4060582.*

With the exception of the flavylium synthesis, the experimental design and work described in this part was carried out by the author.

III.1. Introduction

Synthetic flavylium salts and anthocyanins are both derivatives of 2-phenyl-1-benzopyrylium (Figure III.17). These compounds have several applications, mainly as "greener" colorants, both as food colorants and as dyes. More recently, flavylium salts have found new and high-tech applications, namely in solar energy conversion *(97)*.

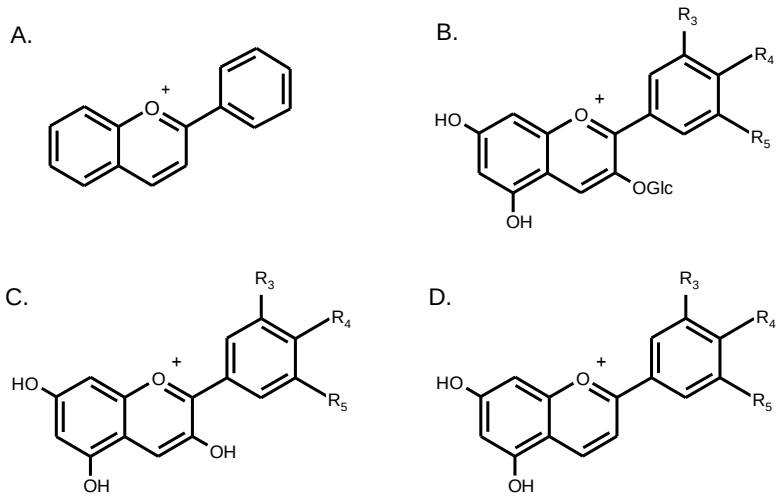

Figure III.17. 2-phenyl-1-benzopyrylium derivatives: flavylium (**A**); anthocyanin (**B**); anthocyanidin (**C**); deoxyanthocyanindin (**D**). R groups can be H, OH or OCH_3.

Synthetic flavylium salts have been associated with natural anthocyanins as the pH and light-dependent network of chemical reactions involving synthetic flavylium compounds is basically identical to that exhibited by natural anthocyanins in acidic and neutral media (Figure II.14). Moreover, the information acquired for the kinetic processes that occur in synthetic flavylium salts have forced a correction of the models and interpretations used for anthocyanins *(236)*. For instance, it is a matter of fact that in the case of common anthocyanins the mole fraction of *trans*-chalcone is very small and by consequence the study of the *cis-trans* isomerization is better carried out if the appropriate synthetic flavylium compounds are used. Bearing this, synthetic flavylium salts can behave as model compounds for natural anthocyanins with the study of these compounds being relevant to the comprehension of the anthocyanins chemistry *(97)*.

For the synthetic flavylium compounds at very low pH values the flavylium cation is the most stable species. After a direct pH jump from equilibrated solutions of the flavylium cation (pH<1) to higher pH values, the base is immediately formed (proton transfer) because the competitive reaction leading to hemiketal is much slower. For example immediately after a pH jump to pH=4.0 equal concentrations of $\mathbf{AH^+}$ and **A**,

are obtained. However for synthetic flavylium salts, and on the opposite to what happens in the most common anthocyanins in which the hemiketal is the major specie at the equilibrium, the most stable species at this pH value is the *trans*-chalcone, and the system evolves to this form at expenses of **AH$^+$** and **A** *(89, 95)*.

The possibility of incorporating anthocyanins and related compounds in matrices such as zeolites, gels and ionic liquids *(237, 238)* have been explored in recent years *(97, 239)*. One of the results of these studies is that the photochromic properties of some synthetic flavylium compounds can be modulated by the nature of the matrices. Among different matrices, cyclodextrins have a great potential for the incorporation of flavylium derivatives because the truncated-shape cone of these oligosaccharides, possess an hydrophilic outer surface and a cavity more or less apolar which makes it ideal to form host-guest inclusion complexes. Moreover, CDs have been widely employed as additives in food, cosmetics and pharmaceutical industries and are thus promising matrices for several applications *(153, 240)*.

In spite of the fact that cyclodextrins promote discoloration of anthocyanins, the so-called anti-copigmentation effect *(143, 144)*, the nature of the species that are stabilized is not yet perfectly identified. Therefore, it is important to clarify the structures of the inclusion complexes from a view point of substrates within the hydrophobic cavities of CD in aqueous solution. In this work the formation of molecular inclusion complexes and the identification of the network species preferentially stabilized by the host (β-CD) were studied through NMR experiments. The model compounds for anthocyanins, 4',7-dihydroxyflavylium, 3',4',7-trihydroxyflavylium and 4'-(2-hydroxyethoxy)-7-hydroxyflavylium were selected (Figure III.18).

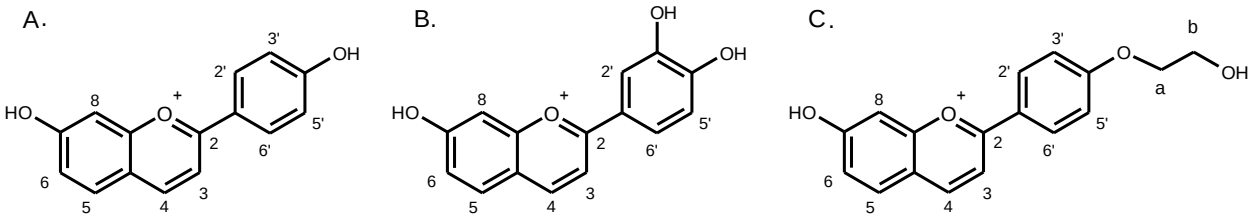

Figure III.18. Chemical structure of 4',7-dihydroxyflavylium (**A**), 3',4',7-trihydroxyflavylium (**B**) and 4'-(2-hydroxyethoxy)-7-hydroxyflavylium (**C**).

III.2. Materials and Methods

III.2.1. Materials

β-CD, D_2O (99.9%) was purchased from Sigma-Aldrich® (Madrid, Spain). NaOD (99.5%) was purchased from Euriso-top® The compounds 4',7-dihydroxyflavylium, 3',4',7-trihydroxyflavylium and 4'-(2-hydroxyethoxy)-7-hydroxyflavylium were synthesized according to the method of Katritzky *(241)*.

III.2.2. NMR samples preparation

To evaluate the interaction between the different equilibrium forms of 4',7-DHF, 3',4',7-THF and 4'-(2-hydroxyethoxy)-7-HF and β-cyclodextrin and to study the inclusion complex formation, approximately 1mM of the macrocycle was dissolved in D_2O at room temperature. Each synthetic flavylium was added at a molar ratio of 1:1 and pH was adjusted to 3.5 by the addition of NaOD. The samples were allowed to equilibrate for at least 12 hours before performing the NMR experiments.

III.2.3. NMR spectroscopy

NMR experiments were recorded on a Bruker Avance III 600 HD or on a Bruker Avance II 400 spectrometer, equipped with 5 mm Cryoprobe Prodigy or PABBO BB probe and pulse gradient units, capable of producing magnetic field pulsed gradients in the z-direction of 50 G/cm or 53 G/cm, respectively. The NMR measurements have been done with standard BRUKER pulse sequences, in D_2O, at 300K and at pH 3.5. ^1H NMR experiments were performed with water suppression using excitation sculpting with gradients *(210)*, acquisition time 1.36 s (or 2.56 s), relaxation delay 2 s (or 1 s), 128 or 256 transients of a spectral width of 10000 Hz (or 5342 Hz) were collected into 32 K time domain points. Typical measuring conditions for the $^1H/^1H$ and 2D spectra (COSY and ROESY) recorded in phase sensitive mode and with water suppression were: relaxation delay 2 s, 64-128 scans, a total 2K data points in *F*2 and 256 data points in *F*1. ROESY experiments were carried out using an intermediate mixing time of 500 ms in the phase-sensitive mode. 2D $^1H/^{13}C$ HSQC and HMBC experiments were carried out with a spectral width of *ca* 10000 Hz (or 6410 Hz) for 1H and 32000 Hz (or 20125 Hz) for 13C, relaxation delay 1.5 s, Fourier Transform (FT) size 2 K × 1K.

III.3. Results and Discussion

III.3.1. NMR spectral characterization

Prior to the study of the interaction between the synthetic flavylium compounds and β-cyclodextrin, a NMR spectral characterization of the equilibrium forms of 4´,7-DHF, 3',4',7-THF and 4'-(2-hydroxyethoxy)-7-HF in aqueous solution at pH 3.5 was performed. Separation of the ^{1}H NMR peaks of each species is possible whenever the rate of interconversions between the several species is slow in comparison with the ^{1}H NMR timescale. This is generally observed for all the processes except for the proton transfer reaction. In this case flavylium cation (**AH^{+}**) is in rapid exchange with quinoidal base (**A**) and the peaks appear in a single set *(96)*.

According to what it was expected based on the network of chemical reactions taking place in these synthetic flavylium salts, the ^{1}H NMR spectra enable one to identify the flavylium cation (in fast equilibrium with quinoidal base) and the *trans*-chalcone (Figure III.19). The assignment of the resonances corresponding to these equilibrium forms was established on the analysis of the mono and bi dimensional (COSY, HSQC, HMBC) NMR spectra. Long range correlations in the ^{1}H/^{13}C HMBC spectra between protons H2',6', H3 and H4 with the carbon C2 at 193 ppm (carbonyl group) were observed, that are in agreement with the presence of the *trans*-chalcone form. Additionally, the isomer *trans* was recognized based on the large coupling constant of 16 Hz between the vicinal protons, H4 and H3. For both equilibrium species, proton H8 was assigned by the observation of a splitting of 2.2 Hz due to long range coupling to proton H6 while proton H4 was assigned based on the observation of a coupling constant of 8.9 Hz due to coupling to proton H3 (only for AH^{+} equilibrium form). Assignment of resonances due to protons H2',6' and protons H3',5' in the two different forms (for 4',7-DHF and 4'-(2-hydroxyethoxy)-7-HF) follows from the relative intensity of two protons expected from these equivalent nuclei. The proton chemical shifts, coupling constants and carbon chemical shifts for the two equilibrium forms of the three synthetic flavylium compounds are presented in Table III.7.

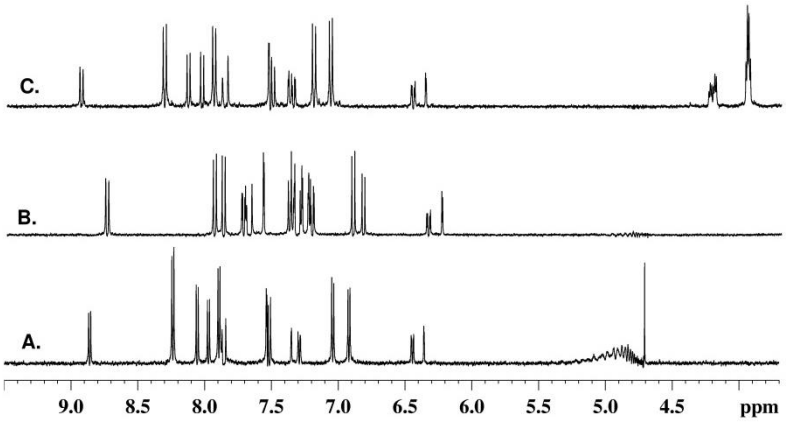

Figure III.19. Expanded ^{1}H spectra of 4´,7-DHF (**A**), 3',4',7-THF (**B**) and 4'-(2-hydroxyethoxy)-7-HF (**C**) in D_2O, at pH 3.5.

Table III.7. ^{1}H and ^{13}C chemical shifts and coupling constants for the two equilibrium forms of 4'-7-DHF, 3',4',7-THF and 4'-(2-hydroxyethoxy)-7-HF in D_2O at pH3.5; *d*, duplet; *dd*, double duplets; *t*, triplet.

4',7-DHF	**Flavylium cation (AH^+)**		***Trans*-chalcone (C*t*)**	
	^{1}H δ (ppm) / *J*(Hz)	^{13}C δ (ppm)	^{1}H δ (ppm) / *J*(Hz)	^{13}C δ (ppm)
H3	8.06 *d (8.9)*	111.9	7.52 *d (16.1)*	119.0
H4	8.86 *d (8.9)*	152.6	7.86 *d (16.1)*	140.9
H5	7.97 *d (9.0)*	132.1	7.54 *d (8.9)*	131.3
H6	7.29 *dd (9.0; 2.2)*	121.3	6.44 *dd (8.9; 2.4)*	108.5
H8	7.35 *d (2.2)*	102.3	6.34 *d (2.4)*	102.7
H2',6'	8.24 *d (9.1)*	132.1	7.89 *d (8.9)*	131.4
H3',5'	7.04 *d (9.1)*	117.0	6.92 *d (8.9)*	115.4
3',4',7-THF	**Flavylium cation (AH^+)**		***Trans*-chalcone (C*t*)**	
	^{1}H δ (ppm) / *J*(Hz)	^{13}C δ (ppm)	^{1}H δ (ppm) / *J*(Hz)	^{13}C δ (ppm)
H3	7.94 *d (9.0)*	112.1	7.33 *d (15.9)*	118.2
H4	8.75 *d (8.9)*	152.1	7.69 *d (16.0)*	140.7
H5	7.88 *d (9.0)*	132.2	7.38 *d (8.8)*	131.2
H6	7.21 *dd (9.0; 2.2)*	121.0	6.34 *dd (8.8; 2.2)*	108.4
H8	7.24 *d (2.0)*	102.3	6.24 *d (2.2)*	102.5
H2'	7.57 *d (2.2)*	115.1	7.29 *d (2.2)*	115.4
H5'	6.91 *d (8.9)*	116.8	6.83 *d (8.6)*	115.1
H6'	7.73 *dd (8.7; 2.2)*	124.7	7.36 *dd (8.8; 2.2)*	123.1
4'-(2-hydroxyethoxy)-7-HF	**Flavylium cation (AH^+)**		***Trans*-chalcone (C*t*)**	
	^{1}H δ (ppm) / *J*(Hz)	^{13}C δ (ppm)	^{1}H δ (ppm) / *J*(Hz)	^{13}C δ (ppm)
H3	8.04 *d (9.8)*	112.0	7.42 *d (16.2)*	118.6
H4	8.84 *d (9.8)*	153.0	7.76 *d (16.2)*	141.4
H5	7.94 *d (9.2)*	132.5	7.43 *d (9.0)*	131.1
H6	7.26 *dd (9.1; 2.2)*	121.2	6.36 *dd (8.8; 2.3)*	108.3
H8	7.29 *d (2.2)*	102.3	6.26 *d (2.3)*	102.3
H2',6'	8.22 *d (9.3)*	132.1	7.85 *d (9.1)*	130.8
H3',5'	7.10 *d (9.3)*	116.1	6.98 *d (9.3)*	114.3
a	4.14 *t (4.4)*	69.6	4.10 *t* (4.4)	69.3
b	3.85 *t (4.6)*	59.5	3.85 *t* (4.6)	59.6

III.3.2. NMR analysis of the inclusion complexes with β-CD: putative structure of the inclusion complexes

Preliminary indications of the formation of inclusion complexes can be derived from the changes in the chemical shift of the guest molecule or of β-cyclodextrin in the ^{1}H NMR spectra. Such chemical shift changes may provide valuable insight into the molecular conformation of the inclusion complexes *(242)*. From the standpoint of the induced chemical shifts of the aromatic protons of 3',4',7-THF in the presence of β-cyclodextrin a clear intermolecular interaction between the *trans*-chalcone and the cyclodextrin could be assumed. Upon the addition of 3',4',7-THF to an aqueous solution of β-cyclodextrin, a downfield shift of the protons of the *trans*-chalcone equilibrium form was observed, with this shift being most prominent for H8 and H4 (0.09 and 0.07 ppm, respectively). This chemical shift alteration may result from the contact, namely from a steric compression effect *(230)*. Regarding the flavylium cation equilibrium form, the proton signals were not differentiated from their initial position or suffered a slight upfield shift upon addition of cyclodextrin, thus indicating a lack of interaction with β-CD Similar chemical shift alteration could be observed for the other two synthetic flavylium salts.

In order to investigate the selective inter-molecular interactions between the synthetic flavylium equilibrium forms with β-cyclodextrin and to determine a more detailed structure of the 1:1 complex, a proton-proton NOE experiment was performed. Rotating frame nuclear Overhauser spectroscopy (ROESY) was applied in order to investigate the structure of the synthetic flavylium salts-β-CD inclusion complex in aqueous solution at pH 3.5 and at equimolar amounts. An intermediate mixing time of 500 ms was selected in order to discriminate the intra and inter-molecular NOEs effects and the evaluation of the intermolecular proximity of protons in the guest specie (synthetic flavylium) to the protons located inside of the cyclodextrin cavity (H3-CD, H5-CD and H6-CD) was performed.

An expanded region of 2D ROESY (600 MHz) spectra of 4´,7-DHF-β-CD complex (1:1) showing the selected intermolecular ROE's between β-cyclodextrin protons and the aromatic protons of 4',7-DHF is shown in Figure III.20 (expanded spectral area).In the 2D ROESY spectra of the complex 4',7-DHF-β-CD, inter-molecular interactions were detected only between the *trans*-chalcone form and β-cyclodextrin. Indeed strong rotating frame nuclear Overhauser effect (ROE) correlations between H3-CD and H5-

CD of β-CD (protons lying on the inner surface of the macrocyclic) and the protons H2',6' and H3',5' for the *trans*-chalcone were detected. The H5-CD also shares important inter-molecular correlations with H3 and with protons H5 and H6 belonging to the A-ring. H3 is also slightly correlated with H3-CD from β-CD. Proton H8 evidences a weak inter-molecular correlation with β-CD's H6-CD proton located in the top of the narrow rim. Collectively, the ROEs correlations observed suggest that the A-ring and H3 of *trans*-chalcone are deeply included in the β-CD cavity. The correlations observed also propose that this ring is closer to the narrow rim of β-CD while B ring is closer to the wide rim. No interactions between the β-CD outer protons (H2-CD and H4-CD) and the *trans*-chalcone protons were detected. Moreover, flavylium cation does not interact at all with β-cyclodextrin as no inter-molecular correlation could be observed between these two species (^{1}H signal labelled with the symbol *).

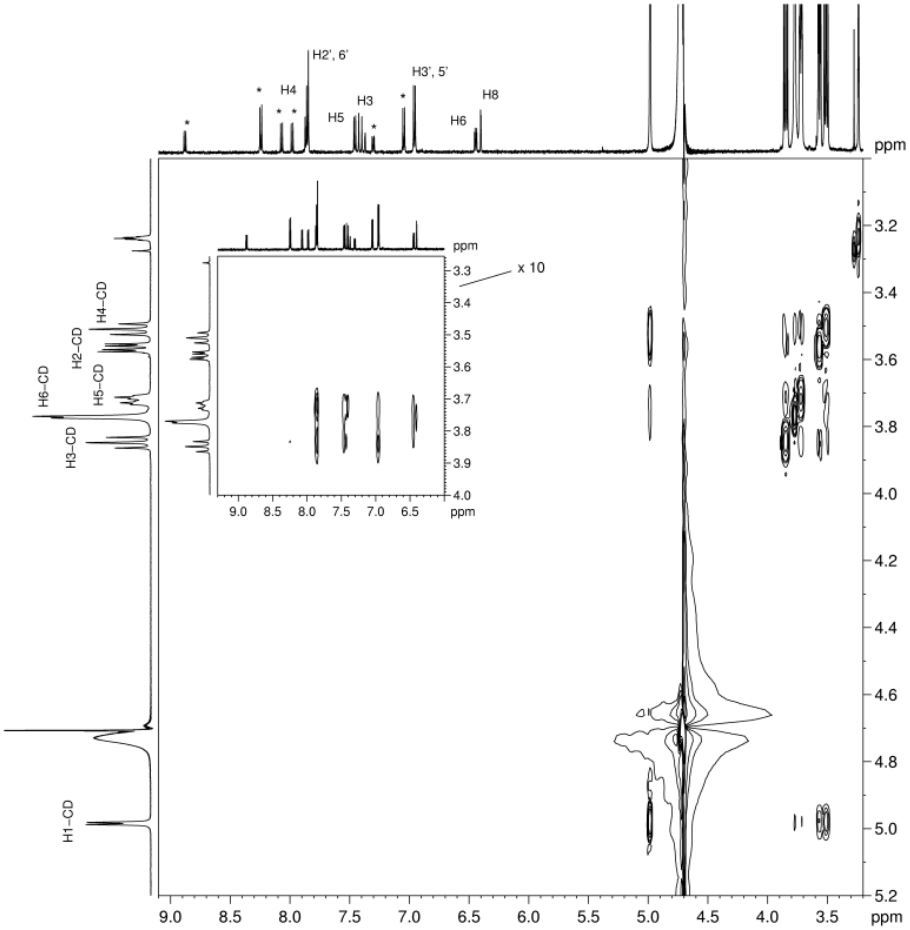

Figure III.20. Expanded region of 2D ROESY (600 MHz) spectra of 4´,7-DHF-β-CD complex (1:1) showing the selected intermolecular ROE's between β-CD protons and the *trans*-chalcone aromatic protons of 4',7-dihydroxyflavylium. The assignment of the resonances peaks of the *trans*-chalcone form was included while the peaks corresponding to the flavylium cation were labeled in the spectrum with the symbol (*).

Concerning the other two synthetic flavylium salts studied, similar results could be obtained regarding the equilibrium specie preferentially interacting with β-CD. In the 2D ROESY spectra no inter-molecular interactions between β-cyclodextrin and the flavylium cation were detected a clear evidence of the lack of contact between these two molecules. In contrast, correlations between the aromatic protons of HF's *trans*-chalcone and β-cyclodextrin were observed, suggesting an intermolecular interaction between these molecules. (Figure III.21).

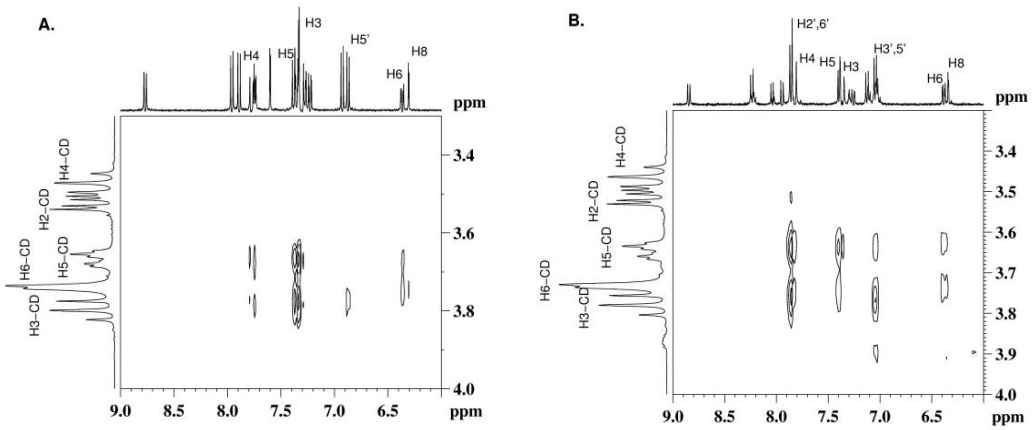

Figure III.21. Expanded region of 2D ROESY (400 MHz) spectra of 3',4´,7-THF-β-cyclodextrin complex (left) showing the selected inter-molecular ROE's between β-CD protons and the *trans*-chalcone aromatic protons of 3',4',7-THF. Expanded region of 2D ROESY (400 MHz) spectra of 4´-(2-hydroxyethoxy)-7-HF-β-cyclodextrin complex (right) showing the selected inter-molecular ROE's between β-CD protons and the *trans*-chalcone aromatic protons of 4´-(2-hydroxyethoxy)-7-HF. The other ^{1}H signals in the spectra correspond to the flavylium cation equilibrium form.

Strong intermolecular interactions between H6-CD from β-cyclodextrin located in the top of the narrow rim and protons H6 and H8 from 3',4',7-THF's A ring were detected. Proton H6 also shares a correlation with H5-CD, suggesting that this ring is deeply included in β-cyclodextrin's cavity close to the primary hydroxyl group side, being closer to the narrow rim. The H5-CD also shares intense inter-molecular correlations with protons H4, H3 and H5. These protons are also slightly correlated with H3-CD from β-cyclodextrin. Proton H5', belonging to the flavylium B ring evidences a strong intermolecular correlation with β-cyclodextrin's H3-CD proton. Regarding protons H2' and H6' no information could be obtained due to the overlapping of the signals. However based on the inter-molecular correlations detected for H5' it could be assumed that this ring is closer to β-cyclodextrin's wide rim. No interactions between the β-CD outer protons (H2-CD and H4-CD) and the *trans*-chalcone protons were detected, a clear evidence of inclusion complex formation.

In the 2D ROESY spectra of the complex 4'-(2-hydroxyethoxy)-7-HF-β-cyclodextrin strong inter-molecular interactions between β-cyclodextrin internal protons and the *trans*-chalcone were clearly observed. Besides this, no interactions between the outer protons (H2-CD and H4-CD) and the *trans*-chalcone protons were detected, a clear evidence of inclusion complex formation.

Regarding the *trans*-chalcone A ring, correlations between H6 and H8 and H6-CD (primary interaction) and H5-CD (weaker interaction) of β-cyclodextrin were clearly distinguished. For the H5 proton a strong interaction with H5-CD and a weaker interaction with H6-CD was detected, which suggests that this part of the molecule is deeply included in β-cyclodextrin's cavity. Regarding protons H4 and H3, strong correlations were detected with H5-CD. The former is also slightly correlated with H6-CD from β-cyclodextrin suggesting again a higher penetration in the macrocyclic. For the protons located in the *trans*-chalcone B ring, strong intermolecular interactions were detected with β–CD's H3-CD and H5-CD protons. Collectively, the ROEs correlations observed propose that the A ring and proton H_4 are deeply included in the cavity being closer to the narrow rim while protons belonging to the B ring are located closer to β-cyclodextrin's wide rim. Concerning the 4' substituent (4.14-3.85 ppm) no interaction was detected with β-cyclodextrin's protons and it could be assumed that this part of the molecule is outside cyclodextrin's cavity.

Compared to similar compounds (4',7-DHF and 3',4',7-THF) the results obtained in the 2D ROESY experiments suggest a higher penetration of this compound and a more efficient interaction between the guest and the host molecule probably due to the decreased polarity.

Based on the inter-molecular interaction observed in the 2D ROESY a possible structure of the inclusion complex 4',7-DHF-β-cyclodextrin is shown on Figure III.22. Similar molecular structures could be obtained for the other synthetic flavyliums.

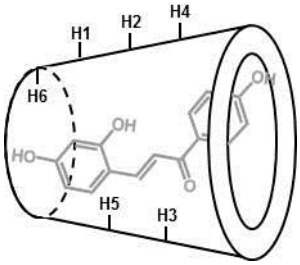

Figure III.22. Possible structure of the inclusion complex of the *trans*-chalcone form of 4',7-DHF and β-CD in D_2O, based on NMR data.

III.4. Conclusion

Through the analysis of the 2D ROESY it was clear the preferential inclusion of one of the equilibrium forms of the synthetic flavylium salts into β-CD cavity. In fact, while the *trans*-chalcone is included in the cyclodextrin cavity as the NMR data strongly indicate, the flavylium cation does no interact with the macrocycle. This could be due to the higher flexibility of the former equilibrium form which allowed the formation of inclusion complexes. Collectively, the results obtained proposed a molecular structure where the synthetic flavylium salts A ring are deeply included in β-CD´s cavity, while the B ring is closer to cyclodextrin wider rim. Decreasing polarity of the guest molecule seems to provide a higher penetration into the host cavity.

IV. INTERACTION BETWEEN ANTHOCYANINS AND CARBOHYDRATES FROM PLANT CELL WALLS

A - Understanding the molecular mechanism of anthocyanins binding to pectin

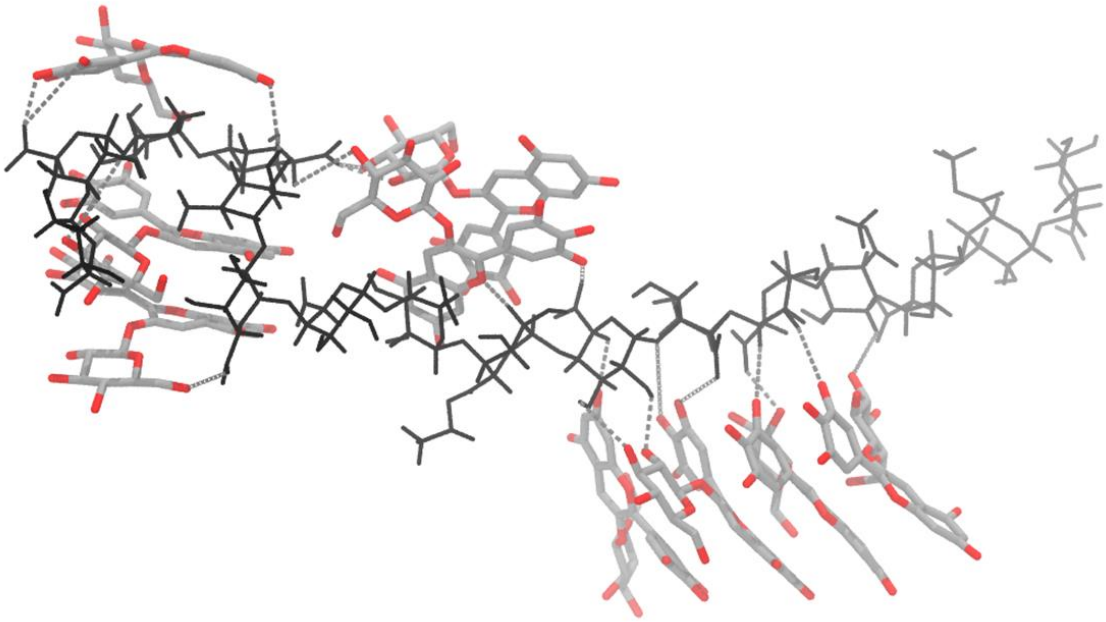

Adapted from:

Fernandes, A., Brás, N., Mateus, N., de Freitas, V.
Understanding the molecular mechanism of anthocyanins binding to pectin*, Langmuir*, **2014***, 30* (28)*, 8516-8527.*
doi: 10.1021/la501879w.

With the exception of the pectin purification and the computational calculations the experimental design and work described in this part was carried out by the author.

IV.1. Introduction

The main interest on anthocyanins arises from their role as water-soluble plant pigments which potentiated its utilization as natural colorants in the food and other industries *(4)*. Another noteworthy property of anthocyanins is their broad range of biological properties, playing an essential role in the prevention of several diseases such as neurological and cardiovascular illnesses, cancer and diabetes *(243)*. Nevertheless, anthocyanins are highly instable and susceptible to degradation *(5)* and their successful application by several industries mainly depends on anthocyanins chemical stability improvements *(91, 137)*. For instance, the color of these compounds is highly pH dependent, due to changes in the concentration of the equilibrium species present in acidic and neutral aqueous solutions (Figure II.14).

Moreover, the interaction between food ingredients such as carbohydrates and anthocyanins has been shown to affect pigments stability and also to modify the equilibrium and rate constants of the flavylium network *(13, 140, 154, 244)*. From a food industry and nutrition perspective, the interaction between anthocyanins and carbohydrates may be relevant since these pigments are biosynthetized in a polysaccharide rich environment where intensive contact between these compounds may occur *(147, 148, 245)*. In fact, anthocyanins are mainly located within the vacuole of the plant cell and with the disruption of plant tissues during the processing of fruits and vegetables an interaction between constituents of cell walls and of the vacuoles may occur *(149)*. As a result, anthocyanins present within plant tissue have the potential to interact with compounds of cell walls particularly pectins, affecting anthocyanins extractability, bioavailability, their color properties and their chemical stability *(147, 156)*.

Pectin is a heterogeneous and complex polysaccharide found in the primary cell walls and middle lamellae of most higher plants, where they give mechanical strength and flexibility due to their interaction with other cell wall components *(246)*. The dominant structural feature of pectin is a linear chain consisting of poly-α-(1→4)-D-galacturonic acid (Gal*p*A) with varying degree of esterification (methylation and/ or acetylation) of the carboxylic acid residues. This backbone also called homogalacturonan can be occasionally interrupted by stretches of rhamnogalacturonans from type I and II *(159)*. Rhamnogalacturonans I are formed by the repeating unit of disaccharides →4)-α-D-Gal*p*A-(1→2)-α-L-Rha*p*-(1→), with the rhamnose residues of the RG fractions being esterified by chains composed mainly of

arabinose and galactose *(162, 163)*. RG II possesses a backbone of (1→4) linked α-D-Gal*p* with side chains containing rhamnose and a variety of rare monosaccharides *(164)*. The composition of pectin varies with the source from which it is isolated, as well as with the conditions used during isolation and purification *(247)*. This carbohydrate is a high value functional food ingredient widely used as gelling agent and stabilizer for instance in jams, jellies and spreads *(138)*.

Interaction between anthocyanins and pectins have been mostly examined primarily focusing the pectin effect on color stability and these works have shown a slight stability enhancement *(136, 138, 139, 147, 154, 248)*. This effect was mostly ascribed to intermolecular association between the carboxylic groups of pectin backbone and anthocyanins in a similar manner as calcium ions are bound in pectin *(249)*. However, in the literature information concerning the structural aspects that govern the interaction between anthocyanins and pectins is scarce.

Therefore, the main goal of this work was to study the mechanism governing the binding of two anthocyanins (cyanidin-3-*O*-glucoside and delphinidin-3-*O*-glucoside) and low methoxylated pectin from *citrus* fruit. The study of this interaction was done by UV-Vis spectroscopy and saturation transfer difference nuclear magnetic resonance (STD NMR) spectroscopy. This latter technique has been used to characterize protein-procyanidin interaction with very promising results *(250, 251)*. However, to the best of our knowledge, this is the first time that this technique was applied to study the binding between carbohydrates (pectin) and anthocyanins. The outcomes achieved should provide a better understanding about anthocyanin-pectin binding from a structural point of view and should provide important information for the development and application of anthocyanins in the food industry but also in the pharmaceutical and cosmetic industries.

IV.2. Materials and Methods

IV.2.1. Materials

D_2O (99.9%), DMSO-d_6 (99.8%), DCl (99%), NaCl and pectin from *citrus* fruits, were purchased from Sigma-Aldrich® (Madrid, Spain). NaOD (99.5%) was purchased from Euriso-top®. Acetic acid (100%) and anhydrous sodium acetate (99.5%) were purchased from VWR® and Fluka®, respectively. All aqueous solutions were prepared

with distilled water. An universal buffer of Theorell Stenhagen was prepared by dissolving 2.25 mL of phosphoric acid (85% w/w), 7.00g of monohydrated citric acid, 3.54g of boric acid and 343 mL of 1 M NaOH solution in water (until 1 L completion) *(189)*. Cyanidin-3-*O*-glucoside (cy3glc) and delphinidin-3-*O*-glucoside (dp3glc) were extracted and purified in the laboratory from blackberries (*Rubus fruticosus*) and grapes (*Vitis vinifera*) respectively, as described elsewhere (Figure IV.1) *(188, 252)*.

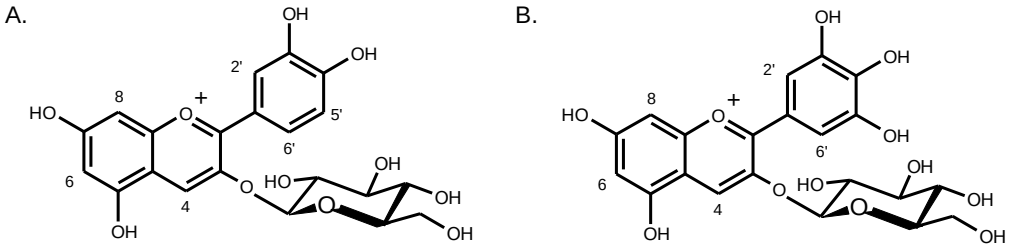

Figure IV.1. Chemical structure of anthocyanins tested in this study (cy3glc, **A** and dp3glc, **B**).

IV.2.2. Purification and analysis of pectin

Pectin from *citrus* fruits was purified by precipitation with ethanol and was analyzed by colorimetric methods and gas chromatography to determine sugar composition and esterification degrees, as described elsewhere *(245, 253, 254)*. According to these analyses it was found that pectin was composed by 85% galacturonic acid, 10% galactose and 5% of other sugars. The degree of methylation and acetylation was determined to be 14% and 1%, respectively.

Molecular weight determination was performed using a Malvern Zetasizer Nano ZS instrument running a Static Light Scattering (SLS) method *(255, 256)*. The samples were studied in sodium chloride at different pectin concentrations at 25º C and the average molecular weight of pectin was found to be 111 kDa.

IV.2.3. UV-Vis absorption spectra

Stock solutions of cy3glc, dp3glc (1.0×10^{-3}M) and pectin from *citrus* fruit (1 $g.L^{-1}$) were prepared at pH 1.5 and 4.0 in acetate buffer (0.1 M). When necessary the pH was adjusted with 1 M NaOH or HCl. Aliquots of 100 μL of the anthocyanin solution were mixed with increasing pectin volumes, corresponding to 0.0–0.4 $g.L^{-1}$ pectin concentration. After equilibration for 120 minutes at 25º C, UV-Vis spectra of the

solution were recorded in 1 nm steps from 360 to 860 nm. Spectrophotometric measurements were carried out in triplicate using a plate reader (Power Wave XS, Bio Tec Instruments) equipped with Gen5 Software.

IV.2.4. pH jumps

The thermodynamic and kinetic constants of a cy3glc-pectin solution were determined by spectrophotometric method, as described elsewhere *(96, 190, 244)*. A stock solution of cy3glc (1.50 x 10^{-4}M) and pectin (4.50 x 10^{-6}M) was prepared in HCl 0.1 M. pH jumps were carried out by adding the necessary amount of NaOH (0.1 M) to neutralize the stock solution of flavylium cation and the necessary amount of an universal buffer solution (at different pH values). The concentration of the buffer (Theorell Stenhagen universal buffer) was maintained low in order to avoid the buffer effects. The absorbance was measured in an UV-vis spectrophotometer (Thermo Scientific Evolution Array UV-vis spectrophotometer) fitted with a thermostated 1.0 cm path length quartz cuvette device at 25º C.

IV.2.5. Dialysis

A dialysis molecular porous membrane tubing (MW cut-off 12-14 KDa, Spectral/Por®) was filled with 4 mL of anthocyanin (cy3glc) and anthocyanin-pectin (cy3glc-pectin) solution and immersed into a flask containing 6 mL of distilled water. The mixtures were prepared at a molar ratio of 16:0 and 16:1 (anthocyanin:pectin) and the pH was adjusted to 1.5 and 4.0. The diffusion of anthocyanins was evaluated by monitoring the absorbance of the dialysate at 512 nm at time 30, 60, 90, 120 and 180 minutes on a UV-Vis spectrophotometer (Thermo Scientific Evolution Array UV-Vis spectrophotometer). The samples were pre-acidified before the absorbance reading. The retention coefficient was calculated for each pH using the equation RC = [1 – (Abs $_{cy3glc:pectin}$ / Abs $_{cy3glc}$)]*100 *(257)*.

IV.2.6. NMR samples preparation

4 μM of purified pectin solution was prepared in DMSO/D_2O (5% DMSO, v/v, 850 μL total volume) and transferred into 5 mm NMR tubes in order to maintain the pectin

concentration constant throughout the STD-NMR experiments. 5% DMSO and temperature of 313 K was used to ensure total anthocyanin solubilization. The anthocyanin solutions at different concentrations were lyophilized and added as a powder, allowing for the same NMR tube to be used for all experiments. Cy3glc and dp3glc were added in the 700 – 4400 μM range. Minimum anthocyanins concentration used in the experiments was restricted by the detection limit for the STD resonances while maximum concentrations tested were limited by anthocyanins solubility. Prior to titration experiments and after the addition of more anthocyanin, the pH of the mixtures was adjusted to 4.0 by the addition of NaOD and DCl. Assays at different pectin concentrations were performed in order to establish the concentration used, limited on the pectin solubility in the NMR solvent and on the solution viscosity. To study the pectin-anthocyanin (cy3glc) interaction at acidic pH (1.5), solutions were prepared in 30% DMSO/D_2O as described before.

IV.2.7. NMR spectroscopy

NMR experiments were recorded on a Bruker Avance III 600 HD spectrometer, operating at 600.13 MHz, equipped with 5 mm CryoProbe Prodigy and pulse gradient units, capable of producing magnetic field pulsed gradients in the z-direction of 50 G/cm. The measurements were done with standard Bruker pulse sequences at 313K. ^{1}H and STD spectra were recorded with a shaped pulse to suppress the water resonance *(258)* using the following parameters: spectral width, 20 ppm; nutation angle, 11 μs and 90º; shaped pulse duration, 2 ms. Selective saturation of pectin off-resonance at 17 ppm and on-resonance at 4.2 ppm was performed through an adaptation of the method described by Gonçalves *et al*. (2011) *(245)*, using a pseudo-two-dimensional (2D) sequence for STD with shaped pulse train alternating between the on- and off-resonances *(259, 260)*. STD-NMR spectra were acquired using EBurp-shaped (pH 4.0) or Gaus 1.1000 (pH 1.5) pulses for selective saturation (50 ms), with a 2.5 μs delay between pulses, which corresponds to a total saturation time of approximately 2.5 s. The number of scans (32), receptor gain value (2050) and relaxation delay (3.5 s) were kept constants*(251)*. To subtract the unprocessed on- and off-resonances spectra, to baseline-correct the resulting difference spectrum and to integrate the areas of cy3glc and dp3glc peaks, the software TopSpin 2.1, Bruker was used.

IV.2.8. Optimization and Molecular Dynamics Simulations

The initial structures of flavylium cation (AH^+_{dp3glc}) and of hemiketal (B_{dp3glc} and B_{cy3glc}) anthocyanin equilibrium forms, were built with the GaussView software *(213)*; whilst the pectin model was constructed with the Glycam Biomolecule Builder *(261)*. The representative model used for pectin has 16 monosaccharide residues with the following sequence: (Gal*p*A-α(1-4))$_{10}$-α(1-4)-Gal*p*A-α(1-2)-Rha*p*-α(1-4)-Gal*p*A-α(1-2)-Rha*p*-α(1-4)-Gal*p*A-α(1-3)-Gal*p*, in which the second and fourth Gal*p*A are methylated, while the eighth Gal*p*A is acetylated. To calculate the optimized geometries and electronic properties for the subsequent parameterization of anthocyanin, the Gaussian 09 suite of programs *(214)* was used. These calculations were performed with the restricted Hartree-Fock method and with the 6-31G (d) basis set. Atomic charges were further recalculated using the RESP algorithm *(215)*. The geometry optimizations and MD simulations were performed using GAFF *(262)* and Glycam2004 force fields *(217-219)* for anthocyanins and carbohydrates, respectively. Explicit solvation (TIP3P water model) was included as a rectangular box with a 12 Å distance between the box edges and any atom within each system. Three MD simulations were performed: the first one with pectin model, 18 flavylium cation molecules (dp3glc) randomly placed around the carbohydrate (with a minimum distance of 20Å) and 7 Cl^- counter-ions; and another two MD simulations with the anthocyanins hemiketal form, (Cy3glc)$_{18}$:pectin and (dp3glc)$_{18}$:pectin systems. The 18 anthocyanins molecules (Cy3glc or dp3glc) were randomly placed around the carbohydrate (with a minimum distance of 20Å) and 11 Na^+ counter-ions. The eighteen anthocyanin molecules used in these simulations reproduce the molar ratio of the experimental conditions used in the NMR studies. All complex geometries were minimized in two stages. Subsequently, an MD simulation of 100 ps at constant volume and temperature, and considering periodic boundaries conditions was runned. This was followed by 45 ns of MD simulation with the NPT ensemble, in which Langevin dynamics was used (collision frequency of 1.0 ps^{-1}) to control the temperature at 303.15 K *(220)*. All simulations were carried out using the AMBER 10.0 simulations package *(216)*. Bond lengths involving hydrogen atoms were constrained using the SHAKE algorithm, and the equations of motion were integrated with a 2 fs time step using the Verlet leapfrog algorithm *(221)*. The Particle-Mesh Ewald (PME) method *(222)* was used to treat long-range interactions, and the nonbonded interactions were truncated with a 10 Å cutoff. The MD trajectories were saved every 2 ps and were analyzed with the PTRAJ module of AMBER 10.0 *(216)* .

IV.3. Results and Discussion

In this work, the interaction between pure anthocyanins and pectin was examined by UV-Vis spectroscopy, saturation transfer difference nuclear magnetic resonance (STD NMR) spectroscopy and Molecular Dynamics simulations (MD). Since cooperative hydrogen bonding (between the oxygen atom of the carbohydrate and the phenolic hydroxyl group) has been recognized to be an important feature for the anthocyanin-pectin interaction *(137)*, this study focused on a fundamental evaluation considering cy3glc and dp3glc exhibiting catechol (two hydroxyl groups) and pyrogallol (three hydroxyl groups) moieties, respectively.

For this study, low methoxylated pectin (14%) from *citrus* fruit was chosen to study the interaction between pectins and anthocyanins. In the literature, some results point out the importance of the degree of esterification of pectins in the stabilization effects of anthocyanins. Indeed, low esterified pectins have shown to provide better anthocyanin stabilization when compared to high esterified pectins *(136, 137, 139, 248)*. On the other hand, some of these works had also revealed that the natural source of pectins is essential for the magnitude of this binding. *Citrus* pectin has been shown to enhance anthocyanins stability, when compared to the corresponding apple pectins or sugar beet pectins. The interaction between anthocyanins and pectin was studied at pH 4.0 and this value was chosen because it is the typical pH of many food matrices *(142, 154)*. At this pH value the neutral hemiketal form (**B**) is expected to be the main equilibrium specie present in solution *(6)*. Since electrostatic forces could also be relevant to the pectin-anthocyanin binding this interaction was also studied in the presence of the flavylium cation at pH 1.5 ($\mathbf{AH^+}$).

To study the binding between these two compounds, STD-NMR spectroscopy was selected. This NMR experiment is a well-known method for probing molecular interactions in solution and it has been widely used to probe low affinity interactions between small ligands and biologically relevant macromolecules (proteins or nucleic acids) *(263, 264)*. Briefly, ligand protons that are in close contact to the receptor (≤ 5Å) receive saturation transfer from the receptor (via spin diffusion, through the nuclear Overhauser effect) and as a result STD NMR signals can be observed. Protons that are not involved in the binding process reveal no STD-NMR signals *(265)*. STD is ideally suitable to receptors with large masses (> 30000 Da) which allow an enhanced spin diffusion and consequently saturation transfer within the receptor and the ligand *(266, 267)*. Thus, the STD was the selected technique to study the interaction between

anthocyanins and pectin. The receptor (pectin from *citrus* fruit) that possesses large molecular mass (~111000 Da, determined by static light scattering – Figure IV.2) should enhance the saturation transfer to the anthocyanin (small ligand, ~500 Da).

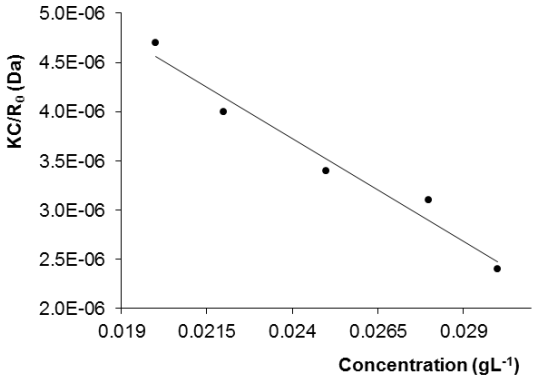

Figure IV.2. Debye plot for molecular weight determination of pectin from *citrus* fruit in sodium chloride.

IV.3.1. UV-Vis absorption spectra

As already reported, much effort has been dedicated to study the interaction between anthocyanins and food carbohydrates, particularly related to anthocyanins stability and color properties *(170, 173, 177)*. Some studies have shown that the presence of mono and polysaccharides produce no change or slightly increase the absorbance of anthocyanin solutions *(139, 140, 154)*. On the other hand, some previous works had shown that the presence of β-cyclodextrin modify dramatically the equilibrium and rate constants of the flavylium network. β-cyclodextrin was shown to promote discoloration of anthocyanins, the so-called anti-copigmentation effect, interacting preferentially with the colorless anthocyanin hemiketal form *(144, 187, 244, 268)*.

In this work, addition of pectin to equilibrated solutions of dp3glc and cy3glc at pH 1.5 and 4.0 does not seem to greatly influence the color of these anthocyanins. Pectin induced a slight increase on anthocyanin visible absorption band λ_{max} (a hiperchromic effect) and a very weak copigmentation effect could be observed (dp3glc: ΔAbs 5% and 11% and cy3glc: ΔAbs 4% and 2% at pH 1.5 and 4.0, respectively). Addition of pectin did not change the shape of the absorption band corresponding to the flavylium form and did not cause any shift in the λ_{max} value. This slight increase could be due to weak hydrophobic interactions occurring between anthocyanins and pectin surface.

Concurrently, to verify the impact of pectin on the equilibrium and rate constants of the anthocyanin network, direct pH jumps from acidic to basic, in thermally equilibrated solutions were performed, as reported elsewhere *(244)*. The interaction between pectin and cy3glc did not cause alteration on the equilibrium and kinetic rate constants of this anthocyanin. Only a very small increase could be perceived on the hydration constant (K_h) which could explain the very weak copigmentation effect observed (Table IV.1). From these two UV-Vis experiments it was perceptible that the impact of this *citrus* pectin on cy3glc color was very limited. However these experiments were performed at one relatively low pectin concentration and in this type of interactions, the water activity influenced by polysaccharides concentration has a detrimental impact on color stabilization.

Table IV.1. Thermodynamic (M^{-1}) and kinetic constants determined by UV-Vis absorption for cy3glc *(244)* and cy3glc-pectin solution ($1.5x10^{-4}$ M-$4.5x10^{-6}$M). Estimated error ≈ 10%.

	Cy3glc	**Cy3glc-pectin**
K'_a (pK'_a)	$1.8x10^{-3}$ (2.8)	$1.5x10^{-3}$ (2.8)
K_a (pK_a)	$2.1x10^{-4}$ (3.7)	$2.1x10^{-4}$ (3.7)
K_h (pK_h)	$1.5x10^{-3}$ (2.7)	$1.7x10^{-3}$ (2.8)
k_h (s^{-1})	0.08	0.09
k_{-h} ($M^{-1}s^{-1}$)	48	55

IV.3.2. STD NMR Studies

Firstly, to guarantee the specificity of STD eliciting resonances and to validate the functionality of the STD pulse sequence chosen, a STD NMR experiment was performed for cyanidin-3-*O*-glucoside and pectin. In this experiment an external capillary containing a 15 mM of phloroglucinol solution was placed into the NMR tube in contact with the anthocyanin and pectin solution. As expected, it was observed that the signals corresponding to phloroglucinol (δ~6 ppm) are not present in the STD spectrum appearing only in the regular ^{1}H spectrum (Figure IV.3).

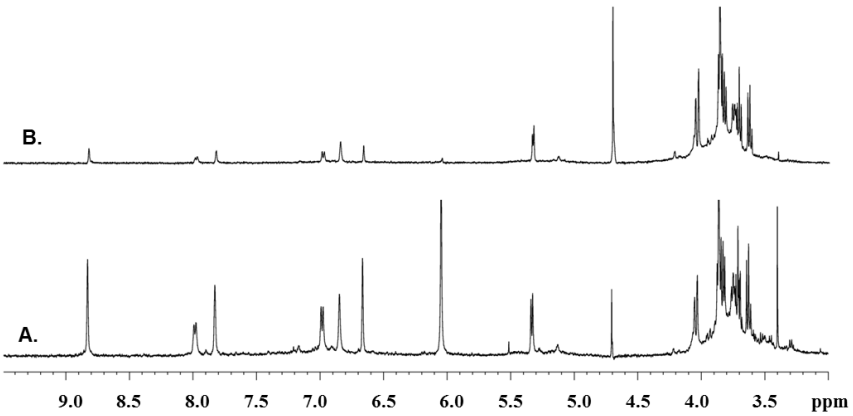

Figure IV.3. ^{1}H spectra recorded in D_2O/DMSO (5%) at 313 K of mixtures of pectin:cy3glc and an external capillary with 15 mM of phloroglucinol (**A**). Corresponding STD spectra of **A**, evidencing the specificity of STD eliciting resonances (**B**).

Also, in the STD experiments it is crucial that the choice of the on-resonance irradiation frequency does not overlap with the ligand resonances*(269)*. Also to confirm that the on-resonance irradiation frequency did not affect the anthocyanins aromatic protons and that the pectin was saturated by the on-resonance irradiation, experiments were performed on solutions of anthocyanins at the maximum concentration tested (cy3glc and dp3glc). For anthocyanins alone, in the difference STD spectrum the anthocyanins aromatic resonances were not visible which indicates that the on-resonance irradiation frequency does not overlap with these resonances (Figure IV.4).

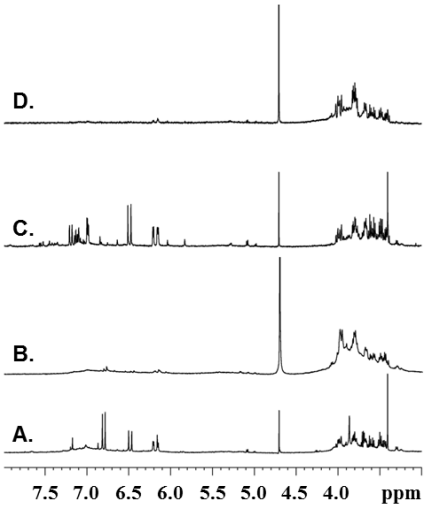

Figure IV.4. ^{1}H spectra recorded in D_2O/DMSO (5%) at 313 K of dp3glc (**A**) and cy3glc (**C**) alone, with the corresponding STD spectra (**B** and **D**, respectively).

On the other hand, the detailed knowledge of the structural characteristics of anthocyanins is of primary significance prior to the investigation of the binding between these pigments and pectin. Therefore, a preliminary NMR spectral characterization of cy3glc and dp3glc in aqueous solution, at pH 1.5 and 4.0 was performed. The assignment of the resonance signals in the ^{1}H NMR spectra of anthocyanin at both pH's was based on the data already published *(6, 223, 268)*. In the ^{1}H spectra of cy3glc and dp3glc represented in Figure IV.5, the hemiketal can be easily identified because of the existence of twin peaks. The labeling of the signals in these ^{1}H spectra corresponds to the numbering of the anthocyanin hemiketal form.

As previously reported, in a STD spectrum only signals of the ligand that are in close contact to the receptor will receive magnetization transfer and consequently will remain in the difference spectrum. Figure IV.5 shows the ^{1}H NMR spectra obtained for a solution of pectin (**A**) and anthocyanin-pectin (dp3glc, **B** and cy3glc, **D**). The corresponding STD spectra of **B** and **D** are displayed in spectra **C** and **E**, respectively. For dp3glc, at the ligand-to-receptor ratio displayed (200:1) it was observed that the saturation induced in pectin after irradiation was transferred to dp3glc protons (**C**). This clearly indicates an interaction between the hemiketal form of anthocyanin and pectin, with protons belonging to the anthocyanin suffering STD amplification. For cy3glc and for the same ligand/receptor ratio, no STD signal could be observed (**E**). Only at a much higher cy3glc-pectin ratio (600:1, **F**) small intensity resonances could be observed in the STD spectrum. This could probably be an indication of a much weaker affinity between these two components and only in the presence of large amount of ligand a weaker interaction could occur. When comparing the binding between these two anthocyanins and pectin it was noticeable that dp3glc bearing a pyrogallol moiety (three hydroxyl groups) seems to interact strongly with pectin when compared to cy3glc with a catechol moiety (two hydroxyl groups). Probably the existence of only two hydroxyl groups instead of three, in ring B resulted in a much weaker cy3glc-pectin interaction. These results are in agreement with those described by other authors *(137)* and they re-enforce the importance of hydrogen bonding in the interaction between anthocyanins and pectin. According to the "egg box model" *(163)* for low methoxylated pectins, analogous hydrogen bonds may be formed, with these hydrogen bonds probably occurring between the carboxyl and hydroxyl groups between the galacturonans of the pectins and the anthocyanin hydroxyl groups *(270)*.

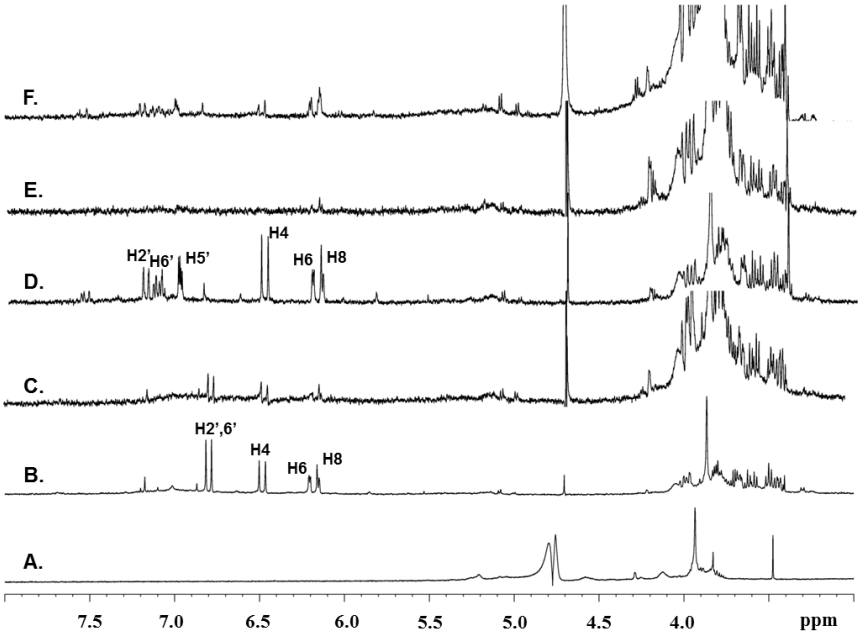

Figure IV.5. ^{1}H spectra recorded in D_2O/DMSO (5%) at pH 4.0 and 313 K of 4 μM pectin (**A**) and mixtures of 4 μM pectin and 700 μM dp3glc (**B**) or cy3glc (**D**). In part **C** and **E** the corresponding STD spectra of **B** and **D**, respectively is represented. Part **F** shows the STD spectra of cy3glc-pectin mixtures at higher anthocyanin:pectin molar ratio.

IV.3.3. Dissociation constant calculations

In order to quantify the strength of this interaction, the binding between anthocyanins and pectin at pH 4.0 was followed by measuring the intensities of selected cy3glc and dp3glc protons observed in the STD spectra with increasing anthocyanin concentration *(251)*. In these titration experiments, K_d, n and Δ_{max} were calculated using the equation previously described for a multisite model (equation *(IV.1)*) *(250)*.

$$A_{obs} = \frac{A_{max}}{2}\left\{\left(1 + \frac{K_d}{n[P_0]} + \frac{T_i}{n[P_0]}\right) - \left(\left[1 + \frac{K_d}{n[P_0]} + \frac{T_i}{n[P_0]}\right]^2\right) - \frac{4[T_i]^{1/2}}{n[P_0]}\right\} \quad (IV.1)$$

where A_{obs} is ΔI_i, the integral intensity variation, A_{max} is I_{imax}, K_d is the dissociation constant expressed in M, $[T_i]$, the total anthocyanin concentration able to fix the pectin, $[P_i]$ the total concentration of pectin and n the number of polyphenol binding sites *(251)*.

The titrations were conducted at high ligand-to-receptor ratios ranging from 200:1 to approximately 1200:1 which correspond to an anthocyanin concentration >> K_d. In this situation the receptor is completely saturated by the ligand. The desirable situation

occurs when [ligand] ≈ K_d, the receptor being half-saturated by ligand *(267)*. However, in this work the selection of anthocyanin concentration was restricted essentially by the detection limit in the STD experiments and for this reason these anthocyanin concentration ranges were chosen. The signals belonging to the hemiketal form B-ring (H_2', H_6' and H_5') were chosen for the titration curves and Figure IV.6 shows the STD titration experiment performed at a fixed pectin concentration (4 μM) and at some representative dp3glc and cy3glc concentrations ranging from 0.7 to 4.4 mM (part **A** and **B**, respectively), at pH 4.0. It is possible to observe that the STD signal of dp3glc and cy3glc resonances increases systematically as anthocyanin concentration rises. As previously reported, and when compared to dp3glc, only at much higher cy3glc-pectin ratio small intensity resonances could be observed in the STD spectra.

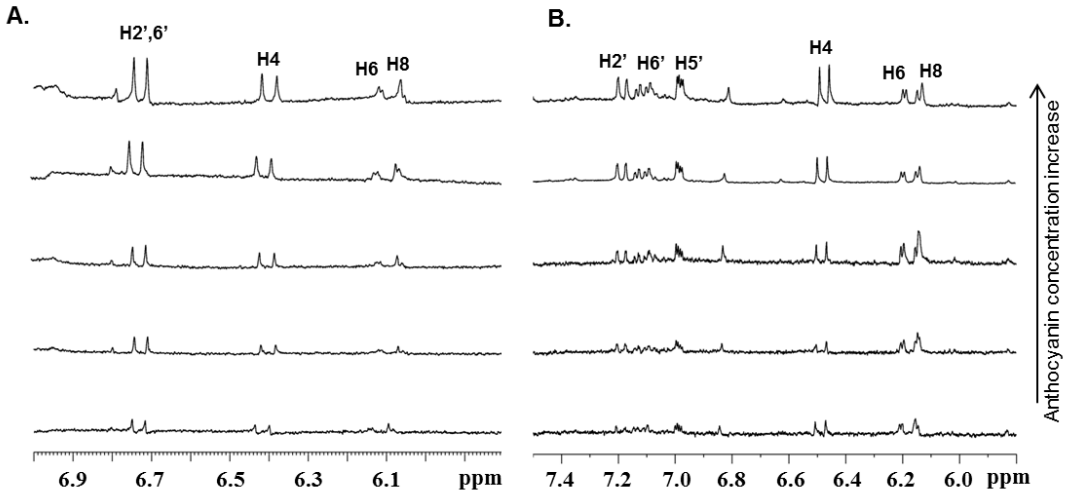

Figure IV.6. Representative spectra from a STD titration on a solution of 4 μM pectin and increasing concentrations of anthocyanin (dp3glc, **A** and cy3glc, **B**). Signals correspond to the protons of the hemiketal form of anthocyanins. STD titration was performed in D_2O/DMSO (5%) at 313 K and at pH 4.0.

Figure IV.7 (**A** and **B**) show the plot of the intensity of the integral for anthocyanins titrations as a function of ligand concentration at a fixed pectin concentration at pH 4.0. The behavior observed during the STD experiments at this pH maintaining the same anthocyanin/pectin ratios, appears to be slightly different. Detailed analysis of this figure shows that when increasing the dp3glc concentration, a curve with a logarithmic tendency could be observed, corresponding to the increase of the occupation of the receptor-binding site *(267)*. The plot of the integral intensity for cy3glc titrations as a function of ligand concentration seems to reveal similar behavior to the one obtained for dp3glc. However, this behavior could only be achieved at a much higher anthocyanin concentration, probably indicating a weaker interaction between cy3glc and pectin. Nevertheless, to ensure that the interaction between pectin and cy3glc

occur in the same manner as for dp3glc, higher anthocyanin concentration should be tested.

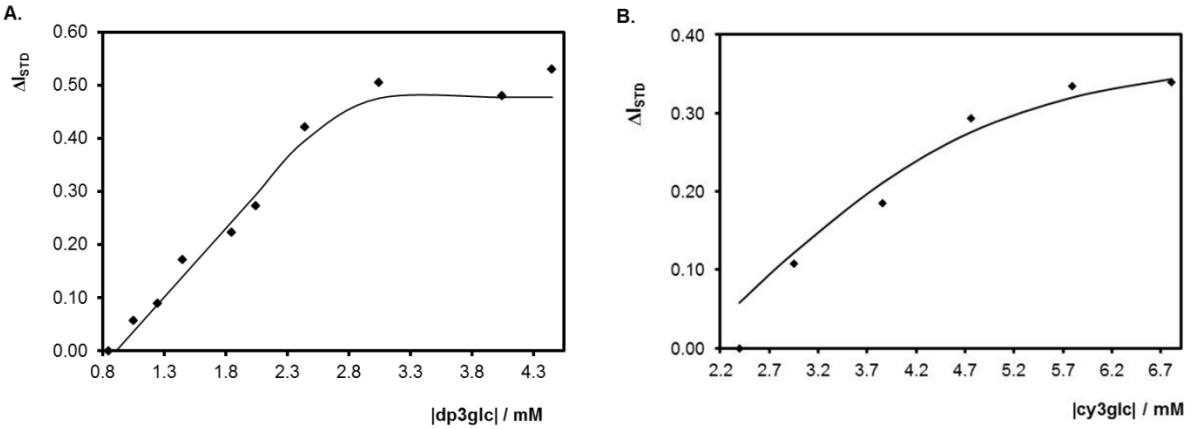

Figure IV.7. Observed (symbols) and fitted (lines) integral intensities of dp3glc and cy3glc hemiketal form proton resonances in STD-NMR spectrum with increasing anthocyanin concentration at pH 4.0 (part **A** and **B**, respectively). The fitting parameters represented in equation *(IV.1)*, K_d, n, Δ_{max}, were calculated using a least-squares fitting routine within the software program Microsoft EXCEL.

The experimental data points (for the hemiketal form of dp3glc and cy3glc) were fitted using equation *(1)*. The best K_d, Δ_{max} and n values obtained for the experimental points fitting are reported in Table IV.2. For the two anthocyanins tested, a K_d > 100 μM was obtained through the fitting of the experimental data, indicating probably a very weak interaction between the hemiketal forms and pectin at pH 4.0. Cy3glc seems to evidence a weaker affinity for pectin compared to dp3glc exhibiting larger K_d and requiring the addition of more ligand to saturate the receptor-binding site. These results once again reinforce the importance of hydrogen bonds to this interaction, with anthocyanins carrying a pyrogallol group exhibiting stronger interaction with pectin.

Table IV.2. K_d, number of binding sites (n) and Δ_{max} for the interaction between dp3glc and cy3glc (hemiketal form) and pectin determined by STD-NMR using equation *(IV.1)*.

	K_d	n	Δ_{max}
dp3glc	180 μM	750	0.59
cy3glc	250 μM	1270	0.30

In the binding of the neutral hemiketal form of anthocyanins (cy3glc and dp3glc) to low esterified pectin, the number of hydroxyl groups at the anthocyanin-B ring seems to be an important feature. Although the experimental data seems to present a logarithmic tendency in the concentration range tested, the dissociation constants obtained

suggested that probably non-specific surface adsorption could be responsible for this binding instead of specific binding sites. In fact, a dialysis experiment performed at pH 4.0 (neutral hemiketal form) had revealed a negligible retardation of passage across the dialysis membrane which probably suggests a non-specific surface. On the other hand, anthocyanins equilibrium forms adsorption on ionic carbohydrate, could also be explained by electrostatic and ionic forces involving charged molecules *(155)* and this raises the question about the interaction between pectin and charged anthocyanin molecules, particularly flavylium cation. Similar to the dialysis experiment performed at pH 4.0, another experiment was conducted at pH 1.5 (flavylium cation form). This form had revealed a much stronger adsorption to pectin surface resulting on a retardation of dialysis membrane passage (retention coefficient, RC = 42% at pH 1.5 and RC = 7% at pH 4.0) (Figure IV.8). This was probably due to the planar structure of the flavylium cation that could either favor interaction with the adsorbent (through the formation of $\pi-\pi$ bonds) or even facilitate the juxtaposition of species in solution onto the already adsorbed molecules involving hydrogen bonds and non-specific charge association of the flavylium cation to the electronegative polysaccharide *(271)*.

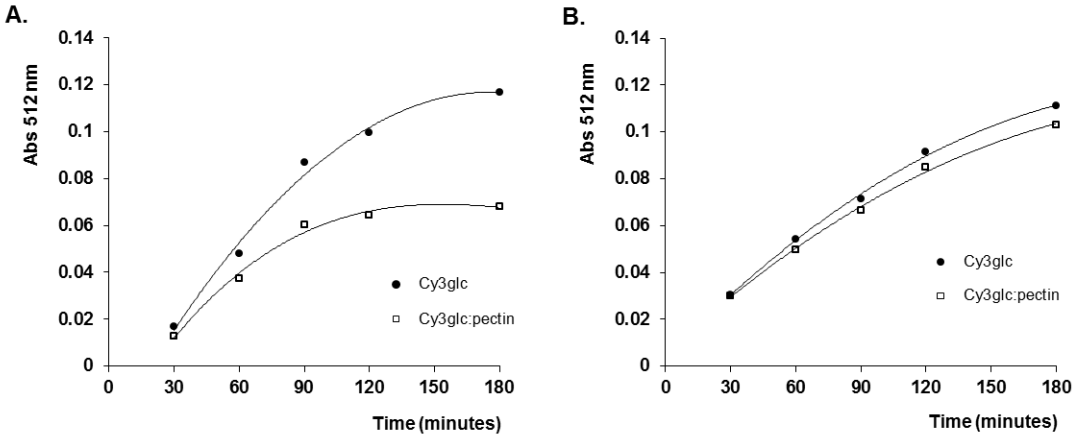

Figure IV.8. Absorbance (512 nm) *versus* time corresponding to cy3glc release from a dialysis membrane alone and in the presence of pectin (16:1 anthocyanin:pectin molar ratio) at pH 1.5 (**A**) and 4.0 (**B**).

As the interaction between anthocyanins and pectin appear to be stronger when the flavylium cation is present at higher concentration, the binding between cy3glc and pectin was also studied at pH 1.5 by STD NMR. Oppositely to the behavior obtained for pH 4.0, at this pH when performing a STD experiment only with pure anthocyanin (control), resonance signals belonging to anthocyanin aromatic protons could be observed in the STD difference spectrum. This behavior could probably be explained by anthocyanins self-association, which facilitates the saturation transfer between anthocyanin molecules. Self-association is a very well-known phenomenon that usually

occurs with the flavylium cation as well as with the quinoidal base *(134)* and is driven by hydrophobic vertical stacking between the anthocyanins to form π–π complexes. This two equilibrium species present a planar hydrophobic structure which allows the formation of these complexes whereas the hemiketal form cannot *(272)*. At pH 4.0 the neutral hemiketal form is the main specie and self-association is probably occuring in a much lower scale. This equilibrium form assumes a non-planar structure which does not allow the vertical π–π stacking. In fact, in a previous work, a systematic study focusing on the concentration dependence of self-association of cy3glc equilibrium species was performed on the basis of the alteration of their self-diffusion coefficients as measured by DOSY experiments *(268)*. The diffusion coefficients were measured for the five cy3glc different species presented in solution and it was possible to observe that the *D* value for the flavylium cation form was significantly affected by the concentration as a result of its self-association. For the neutral hemiketal, the diffusion coefficient was practically unchanged with concentration decrease. Bearing this, to minimize anthocyanins self-association phenomenon, DMSO was added to the anthocyanin-pectin solution and a more selective pulse program were used *(240)*. In this case, in the STD spectrum (control) the cy3glc aromatic resonances were not visible.

As it can be seen in Figure IV.9 (part **A**), as anthocyanin concentration rises, the STD resonance signals of the flavylium cation also increases with resonances from cy3glc anthocyanin protons appearing in the STD spectra. The experimental data points obtained were also fitted using equation *(1)* and a logarithmic curve could be obtained resulting on a $K_d \approx 2$ μM (part **B**). Compared to pH 4.0, the cy3glc flavylium cation appears to be a much stronger binder to pectin in accordance to the preliminary results obtained in the dialysis experiments with non-specific charge association probably effecting this interaction.

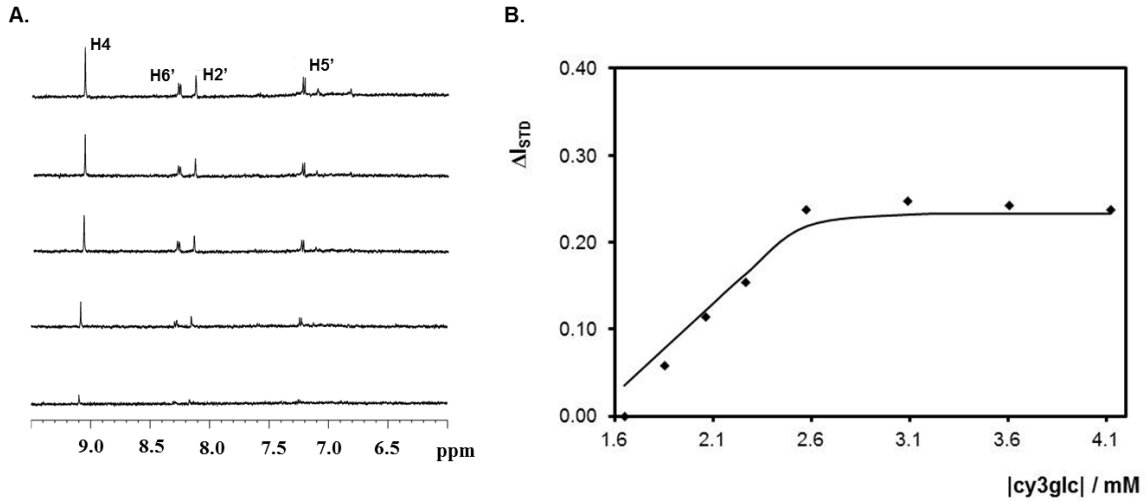

Figure IV.9. Representative spectra from a STD titration on a solution of 4 μM pectin and increasing concentrations of cy3glc ranging from 1 to 4 mM (**A**). STD titration was performed in D_2O/DMSO (30%) at 313 K and at pH 1.5. Respective observed (symbols) and fitted (lines) integral intensities of cy3glc flavylium cation proton resonances in STD NMR spectrum with increasing anthocyanin concentration, resulting on n = 575 and Δ_{max} = 0.24 (**B**).

IV.3.4. Molecular Dynamics simulations

To better characterize the conformational behavior between the charged (flavylium cation) and neutral (hemiketal) anthocyanin molecules with a representative model of pectin in aqueous solution, computational studies were additionally carried out. To this regard, three MD simulations of 45 ns each were performed. Figure IV.10 shows the root-mean-square deviation (RMSD) along the MD simulation, for the pectin molecule, in regards to its initial structure. In all simulations, it was observed that after the first nanosecond the RMSD values stabilize and have variations with a maximum of 2 Å during the remaining of the simulation. This supports the overall stability and equilibration of the pectin structures.

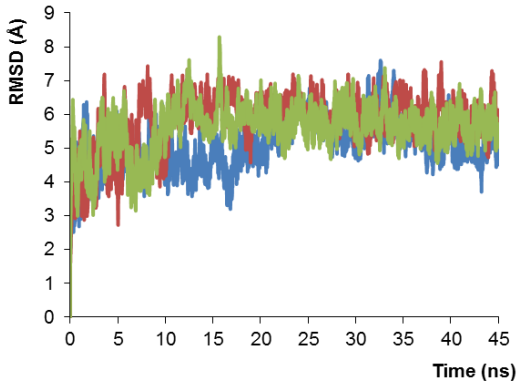

Figure IV.10. RMSD values obtained for the pectin residues along each MD simulation. Blue, green and red lines correspond to AH^{+}_{dp3glc}, B_{dp3glc} and B_{cy3glc}, respectively.

To analyze the binding between anthocyanins and pectin, several representative structures of the systems were extracted during the simulations (Figure IV.11). The formation of stable complexes, involving anthocyanin molecules and some pectin's monosaccharides, was observed. Concerning the flavylium cation (AH^{+}_{dp3glc}), initially there is a binding of 3 molecules around the polysaccharide (Figure IV.11-A). During the extent of the simulation, there is an additional binding of more anthocyanins to pectin. As can be observed in the same figure, this binding increased during the simulation: after ca. 4 ns simulation 5 AH^{+}_{dp3glc} molecules interact with pectin and 9 molecules interact at 20 ns. The latter structural arrangement (with 50% of AH^{+}_{dp3glc} molecules bound to pectin) was maintained throughout the final 25 ns of simulation, revealing its higher stability. The large planar structure (A-C and B rings) and the positive charge of these compounds greatly contribute to their strong interaction with the sugar rings, hydroxyl and carboxylate groups of pectin. It was observed the occurrence of self-association of two or four anthocyanins that are perfectly aligned between themselves by their large planar surfaces or with the pectin rings. The binding of the flavylium cation molecules to pectin occurs mainly by hydrogen bonds and dispersive contacts, and some of these interactions are depicted and described in Table IV.3. The short length of the exemplified H-bonds (*e.g.* H-C4-$_{dp3glc}$ to H-C6-$_{Rha12}$ or H-C2'-$_{dp3glc}$ to H-C1-$_{GalA8\ (acetylated)}$) and the small distances between the non-polar CH groups of both molecules reinforces the strong binding of these compounds to the pectin. Furthermore, the A-C nucleus provides a huge roughly planar polarizable surface that is strategically available to establish an accessible surface to interact with pectin's ring planes. The small proximity between some of these planes (described in Table IV.3) allows the establishment of optimized π–π stacking interactions that contributes to the higher stability of the global complex.

Additionally, the simulations of the anthocyanin hemiketal form $(B_{cy3glc})_{18}$:pectin and $(B_{dp3glc})_{18}$:pectin systems reveal that the binding of these molecules to pectin is smaller than the one observed for flavylium cation. In the case of B_{cy3glc} molecules, the maximum binding was achieved after 10 ns of simulation and it was only 17% (3 molecules, as seen on Figure IV.11). Concerning B_{dp3glc}, a sequential binding was observed, i.e., 2, 3, 4 and 5 molecules were bound to pectin at respectively 3.6 ns, 13.5 ns , 14.4 ns and 28 ns (Figure IV.11, respectively). The later structural arrangement (28% of binding) was maintained throughout the remaining of the simulation. The presence of the hydroxyl group at C_2 atom slightly decreases the planarity of the strict A-C-B surface of each compound, which may be responsible for their weak interaction with the polysaccharide. Their stellated structures make these molecules interact with each other, forming clusters between themselves (as seen in B_{cy3glc} simulation after 34 ns), which prevent a large interaction with pectin. It was also observed that the pectin tends to adopt a semi-coiled structure in the absence of anthocyanin binding.

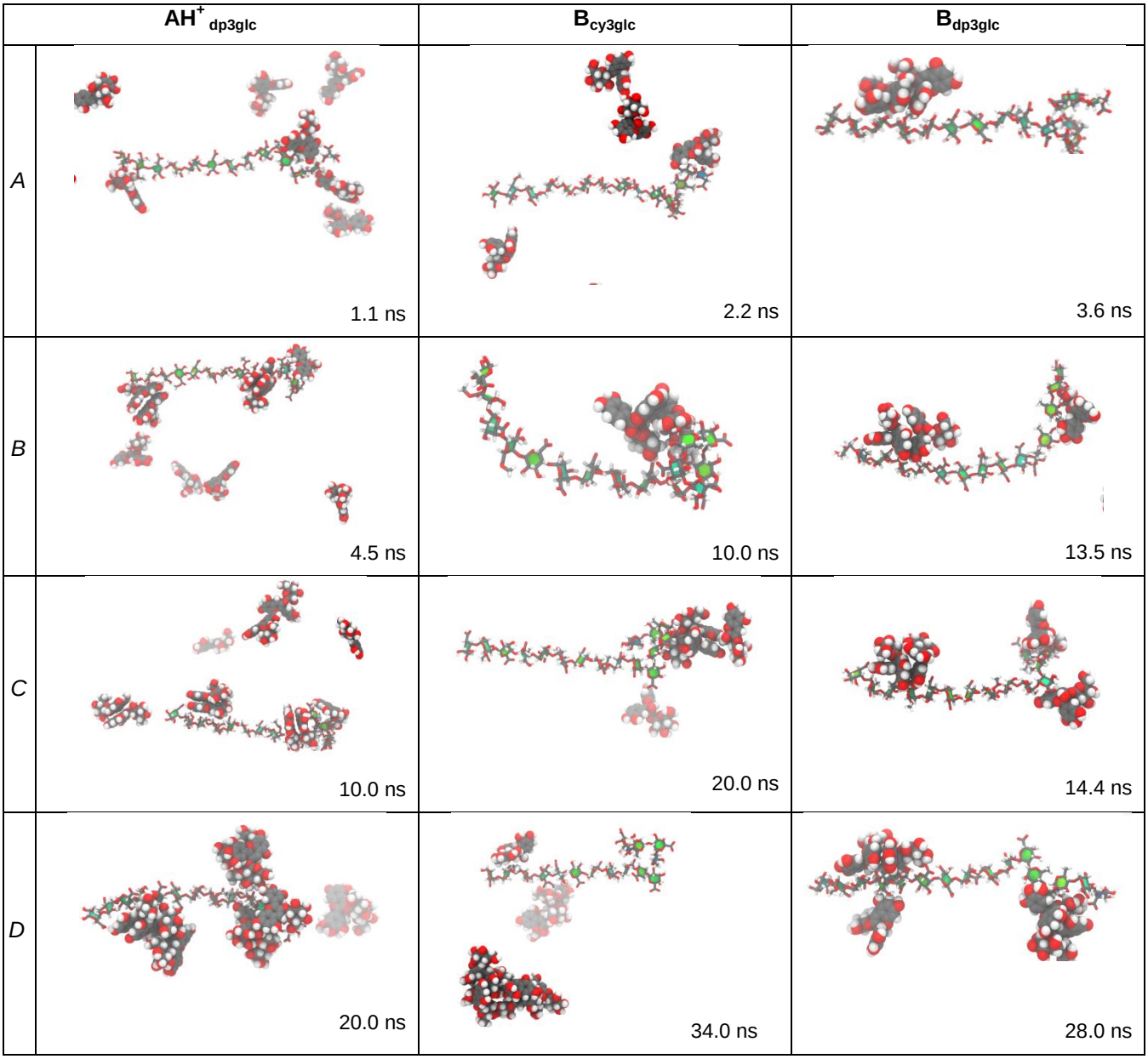

Figure IV.11. Representation of several geometries of AH^{+}_{dp3glc}:pectin, B_{cy3glc}:pectin and B_{dp3glc}:pectin systems along the course of each MD simulation. The pectin and anthocyanins molecules are depicted with sticks and van deer Waals (respectively) and are colored by atom type. Each panel represents an expansion of the total anthocyanin:pectin system.

Table IV.3. Representation of examples of some interactions established between the dp3glc (**AH^+**) molecules and pectin. The distances correspond to the average values of the last 10 ns of simulation. A snapshot from the MD simulation is also displayed, where the interactions are depicted by dashed lines. The dp3glc carbons and protons labeling corresponds to the numbering of the anthocyanin hemiketal form

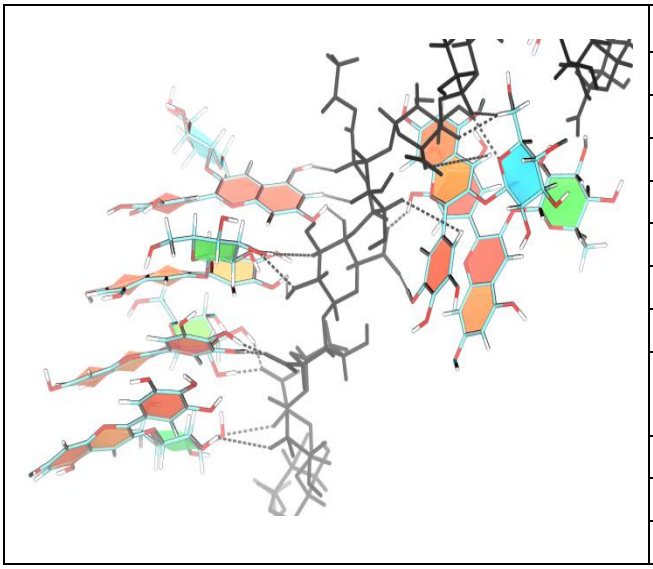

Interaction	Distance / Å
HO-C3'-dp3glc to COO^--Gal*p*A_7	3.5 ± 2.6
HO6(Glc)-dp3glc to COO^--Gal*p*A_{10}	1.7 ± 0.2
HO6(Glc)-dp3glc to HO3-Gal*p*A_9	3.2 ± 1.0
HO4(Glc)-dp3glc to COO^--Gal*p*A_{13}	2.8 ± 1.5
HO3(Glc)-dp3glc to COO^--Gal*p*A_{13}	2.1 ± 0.5
HO-C5-dp3glc to COO^--Gal*p*A_{10}	1.7 ± 0.2
HO6(Glc)-dp3glc to COO^--Gal*p*A_{11}	2.0 ± 0.9
H-C2'-dp3glc to H-C1-GalA_8(acetylated)	3.2 ± 1.2
H-C4-dp3glc to H-C6-Rha*p*$_{12}$	2.5 ± 0.4
AC ring-dp3glc to Gal*p*A_9 ring	5.4 ± 1.7
AC ring-dp3glc to Gal*p*A_{10} ring	6.6 ± 1.0

Similarly to the flavylium cation, both neutral anthocyanins interact with pectin residues by hydrophobic contacts (direct $\pi-\pi$ stacking and strong van der Waals interactions) between their large planar surfaces. With this interaction there is a concomitant high-energy release of water molecules from the solvation shells (hydrophobic effect). Furthermore, the binding driving force could also be strengthened by H-bonds involving the numerous hydroxyl groups from anthocyanin units and galacturonic acid moieties. Figure IV.12 shows some examples of these interactions. When comparing both anthocyanins (hemiketal form), it was observed that B_{dp3glc} interacts more with pectin than B_{cy3glc}. This is probably due to the additional hydroxyl group in the B ring of dp3glc, which grants a more hydrophilic character to this molecule. Similarly to AH^+_{dp3glc}, small distances were evidenced, which is in agreement with the NMR results presented in this work.

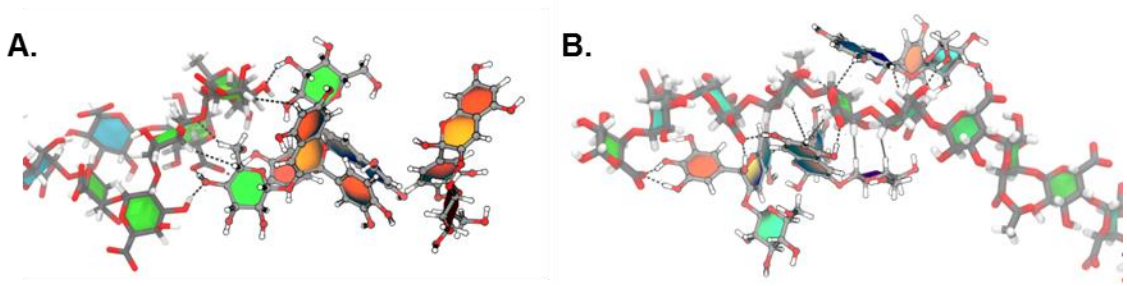

Figure IV.12. Representation of some interactions with pectin established between the cy3glc (**A**) and dp3glc (**B**) molecules (present in the hemiketal equilibrium form).

Figure IV.13 shows the Solvent-Accessible Surface Area (SASA) values that were determined for the pectin residues during each MD simulation. These values evaluate the surface area of pectin that is accessible to a solvent probe, which could indicate the extension of anthocyanins' binding. It was observed that the SASA value of pectin decreases much faster in the presence of AH^+_{dp3glc} molecules than in the presence of the B_{cy3glc} and B_{dp3glc} molecules, which suggests a larger binding extension of the former compound. In the $(AH^+_{dp3glc})_{18}$:pectin simulation, the SASA value rapidly decreases from 2716.5 ± 95.6 $Å^2$ (1^{st} ns) to 2117.5 ± 73.7 $Å^2$ (6^{th} ns), and finally to 1919.6 ± 69.5 $Å^2$ in the last nanosecond of simulation. However, in the other two systems (B_{cy3glc} and B_{dp3glc}, respectively), the initial SASA value (~ 2700 $Å^2$) only decreases in the last nanosecond of simulation to 2349.3 ± 37.0 $Å^2$ and 2210.4 ± 39.0 $Å^2$.

Overall, all these computational data suggest that the extension of polyphenols binding to pectin is the following: AH^+ > B which is in agreement with the experimental NMR studies performed. Simultaneously to calculate the SASA value, an MD simulation (20 ns) with the pectin model alone was performed. The SASA value of the initial extended structure of pectin is 2725.9 ± 52.4 $Å^2$ (first nanosecond). However, after this time, the pectin structure starts to adopt a semi-coiled (or partial-folded) geometry, which causes the decrease in the SASA value. A 10.1 % maximum SASA's decrease was attained in the last nanosecond of simulation (2451.9 ± 30.5 $Å^2$).

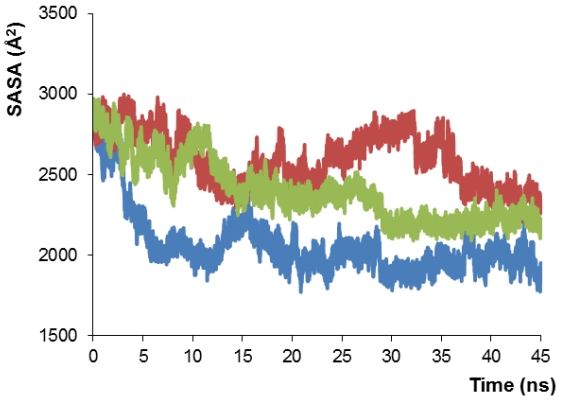

Figure IV.13. Solvent-Accessible Surface Area (SASA) values obtained for the pectin model. Blue, green and red lines correspond to AH^{+}_{dp3glc}, B_{dp3glc} and B_{cy3glc}, respectively.

IV.4. Conclusions

For the first time the study of the interaction between anthocyanins and low esterified pectin was evaluated through STD NMR spectroscopy and Molecular Dynamics simulation. This methodology allowed the measurement of weak interactions occurring between anthocyanins and this polysaccharide and the results presented herein indicate that this interaction probably occurs through hydrogen bonding and hydrophobic interactions. For these reason, the number of hydroxyl groups in the ligand seems to affect this binding. As only low esterified pectin was studied it was not possible to outline how this interaction was affected by the pectin type (particularly the degree of esterification). In the presence of the flavylium cation a much stronger interaction between anthocyanins and pectin could be perceived. Pectin impact on the thermodynamic and kinetic constants was very restricted causing only a small increase on the K_h.

From a food industry perspective these results contribute to the elucidation of the interaction between anthocyanins and food carbohydrates increasing the knowledge regarding the phenomena that drive the extraction and stabilization of these natural colorants.

V. ANTHOCYANIN'S ASSOCIATION MECHANISMS

A - Study of Anthocyanins Self-Association by NMR spectroscopy

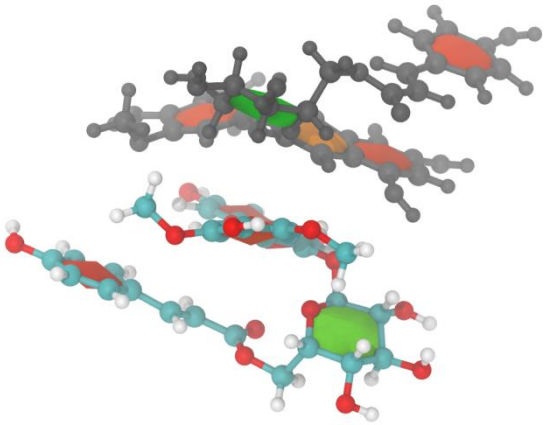

Adapted from:

Fernandes, A., Brás, N., Mateus, N., de Freitas, V.
Study of Anthocyanins Self-Association by NMR spectroscopy*, New Journal of Chemistry*, **submitted**

With the exception of the computational calculations all experimental design and work described in this part was carried out by the author.

V.1. Introduction

An attractive and stable color is a fundamental aspect for the food industry since it plays a very important role in the consumer´s choice and oftentimes adds a value to the food *(5)*. Therefore for optimal color retention, artificial dyes have been commonly added by the food industry. Nevertheless, the safety of these colorants has been questioned, leading to a reduction in the number of permitted colorants and to a worldwide tendency towards the consumption of natural products *(116, 273, 274)*.

Replacing synthetic dyes with natural colorants poses a challenge due to the higher stability of synthetic colorants with respect to light, oxygen, temperature and pH, among other factors *(275)*. Anthocyanins are well established as natural colorants mainly because of their availability as by-products of the wine industry *(276)*. Besides the color attributes, interest in anthocyanins has increased because of their possible health benefits to the consumers *(12, 277)* and these characteristics make anthocyanins a worthy substitute to synthetic dyes. However, their use as food colorants has been limited due to their relatively low stability *(5)*. Anthocyanins are structurally dependent on the conditions and composition of the media where they are dissolved and suffer interactions among them and with other compounds that influence their structural equilibria and modify their color. One of the most important parameter for anthocyanins stability is the pH value of a system *(278)* and in fact, the main obstacle in using anthocyanins derive from their loss of color in non-acidic media. Anthocyanins undergo reversible structural transformations with the pH, which is accompanied by dramatic changes in color. At pH 3 or bellow, anthocyanins exist predominantly as a flavylium cation (**AH^+**) with their color ranging from orange to bluish-red (depending on the chemical structure). As the pH is raised, proton transfer and hydration reactions occur giving rise to the purplish quinoidal base (**A**) and to the colorless hemiketal (**B**), respectively. This latter undergoes a ring opening producing the *cis*-chalcone (**C*c***) which further isomerizes originating the *trans*-chalcone (**C*t***) *(89, 94, 95)*. Due to these transformations with pH, the hydrophilic anthocyanins are most common applied in acidic food systems (pH<3), to ensure the predominance of the colored flavylium cation *(5)*.

Research involving the development of strategies for the stabilization of these pigments has found that this can be achieved by copigmentation, a phenomenon in which pigments associate with other compounds resulting in a color enhancement and in more stable colors *(64, 279)*. In food science, this phenomenon is considered a very

important interaction as color is one of the main quality factors. Copigmentation occurs in different ways, namely by inter-molecular association between colorless copigments and anthocyanins *(80)*, intra-molecular copigmentation, which is an interaction between the chromophore and non-chromophoric parts of the same molecule *(280)* and by self-association, which is an inter-molecular association between anthocyanindin nuclei *(281)* or between anthocyanindin nuclei and aromatic acyl groups *(282)* (Figure V.1). All these mechanisms involve hydrophobic vertical π-stacking of the chromophore, thus protecting it from the nucleophilic attack of water and preventing, at least in part, the formation of colorless hemiketal and chalcone forms. The intra-molecular copigmentation is restricted to anthocyanins which are acylated by phenolic acids. Indeed, when acylation occurs through the position 6 of the sugar, the free rotation of the acyl group is possible, allowing the folding of the molecule and intra-molecular stacking of the acyl group with the pyrylium ring of the flavylium cation *(5)*.

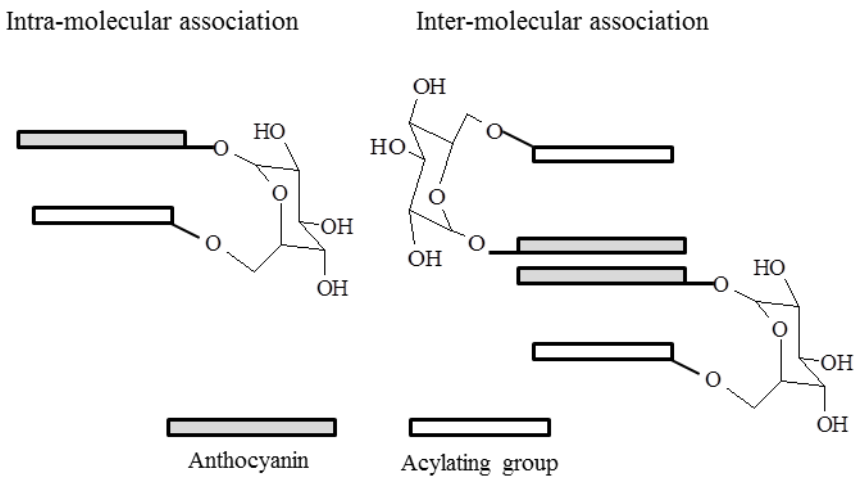

Figure V.1. Schematic representation of intra and inter-molecular association in acylated anthocyanins. Adapted from Mistry *et al*.,1991 *(283)*.

A subset of copigmentation involving anthocyanins is the case of self-association in relatively concentrated solutions and this interaction has been evidenced by several techniques including UV-vis absorption spectroscopy, circular dichroism and NMR *(6, 88, 128, 131, 132, 281, 284, 285)*. This process takes place with the flavylium cation as well as with the quinoidal base. Cross aggregation involving flavylium cation and *trans*-chalcone has also been described *(134)*. Beyond its marked role in anthocyanins chemical stabilization, anthocyanins inter- and intra-molecular interactions must also be considered for anthocyanins biovailability purposes and it is therefore essential to clarify these mechanisms.

In this work it is presented a study dealing with anthocyanins self-association (inter- and intra-molecular interactions) in the flavylium form and the relationship between anthocyanin structure and their tendency to self-associate. Two structurally related anthocyanins where used: mono-acylated malvidin-3-*O*-coumaroylglucoside and non-acylated anthocyanin, malvidin-3-*O*-glucoside were studied. Anthocyanins self-association was assessed by different NMR parameters, such as proton chemical shifts ($^1H\delta$), translational diffusion coefficients (*D*) and NOE correlations.

V.2. Materials and Methods

V.2.1. Materials

D_2O (99.9%), DMSO-d_6 (99.8%) and DCl (99%) were purchased from Sigma-Aldrich® (Madrid, Spain). Malvidin-3-*O*-glucoside (mv3glc) and malvidin-3-*O*-coumaroylglucoside (mv3cumglc) (Figure V.2) were extracted and purified in the laboratory from a young red table wine (*Vitis vinifera* L. varietal caste Touriga Nacional) by semipreparative HPLC using a reversed-phase C18 column (250 mm x 4.6 mm i.d.) as described elsewhere *(252)*.

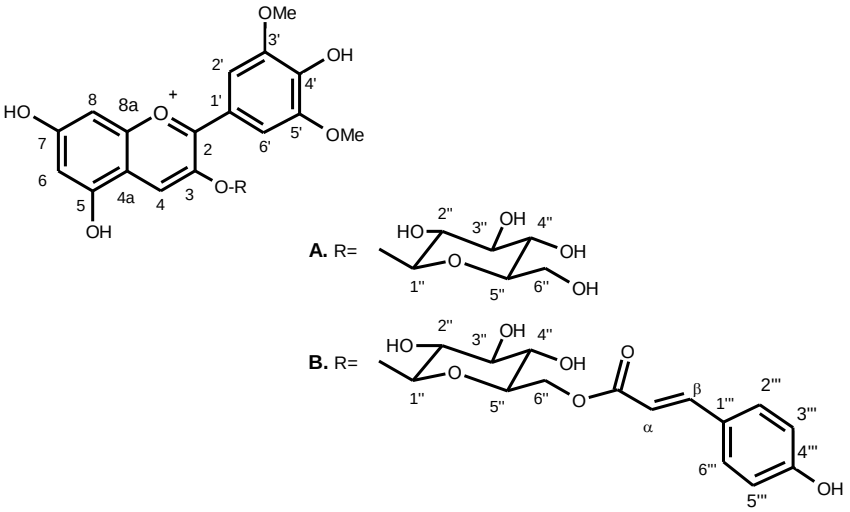

Figure V.2. Structure of mv3glc and mv3cumglc obtained from red wine (*Vitis vinifera* L.).

V.2.2. NMR samples preparation

Solutions of anthocyanins (mv3glc and mv3cumglc) were prepared in D_2O/DMSO d_6 (7:3 v/v) or in D_2O at room temperature and pH was adjusted to pH 1.0 by the addition of DCl. pH measurements were made in a pH meter WTW pH 320 fitted with a standard glass Crison ® 5209 electrode. The calibration was made with standard aqueous buffers at pH 4.0 and 1.0 from Crison®. Before performing the NMR experiments (DOSY and ^{1}H) the pH was checked and adjusted to 1.0 whenever necessary. After pH adjustment, the samples were allowed to equilibrate for one hour before the NMR study to guaranty sample stability and to ensure that the equilibrium between all sample components was entirely achieved and at the intended pH.

V.2.3. NMR spectroscopy

NMR experiments were recorded on a Bruker Avance II spectrometer, operating at 400.13 MHz (^{1}H), equipped with 5 mm PABBO BB Probe and pulse gradient units, capable of producing magnetic field pulsed gradients in the z-direction of 53 G/cm. The NMR measurements have been done with standard BRUKER pulse sequences in D_2O/DMSO (7:3) or D_2O at 300 K. ^{1}H NMR experiments were performed with water suppression using excitation sculpting with gradients *(210)*, acquisition time 1.36 s, relaxation delay 2 s and128 or 256 transients of a spectral width of 10000 Hz were collected into 32 K time domain points. Typical measuring conditions for the ^{1}H/^{1}H and 2D spectra (COSY) recorded in phase sensitive mode and with water suppression were: relaxation delay 2 s, 64-128 scans, a total 2K data points in *F*2 and 256 data points in *F*1 over a spectral width of 10000 Hz. 2D ^{1}H COSY and ^{13}C HSQC and HMBC experiments were carried out with a spectral width of *ca* 10000 Hz for ^{1}H and 32000 Hz for ^{13}C, relaxation delay 1.5 s, Fourier transform (FT) size 2 K × 1K. Multiplicities were recorded as singlets (*s*), doublets (*d*), triplets (*t*), doublets of doublets (*dd*), multiplets (*m*) and unresolved (*).The delay for the long-range C/H coupling constant was optimized to 7 Hz. The two-dimensional nuclear Overhauser effect spectroscopy (NOESY) experiments were acquired in phase-sensitive mode with optimized mixing time of 400 ms. Generally, 64 scans and 512 F1 slices were obtained and the spectral width was 6500 Hz.

V.2.4. Diffusion Ordered NMR experiments

Proton registered diffusion-ordered (^{1}H DOSY) spectroscopy was used to measure translational diffusion coefficients (*D*) and was performed on a Bruker Avance III 600 HD spectrometer, equipped with 5 mm CryoProbe Prodigy and pulse gradient units, capable of producing magnetic field pulsed gradients in the z-direction of 50 G/cm. DOSY experiments were acquired using the bipolar longitudinal eddy current delay (BPPLED – Bipolar Pulsed Field Gradient Longitudinal Eddy Delay) pulse sequence *(211)*. The experimental conditions (5mm NMR tubes, temperature of 300 K, no sample rotation and high air flow of 535 L/h to avoid convections in the samples) for all DOSY experiments were kept constant. Before the NMR experiments, the temperature was equilibrated and maintained at 300 K, as measured using the spectrometer thermocouple system. Typically, in each experiment a number of 16 spectra of 32K data points and 128 or 256 scans were collected, with values for the duration of the magnetic field pulse gradients (δ) of 2.4 ms, diffusion times (Δ) of 120 ms and an eddy current delay set to 5 ms. The pulse gradient (g) was incremented from 2 to 98% of the maximum gradient strength in a linear ramp. The spectra were processed with the Bruker Topspin software package (version 3.2).

V.2.5. Optimization and Molecular Dynamics simulations

The 3D structure of mv3cumglc molecule was prepared with the GaussView software *(286)*. To obtain the optimized geometries and electronic properties for its subsequent parameterization, the Gaussian 09 suite of programs *(287)* was used. These calculations were performed with the restricted Hartree-Fock method and with the 6-31G(d) basis set. Atomic charges were further recalculated using the RESP algorithm *(215)*. The geometry optimization and MD simulations were performed using GAFF force field *(262)*. Explicit solvation (TIP3P water model) was included as a rectangular box with a 12 Å distance between the box edges and any atom within each system. Two systems were studied: *i*) one mv3cumglc and one Cl^- counter-ion and *ii*) two mv3cumglc and two Cl^- counter-ions. All complex geometries were minimized in two stages. Subsequently, MD simulations of 100 ps at constant volume and temperature, and considering periodic boundaries conditions were performed. These were followed by 5 and 50 ns of MD simulation with the NPT ensemble, in which Langevin dynamics was used (collision frequency of 1.0 ps^{-1}) to control the temperature at 303.15 K *(220)*. All simulations were carried out using the AMBER 12.0 *(288)*

simulations package. Bond lengths involving hydrogen atoms were constrained using the SHAKE algorithm, and the equations of motion were integrated with a 2 fs time step using the Verlet leapfrog algorithm *(221)*. The Particle-Mesh Ewald (PME) method *(222)* was used to treat long-range interactions, and the nonbonded interactions were truncated with a 10 Å cutoff. The MD trajectories were saved every 2 ps and were analyzed with the PTRAJ module of AMBER 12.0 *(288)*.

V.3. Results and Discussion

A synergistic combination of NMR techniques such as diffusion ordered spectroscopy (DOSY), ^{1}H and nuclear Overhauser effects (NOE) can bring valuable information regarding the structure and the molecular association (intra and inter-association) of multicomponent systems. DOSY is a well-established technique for characterizing the structure of intermolecular systems since the self-diffusion coefficients of these systems depend on their molecular size, weight and shape *(232)*. Additionally, NOESY experiments can provide valuable information in mapping specific through-space internuclear distances and can also provide information regarding anthocyanins intra and inter-molecular association.

V.3.1. NMR spectral characterization

Initially a NMR spectral characterization of malvidin-3-*O*-coumaroylglucoside (mv3cum-glc) was performed in order to better understand the molecular structure and the possibility of intra- and/or inter-molecular association. The assignment of the corresponding resonances was established using 1D and 2D techniques (COSY, HSQC, HMBC) in D_2O/DMSO (7:3) and by comparison with the data previously published *(289, 290)*. Malvidin-3-*O*-glucoside structure was assessed by NMR by comparison with the data already published *(223)*. ^{1}H chemical shifts were assigned using 2D NMR (COSY) experiments, while ^{13}C resonances were assigned using 2D NMR techniques (HMBC and HSQC) (Table V.1). NOESY experiments were performed in order to provide specific information regarding the spatial proximity between protons and allowed the determination of sugar binding sites on anthocyanidin nucleus. The connecting position on sugars of acyl residue was determined by HMBC measurements.

Table V.1. Proton chemical shifts (δ^{1}H), coupling constants and carbon chemical shifts (δ^{13}C) for malvidin-3-*O*-coumaroylglucoside in D_2O/DMSO (7:3) at pH 1.0.

Position	δ ^{1}H (ppm); *J*(Hz)	δ ^{13}C (ppm)
Aglycone moiety		
H2	-	161.1
H3	-	142.9
H4	8.65 (*s*)	135.2
H4a	-	111.8
H5	-	156.8
H6	6.36 (*s*)	100.8
H7	-	*n.a.*
H8	6.63 (*s*)	100.6
H8a	-	155.3
H1'	-	118.1
H2', 6'	7.58 (*s*)	108.6
H4'	-	147.9
H3', 5'	-	143.6
3', 5'-OMe	3.87 (*s*)	56.1
Glucose moiety		
H1''	5.43 (*d*, 7.5)	100.8
H2''	3.73 (*t*, *)	73.2
H3''	3.68 (*t*, 6.8)	75.6
H4''	3.50 (*t*, 9.0)	70.1
H5''	3.81 (*m*)	73.9
H6a''	4.35 (*dd*, 7.4; 12.1)	62.9
H6b''	4.46 (*dd*, 2.6; 12.3)	62.9
Coumaroyl group		
CO_2	-	125.5
α	5.96 (*d*, 16.7)	130.3
β	7.09 (*d*, 16.7)	115.7
H1'''	-	158.8
H2''', 6'''	7.05 (*d*, 8.5)	113.4
H3''', 5'''	6.68 (*d*, 8.5)	145.4
H4'''	-	167.7

V.3.2. NOE effects

The changes of NOE for the species in the solution can provide reliable information regarding the molecular proximity of protons and allows the discrimination of the NOE resulting from the self-association of anthocyanins (inter-molecular NOE) and NOE

resulting from intra-molecular interactions between the anthocyanin protons. Data from the NOESY spectra performed on mv3cumglc and acquired at 300 K in D_2O/DMSO (7:3) pointed to a structure where the coumaroyl group was oriented towards the anthocyanin chromophore (Figure V.3). In fact, cross peaks between protons H6 and H8 of the anthocyanidin moiety and proton Hα of the aromatic acyl function (^{1}Hδ 5.96 ppm) could be detected. Besides this, other weak correlations could be observed in the NOESY spectra, corresponding to the pairs OMe/H2''', 6''' or OMe/H3''', 5''' and to the pair H2',6'/Hα. As sugar acylation occurs at position C-6, the free rotation and the subsequent folding of the coumaroyl group over the flavylium nucleous is possible. These cross peaks detected clearly prove the existence of intra-molecular copigmentation for this monoacylated anthocyanin. The formation of these intra-molecular complexes seems to involve both the double bond and aromatic ring of coumaroyl residue and they may occur on the top or on the bottom of the flavylium nucleus.

Furthermore, detailed analysis of the NOESY spectrum also reveals the possibility of inter-molecular association. This association could be explained by the existence through-space interactions between protons belonging to distant parts of the molecule: cross peaks between H4 and protons from the methoxy group (B-ring) and between H4 and H2',6' protons, presumably indicating inter-molecular association.

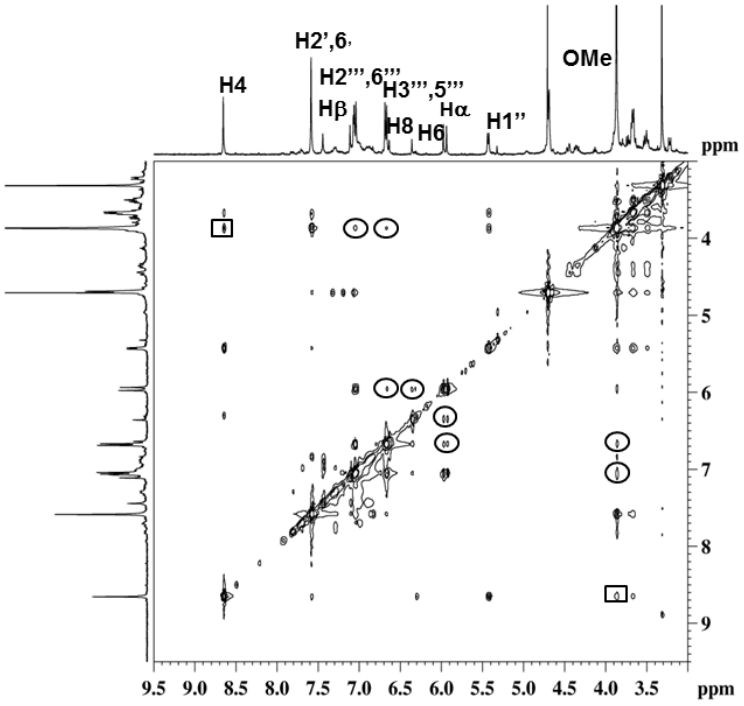

Figure V.3. Portion of the 2D NOESY spectra of mv3cumglc (1.4 mM) acquired in D_2O/DMSO (7:3) with a mixing time of 400 ms, showing some of the characteristic inter-molecular (in boxes) and intra-molecular (in circles) NOE interactions. The assignment of resonances of mv3cumglc are also included.

The self-association constant, K_{ass}, of anthocyanins was obtained through an adaptation of the methodology reported in the literature *(225)*. This association constant was determined by following the evolution of either the chemical shift (δ) or the diffusion coefficient (*D*) with respect to anthocyanin concentration (between 0.4 to 2.0 mM). The observed chemical shift (or diffusion coefficient) changes were least-squares fitted to equation *(V.1) (291)*:

$$A_{obs} = A_{free} - \left[\left(\left|A_{aggregate} - A_{free}\right|\right)K_{ass}C_0\left\{2/\left[1 + (K_{ass}C_0 + 1)^{1/2}\right]\right\}\right]^2 \quad (V.1)$$

where A_{obs} is the observed proton chemical shift (or diffusion coefficient), A_{free} is the proton chemical shift (or diffusion coefficient) of the non-associated (free) anthocyanin, $A_{aggregate}$ is the proton chemical shift (or diffusion coefficient) of the aggregated anthocyanin and C_0 is the total anthocyanin concentration. This equation can be used to determine K_{ass} from *D* value assuming that the T2 relaxation is negligible *(225)*.

V.3.3. ^{1}H NMR chemical shifts variation

^{1}H chemical shifts are very sensitive to the magnetic anisotropy of aromatic systems and thus can serve as a probe for the spatial proximity of aromatic rings to specific protons, therefore revealing an intra-molecular interaction. Moreover, concentration dependence of ^{1}H chemical shifts helps to differentiate between inter- and intra-molecular since such dependencies can be observed only in the case of inter-molecular interactions *(289)*. In the ^{1}H NMR spectra, malvidin-3-*O*-coumaroylglucoside bearing an acyl group displayed an upfield shift of the flavylium nucleus relative to the nonacylated anthocyanins (malvidin-3-*O*-glucoside). This chemical shift alteration was proposed to be an indicator of the shielding of the anthocyanidin caused by intra-molecular association between the anthocyanidin and the acyl moiety *(292)*. This upfield shift was more striking for A and C-ring protons ($\Delta\delta$ ~0.15 and 0.20 ppm, respectively) than for B-ring protons (~0.06 ppm). Concurrently, evaluation of the δ^{1}H with anthocyanin concentration also indicated a concentration dependence on chemical shift which mean that inter-molecular associations (self-association) should also be considered as possible stabilization mechanisms. This ^{1}Hδ upfield and concentration dependence was in agreement to the results obtained in the NOESY experiments which revealed the occurrence of both intra and inter-molecular associations in mv3cumglc.

In order to understand the role of inter-molecular associations in the shielding of mv3cumglc protons, ^{1}Hδ concentration dependence of acylated anthocyanin was compared to the behavior observed for mv3glc (non-acylated), in which self-association is known to occur. When comparing the ranges of proton chemical shifts for both anthocyanins significant differences could be detected (Figure V.4). Even at the lowest concentration tested, mv3cumglc's H4 remains shielded compared to the non-acylated anthocyanin (δH4 at 8.77 ppm in mv3cumglc compared with 8.91 in mv3glc). These results seem to indicate a higher shielding of anthocyanin rings and that the intra-molecular complexes formed by acylated anthocyanins were held together, existing even in diluted solutions. Regarding H2',6' chemical shifts ranges, the differences between acylated and non-acylated anthocyanins are smaller (δH2',6' at 7.72 ppm in mv3cumglc compared with 7.81 in mv3glc). Furthermore, when only inter-molecular association is present (*e.g.* mv3glc), anthocyanins shielding due to the magnetic anisotropy of the π-electron system of another flavylium nucleus disappears rapidly upon dilution of the solution ($\Delta\delta$H4 ~0.12 ppm in mv3cumglc compared with $\Delta\delta$H4 ~0.15

ppm in mv3glc in the same concentration range). This could be an indication that inter-molecular interactions in the form of self-association are not held together strongly enough to withstand the effects of dilution.

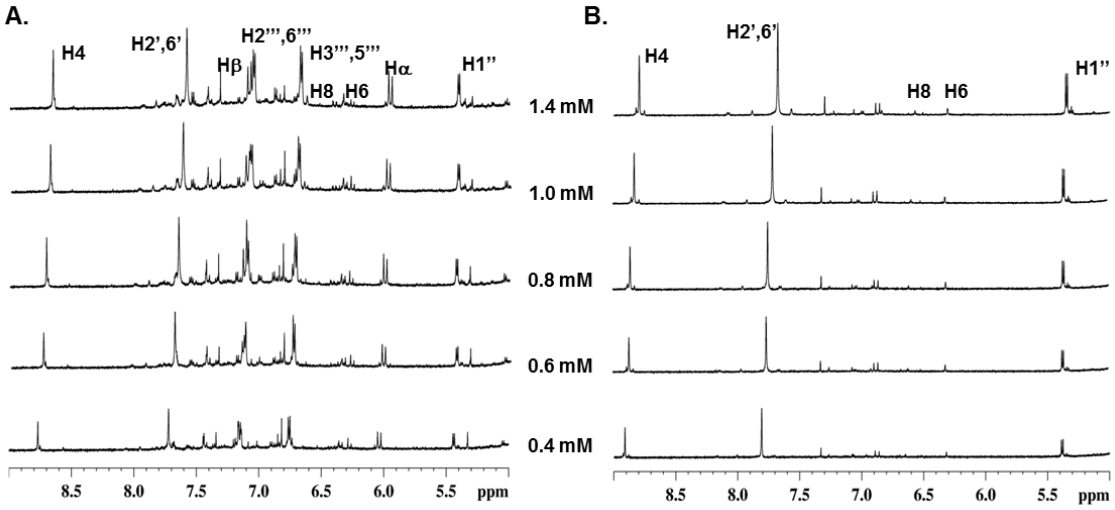

Figure V.4. ^{1}H NMR spectra of mv3cumglc (**A**) and mv3glc (**B**) in D_2O/DMSO (7:3) as a function of anthocyanin concentration.

For mv3cumglc and mv3glc, proton chemical shifts from both C (H4) and B (H2',6') rings and H3''',5''' (for mv3cumglc) were used to evaluate the concentration dependence. This dependence and the fitting of the experimental data using equation (*V.1*) (where $A_{obs} = \delta_{obs}$) are shown in Figure V.5. The fitting of the experimental chemical shift variation are consistent with the isodesmic model used in which the self-association of anthocyanins occurs at low concentration in an indefinite non-cooperative way to form stacks (with 2, 3, 4, or more molecules) where the equilibrium constant K_{ass} is always the same for each step *(291)*. An isodesmic model had already been used to study the self-aggregation in anthocyanidin-3-glucoside *(6)*.

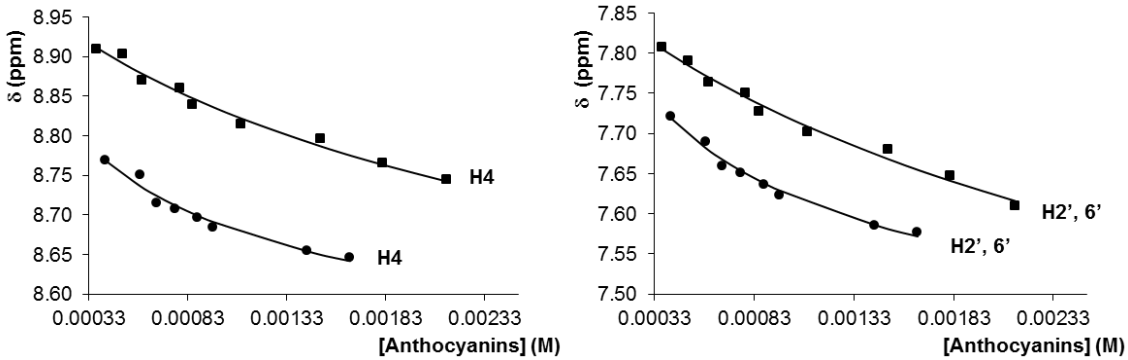

Figure V.5.Proton chemical shift variation (δ^{1}H) of the protons H4 and H2',6' *versus* mv3cumglc (•) and mv3glc (▪) concentration (M) in D_2O/DMSO (7:3). Solid lines represent the best fit obtained using equation *(V.1)*.

From the chemical shifts variation and data analysis, the association constant (K_{ass}) together with the free (δ_{free}) and aggregated ($\delta_{aggregate}$) chemical shifts could be obtained for acylated and non-acylated anthocyanins. K_{ass} for non-acylated anthocyanins (mv3glc) was found to be approximately 800 M^{-1} while for acylated anthocyanins the K_{ass} value obtained increased approximately by 2-fold by comparison with mv3glc, evidencing that the presence of an acyl substituent could result in a superior affinity towards aggregation (Table V.2). This higher association constant could be an indication of a multi-aggregation phenomenon in which self-association (inter-molecular) is combined with intra-molecular stacking with molecules being locked into each other and resulting in much higher affinity towards self-association. Compared to the data published by Leydet *et al* (2012), mv3glc K_{ass} value determined in this study was smaller (800 M^{-1} compared to 1738 M^{-1}) *(6)*. However, due to anthocyanins solubility our experiments where performed in D_2O/DMSO and the use of organic solvents could be responsible for the disruption of copigmentation stacks resulting in the weakening of hydrophobic interactions *(111)*.

Table V.2. Association constants (K_{ass}) determined by chemical shift variation and chemical shifts of anthocyanins characteristic protons (H4, H2',6' and H3''',5''') in aggregated ($\delta_{aggregate}$) and free (δ_{free}) states at 300 K in D_2O/DMSO (7:3).

	Mv3glc		**Mv3cumglc**		
	H4	H2',6'	H4	H2',6'	H3''',5'''
K_{ass} (M^{-1})	819 ± 40		1402 ± 164		
δ_{free} (ppm)	8.98	7.87	8.84	7.81	6.81
$\delta_{Agreggate}$ (ppm)	8.74	7.60	8.65	7.61	8.769
χ^2	5.0×10^{-4}	4.6×10^{-4}	6.9×10^{-4}	2.4×10^{-4}	8.9×10^{-5}

V.3.4. Diffusion Ordered spectroscopy (DOSY)

The self-association of anthocyanins was also characterized by following the evolution of the diffusion coefficient (*D*) with respect to anthocyanin concentration. The diffusion coefficients (*D*) determined for different concentration were obtained by measuring the signal intensity at more than one place in the spectra. The diffusion measurements using DOSY were performed under identical experimental conditions taking special attention on the pH and temperature of the samples. A progressive decrease of *D* was observed as the anthocyanin concentration increase, in agreement with the increase of the overall complex size and higher hydrodynamic diameter

(Figure V.6). The fact that the diffusion coefficient values decrease with increasing anthocyanin concentration clearly demonstrates that anthocyanins can be organized in larger molecular structures. Similarly to the chemical shifts, diffusion coefficients were fitted using equation *(V.1)* (where $A_{obs} = D_{obs}$) which allowed the determination of K_{ass}, the diffusion coefficient of the anthocyanin in its free form (D_{free}) as well as the *D* value in its aggregated form ($D_{aggregate}$). Values of 3.1 and $2.4x10^{-10}$ $m^2.s^{-1}$ for mv3glc and mv3cumglc were found at the lower concentration tested and they corresponded to anthocyanins values in their free form (D_{free}). The equilibrium constant for the acylated malvidin was found to be higher than for the non-acylated anthocyanin (approximately 2-fold) in agreement with the chemical shift variation and once again suggesting a higher affinity of acylated anthocyanins to self-associate (Figure V.6). It is noteworthy that similar K_{ass} value was obtained whatever the variation monitored (chemical shift or diffusion coefficient).

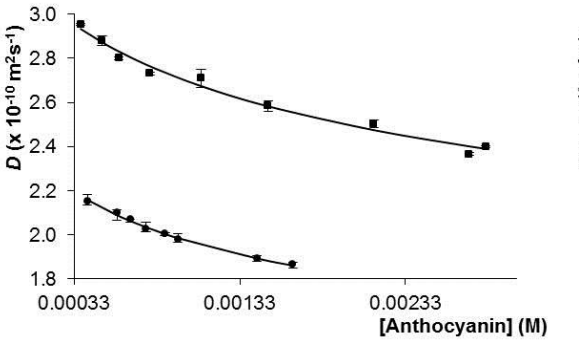

Figure V.6. Diffusion coefficient variation (*D*) *versus* mv3glc (▪) and mv3cumglc (•) concentration (M) in D_2O/DMSO (7:3). Solid lines represent the best fit obtained using equation *(V.1)* with K_{ass} = 1002 and 2203 M^{-1}, D_{free} = 3.1 and $2.4x10^{-10}$ $m^2.s^{-1}$ and $D_{aggregate}$ = 2.5 and $2.0x10^{-10}$ $m^2.s^{-1}$ for mv3glc and mv3cumglc, respectively. Accuracy was estimated to approximately 15%.

For other polyphenols like procyanidins, micellarization is a phenomenon well-known to occur *(225, 226)* and by plotting *D* value against the inverse concentration an approximated cac (critical aggregation concentrations) could be obtained. For mv3glc and mv3cumglc similar data analysis was performed and Figure V.7 illustrates the evolution of *D* as a function of inverse anthocyanin concentration for mv3glc and mv3cumglc. Similarly to the behavior observed for procyanidins *(225)*, when plotting *D versus* inverse anthocyanin concentration two linear variations could be observed corresponding to the behavior at low and high concentration. The intercept of the two straight lines allowed the determination of the cac probably suggesting that a micellization process takes place at that particular concentration (arrows in Figure V.7). In D_2O/DMSO the approximated cac value determined for both anthocyanins were very similar (0.40 $g.L^{-1}$ and 0.39 $g.L^{-1}$ for mv3cumglc and mv3glc, respectively). This could

probably indicate that the aggregation phenomenon occur at low concentration in these anthocyanins in accordance to the high tendency for these anthocyanins to self-associate. However special care should be taken when assuming the existence of a colloidal behavior since the present study only considered the case of anthocyanins self-association in D_2O/DMSO and in the 0.4 – 2.0 mM range and a higher range of concentrations should be tested.

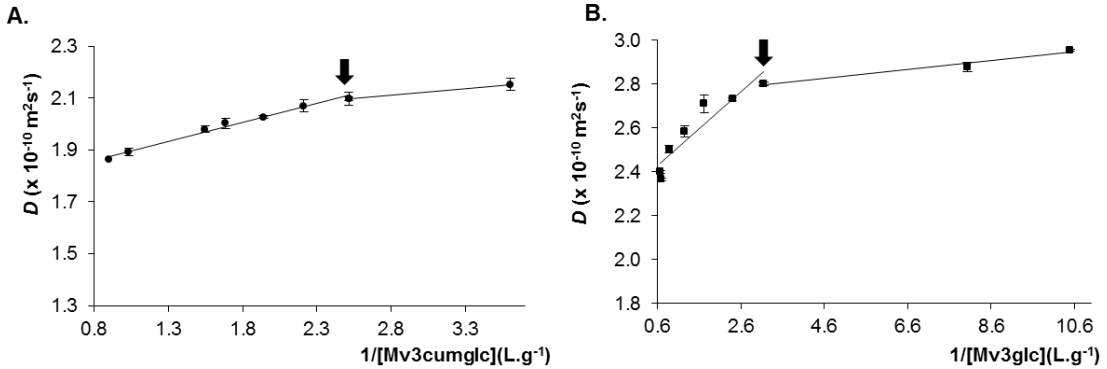

Figure V.7. Diffusion coefficient variation (*D*) *versus* mv3cumglc (•) and mv3glc (▪) inverse concentration ($L.g^{-1}$) for the determination of cac's values (shown as arrows).

V.3.5. Self-association of malvidin-3-O-glucoside in aqueous solution

In order to understand the impact of organic solvents, particularly DMSO, on anthocyanins self-association process, similar experiments were performed in D_2O solution. However, due to solubility issues this study could only be performed with mv3glc since it was not possible to obtain a clear and stable solution of mv3cumglc in D_2O. Malvidin-3-*O*-glucoside self-association constant (K_{ass}) was determined through diffusion coefficient (*D*) variation in D_2O. In aqueous solution this value increased, in comparison to the values obtained in D_2O/DMSO to 1245 M^{-1}. This increase could be due to the strengthening of the hydrophobic π–π interactions between anthocyanins molecules in aqueous solution and resulting in a higher affinity to self-associate. Simultaneously mv3glc's cac value in water was determined.

V.3.6. Molecular Dynamics simulations

To better characterize the conformational behavior of mv3cumglc molecules in an aqueous environment, computational studies were additionally carried out. To this regard, two MD simulations were performed. A structural analysis was done, in

particular the study of the inter-molecular and intra-molecular interactions within mv3cumlc molecules. Figure V.8 shows a representative structure of mv3cumglc molecules that were extracted during the two simulations. In regards to the first MD simulation (**A**), the mv3cumglc tends to adopt a folded geometry, in which the aromatic catechol group interacts by π stacking with the B ring or with A ring (see Figure V.8-A) and these interactions are in agreement with the NMR results presented in this work.

In the simulation with two anthocyanins (**B**), the formation of stable assembly involving both mv3cumglc molecules that are perfectly aligned between themselves by their large planar surfaces was observed after 16.8 ns (see Figure V.8-B). The later structural arrangement was maintained throughout the remaining 33.2 ns of simulation, revealing its higher stability.

This interaction occurs mainly by dispersive contacts (direct $\pi-\pi$ stacking and van der Waals interactions) because the AC and B nucleus provides a huge roughly planar polarizable surface that is strategically available to interact with the hydrophobic AC and B planes of the other polyphenol. Further, the binding driving force could also be strengthened by H-bonds involving the numerous hydroxyl groups from these polyphenols. The small proximity between these planes allows the establishment of optimized π stacking interactions that contribute to the higher stability of the global complex. With this interaction there is a concomitant high-energy release of water molecules from the solvation shells (hydrophobic effect). Similarly, to the simulation with only one mv3cumglc molecule, it was also observed that each anthocyanin molecule adopt a folded structure, in which the catechol group establishes hydrophobic and hydrophilic interactions with the other AC and B planes of the respective molecule.

Furthermore, Figure V.8 depicts some distances established between the non-polar hydrogen atoms of the same or different anthocyanin molecules as it was observed by NOESY experiments. Small distances (approximately 2 Å) was established between protons of the anthocyanidin moiety and protons from the aromatic acyl residue like OMe proton and proton H3'''5''' and between Hα and H2',6'. Similarly, distances of 2.2 and 2.8 Å could be observed between protons belonging to different anthocyanin moieties like H4/H2',6' and H4/OMe, respectively.

The exemplified distances confirm the existence of intra-molecular and inter-molecular interactions (evidenced in the NMR experiments) between these molecules in solution. In particular, their short distance reinforces the strong binding between the two different mv3cumglc molecules within the stable complex.

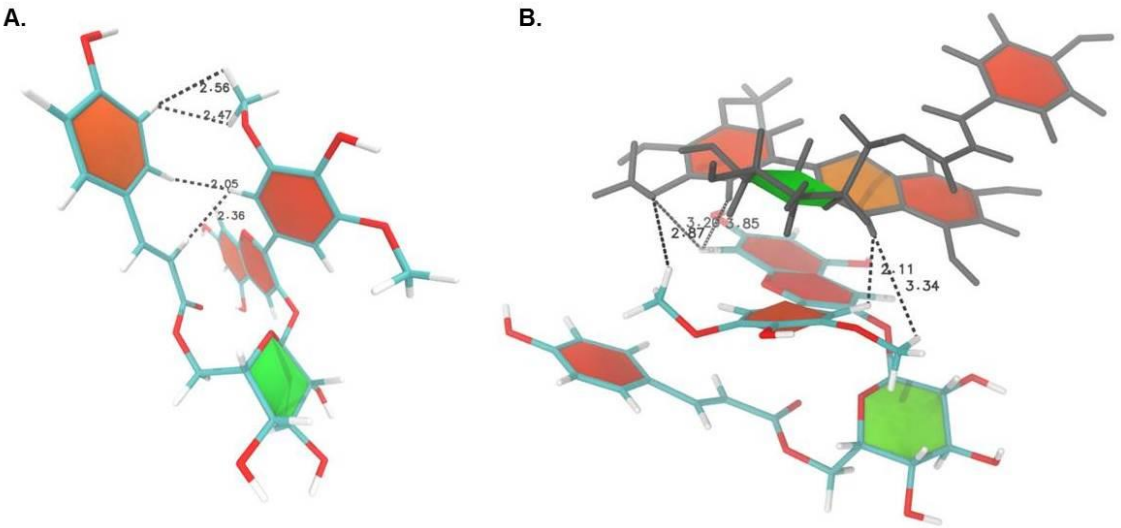

Figure V.8. Illustration of representative geometries of one and two molecules of mv3cumglc in an aqueous solution along each MD simulation. Some intra-molecular (**A**) and inter-molecular (**B**) interactions were also identified. The mv3cumglc molecules are depicted with sticks and are colored by atom type or gray.

V.4. Conclusions

In summary NMR spectroscopy (^{1}H, NOESY and DOSY) has been applied in this work to study the intra- and inter-molecular association processes in malvidin-3-*O*-cumaroylglucoside and malvidin-3-*O*-glucoside. Two processes of interaction seem to occur in acylated anthocyanins: formation of intra-molecular complexes that involves both the double bond and the coumaric acid aromatic ring and inter-molecular interaction resulting in the formation of larger aggregates. Acyl substituents seem to favor the flavylium cation aggregation with this compound showing a higher affinity to self-associate. This higher tendency to aggregate could also be reflected in the cac value, which occurred at lower concentration. The computational data support and clarify the structure of the intra and inter-molecular complexes formed.

The results obtained in this work provide important information regarding anthocyanin color stabilization a major issue for the development of natural components for food industry.

VI. Concluding Remarks and Future Work

Interest in anthocyanins has increased substantially over the past decades, and it is expected to continue to increase. From the standpoint of consumers, there is an increased awareness and interest about the potential impact of anthocyanins on food and health, and with this, an increasing demand for natural ingredients in contrast to the use of synthetic and/ or artificial ingredients in foods. This, in turn is stimulating the food industry toward the incorporation of more natural ingredients into foods, including the use of anthocyanin-based colorants as an alternative to the use of synthetic dyes. However, the use of anthocyanin-based colorants presents a number of challenges, including stability to processing and storage, compatibility with the matrix, their ability to produce the desired color as well as the fact that they may interact with other food components *(12)*. In the last years, a lot of effort has been made towards the development of anthocyanins stabilization mechanisms. However, owing to the diversity complexity and variability of anthocyanins chemical structure, this is an area that is in continuous development.

Bearing this, the main goals of this project was to gain knowledge regarding the interaction between anthocyanins and some food carbohydrates namely cyclodextrins and pectin. The results obtained in this work provide important information regarding anthocyanin color stabilization a major issue for the development of natural components for food industry. This study also allowed to verify that the selected carbohydrates can influence the chemistry of anthocyanin, affecting not only the network of chemical reaction but also anthocyanins stability. Larger polymers, like pectin, seem also to play an important role on anthocyanins extraction.

Although anthocyanins thermal stability increased due to the interaction with β-cyclodextrins, molecular inclusion also induced a clear change in the color of the anthocyanin solution causing a strong decrease in the anthocyanin visible absorption band (anti-copigmentation effect). The presence of this macrocycle produced an alteration on anthocyanins equilibrium and kinetic constants namely on the hydration constant. In fact, in the presence of β-CD the pigment hydration equilibrium was shifted towards the formation of more colorless forms through the flavylium cation which result in the loss of color.

Based on these results and also through NMR studies (DOSY and ROESY) and theoretical studies it was possible to establish the equilibrium form interacting preferentially with β-CD. The observed chemical shift displacements of protons

belonging to the hemiketal, together with the diffusion coeficients measurements and the NOE studies have anticipated the formation of an inclusion complex between the hemiketal equilibrium form and β-CD. The anthocyanin hemiketal equilibrium specie formed a 1:1 inclusion complex with β-cyclodextrin in which the pyranic C ring was deeply included inside the β-CD cavity while B ring lies on the plan of the wider rim of β-CD. The sugar unit was left outside the cavity.

One of the main conclusions to be highlighted is the possible occurrence of interactions between anthocyanins and carbohydrates present plant cell walls. With the disruption of plant tissues an interaction between the constituents of cell walls and of the vacuoles may occur. In this work, for the first time we report a methodology of STD-NMR to the study of the binding between anthocyanins and polymeric carbohydrates (low methoxylated pectins). This methodology allowed the measurement of weak interactions occurring between anthocyanins and this polysaccharide and the determination of the affinity between different anthocyanin equilibrium forms and pectin. This interaction was probably driven by hydrogen bonding and hydrophobic interactions and a variation in the extent of the interaction between the flavylium cation and the hemiketal equilibrium form was noticed with the charged specie revealing a stronger interaction with pectin. Structural aspects of anthocyanin molecule seem also to affect the binding between these two components with anthocyanins bearing a pyrogallol group revealing to be a stronger binder to pectin (compared to anthocyanins with a catechol group).

The occurrence of two stabilizing mechanisms, namely intra-molecular and inter-molecular co-pigmentation was found to occur on anthocyanins. Acyl substituents seem to favor the flavylium cation aggregation and acylated anthocyanin was found to self-associate with a higher affinity constant compared to the non-acylated anthocyanin resulting in the formation of larger aggregates. This higher tendency to aggregate could also be reflected in the cac value, which occurred at lower concentration.

The results present herein contribute to a better knowledge regarding the chemistry of anthocyanins, particularly important for the interaction between these natural pigments and carbohydrates usually used in the food, cosmetic and pharmaceutical industries. This project addresses a current thematic and although the relevance of the results obtained in this work and the progress made in recent years, this reflects only

the starting point for the study of anthocyanin-carbohydrate interaction from a fundamental and structural point of view.

Future work should address the understanding of the impact of these associations in anthocyanin's color and chemical stability. Besides this, anthocyanin-carbohydrate interaction is a very important issue regarding anthocyanin's extraction from plant material during plant processing to obtain colorants and drinks (wine, fruit juices). Also, depending on the tendency to interact with selected polysaccharides, changes in anthocyanin's bioavailability and hence on their biological properties should be expected.

Experimental approach should be related with some anthocyanin and carbohydrate structural features and how these features affect this interaction. Future work should also be related with the presence of different substrates (*e.g*. procyanidins, proteins, metal ions) and medium conditions (*e.g.* pH, temperature, ionic strength) and how these aspects may affect the specificity of the binding between different polysaccharides and anthocyanins.

REFERENCES

(1) Munin, A.; Edwards-Lévy, F., Encapsulation of Natural Polyphenolic Compounds: a Review. *Pharmaceutics,* **2011**, *3*, 793-829.

(2) Clydesdale, F. M., Color as a factor in food choice. *Crit. Rev. Food Sci.,* **1993**, *33*, 83-101.

(3) McCann, D.; Barrett, A.; Cooper, A.; Crumpler, D.*, et al.*, Food additives and hyperactive behaviour in 3-year-old and 8/9-year-old children in the community: a randomised, double-blinded, placebo-controlled trial. *The Lancet,* **2007**, *370*, 1560-1567.

(4) Delgado-Vargas, F.; Paredes-López, O., Pigments as Food Colorants. In *Natural Colorants for Food and Nutraceutical Uses*, CRC Press: 2003.

(5) Giusti, M. M.; Wrolstad, R. E., Acylated anthocyanins from edible sources and their applications in food systems. *Biochem. Eng. J.,* **2003**, *14*, 217-225.

(6) Leydet, Y.; Gavara, R.; Petrov, V.; Diniz, A. M.*, et al.*, The effect of self-aggregation on the determination of the kinetic and thermodynamic constants of the network of chemical reactions in 3-glucoside anthocyanins. *Phytochemistry,* **2012**, *83*, 125-135.

(7) Markakis, P., Stability of Anthocyanins in Foods. In *Anthocyanins As Food Colors*, Markakis, P., Ed. Academic Press: 1982; pp 163-180.

(8) Bridle, P.; Timberlake, C. F., Anthocyanins as natural food colours-selected aspects. *Food Chem.,* **1997**, *58*, 103-109.

(9) Clifford, M. N., Anthocyanins - nature, occurrence and dietary burden. *J. Sci. Food Agric.,* **2000**, *80*, 1063-1072.

(10) Kong, J. M.; Chia, L. S.; Goh, N. K.; Chia, T. F.*, et al.*, Analysis and biological activities of anthocyanins. *Phytochemistry,* **2003**, *64*, 923-933.

(11) Kähkönen, M. P.; Heinämäki, J.; Ollilainen, V.; Heinonen, M., Berry anthocyanins: isolation, identification and antioxidant activities. *J. Sci. Food Agric.,* **2003**, *83*, 1403-1411.

(12) He, J. A.; Giusti, M. M., Anthocyanins: Natural Colorants with Health-Promoting Properties. In *Annual Review of Food Science and Technology, Vol 1*, Doyle, M. P.; Klaenhammer, T. R., Eds. Annual Reviews: Palo Alto, 2010; Vol. 1, pp 163-187.

(13) Cavalcanti, R. N.; Santos, D. T.; Meireles, M. A. A., Non-thermal stabilization mechanisms of anthocyanins in model and food systems—An overview. *Food Res. Int.,* **2011**, *44*, 499-509.

(14) Harborne, J. B.; Williams, C. A., Advances in flavonoid research since 1992. *Phytochemistry,* **2000**, *55*, 481-504.

(15) Kennedy, D. O.; Wightman, E. L., Herbal Extracts and Phytochemicals: Plant Secondary Metabolites and the Enhancement of Human Brain Function. *Adv. Nutr.,* **2011**, *2*, 32-50.

(16) Manach, C.; Scalbert, A.; Morand, C.; Remesy, C.*, et al.*, Polyphenols: food sources and bioavailability. *Am. J. Clin. Nutr.,* **2004**, *79*, 727-747.

(17) Cheynier, V., Polyphenols in foods are more complex than often thought. *Am. J. Clin. Nutr.,* **2005**, *81*, 223S-229S.

(18) Lesschaeve, I.; Noble, A. C., Polyphenols: factors influencing their sensory properties and their effects on food and beverage preferences. *Am. J. Clin. Nutr.,* **2005**, *81*, 330S-335S.

(19) Scalbert, A.; Manach, C.; Morand, C.; Rémésy, C.*, et al.*, Dietary Polyphenols and the Prevention of Diseases. *Crit. Rev. Food Sci.,* **2005**, *45*, 287-306.

(20) Renaud, S.; de Lorgeril, M., Wine, alcohol, platelets, and the French paradox for coronary heart disease. *The Lancet,* **1992**, *339*, 1523-1526.

(21) Milner, J. A., Reducing the risk of cancer. In *Functional Foods: Designer Foods, Pharmafoods, Nutraceuticals*, Goldberg, I., Ed. Chapman & Hall: New York, USA, 1994; pp 39-70.

(22) Tsao, R., Chemistry and Biochemistry of Dietary Polyphenols. *Nutrients,* **2010**, *2*, 1231-1246.

(23) Dangles, O., Antioxidant Activity of Plant Phenols: Chemical Mechanisms and Biological Significance. *Curr. Org. Chem.,* **2012**, *16*, 692-714.

(24) Shahidi, F.; Naczk, M., *Food phenolics: sources, chemistry, effects and applications*. Technomics Publishing Co: Lancaster, PA, 1995.

(25) Quideau, S.; Deffieux, D.; Douat-Casassus, C.; Pouységu, L., Plant Polyphenols: Chemical Properties, Biological Activities, and Synthesis. *Angew. Chem. Int. Ed.,* **2011**, *50*, 586-621.

(26) Andersen, Ø.; Markham, K., *Flavonoids: chemistry, biochemistry and applications*. CRC Press: Boca Raton, Florida, 2006.

(27) El Gharras, H., Polyphenols: food sources, properties and applications – a review. *Int. J. Food Sci. Tech.,* **2009**, *44*, 2512-2518.

(28) Scalbert, A.; Williamson, G., Dietary Intake and Bioavailability of Polyphenols. *Journal of Nutrition,* **2000**, *130*, 2073-2085.

(29) Monagas, M.; Bartolomé, B.; Gómez-Cordovés, C., Updated Knowledge About the Presence of Phenolic Compounds in Wine. *Crit. Rev. Food Sci.,* **2005**, *45*, 85-118.

(30) Arts, I. C. W.; van de Putte, B.; Hollman, P. C. H., Catechin Contents of Foods Commonly Consumed in The Netherlands. 1. Fruits, Vegetables, Staple Foods, and Processed Foods. *J. Agric. Food. Chem.,* **2000**, *48*, 1746-1751.

(31) Arts, I. C. W.; van de Putte, B.; Hollman, P. C. H., Catechin Contents of Foods Commonly Consumed in The Netherlands. 2. Tea, Wine, Fruit Juices, and Chocolate Milk. *J. Agric. Food. Chem.,* **2000**, *48*, 1752-1757.

(32) Scalbert, A., Antimicrobial properties of tannins. *Phytochemistry,* **1991**, *30*, 3875-3883.

(33) Harborne, A. J., *Phytochemical Methods A Guide to Modern Techniques of Plant Analysis*. 3 rd ed.; Chapman & Hall: London, 1998.

(34) Naczk, M.; Oickle, D.; Pink, D.; Shahidi, F., Protein Precipitating Capacity of Crude Canola Tannins: Effect of pH, Tannin, and Protein Concentrations. *J. Agric. Food. Chem.,* **1996**, *44*, 2144-2148.

(35) Foo, L. Y.; Lu, Y.; McNabb, W. C.; Waghorn, G.*, et al.*, Proanthocyanidins from *Lotus pedunculatus*. *Phytochemistry,* **1997**, *45*, 1689-1696.

(36) Muller-harvey, I.; B., M. A., Tannins: their biochemistry and nutritional properties. *Adv. Plant Cell Biochem. Biotechnol.,* **1992**, *1*, 151-217.

(37) Takeoka, G. R.; Dao, L. T., Anthocyanins. In *Methods of Analysis for Functional Foods and Nutraceuticals*, 2nd Edition ed.; Hurst, J., Ed. CRC Press, Taylor & Francis Group: Boca Raton, Florida, 2002; pp 247-276.

(38) Andersen, Ø.; Jordheim, M. In *Anthocyanins - food applications* 5th International Conference on Pigments in Foods - For Quality and Health, Helsinki, Finland, 2008; Helsinki, Finland, 2008.

(39) Delgado-Vargas, F.; Paredes-Lopez, O., Anthocyanins and betalains. In *Natural Colorants for Food and Nutraceutical Uses*, CRC Press, Taylor & Francis Group: Boca Raton, Florida, 2003; pp 167-219.

(40) Andersen, O.; Jordheim, M., Basic anthocyanin chemistry and dietary sources. In *Anthocyanins in Health and Disease*, Wallace, T. C.; Giusti, M., Eds. CRC Press: Boca Raton, Florida, USA, 2013; pp 13-90.

(41) Harborne, J. B., Phenolic compounds. In *Phytochemical Methods - A Guide to Modern Techniques of Plant Analysis* chapman & Hall: New York, 1998; pp 66-74.

(42) Cooper-Driver, G. A.; Bhattacharya, M., Role of phenolics in plant evolution. *Phytochemistry,* **1998**, *49*, 1165-1174.

(43) Mazza, G.; Miniati, E., Grapes. In *Anthocyanins in Fruits, Vegetables and Grains*, Mazza, G.; Miniati, E., Eds. CRC Press, Taylor & Francis Group: Boca Raton, Florida, 1993; pp 149-199.

(44) Wang, H.; Cao, G.; Prior, R. L., Oxygen Radical Absorbing Capacity of Anthocyanins. *J. Agric. Food. Chem.,* **1997**, *45*, 304-309.

(45) Tamura, H.; Yamagami, A., Antioxidative activity of monoacylated anthocyanins isolated from Muscat Bailey A grape. *J. Agric. Food. Chem.,* **1994**, *42*, 1612-1615.

(46) Rice-Evans, C. A.; Miller, N. J., Antioxidant activities of flavonoids as bioactive components of food. *Biochem Soc Trans,* **1996**, *24*, 790-795.

(47) Prior, R. L.; Cao, G.; Martin, A.; Sofic, E.*, et al.*, Antioxidant Capacity As Influenced by Total Phenolic and Anthocyanin Content, Maturity, and Variety of *Vaccinium* species. *J. Agric. Food. Chem.,* **1998**, *46*, 2686-2693.

(48) Degenhardt, A.; Knapp, H.; Winterhalter, P., Separation and Purification of Anthocyanins by High-Speed Countercurrent Chromatography and Screening for Antioxidant Activity. *J. Agric. Food. Chem.,* **2000**, *48*, 338-343.

(49) Rice-Evans, C. A.; Miller, N. J.; Paganga, G., Structure-antioxidant activity relationships of flavonoids and phenolic acids. *Free Radical Biol. Med.,* **1996**, *20*, 933-956.

(50) Timberlake, C. F.; Henry, B. S., Anthocyanins as natural food colorants. *Prog Clin Biol Res,* **1988**, *208*, 107-121.

(51) Lietti, A.; Cristoni, A.; Picci, M., Studies on *Vaccinium myrtillus* anthocyanosides. I. Vasoprotective and anti-inflamatory activity. *Arzneim.-Forsch.,* **1976**, *26*, 829-32.

(52) Seeram, N. P.; Bourquin, L. D.; Nair, M. G., Degradation Products of Cyanidin Glycosides from Tart Cherries and Their Bioactivities. *J. Agric. Food. Chem.,* **2001**, *49*, 4924-4929.

(53) Kamei, H.; Kojima, T.; Hasegawa, M.; Koide, T.*, et al.*, Suppression of tumor cell growth by anthocyanins in vitro. *Cancer Invest.,* **1995**, *13*, 590-4.

(54) Hou, D. X., Potential mechanisms of cancer chemoprevention by anthocyanins. In *Current Molecular Medicine*, 2003; Vol. 3, pp 149-159.

(55) Akhmadieva, A. K.; Zaichkina, S. I.; Ruzieva, R. K.; Ganassi, E. E., The protective action of a natural preparation of anthocyan (pelargonidin-3,5-diglucoside). *Radiobiologiia,* **1993**, *33*, 433-5.

(56) Tsuda, T.; Horio, F.; Uchida, K.; Aoki, H.*, et al.*, Dietary Cyanidin 3-O-β-D-Glucoside-Rich Purple Corn Color Prevents Obesity and Ameliorates Hyperglycemia in Mice. *J. Nutr.,* **2003**, *133*, 2125-2130.

(57) Eder, R., Pigments. In *Food Analysis by HPLC*, Nollet, L., Ed. Marcel Dekker: Monticello, NY, 2000; pp 845-880.

(58) Heredia, F. J.; Francia-Aricha, E. M.; Rivas-Gonzalo, J. C.; Vicario, I. M.*, et al.*, Chromatic characterization of anthocyanins from red grapes - I. pH effect. *Food Chem.,* **1998**, *63*, 491-498.

(59) Honda, T.; Saito, N., Recent progress in the chemistry of polyacylated anthocyanins as flower color pigments. *Heterocycles,* **2002**, *56*, 633-692.

(60) Otsuki, T.; Matsufuji, H.; Takeda, M.; Toyoda, M.*, et al.*, Acylated anthocyanins from red radish (*Raphanus sativus* L.). *Phytochemistry,* **2002**, *60*, 79-87.

(61) Fossen, T.; Øvstedal, D. O.; Slimestad, R.; Andersen, Ø. M., Anthocyanins from a Norwegian potato cultivar. *Food Chem.,* **2003**, *81*, 433-437.

(62) Andersen, Ø. M.; Fossen, T., Anthocyanins with an unusual acylation pattern from stem of *Allium victorialis*. *Phytochemistry,* **1995**, *40*, 1809-1812.

(63) Borkowski, T.; Szymusiak, H.; Gliszczynska-Swiglo, A.; Tyrakowska, B., The effect of 3-O-beta-glycosylation on structural transformations of anthocyanins. *Food Res. Int.,* **2005**, *38*, 1031-1037.

(64) Dangles, O.; Saito, N.; Brouillard, R., Anthocyanin intramolecular copigment effect. *Phytochemistry,* **1993**, *34*, 119-124.

(65) Francis, F. J., A new group of food colorants. *Trends Food Sci.Tech.,* **1992**, *3*, 27-30.

(66) Francis, F. J.; Markakis, P. C., Food colorants: Anthocyanins. *Crit. Rev. Food Sci.,* **1989**, *28*, 273 - 314.

(67) Wu, X.; Beecher, G. R.; Holden, J. M.; Haytowitz, D. B.*, et al.*, Concentrations of Anthocyanins in Common Foods in the United States and Estimation of Normal Consumption. *J. Agric. Food. Chem.,* **2006**, *54*, 4069-4075.

(68) Shahidi, F.; Naczk, M., Contribution of phenolic compounds to flavor and color characteristics of foods. In *Phenolics in Foods and Nutraceuticals*, CRC Press: Boca Raton, Florida, 2004; pp 443-461.

(69) de Pascual-Teresa, S.; Moreno, D.; García-Viguera, C., Flavanols and Anthocyanins in Cardiovascular Health: A Review of Current Evidence Flavanols and Anthocyanins in Cardiovascular Health. *Int J Mol Sci. ,* **2010**, *11*, 1679-1703.

(70) Brouillard, R., Chemical Structure of Anthocyanins. In *Anthocyanins As Food Colors*, Markakis, P., Ed. Academic Press: 1982; pp 1-40.

(71) WHO, Toxicological evaluation of certain food additives. In Addit., F. W. E. C. F., Ed. Geneva, 1982.

(72) Wrolstad, R. E., Anthocyanins. In *Natural food colorants: science and technology* Lauro, G. J.; Francis, F. J., Eds. Dekker, M.: New York, 2000.

(73) Fulcrand, H.; Atanasova, V.; Salas, E.; Cheynier, V., The fate of anthocyanins in wine: are there determining factors? In *Red wine color: Revealing the Mysteries*, Waterhouse, A. L.; Kennedy, J. A., Eds. 2004; pp 68-88.

(74) Berké, B.; Chèze, C.; Vercauteren, J.; Deffieux, G., Bisulfite addition to anthocyanins: revisited structures of colourless adducts. *Tetrahedron Lett.,* **1998**, *39*, 5771-5774.

(75) Jordheim, M.; Fossen, T.; Songstad, J.; Andersen, Ø. M., Reactivity of Anthocyanins and Pyranoanthocyanins. Studies on Aromatic Hydrogen–Deuterium Exchange Reactions in Methanol. *J. Agric. Food. Chem.,* **2007**, *55*, 8261-8268.

(76) Remy-Tanneau, S.; Le Guernevé, C.; Meudec, E.; Cheynier, V., Characterization of a Colorless Anthocyanin−Flavan-3-ol Dimer Containing Both Carbon−Carbon and Ether Interflavanoid Linkages by NMR and Mass Spectrometry. *J. Agric. Food. Chem.,* **2003**, *51*, 3592-3597.

(77) Bueno, J. M.; Sáez-Plaza, P.; Ramos-Escudero, F.; Jiménez, A. M.*, et al.*, Analysis and Antioxidant Capacity of Anthocyanin Pigments. Part II: Chemical Structure, Color, and Intake of Anthocyanins. *Crit. Rev. Anal. Chem.,* **2012**, *42*, 126-151.

(78) Fulcrand, H.; Benabdeljalil, C.; Rigaud, J.; Cheynier, V.*, et al.*, A new class of wine pigments generated by reaction between pyruvic acid and grape anthocyanins. *Phytochemistry,* **1998**, *47*, 1401-1407.

(79) Santos-Buelga, C.; De Freitas, V., Influence of Phenolics on wine organoleptic properties. In *Wine Chemistry and Biochemistry*, Moreno-Arribas, M. V.; Polo, M. C., Eds. Springer: 2009; pp 529-570.

(80) Mazza, G.; Brouillard, R., The mechanism of co-pigmentation of anthocyanins in aqueous solutions. *Phytochemistry,* **1990**, *29*, 1097-1102.

(81) Brouillard, R.; Dangles, O., Flavonoids and flower colour. In *The Flavonoids: Advances in Research since 1986*, Harborne, J. B., Ed. Chapman & Hall: London, 1994; pp 565–588.

(82) Cabrita, L.; Fossen, T.; Andersen, Ø. M., Colour and stability of the six common anthocyanidin 3-glucosides in aqueous solutions. *Food Chem.,* **2000**, *68*, 101-107.

(83) Torskangerpoll, K.; Andersen, Ø. M., Colour stability of anthocyanins in aqueous solutions at various pH values. *Food Chem.,* **2005**, *89*, 427-440.

(84) Fleschhut, J.; Kratzer, F.; Rechkemmer, G.; Kulling, S. E., Stability and biotransformation of various dietary anthocyanins in vitro. *Eur J Nutr,* **2006**, *45*, 7-18.

(85) von Elbe, M.; Shwartz, R., Colorants. In *Food Chem.*, Fennema, O., Ed. Marcel Dekker, Inc: New York, 1996; pp 681-694.

(86) Bakker, J.; Timberlake, C. F., Isolation, Identification, and Characterization of New Color-Stable Anthocyanins Occurring in Some Red Wines. *J. Agric. Food. Chem.,* **1997b**, *45*, 35-43.

(87) Mateus, N.; de Freitas, V., Evolution and stability of anthocyanin-derived pigments during port wine aging. *J. Agric. Food. Chem.,* **2001b**, *49*, 5217-5222.

(88) Asen, S.; Stewart, R. N.; Norris, K. H., Co-pigmentation of anthocyanins in plant tissues and its effect on color. *Phytochemistry,* **1972**, *11*, 1139-1144.

(89) Brouillard, R.; Lang, J., The hemiacetal-cis-chalcone equilibrium of malvin, a natural anthocyanin. *Can. J. Chem.,* **1990**, *68*, 755.

(90) Ahmed, J.; Shivhare, U. S.; Raghavan, G. S. V., Thermal degradation kinetics of anthocyanin and visual colour of plum puree. *Eur. Food Res. Technol.,* **2004**, *218*, 525-528.

(91) Rein, M. J.; Heinonen, M., Stability and Enhancement of Berry Juice Color. *J. Agric. Food. Chem.,* **2004**, *52*, 3106-3114.

(92) Jackman, R. L.; Yada, R. Y.; Tung, M. A.; Speers, R. A., Anthocyanins as food colorants - a review. *J. Food Biochem.,* **1987**, *11*, 201-247.

(93) Furtado, P.; Figueiredo, P.; Chaves das Neves, H.; Pina, F., Photochemical and thermal degradation of anthocyanidins. *J. Photochem. Photobiol. A - Chem.,* **1993**, *75*, 113-118.

(94) Brouillard, R.; Delaporte, B., Chemistry of anthocyanin pigments. 2. Kinetic and thermodynamic study of proton transfer, hydration, and tautomeric reactions of malvidin 3-glucoside. *J. Am. Chem. Soc.,* **1977**, *99*, 8461-8468.

(95) Brouillard, R.; Dubois, J. E., Mechanism of the structural transformations of anthocyanins in acidic media. *J. Am. Chem. Soc.,* **1977**, *99*, 1359-1364.

(96) Pina, F., Thermodynamics and kinetics of flavylium salts. Malvidin revisited. *J. Chem. Soc., Faraday Trans.,* **1998**, *94*, 2109-2116.

(97) Pina, F.; Melo, M. J.; Laia, C. A. T.; Parola, A. J.*, et al.*, Chemistry and applications of flavylium compounds: a handful of colours. *Chem. Soc. Rev.,* **2012**, *41*, 869-908.

(98) Preston, N. W.; Timberlake, C. F., Separation of anthocyanin chalcones by high-performance liquid chromatography. *J. Chromatogr. A,* **1981**, *214*, 222-228.

(99) Santos, H.; Turner, D. L.; Lima, J. C.; Figueiredo, P.*, et al.*, Elucidation of the multiple equilibria of malvin in aqueous solution by One- and two-dimensional NMR. *Phytochemistry,* **1993**, *33*, 1227-1232.

(100) Asenstorfer, R. E.; Iland, P. G.; Tate, M. E.; Jones, G. P., Charge equilibria and p*K*a of malvidin-3-glucoside by electrophoresis. *Anal. Biochem.,* **2003**, *318*, 291-299.

(101) Sadilova, E.; Carle, R.; Stintzing, F. C., Thermal degradation of anthocyanins and its impact on color and in vitro antioxidant capacity. *Mol. Nutrit. Food Res.,* **2007**, *51*, 1461-1471.

(102) Sadilova, E.; Stintzing, F. C.; Carle, R., Thermal Degradation of Acylated and Nonacylated Anthocyanins. *J. Food Sci.,* **2006**, *71*, C504-C512.

(103) Cevallos-Casals, B. A.; Cisneros-Zevallos, L., Stability of anthocyanin-based aqueous extracts of Andean purple corn and red-fleshed sweet potato compared to synthetic and natural colorants. *Food Chem.,* **2004**, *86*, 69-77.

(104) Fossen, T.; Andersen, Ø. M., Cyanidin 3-*O*-(6″-Succinyl-β-glucopyranoside) and other anthocyanins from *Phragmites Australis*. *Phytochemistry,* **1998**, *49*, 1065-1068.

(105) Kırca, A.; Özkan, M.; Cemeroğlu, B., Effects of temperature, solid content and pH on the stability of black carrot anthocyanins. *Food Chem.,* **2007**, *101*, 212-218.

(106) Osmani, S. A.; Halkjær Hansen, E.; Malien-Aubert, C.; Olsen, C.-E.*, et al.*, Effect of Glucuronosylation on Anthocyanin Color Stability. *J. Agric. Food. Chem.,* **2009**, *57*, 3149-3155.

(107) Bąkowska, A.; Kucharska, A. Z.; Oszmiański, J., The effects of heating, UV irradiation, and storage on stability of the anthocyanin–polyphenol copigment complex. *Food Chem.,* **2003**, *81*, 349-355.

(108) Cruz, L.; Petrov, V.; Teixeira, N.; Mateus, N.*, et al.*, Establishment of the Chemical Equilibria of Different Types of Pyranoanthocyanins in Aqueous Solutions: Evidence for the Formation of Aggregation in Pyranomalvidin-3-*O*-coumaroylglucoside-(+)-catechin. *J. Phys. Chem. B,* **2010**, *114*, 13232-13240.

(109) Oliveira, J.; Mateus, N.; de Freitas, V., Previous and recent advances in pyranoanthocyanins equilibria in aqueous solution. *Dyes Pigments,* **2014**, *100*, 190-200.

(110) Oliveira, J.; Brás, N. F.; da Silva, M. A.; Mateus, N.*, et al.*, Grape anthocyanin oligomerization: A putative mechanism for red color stabilization? *Phytochemistry,* **2014**, *105*, 178-185.

(111) Boulton, R., The Copigmentation of Anthocyanins and Its Role in the Color of Red Wine: A Critical Review. *American Journal of Enology and Viticulture,* **2001**, *52*, 67-87.

(112) Dangles, O.; Elhabiri, M.; Brouillard, R., Kinetic and thermodynamic investigation of the aluminium-anthocyanin complexation in aqueous solution. *J. Chem. Soc., Perkin Trans. 2,* **1994**, 2587-2596.

(113) Moncada, M. C.; Moura, S.; Melo, M. J.; Roque, A.*, et al.*, Complexation of aluminum (III) by anthocyanins and synthetic flavylium salts: A source for blue and purple color. *Inorg. Chim. Acta,* **2003**, *356*, 51-61.

(114) Yoshida, K.; Kitahara, S.; Ito, D.; Kondo, T., Ferric ions involved in the flower color development of the Himalayan blue poppy, *Meconopsis grandis*. *Phytochemistry,* **2006**, *67*, 992-998.

(115) Schreiber, H. D.; Swink, A. M.; Godsey, T. D., The chemical mechanism for Al^{3+} complexing with delphinidin: A model for the bluing of *hydrangea sepals*. *J. Inorg. Biochem.,* **2010**, *104*, 732-739.

(116) Castañeda-Ovando, A.; Pacheco-Hernández, M. L.; Páez-Hernández, M. E.; Rodríguez, J. A.*, et al.*, Chemical studies of anthocyanins: A review. *Food Chem.,* **2009**, *113*, 859-871.

(117) Brouillard, R.; Chassaing, S.; Fougerousse, A., Why are grape/fresh wine anthocyanins so simple and why is it that red wine color lasts so long? *Phytochemistry,* **2003**, *64*, 1179-1186.

(118) Williams, M.; Hrazdina, G., Anthocyanins as food colorants: effect of pH on the formation of anthocyanin-rutin complexes. *J. Food Sci.,* **1979**, *44*, 66-68.

(119) Scheffeldt, P.; Hrazdina, G., Co-pigmentation of anthocyanins under physiological conditions. *J. Food Sci.,* **1978**, *43*, 517-520.

(120) Brouillard, R.; Mazza, G.; Saad, Z.; Albrecht-Gary, A. M.*, et al.*, The co-pigmentation reaction of anthocyanins: a microprobe for the structural study of aqueous solutions. *J. Am. Chem. Soc.,* **1989**, *111*, 2604-2610.

(121) Brouillard, R.; Wigand, M.-C.; Dangles, O.; Cheminat, A., pH and solvent effects on the copigmentation reaction of malvin with polyphenols, purine and pyrimidine derivatives. *J. Chem. Soc., Perkin Trans. 2,* **1991**, 1235-1241.

(122) Eiro, M. J.; Heinonen, M., Anthocyanin Color Behavior and Stability during Storage: Effect of Intermolecular Copigmentation. *J. Agric. Food. Chem.,* **2002**, *50*, 7461-7466.

(123) Markovic, J. M. D.; Petranovic, N. A.; Baranac, J. M., A spectrophotometric study of the copigmentation of malvin with caffeic and ferulic acids. *J. Agric. Food. Chem.,* **2000**, *484*, 5530-5536.

(124) Rein, M. Copigmentation reactions and color stability of berry anthocyanins. Helsinki, Helsinki, Finland, 2005.

(125) Brouillard, R., The *in vivo* expression of anthocyanin colour in plants. *Phytochemistry,* **1983**, *22*, 1311-1323.

(126) Lambert, S. G.; Asenstorfer, R. E.; Williamson, N. M.; Iland, P. G.*, et al.*, Copigmentation between malvidin-3-glucoside and some wine constituents and its importance to colour expression in red wine. *Food Chem.,* **2011**, *125*, 106-115.

(127) Timberlake, C. F.; Bridle, P., The anthocyanins. In *The flavonoids*, Harborne, J. B.; Mabry, T. J.; Mabry, H., Eds. Chapman & hall: london, 1975; pp 214-266.

(128) Hoshino, T.; Matsumoto, U.; Harada, N.; Goto, T., Chiral exciton coupled stacking of anthocyanins: interpretation of the origin of anomalous CD induced by anthocyanin association. *Tetrahedron Lett.,* **1981**, *22*, 3621-3624.

(129) González-Manzano, S.; Mateus, N.; de Freitas, V.; Santos-Buelga, C., Influence of the degree of polymerisation in the ability of catechins to act as anthocyanin copigments. *Eur. Food Res. Technol.,* **2008**, *227*, 83-92.

(130) Goto, T.; Kondo, T., Structure and Molecular Stacking of Anthocyanins—Flower Color Variation. *Angewandte Chemie International Edition in English,* **1991**, *30*, 17-33.

(131) Hoshino, T.; Matsumoto, U.; Goto, T., Evidences of the self-association of anthocyanins I. Circular Dichroism of cyanin anhydrobase. *Tetrahedron Lett.,* **1980**, *21*, 1751-1754.

(132) Hoshino, T.; Matsumoto, U.; Goto, T.; Harada, N., Evidence for the self-association of anthocyanins IV. PMR spectroscopic evidence for the vertical stacking of anthocyanin molecules. *Tetrahedron Lett.,* **1982**, *23*, 433-436.

(133) Andersen, Ø. M.; Jordheim, M., Anthocyanins. In *eLS*, John Wiley & Sons, Ltd: 2001.

(134) Houbiers, C.; Lima, J. C.; Maçanita, A. L.; Santos, H., Color Stabilization of Malvidin 3-Glucoside: Self-Aggregation of the Flavylium Cation and Copigmentation with the *Z*-Chalcone Form. *J. Phys. Chem. B,* **1998**, *102*, 3578-3585.

(135) Dangles, O.; Saito, N.; Brouillard, R., Kinetic and thermodynamic control of flavylium hydration in the pelargonidin-cinnamic acid complexation. Origin of the extraordinary flower color diversity of *Pharbitis nil*. *J. Am. Chem. Soc.,* **1993**, *115*, 3125-3132.

(136) Kopjar, M.; PiliŽota, V.; Tiban, N. N.; ŠubariĆ, D.*, et al.*, Strawberry jams: influence of differnt pectins on colour and textural properties. *Czech J. Food Sci.,* **2009**, *27*, 20-28.

(137) Buchweitz, M.; Speth, M.; Kammerer, D. R.; Carle, R., Impact of pectin type on the storage stability of black currant (*Ribes nigrum* L.) anthocyanins in pectic model solutions. *Food Chem.,* **2013**, *139*, 1168-1178.

(138) Poiana, M. A.; Munteanu, M. F.; Bordean, D. M.; Gligor, R.*, et al.*, Assessing the effects of different pectins addition on color quality and antioxidant properties of blackberry jam. *Chem. Cent. J.,* **2013**, *7*, 1-13.

(139) Hubbermann, E. M.; Heins, A.; Stöckmann, H.; Schwarz, K., Influence of acids, salt, sugars and hydrocolloids on the colour stability of anthocyanin rich black currant and elderberry concentrates. *Eur. Food Res. Technol.,* **2006**, *223*, 83-90.

(140) Lewis, C. E.; Walker, J. R. L.; Lancaster, J. E., Effect of polysaccharides on the colour of anthocyanins. *Food Chem.,* **1995**, *54*, 315-319.

(141) Yamada, T.; Komiya, T.; Akaki, M., Formation of an Inclusion Complex of Anthocyanin with Cyclodextrin. *Agric. Biol. Chem.,* **1980**, *44*, 1411-1413.

(142) Mourtzinos, I.; Makris, D. P.; Yannakopoulou, K.; Kalogeropoulos, N.*, et al.*, Thermal Stability of Anthocyanin Extract of *Hibiscus sabdariffa* L. in the Presence of b-Cyclodextrin. *J. Agric. Food. Chem.,* **2008**, *56*, 10303-10310.

(143) Dangles, O.; Stoeckel, C.; Wigand, M. C.; Brouillard, R., Two very distinct types of anthocyanin complexation: Copigmentation and inclusion. *Tetrahedron Lett.,* **1992**, *33*, 5227-5230.

(144) Dangles, O.; Wigand, M. C.; Brouillard, R., Anthocyanin anti-copigment effect. *Phytochemistry,* **1992**, *31*, 3811-3812.

(145) Wrolstad, R. E.; Skrede, G.; Lea, P. E. R.; Enersen, G., Influence of Sugar on Anthocyanin Pigment Stability in Frozen Strawberries. *J. Food Sci.,* **1990**, *55*, 1064-1065.

(146) Rubinskiene, M.; Viskelis, P.; Jasutiene, I.; Viskeliene, R.*, et al.*, Impact of various factors on the composition and stability of black currant anthocyanins. *Food Res. Int.,* **2005**, *38*, 867-871.

(147) Padayachee, A.; Netzel, G.; Netzel, M.; Day, L.*, et al.*, Binding of polyphenols to plant cell wall analogues – Part 1: Anthocyanins. *Food Chem.,* **2012**, *134*, 155-161.

(148) Le Bourvellec, C. Association entre les procyanidols et les polymères pariétaux de pommes: quantification et conséquences. Universite de Rennes I, 2003.

(149) Rodríguez, R.; Jaramillo, S.; Heredia, A.; Guillén, R.*, et al.*, Mechanical properties of white and green asparagus: changes related to modifications of cell wall components. *J. Sci. Food Agric.,* **2004**, *84*, 1478-1486.

(150) Chanliaud, E.; Gidley, M. J., In vitro synthesis and properties of pectin/*Acetobacter xylinus* cellulose composites. *The Plant Journal,* **1999**, *20*, 25-35.

(151) Prasanna, V.; Prabha, T. N.; Tharanathan, R. N., Fruit Ripening Phenomena–An Overview. *Crit. Rev. Food Sci.,* **2007**, *47*, 1-19.

(152) Saura-Calixto, F.; Díaz-Rubio, M. E., Polyphenols associated with dietary fibre in wine: A wine Polyphenols gap? *Food Res. Int.,* **2007**, *40*, 613-619.

(153) Loftsson, T.; Másson, M.; Brewster, M. E., Self-association of cyclodextrins and cyclodextrin complexes. *J. Pharm. Sci.,* **2004**, *93*, 1091-1099.

(154) Mazzaracchio, P.; Pifferi, P.; Kindt, M.; Munyaneza, A.*, et al.*, Interactions between anthocyanins and organic food molecules in model systems. *Int. J. Food Sci. Tech.,* **2004**, *39*, 53-59.

(155) de Freitas, V.; Carvalho, E.; Mateus, N., Study of carbohydrate influence on protein-tannin aggregation by nephelometry. *Food Chem.,* **2003**, *81*, 503-509.

(156) Le Bourvellec, C.; Bouchet, B.; Renard, C. M. G. C., Non-covalent interaction between procyanidins and apple cell wall material. Part III: Study on model polysaccharides. *Biochim. Biophys. Acta,* **2005**, *1725*, 10-18.

(157) Parada, J.; Aguilera, J., Food microstructure affects the bioavailability of several nutrients. *J. Food Sci.,* **2007**, *72.*, 21-32.

(158) Watrelot, A. A.; Le Bourvellec, C.; Imberty, A.; Renard, C. M. G. C., Neutral sugar side chains of pectins limit interactions with procyanidins. *Carbohydr. Polym.,* **2014**, *99*, 527-536.

(159) Caffall, K. H.; Mohnen, D., The structure, function, and biosynthesis of plant cell wall pectic polysaccharides. *Carbohydr. Res.,* **2009**, *344*, 1879-1900.

(160) Ochoa-Villarreal, M.; Aispuro-Hernández, E.; Martínez-Téllez, M. Á.; Vargas-Arispuro, I., Plant Cell Wall Polymers: Function, Structure and Biological Activity of Their Derivatives. In *Polymerization*, Souza Gomes, A., Ed. 2012; pp 63-86.

(161) Watrelot, A. A.; Le Bourvellec, C.; Imberty, A.; Renard, C. M. G. C., Interactions between Pectic Compounds and Procyanidins are Influenced by Methylation Degree and Chain Length. *Biomacromolecules,* **2013**, *14*, 709-718.

(162) Ridley, B. L.; O'Neill, M. A.; Mohnen, D., Pectins: structure, biosynthesis, and oligogalacturonide-related signaling. *Phytochemistry,* **2001**, *57*, 929-967.

(163) Voragen, A.; Coenen, G.-J.; Verhoef, R.; Schols, H., Pectin, a versatile polysaccharide present in plant cell walls. *Struct. Chem.,* **2009**, *20*, 263-275.

(164) Pérez, S.; Rodríguez-Carvajal, M. A.; Doco, T., A complex plant cell wall polysaccharide: rhamnogalacturonan II. A structure in quest of a function. *Biochimie,* **2003**, *85*, 109-121.

(165) Szejtli, J., Cyclodextrins. In *Chemical and Functional Properties of Food Saccharides*, Tomasik, P., Ed. CRC Press: Cracow, 2003.

(166) Del Valle, E. M. M., Cyclodextrins and their uses: a review. *Process Biochem.,* **2004**, *39*, 1033-1046.

(167) Mourtzinos, I.; Salta, F.; Yannakopoulou, K.; Chiou, A.*, et al.*, Encapsulation of olive leaf extract in b-cyclodextrin. *J. Agric. Food. Chem.,* **2007**, *55*, 8088-8094.

(168) Pegg, R. B.; Shahidi, F., Encapsulation, stabilization, and Controlled Release of Food Ingredients and Bioactives. In *Handbook of Food Preservation*, 2 ed.; Taylor & Frances Group, L., Ed. 2007.

(169) Szejtli, J., Introduction and General Overview of Cyclodextrin Chemistry. *Chem. Rev.,* **1998**, *98*, 1743-1754.

(170) Burin, V. M.; Rossa, P. N.; Ferreira-Lima, N. E.; Hillmann, M. C. R.*, et al.*, Anthocyanins: optimisation of extraction from Cabernet Sauvignon grapes, microcapsulation and stability in soft drink. *Int. J. Food Sci. Tech.,* **2011**, *46*, 186-193.

(171) Idham, Z.; Muhamad, I. I.; Sarmidi, M. R., Degradation kinetics and color stability of spray-dried encapsulated anthocyanins from *Hibiscus sabdariffa* L. *J. Food Process. Eng.,* **2012**, *35*, 522-542.

(172) Brouillard, R.; Chassaing, S.; Isorez, G.; Kueny-Stotz, M.*, et al.*, The visible flavonoids or anthocyanins: from research to applications. In *Recent Advances in Polyphenols Research*, Santos-Buelga, C.; Escribano-Bailon, M.; Lattanzio, U., Eds. John Wiley & Sons Ltd.: 2010; Vol. 2, pp 1-23.

(173) Ersus, S.; Yurdagel, U., Microencapsulation of anthocyanin pigments of black carrot (*Daucuscarota* L.) by spray drier. *J. Food Eng.,* **2007**, *80*, 805-812.

(174) Brouillard, R., In *Anthocyanins as Food Colors*, Markakis, P., Ed. Academic Press: New York, 1982.

(175) Xiong, S.; Melton, L. D.; Easteal, A. J.; Siew, D., Stability and Antioxidant Activity of Black Currant Anthocyanins in Solution and Encapsulated in Glucan Gel. *J. Agric. Food. Chem.,* **2006**, *54*, 6201-6208.

(176) Selim, K. A.; Khalil, K. E.; Abdel-Bary, M. S.; Abdel-Azeim, N. A., Extraction, Encapsulation and Utilization of Red Pigments from Roselle (*Hibiscus sabdariffa* L.) as Natural Food Colourants. *Alexandria Journal Food Science and Technology,* **2008**, 7-20.

(177) Cai, Y. Z.; Corke, H., Production and Properties of Spray-dried *Amaranthus* Betacyanin Pigments. *J. Food Sci.,* **2000**, *65*, 1248-1252.

(178) Chandra, A.; Nair, M. G.; Iezzoni, A. F., Isolation and stabilization of anthocyanins from tart cherries (*Prunus cerasus* L.). *J. Agric. Food. Chem.,* **1993**, *41*, 1062-1065.

(179) Hendy, G. M.; Breslin, C. B., A spectrophotometric and NMR study on the formation of an inclusion complex between dopamine and a sulfonated cyclodextrin host. *J. Electroanal. Chem.,* **2011**, *661*, 179-185.

(180) Cai, Y.; Gaffney, S. H.; Lilley, T. H.; Magnolato, D*., et al.*, Polyphenol interactions. Part 4. Model studies with caffeine and cyclodextrins. *J. Chem. Soc., Perkin Trans. 2,* **1990**, 2197-2209.

(181) Ishizu, T.; Kintsu, K.; Yamamoto, H., NMR Study of the Solution Structures of the Inclusion Complexes of β-Cyclodextrin with (+)-Catechin and (−)-Epicatechin. *J. Phys. Chem. B,* **1999**, *103*, 8992-8997.

(182) Ishizuka, Y.; Fujiwara, M.; Kanazawa, K.; Nemoto, T*., et al.*, Three-dimensional structure of the inclusion complex between phloridzin and β-cyclodextrin. *Carbohydr. Res.,* **2002**, *337*, 1737-1743.

(183) Divakar, S., A structural study of the naringin-b-cyclodextrin complex. *J. Incl. Phenom. Macrocyc.l Chem.,* **1993**, *15*, 305-316.

(184) Divakar, S.; Maheswaran, M. M., Structural Studies on Inclusion Compounds of β-Cyclodextrin with Some Substituted Phenols. *J. Incl. Phenom. Macrocyc.l Chem.,* **1997**, *27*, 113-126.

(185) Nagatomo, S., Cyclodextrins: Expanding the development of their functions and applications. *Chem. Econ. Eng. Rev.,* **1985**, *17*, 28-34.

(186) Tamura, H.; Takada, M.; Yamagami, A.; Shiomi, K., The Color Stability and Antioxidative Activity of an Anthocyanin and g-Cyclodextrin Complex. In *Functional Foods for Disease Prevention I*, American Chemical Society: 1998; Vol. 701, pp 157-171.

(187) Dangles, O.; Brouillard, R., Inclusion of natural pigments into cyclodextrins. Natural pigments in competitive spectrophotometric studies of host–guest systems. In *Minutes of the Sixth International Symposium on Cyclodextrins*, Hedges, A. R., Ed. Editions de Santé: Paris, 1992; pp 117-122.

(188) Azevedo, J.; Fernandes, I.; Faria, A.; Oliveira, J*., et al.*, Antioxidant properties of anthocyanidins, anthocyanidin-3-glucosides and respective portisins. *Food Chem.,* **2010**, *119*, 518-523.

(189) Küster, W. F.; Thiel, A., *Tabelle per le Analisi Chimiche e Chimico-Fisiche*. 12 ed.; Hoepli: Milano, 1982.

(190) Nave, F.; Petrov, V.; Pina, F.; Teixeira, N.*, et al.*, Thermodynamic and Kinetic Properties of a Red Wine Pigment: Catechin-(4,8)-malvidin-3-O-glucoside. *J. Phys. Chem. B,* **2010**, *114*, 13487-13496.

(191) Sabbah, R.; Xu-wu, A.; Chickos, J. S.; Leitão, M. L.*, et al.*, Reference materials for calorimetry and differential thermal analysis. *Thermochim. Acta,* **1999**, *331*, 93–204.

(192) Tønnesen, H. H.; Másson, M.; Loftsson, T., Studies of curcumin and curcuminoids. XXVII. Cyclodextrin complexation: solubility, chemical and photochemical stability. *Int. J. Pharm.,* **2002**, *244*, 127-135.

(193) Atkins, P. W., *Physical Chemistry*. 6th ed.; Oxford University Press: Oxford, 1998.

(194) Macanita, A. L.; Moreira, P. F.; Lima, J. C.; Quina, F. H.*, et al.*, Proton transfer in anthocyanins and related flavylium salts. Determination of ground-state rate constants with nanosecond laser flash photolysis. *J. Phys. Chem. A,* **2002**, *106*, 1248-1255.

(195) Brouillard, R.; Delaporte, B.; Dubois, J. E., Chemistry of anthocyanin pigments. 3. Relaxation amplitudes in pH-jump experiments. *J. Am. Chem. Soc.,* **1978**, *100*, 6202-6205.

(196) Pina, F., Thermodynamics and kinetics of flavylium salts - Malvin revisited. *J. Chem. Soc.-Faraday Trans.,* **1998**, *94*, 2109-2116.

(197) Pina, F.; Benedito, L.; Melo, M. J.; Parola, A. J.*, et al.*, Photochemistry of 3,4'-dimethoxy-7-hydroxyflavylium chloride - Photochromism and excited-state proton transfer. *J. Chem. Soc.-Faraday Trans.,* **1996**, *92*, 1693-1699.

(198) Quina, F.; Freitas, A.; Maçanita, A. L.; da Silva, P.*, et al.*, the (photo)chemistry of anthocyanins. *The Spectrum,* **2006**, *19*.

(199) Petrov, V.; Pina, F., Analytical resolution of the reaction rates of flavylium network by Laplace transform. *J. Math. Chem.,* **2010**, *47*, 1005-1026.

(200) Pina, F.; Benedito, L.; Melo, M. J.; Parola, A. J.*, et al.*, Photochemistry of 3,4'-dimethoxy-7-hydroxyflavylium chloride. Photochromism and excited-state proton transfer. *J. Chem. Soc., Faraday Trans.,* **1996**, *92*, 1693-1699.

(201) Formosinho, S. J.; Arnaut, L. G., Excited-state proton transfer reactions II. Intramolecular reactions. *J. Photochem. Photobiol. A - Chem.,* **1993**, *75*, 21-48.

(202) Ozkan, M.; Yemenicioglu, A.; Asefi, N.; Cemeroglu, B., Degradation kinetics of anthocyanins from sour cherry, pomegranaye, and strawberry juices by hydrogen peroxide. *J. Food Sci.,* **2002**, *67*, 525-529.

(203) Gradinaru, G.; Biliaderis, C. G.; Kallithraka, S.; Kefalas, P.*, et al.*, Thermal stability of *Hibiscus sabdariffa* L. anthocyanins in solution and in solid state: effects of copigmentation and glass transition. *Food Chem.,* **2003**, *83*, 423-436.

(204) Pralhad, T.; Rajendrakumar, K., Study of freeze-dried quercetin-cyclodextrin binary systems by DSC, FT-IR, X-ray diffraction and SEM analysis. *J. Pharm. Biomed. Anal.,* **2004**, *34*, 333-339.

(205) Thaning, J.; Stevensson, B.; Östervall, J.; Naidoo, K. J.*, et al.*, NMR Studies of Molecular Conformations in α-Cyclodextrin. *J. Phys. Chem. B,* **2008**, *112*, 8434-8436.

(206) Rymdén, R.; Carlfors, J.; Stilbs, P., Substrate binding to cyclodextrins in aqueous solution: A multicomponent self-diffusion study. *Journal of Inclusion Phenomena,* **1983**, *1*, 159-167.

(207) Howard, L. R.; Brownmiller, C.; Prior, R. L.; Mauromoustakos, A., Improved Stability of Chokeberry Juice Anthocyanins by β-Cyclodextrin Addition and Refrigeration. *J. Agric. Food. Chem.,* **2013**, *61*, 693-699.

(208) Tamura, H.; Takada, M.; Yamagami, A.; Shiomi, K., The Color Stability and Antioxidative Activity of an Anthocyanin and ?-Cyclodextrin Complex. In *Functional Foods for Disease Prevention I*, American Chemical Society: 1998; Vol. 701, pp 157-171.

(209) Popov, K.; Rönkkömäki, H.; Lajunen, L. H. J., Guidelines for NMR measurements for determination of high and low pK_a values (IUPAC Technical Report). *Pure Appl. Chem.,* **2006**, *78*, 663-675.

(210) Hwang, T. L.; Shaka, A. J., Water Suppression That Works. Excitation Sculpting Using Arbitrary Wave-Forms and Pulsed-Field Gradients. *Journal of Magnetic Resonance, Series A,* **1995**, *112*, 275-279.

(211) Wu, D. H.; Chen, A. D.; Johnson, C. S., An Improved Diffusion-Ordered Spectroscopy Experiment Incorporating Bipolar-Gradient Pulses. *Journal of Magnetic Resonance, Series A,* **1995**, *115*, 260-264.

(212) Matsumoto, N.; Yamada, M.; Kurakata, Y.; Yoshida, H.*, et al.*, Crystal structures of open and closed forms of cyclo/maltodextrin-binding protein. *Febs Journal,* **2009**, *276*, 3008-3019.

(213) Gaussian Inc., C. O. P., Bldg. 6, Pittsburgh, PA 15106, USA.

(214) Frisch, M. J.; G. W. Trucks; H. B. Schlegel; Scuseria, G. E.*, et al.*, Gaussian 09. **2009**.

(215) Bayly, C. I.; Cieplak, P.; Cornell, W. D.; Kollman, P. A., A Well-Behaved Electrostatic Potential Based Method Using Charge Restraints for Deriving Atomic Charges - the Resp Model. *J. Phys. Chem.,* **1993**, *97*, 10269-10280.

(216) Case, D. A.; Darden, T. A.; Cheatham, I. T. E.; Simmerling, C. L.*, et al.*, AMBER 10, University of California, San Francisco. **2008**.

(217) Kirschner, K. N.; Woods, R. J., Solvent interactions determine carbohydrate conformation. *Proceedings of the National Academy of Sciences of the United States of America,* **2001**, *98*, 10541-10545.

(218) Kirschner, K. N.; Woods, R. J., Quantum mechanical study of the nonbonded forces in water-methanol complexes. *J. Phys. Chem. A,* **2001**, *105*, 4150-4155.

(219) Basma, M.; Sundara, S.; Calgan, D.; Vernali, T.*, et al.*, Solvated ensemble averaging in the calculation of partial atomic charges. *J. Comput. Chem.,* **2001**, *22*, 1125-1137.

(220) Izaguirre, J. A.; Catarello, D. P.; Wozniak, J. M.; Skeel, R. D., Langevin stabilization of molecular dynamics. *J. Chem. Phys.,* **2001**, *114*, 2090-2098.

(221) Ryckaert, J. P.; Ciccotti, G.; Berendsen, H. J. C., Numerical-Integration of Cartesian Equations of Motion of a System with Constraints - Molecular-Dynamics of N-Alkanes. *J. Comput. Phys.,* **1977**, *23*, 327-341.

(222) Essmann, U.; Perera, L.; Berkowitz, M. L.; Darden, T.*, et al.*, A Smooth Particle Mesh Ewald Method. *J. Chem. Phys.,* **1995**, *103*, 8577-8593.

(223) Jordheim, M.; Fossen, T.; Andersen, Ø. M., Characterization of Hemiacetal Forms of Anthocyanidin 3-*O*-β-Glycopyranosides. *J. Agric. Food. Chem.,* **2006**, *54*, 9340-9346.

(224) Ishizu, T.; Hirata, C.; Yamamoto, H.; Harano, K., Structure and intramolecular flexibility of β-cyclodextrin complex with (−)-epigallocatechin gallate in aqueous solvent. *Magn. Reson. Chem.,* **2006**, *44*, 776-783.

(225) Pianet, I.; André, Y.; Ducasse, M. A.; Tarascou, I.*, et al.*, Modeling Procyanidin Self-Association Processes and Understanding Their Micellar Organization: A Study by Diffusion NMR and Molecular Mechanics. *Langmuir,* **2008**, *24*, 11027-11035.

(226) Cala, O.; Dufourc, E. J.; Fouquet, E.; Manigand, C.*, et al.*, The Colloidal State of Tannins Impacts the Nature of Their Interaction with Proteins: The Case of Salivary Proline-Rich Protein/Procyanidins Binding. *Langmuir,* **2012**, *28*, 17410-17418.

(227) Polyakov, N. E.; Leshina, T. V.; Hand, E. O.; Petrenko, A.*, et al.*, β-Ionone cyclodextrins inclusion complexes: ^{1}H NMR study and photolysis. *J. Photochem. Photobiol. A - Chem.,* **2004**, *161*, 261-267.

(228) Ishizu, T.; Kajitani, S.; Tsutsumi, H.; Yamamoto, H.*, et al.*, Diastereomeric difference of inclusion modes between (−)-epicatechin gallate, (−)-epigallocatechin gallate and (+)-gallocatechin gallate, with β-cyclodextrin in aqueous solvent. *Magn. Reson. Chem.,* **2008**, *46*, 448-456.

(229) Upadhyay, S. K.; Kumar, G., NMR and molecular modelling studies on the interaction of fluconazole with b-cyclodextrin. *Chem. Cent. J.,* **2009**, *3*.

(230) Wood, D. J.; Hruska, F. E.; Saenger, W., Proton NMR study of the inclusion of aromatic molecules in a-cyclodextrin. *J. Am. Chem. Soc.,* **1977**, *99*, 1735-1740.

(231) Job, P., Formation and stability of inorganic complexes in solution. *Anal. Chim.,* **1928**, *9*.

(232) Brand, T.; Cabrita, E. J.; Berger, S., Intermolecular interaction as investigated by NOE and diffusion studies. *Prog. Nucl. Magn. Reson. Spectrosc.,* **2005**, *46*, 159-196.

(233) Cohen, Y.; Avram, L.; Frish, L., Diffusion NMR Spectroscopy in Supramolecular and Combinatorial Chemistry: An Old Parameter—New Insights. *Angew. Chem. Int. Ed.,* **2005**, *44*, 520-554.

(234) Avram, L.; Cohen, Y., Complexation in Pseudorotaxanes Based on α-Cyclodextrin and Different α,ω-Diaminoalkanes by NMR Diffusion Measurements. *The Journal of Organic Chemistry,* **2002**, *67*, 2639-2644.

(235) Fielding, L., Determination of Association Constants (K_a) from Solution NMR Data. *Tetrahedron,* **2000**, *56*, 6151-6170.

(236) McClelland, R. A.; Gedge, S., Hydration of the flavylium ion. *J. Am. Chem. Soc.,* **1980**, *102*, 5838-5848.

(237) Pina, F.; Hatton, T. A., Photochromic Soft Materials: Flavylium Compounds Incorporated into Pluronic F-127 Hydrogel Matrixes. *Langmuir,* **2008**, *24*, 2356-2364.

(238) Pina, F.; Lima, J. C.; Parola, A. J.; Afonso, C. A. M., Thermal and Photochemical Properties of 4′,7-dihydroxyflavylium in Water-Ionic Liquids Biphasic Systems. A Novel Approach to a Write-Read-Erase Molecular Switching System. *Angew. Chem., Int. Ed.,* **2004**, *43*, 1525-1527.

(239) Pina, F.; Petrov, V.; Laia, C. A. T., Photochromism of flavylium systems. An overview of a versatile multistate system. *Dyes Pigments,* **2012**, *92*, 877-889.

(240) Flavonoids and flower colour. In *The Flavonoids: advances in research since 1986*, Harborne, J. B., Ed. Chapman & Hall/CRC: 1993; pp 565-589.

(241) Katritzky, A. R.; Czerney, P.; Levell, J. R.; Du, W., Molecular Engineering of Benzo[b]pyrylium Salts by Indirect Electrophilic Substitution. *Eur. J. Org. Chem.,* **1998**, *1998*, 2623-2629.

(242) Kim, H.; Choi, J.; Jung, S., Inclusion complexes of modified cyclodextrins with some flavonols. *J. Incl. Phenom. Macrocyc.l Chem.,* **2009**, *64*, 43-47.

(243) Konczak, I.; Zhang, W., Anthocyanins: More Than Nature's Colours. *J. Biomed. Biotechnol.,* **2004**, *2004*, 239-240.

(244) Fernandes, A.; Sousa, A.; Azevedo, J.; Mateus, N.*, et al.*, Effect of cyclodextrins on the thermodynamic and kinetic properties of cyanidin-3-*O*-glucoside. *Food Res. Int.,* **2013**, *51*, 748-755.

(245) Gonçalves, R.; Mateus, N.; De Freitas, V., Influence of Carbohydrates on the Interaction of Procyanidin B3 with Trypsin. *J. Agric. Food. Chem.,* **2011**, *59*, 11794-11802.

(246) Rosenbohm, C.; Lundt, I.; Christensen, T. I. E.; Young, N. G., Chemically methylated and reduced pectins: preparation, characterisation by ^{1}H NMR spectroscopy, enzymatic degradation, and gelling properties. *Carbohydr. Res.,* **2003**, *338*, 637-649.

(247) Aina, V. O.; Barau, M. M.; Mamman, O. A.; Zakari, A.*, et al.*, Extraction and Characterization of Pectin from Peels of Lemon (*Citrus limon*), Grape Fruit (*Citrus paradisi*) and Sweet Orange (*Citrus sinensis*). *Br. J. Clin. Pharmacol.,* **2012**, *3*, 259-262.

(248) Holzwarth, M.; Korhummel, S.; Siekmann, T.; Carle, R.*, et al.*, Influence of different pectins, process and storage conditions on anthocyanin and colour retention in strawberry jams and spreads. *LWT - Food Science and Technology,* **2013**, *52*, 131-138.

(249) Belitz, H. D.; Grosch, W.; Shieberle, P., *Food Chemistry*. 4 ed.; 2009.

(250) Charlton, A. J.; Baxter, N. J.; Khan, M. L.; Moir, A. J. G., *et al.*, Polyphenol/Peptide Binding and Precipitation. *J. Agric. Food. Chem.,* **2002**, *50*, 1593-1601.

(251) Gonçalves, R.; Mateus, N.; Pianet, I.; Laguerre, M., *et al.*, Mechanisms of Tannin-Induced Trypsin Inhibition: A Molecular Approach. *Langmuir,* **2011**, *27*, 13122-13129.

(252) Pissarra, J.; Mateus, N.; Rivas-Gonzalo, J.; Santos Buelga, C., *et al.*, Reaction Between Malvidin 3-Glucoside and (+)-Catechin in Model Solutions Containing Different Aldehydes. *J. Food Sci.,* **2003**, *68*, 476-481.

(253) Coimbra, M. A.; Waldron, K. W.; Selvendran, R. R., Isolation and characterisation of cell wall polymers from olive pulp (*Olea europaea* L.). *Carbohydr. Res.,* **1994**, *252*, 245-262.

(254) Nunes, C.; Rocha, S. M.; Saraiva, J.; Coimbra, M. A., Simple and solvent-free methodology for simultaneous quantification of methanol and acetic acid content of plant polysaccharides based on headspace solid phase microextraction-gas chromatography (HS-SPME-GC-FID). *Carbohydr. Polym.,* **2006**, *64*, 306-311.

(255) Puskás, I.; Szemjonov, A.; Fenyvesi, É.; Malanga, M., *et al.*, Aspects of determining the molecular weight of cyclodextrin polymers and oligomers by static light scattering. *Carbohydr. Polym.,* **2013**, *94*, 124-128.

(256) Yuliarti, O.; Matia-Merino, L.; Goh, K. K. T.; Mawson, J. A., *et al.*, Effect of Celluclast 1.5L on the Physicochemical Characterization of Gold Kiwifruit Pectin. *Int. J. Mol. Sci.,* **2011**, *12*, 6407-6417.

(257) Gonçalves, F. J.; Rocha, S. M.; Coimbra, M. A., Study of the retention capacity of anthocyanins by wine polymeric material. *Food Chem.,* **2012**, *134*, 957-963.

(258) Piotto, M.; Saudek, V.; Sklenář, V., Gradient-tailored excitation for single-quantum NMR spectroscopy of aqueous solutions. *J. Biomol. NMR,* **1992**, *2*, 661-665.

(259) Mayer, M.; Meyer, B., Characterization of Ligand Binding by Saturation Transfer Difference NMR Spectroscopy. *Angew. Chem. Int. Ed.,* **1999**, *38*, 1784-1788.

(260) Meyer, B.; Peters, T., NMR Spectroscopy Techniques for Screening and Identifying Ligand Binding to Protein Receptors. *Angew. Chem. Int. Ed.,* **2003**, *42*, 864-890.

(261) Woods Group. (2005-2014) GLYCAM Web. Complex Carbohydrate Research Center, U. o. G., Athens, GA. (http://www.glycam.com).

(262) Wang, J. M.; Wolf, R. M.; Caldwell, J. W.; Kollman, P. A., *et al.*, Development and testing of a general amber force field. *J. Comput. Chem.,* **2004**, *25*, 1157-1174.

(263) Lepre, C. A.; Moore, J. M.; Peng, J. W., Theory and Applications of NMR-Based Screening in Pharmaceutical Research. *Chem. Rev.,* **2004**, *104*, 3641-3676.

(264) Viegas, A.; Manso, J.; Nobrega, F. L.; Cabrita, E. J., Saturation-Transfer Difference (STD) NMR: A Simple and Fast Method for Ligand Screening and Characterization of Protein Binding. *J. Chem. Educ.,* **2011**, *88*, 990-994.

(265) Haselhorst, T.; Lamerz, A. C.; Itzstein, M. V., Saturation Transfer Difference NMR Spectroscopy as a Technique to Investigate Protein-Carbohydrate Interactions in Solution. In *Glycomics*, Packer, N.; Karlsson, N., Eds. Humana Press: 2009; Vol. 534, pp 375-396.

(266) Perez-Victoria, I.; Kemper, S.; Patel, M. K.; Edwards, J. M.*, et al.*, Saturation transfer difference NMR reveals functionally essential kinetic differences for a sugar-binding repressor protein. *Chem. Commun.,* **2009**, 5862-5864.

(267) Krishnan, V., Ligand screening by saturation-transfer difference (STD) NMR spectroscopy. *Curr. Anal. Chem.,* **2005**, *1*, 307-320.

(268) Fernandes, A.; Ivanova, G.; Brás, N. F.; Mateus, N.*, et al.*, Structural characterization of inclusion complexes between cyanidin-3-O-glucoside and β-cyclodextrin. *Carbohydr. Polym.,* **2014**, *102*, 269-277.

(269) Mayer, M.; Meyer, B., Group Epitope Mapping by Saturation Transfer Difference NMR To Identify Segments of a Ligand in Direct Contact with a Protein Receptor. *J. Am. Chem. Soc.,* **2001**, *123*, 6108-6117.

(270) Buchweitz, M.; Speth, M.; Kammerer, D. R.; Carle, R., Stabilisation of strawberry (*Fragaria x ananassa Duch.*) anthocyanins by different pectins. *Food Chem.,* **2013**, *141*, 2998-3006.

(271) Giles, C. H.; MacEwan, T. H.; Nakhwa, S. N.; Smith, D., Studies in adsorption. Part XI. A system of classification of solution adsorption isotherms, and its use in diagnosis of adsorption mechanisms and in measurement of specific surface areas of solids. *J. Chem. Soc.,* **1960**, 3973-3993.

(272) Terrier, N.; Poncet-Legrand, C.; Cheynier, V., Flavanols, Flavonols and Dihydroflavonols. In *Wine Chemistry and Biochemistry*, Moreno-Arribas, M. V.; Polo, M. C., Eds. Springer: 2009; pp 463-508.

(273) Yamakawa, Y.; Oosuna, H.; Yamakawa, T.; Aihara, M.*, et al.*, Cochineal extract-induced immediate allergy. *J. Dermatol.,* **2009**, *36*, 72-74.

(274) Arnold, L. E.; Lofthouse, N.; Hurt, E., Artificial Food Colors and Attention-Deficit/Hyperactivity Symptoms: Conclusions to Dye for. *Neurotherapeutics,* **2012**, *9*, 599-609.

(275) Bakowska-Barczak, A., Acylated anthocyanins as stable, natural food colorants - a review. *Pol. J. Food Nutrit. Sci.,* **2005**, *14/55*, 107-116.

(276) Maier, T.; Fromm, M.; Schieber, A.; Kammerer, D. R.*, et al.*, Process and storage stability of anthocyanins and non-anthocyanin phenolics in pectin and gelatin gels enriched with grape pomace extracts. *Eur. Food Res. Technol.,* **2009**, *229*, 949-960.

(277) Delgado-Vargas, F.; Jiménez, A. R.; Paredes-López, O., Natural Pigments: Carotenoids, Anthocyanins, and Betalains- Characteristics, Biosynthesis, Processing, and Stability. *Crit. Rev. Food Sci.,* **2000**, *40*, 173 - 289.

(278) Mazza, G.; Brouillard, R., Recent developments in the stabilization of anthocyanins in food products. *Food Chem.,* **1987**, *25*, 207-225.

(279) Davies, A. J.; Mazza, G., Copigmentation of simple and acylated anthocyanins with colorless phenolic compounds. *J. Agric. Food. Chem.,* **1993**, *41*, 716-720.

(280) Yoshida, K.; Kondo, T.; Goto, T., Intramolecular stacking conformation of gentiodelphin, a diacylated anthocyanin from *Gentiana makinoi*. *Tetrahedron,* **1992**, *48*, 4313-4326.

(281) Hoshino, T., Self-association of flavylium cations of anthocyanidin 3,5-diglucosides studied by circular dichroism and ^{1}H NMR *Phytochemistry,* **1992**, *31*, 647-653.

(282) Nerdal, W.; Andersen, Ø. M., Intermolecular aromatic acid association of an anthocyanin (petanin) evidenced by two-dimensional nuclear overhauser enhancement nuclear magnetic resonance experiments and distance geometry calculations. *Phytochem. Anal.,* **1992**, *3*, 182-189.

(283) Mistry, T.; Cai, Y.; Lilley, T. H.; Haslam, E., Polyphenol interactions. Part 5. Anthocyanin co-pigmentation. *J. Chem. Soc., Perkin Trans. 2,* **1991**, 1287-1296.

(284) Hoshino, T., An approximate estimate of self-association constants and the self-stacking conformation of Malvin quinonoidal bases studied by ^{1}H NMR. *Phytochemistry,* **1991**, *30*, 2049-2055.

(285) Hoshino, T.; Goto, T., Effects of pH and concentration on the self-association of malvin quinonoidal base — electronic and circular dichroic studies. *Tetrahedron Lett.,* **1990**, *31*, 1593-1596.

(286) Gaussian Inc., C. O. P., Bldg. 6, Pittsburgh, PA 15106, USA.

(287) Frisch, M. J., G. W. Trucks, H. B. Schlegel, Scuseria, G. E.; Robb, M. A.; Cheeseman, J. R.; Scalmani, G.; Barone, V.; Mennucci, B.; Petersson, G. A.; Nakatsuji, H.; Caricato, M.; Li, X.; Hratchian, H. P.; Izmaylov, A. F.; Bloino, J.; Zheng, G.; Sonnenberg, J. L.; Hada, M.; Ehara, M.; Toyota, K.; Fukuda, R.; Hasegawa, J.; Ishida, M.; Nakajima, T.; Honda, Y.; Kitao, O.; Nakai, H.; Vreven, T.; Montgomery, Jr., J. A.; Peralta, J. E.; Ogliaro, F.; Bearpark, M.; Heyd, J. J.; Brothers, E.; Kudin, K. N.; Staroverov, V. N.; Kobayashi, R.; Normand, J.; Raghavachari, K.; Rendell, A.; Burant, J. C.; Iyengar, S. S.; Tomasi, J.; Cossi, M.; Rega, N.; Millam, N. J.; Klene, M.; Knox, J. E.; Cross, J. B.; Bakken, V.; Adamo, C.; Jaramillo, J.; Gomperts, R.; Stratmann, R. E.; Yazyev, O.; Austin, A. J.; Cammi, R.; Pomelli, C.; Ochterski, J. W.; Martin, R. L.; Morokuma, K.; Zakrzewski, V. G.; Voth, G. A.; Salvador, P.; Dannenberg, J. J.; Dapprich, S.; Daniels, A. D.; Farkas, Ö.; Foresman, J. B.; Ortiz, J. V.; Cioslowski, J.; Fox, D. J. *Gaussian 09*, Revision A.1; Gaussian, Inc.: Wallingford CT, 2009.

(288) D.A. Case, T. A. D., T.E. Cheatham, III, C.L. Simmerling, J. Wang, R.E. Duke, R.; Luo, R. C. W., W. Zhang, K.M. Merz, B. Roberts, S. Hayik, A. Roitberg, G. Seabra,; J. Swails, A. W. G., I. Kolossváry, K.F. Wong, F. Paesani, J. Vanicek, R.M. Wolf, J. Liu,; X. Wu, S. R. B., T. Steinbrecher, H. Gohlke, Q. Cai, X. Ye, J. Wang, M.-J. Hsieh, G.*, et al. AMBER 12, University of California, San Francisco*, 2012.

(289) Gakh, E. G.; Dougall, D. K.; Baker, D. C., Proton nuclear magnetic resonance studies of monoacylated anthocyanins from the wild carrot: Part 1. Inter- and intra-molecular interactions in solution. *Phytochem. Anal.,* **1998**, *9*, 28-34.

(290) Oliveira, J.; de Freitas, V.; Mateus, N., A novel synthetic pathway to vitisin B compounds. *Tetrahedron Lett.,* **2009**, *50*, 3933-3935.

(291) Baxter, N. J.; Williamson, M. P.; Lilley, T. H.; Haslam, E., Stacking interactions between caffeine and methyl gallate. *J. Chem. Soc., Faraday Trans.,* **1996**, *92*, 231-234.

(292) Gläßgen, W.; Wray, V.; Strack, D.; Metzger, J.*, et al.*, Anthocyanins from cell suspension cultures of *Daucus carota*. *Phytochemistry,* **1992**, *31*, 1593-1601.